Development of the UMAC-Based Control System with Application to 5-Axis Ultraprecision Micromilling Machines

A thesis submitted for the degree of
Doctor of Philosophy

by

Mohd Khalid Mohd Nor

School of Engineering and Design,
Brunel University

February 2010

Abstract

Increasing demands from end users in the fields of optics, defence, automotive, medical, aerospace, etc. for high precision 3D miniaturized components and microstructures from a range of materials have driven the development in micro and nano machining and changed the manufacturing realm. Conventional manufacturing processes such as chemical etching and LIGA are found unfavourable or limited due to production time required and have led mechanical micro machining to grow further. Mechanical micro machining is an ideal method to produce high accuracy micro components and micro milling is the most flexible enabling process and is thus able to generate a wider variety of complex micro components and microstructures.

Ultraprecision micromilling machine tools are required so as to meet the accuracy, surface finish and geometrical complexity of components and parts. Typical manufacturing requirements are high dimensional accuracy being better than 1 micron, flatness and roundness better than 50 nm and surface finish ranging between 10 and 50 nm. Manufacture of high precision components and parts require very intricate material removal procedure. There are five key components that include machine tools, cutting tools, material properties, operation variables and environmental conditions, which constitute in manufacturing high quality components and parts. End users assess the performance of a machine tool based on the dimensional accuracy and surface quality of machined parts including the machining time.

In this thesis, the emphasis is on the design and development of a control system for a 5-axis bench-type ultraprecision micromilling machine- Ultra-Mill. On the one hand, the developed control system is able to offer high motion and positioning accuracy, dynamic stiffness and thermal stability for motion control, which are essential for achieving the machining accuracy and surface finish desired. On the other hand, the control system is able to undertake in-process inspection and condition monitoring of the machine tool and process.

The control of multi-axis precision machines with high-speed and high-accuracy motions and positioning are desirable to manufacture components with high accuracy and complex features to increase productivity and maintain machine stability, etc. The

development of the control system has focused on fast, accurate and robust positioning requirements at the machine system design stage. Apart from the mechanical design, the performance of the entire precision systems is greatly dependent on diverse electrical and electronics subsystems, controllers, drive instruments, feedback devices, inspection and monitoring system and software. There are some variables that dynamically alter the system behaviour and sensitivity to disturbance that are not ignorable in the micro and nano machining realm.

In this research, a structured framework has been developed and integrated to aid the design and development of the control system. The framework includes critically reviewing the state of the art of ultraprecision machining tools, understanding the control system technologies involved, highlighting the advantages and disadvantages of various control system methods for ultraprecision machines, understanding what is required by end-users and formulating what actually makes a machine tool be an ultraprecision machine particularly from the control system perspective.

In the design and development stage, the possession of mechatronic know-how is essential as the design and development of the Ultra-Mill is a multidisciplinary field. Simulation and modelling tool such as Matlab/Simulink is used to model the most suitable control system design. The developed control system was validated through machining trials to observe the achievable accuracy, experiments and testing of subsystems individually (slide system, tooling system, monitoring system, etc.).

This thesis has successfully demonstrated the design and development of the control system for a 5-axis ultraprecision machine tool- Ultra-Mill, with high performance characteristics, fast, accurate, precise, etc. for motion and positioning, high dynamic stiffness, robustness and thermal stability, whereby was provided and maintained by the control system.

Acknowledgements

I would like to express my deepest gratitude to the people who have helped and guided in working to realize this research project.

Firstly, I would like to thank my supervisor, Professor Kai Cheng for his guidance, assistance, time, effort and never ending patience to make this project a success.

Not forgetting my fellow laboratory researchers Dr. Dehong Huo, Mr. Paul Yates, Mr. Lei Zhou, Mr. Tao Wu and Dr. Xizhi Sun for their support and help through one-on-one or group meetings.

I would like also thank Brunel University and Delta Tau UK Ltd. for financing my PhD studies. I am thankful to the EU FP6 MASMICRO project partners for the constructive discussions especially Dr. Frank Wardle who is constantly monitoring the progress of the project.

I would also like to express my gratitude to my family for supporting me and providing me endless encouragement and my girlfriend, Mahani Baharum for her support and motivation. Lastly, I would like to thank my friends and colleagues for all their help and support.

This project is dedicated to those mentioned above.

Table of Contents

Abbreviations

ACC	Adaptive control constraint
ACO	Adaptive control optimization
AE	Acoustic emission
APT	Automatically programmed tool
ATC	Automatic tool changer
BSI	British standards institution
CAD	Computer aided drawing
CAM	Computer aided manufacturing
CAN	Controller area network
CCC	Cross coupled controller
CFD	Computational fluid dynamics
CE	European conformity
CMM	Coordinate measuring machine
CNC	Computer numerical controlled
DC	Direct current
DSP	Digital signal processing
EDM	Electrical discharge machining
EMC	Electromagnetic compatibility
EMI	Electromagnetic interference
EU	European Union
FMS	Flexible manufacturing system
GAC	Geometric adaptive compensation
GM	General Motors

HFE	Human factor engineering
HTM	Homogeneous transformation matrices
ISO	International Organization for Standardization
LIGA	Lithography
MASMICRO	Mass-Manufacture of Miniature/Micro Products
MCU	Machine control unit
MIT	Massachusetts Institute of Technology
mMT	Meso-micro machine tool
MOSAIC	Machine tool open system advanced intelligent controller
NC	Numerical controlled
NGC	Next generation controller
OAC	Open architecture controller
OMAC	Open modular architecture controllers
OSACA	Open system architecture for controls within automation systems
OSEC	Open system environment for controller
PC	Personal computer
PID	Proportional integral derivative controller
PLC	Programmable logic controller
PWM	Pulse width modulation
Ra	Arithmetical mean roughness of a surface
SE	Shielding effectiveness
SERCOS	Serial real-time communication system
TCM	Tool condition monitoring

TLM	Transmission line matrix
UBCOAC	University of British Columbia open architecture controller
UMAC	Universal motion and automation controller
UMOAC	University of Michigan Open Architecture Controller
ZPTEC	Zero pole error tracking controller

Nomenclature

A	*absorption*
$AV(n)$	*actual velocity in servo cycle n*
B	*friction coefficient*
B_{emf}	*back emf (V/m/a)*
b	*Re-reflection*
CA	*the commanded acceleration in servo cycle n*
$CMDout(n)$	*16-bit output command in servo cycle n*
CV	*the commanded velocity in servo cycle n*
DAC_{out}	*the 16-bit output command in servo cycle n*
f	*force (N)*
f_p	*peak force (N)*
f_{rms}	*continuous force (N)*
F_D	*friction force*
FE	*following error*
F_T	*motor force (N)*
G_{FF}	*feedforward gain*
I_p	*peak current (A)*
I_{rms}	*continuous current (A)*
I_M	*motor current (A)*
IE	*the integrated following error in servo cycle n*
$Ixx08$	*internal position scaling term for motor xx*
$Ixx09$	*internal position scaling term for motor xx*
$Ixx30$	*proportional gain value motor xx*

Ixx31	*velocity feedforward gain value for motor xx*
Ixx32	*derivative gain value for motor xx*
Ixx33	*integral gain value for motor xx.*
Ixx35	*acceleration feedforward gain value for motor xx*
IE(n)	*integrated following error in servo cycle n*
J	*total inertia* (kg/m^2)
K_{Aff}	*acceleration feedforward gain*
K_{Amp}	*amplifier gain (N/A)*
K_d	*derivative gain*
K_i	*integral gain*
K_p	*proportional gain*
K_{sp}	*internal position scaling term for motor xx*
K_{sv}	*internal position scaling term for motor xx*
K_t	*motor force constant (N/A)*
K_{Vff}	*velocity feedforward gain*
M	*Mass*
R	*reflection*
R_c	*coil resistance (R)*
t	*time (s)*
T	*torque (Nm)*
v	*velocity (m/s)*
$\tilde{v}$	*acceleration* (m/s^2)
V	*maximum speed (m/s)*
V_{ampmax}	*amplifier maximum bus voltage (V)*
V_{Dmin}	*minimum drive voltage (V)*

ω	*angular velocity (rad/s)*
$\tilde{\omega}$	*angular acceleration (rad/s^2)*

List of Figures

Chapter 1

Chapter 2

Chapter 3

Chapter 4

Chapter 5

Chapter 6

Chapter 7

Chapter 8

List of Tables

Chapter 1

Introduction

1.1. Background of the Research

Precision and micro manufacturing is becoming a critical requirement due to the rapidly increasing need for high precision three dimensional miniature products or components with micro-features in the fields of optics, aerospace, medical, etc. In fulfilling these demands, the involvement of industries and university research groups in ultraprecision machine tool research, design and integration sectors have increased rapidly nowadays. Micro and nano manufacturing is a timely and fast moving field with many product and equipment design concepts emerged and catering to the need of miniaturization (Mihalik, 2006). Figure 1.1 shows the timeline of achievable machining accuracy driven by precision and micro/nano manufacturing.

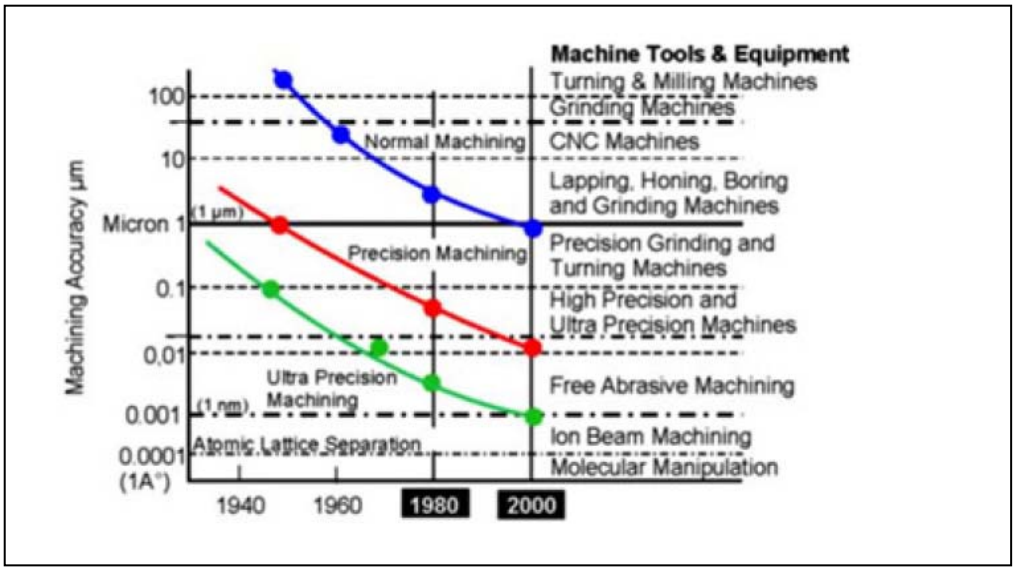

Fig. 1.1 The development of achievable machining accuracy (Byrne et al, 2003)

Micro mechanical cutting is normally not common in fabrication of micro components. Research groups investigated the potential of employing LIGA (a photo-lithography method using a synchrotron), laser, ultrasonic, ion beam and micro-EDM machining processes for manufacture of micro components (Chae et al, 2006; Madou 1997; Alting et al, 2003; Masuzawa 2000) but these processes are not productive and limited compared to mechanical cutting.

Employing mechanical cutting process in the micro and nano region, certain mechanical and electrical requirements must be met. In terms of mechanical, the machine base and moving structures must be able to withstand mechanical force disturbances that could be seen as imperfections of the machined parts. Electrical wise, the control system employed must be able to provide fast, accurate, repeatable, smooth and robust. motions. This is an important requirement when machining at the level of micro and nano. Machining at pico level might lead to more usage of laser systems to guarantee the accuracies required.

Observing the parts size in micro or nano machining and manufacturing, the size of current ultraprecision machine tools being employed on the shop floors are big. This could be uneconomical resulting in resources wastage. Designing and integrating smaller and compact ultraprecision machine tools which require smaller floor space and lower resources for manufacturing is the aim of many. At the same time, the performance of the ultraprecision machine tool should be compromised.

In this thesis, research on the requirements of control systems for a micromilling machine is investigated. The research on the evolving precision engineering research is underlined and understood in this thesis. Apart from the requirements of the control system, the motivation for miniaturization of machine tools is also investigated and research on implementation is highlighted in the thesis.

At Brunel University in conjunction with the EU MASMICRO (Mass-Manufacture of Miniature/Micro Products, contract no.: NMP2-CT-2004-500095-2) project two micro-machining machines were built. For the EU MASMICRO project, the main aim is designing and building a 5-axis ultraprecision micromilling machine. In order to achieve the aim, a 3-axis diamond turning test-bed was built in the knowledge build-up stage. Several subsystems that will be employed in the micromilling were firstly tested using this test-bed. The research conducted in this thesis is focused on the control system design and requirements for micro-machining.

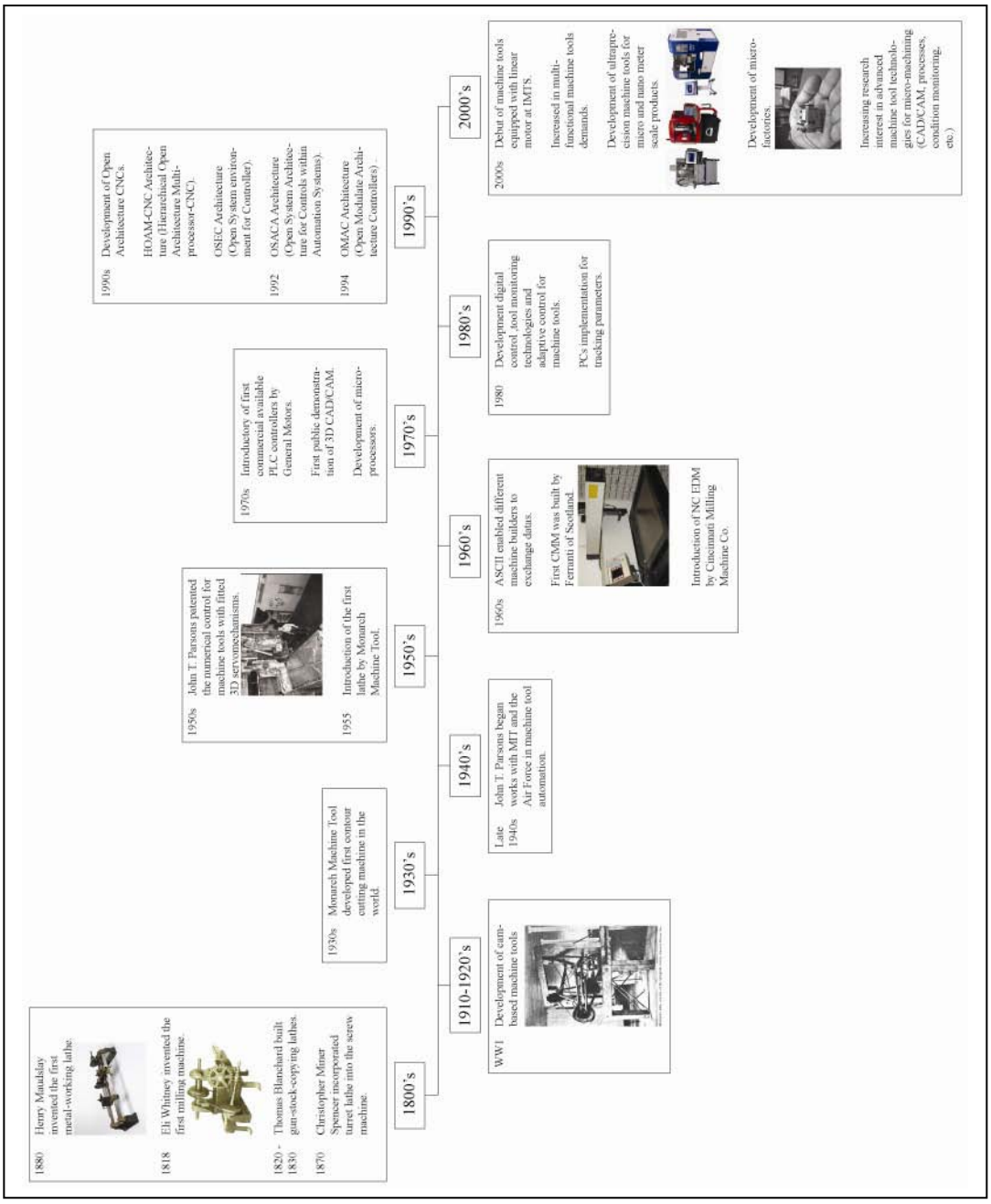

Fig. 1.2 Timeline of CNC evolution

1.2. History of the CNC Control System

The first known lathes for wood-working were used during the Biblical time. Henry Maudslay is responsible for inventing the first metal-working lathe in 1800. The design was relatively simple as it had a clamp for workpieces and a spindle. The rotation of the clamped workpiece would enable the cutting tool to machine its surface. The operator who observed controls the dials on the handwheels in order to move the workpiece accurately. Eli Whitney had invented in 1818 the first milling machine. The operating principles are similar to that of the lathe invented by Henry Maudslay. Operating these machines was really exhausting and the ability to produce the workpieces with same accuracy was limited. Consequently, the number of poorly machined and unusable workpeices was high.

The initial attempt to invent an automated machine tool also dates back to the 1800s. This initiative for automatic control of the machine tool was inspired by the use of cams in musical boxes and cuckoo clocks. Between 1820s and 1830s, gun-stock-copying lathes were built by Thomas Blanchard. In 1870, Christopher Miner Spencer was responsible turret lathe into the screw machine. By World War 1, automation based on cams was already quite advanced. The cam-based machines were difficult to set up but once set up correctly, they are capable of producing excellent repeatability.

The CNC machines operating now in many factory shopfloors or research centres are inspired by the work of John T. Parsons during the late 1940s and early 1950s. Parsons was involved in machining which required high precision. Since IBM was an established computer manufacturer at that time, Parsons decided to use an IBM computer to make more accurate contour guides. With this idea, Parsons was awarded a contract by the American Air Force for his invention of the automatic contour cutting machine invention. Using this invention with controlled servomotors, Parsons was able to machine large, complex and expensive parts for the American Air Force with high accuracy. The American Air Force and Massachusetts Institute of Technology (MIT) worked with Parsons on these projects.

During the 1950s, General Motors (GM) was also active in machine tool field. They managed to build machine tools based on tracing technology. The approach was dubbed

"record and playback". This approach used memory storage space to copy and record the movement of a machinist.

The punch card technology emerged during the 1950s. The machines during time used direct current electric driven motors for machine movements. The electric signal that drives the movements came from tape or punched-cards. The holes in them dictated the movements. The electric pulses were managed by a computer which had no memory space from the tapes or cards moved the machines precisely. The machines were called Numerical Controlled (NC) machines.

During 1960s, MIT was focused on CAD development and the development of APT programming language was conducted by Aircraft Industries Association (AIA) and Illinois Institute of Technology Research. During this time, the second batch of transistorized computers were available with larger information processing capabilities. During this time, prices of computers plunged due to introduction of minicomputers. This made it cheaper to employ computers for motor control and feedback handling and would enable every machine to be equipped with computers for process handling.

The development of microprocessors in the 1970s has led the CNC technology to reduce in cost. In this time, General Motors developed the first Programmable Logic Controller (PLC). During the 1980s, digital control was introduced. At the same time, tool monitoring technologies and adaptive control for machine tools have evolved.

With the introduction of Open Architecture Controller (OAC) in the 1990s, machine tool technologies have evolved. In computing, the definition of open architecture means:

> ***Open systems are computer systems that provide some combination of interoperability, portability, and open software standards. (It can also mean specific installations that are configured to allow unrestricted access by people and/or other computers)***(Wikipedia, 2009a).

Several key characteristics of open architecture controllers which appeal to the machine tool industries are (Asato et al, 2002):

Transparent – the system should be known completely to the end users.

Transportable – the control software could be transported to a personal microcomputer.

Transplantable – the control software could be modernized.

Liveliness – the machine should be able to function immediately without extra cost after a changed in the software and hardware.

Re-configurable – the user should be able to configure the controller functions more than once.

During this period many university research groups working with industries research the potential of OAC for machine tools. OAC technology is driven by the rapid movement in the computing technologies. Adopting these technologies provides open-ended possibilities for what machine tools could achieve for the future.

In the 2000s, came the introduction of machine tools adopting the linear motor technologies. During this period, the demand for multi-functional machine tools that could mill and turn has increased (Moriwaki, 2008). The machining accuracy currently has reached the nano meter level. Figure 1.3 illustrates the dimensional size in mechanical micro machining.

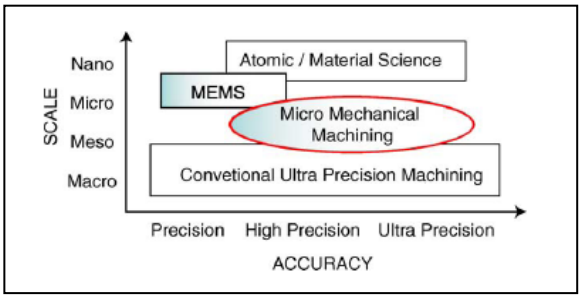

Fig. 1.3 Trend of dimensional size in micro-mechanical machining (Chae et al, 2006)

Achieving this, the need for ultraprecision machines with high accuracy, speed, repeatability, etc. is compulsory. At the moment, the technologies of motion controllers, drive systems, encoders/sensors, CAM packages, etc. are changing rapidly which would lead to more sophisticated user-friendly machine tools integration. The future requires the machine tools to automatically operate themselves with very little or no human intervention. Abilities for a machine to run the machining sequences, provide self-condition monitoring/diagnosing, quality inspection, packaging, etc. is the vision for the future with low implementation cost.

1.3. Nature of Micromilling

As this research involves the development of a 5-axis ultraprecision micromilling machine, this section will discuss the nature of micromilling in brief. Micromilling is the scaled down version of traditional macro-milling which lies in the mechanical cutting category. In this category, the main element that is used to remove material is force. The cutting tools or micro-tools commonly used in micromilling ranges between 20 and 500 µm in diameter. Micromilling processes typically employ high speed spindles with speeds starting from 100,000 rpm. Figure 1.4 illustrates examples of micro-tools.

(a) Ball nose endmill (b) Micro-drill

Fig. 1.4 Examples of micro-tools

Micromilling processes have applications in lithography, medicine, optics and micro-injection moulding. The micromilling processes is the most flexible to create 3D surfaces from a variety of engineering materials (Weck et al, 1997). It has been found that in micromilling processes tungsten carbide tools are more suitable (Masuzawa, 2000).

In the micromilling realm, the knowledge of macro-milling cannot be directly applied. More research must be conducted to understand the micromilling cutting process dynamics. The cutting forces involved in micromilling processes are minute compared to the forces in macro-milling.

Generally, ultraprecision machine tools are used for micromilling processes. These machine tools are mechanically and electrically very robust. The machine tool structure must have high static and dynamic stiffness with high thermal stability which only allow minute deformation. From the control system point of view, the controller and the drive systems must provide accurate, fast and smooth motion and positioning with high repeatability. Common commercial ultraprecision machine tools are illustrated in Figure 1.5.

(a) Robonano by Fanuc

(b) Microgantry nano 3/5x by Kugler

(c) Nanotech 250PL by Moore Technology

(d) Nanoform 250 Ultra by Precitech

Fig. 1.5 Commercial ultraprecision machine tools

1.3.1 Characteristics of the Control System for Micromilling Process

In micromilling or micromanufacturing, there are two types of controls that are widely implemented, one being closed and the other being open architecture. Machine tool manufacturers employ these two kinds of architectures although many research groups emphasize the usage of open architecture control.

The controllers are not only used for motion control but also for process control. Employment of various types of sensors enables the condition of the machine tool and machining process constantly being monitored. Table 1.1 illustrates the various types of commercially available controllers.

Table 1.1 Characteristics of machine tool controllers

Type	PC-based open architecture controller			Non PC-based architecture controller		
Manufacturer	Aerotech (Aerotech, n.d.)	Delta Tau (Delta Tau, n.d.)	PMC (PMC, n.d.)	Mitsubishi (Mitsubishi, n.d.)	GE Fanuc (Fanuc, n.d.)	Siemens (Siemens, n.d.)
Controller	A3200 Unidex600	UMAC	DCX-PCI300	Nanometer control CNC system 700 series	Fanuc 15i	SINUMERIK 840D
Axes	32 axes of synchronized motion control	Up to 32 axes	Up to 16 axes	Up to 16 axes and maximum simultaneous control	Up to 24 axes	Up to 31 axes
Processor	Motorola 56000 family of DSP	Motorola 56300 serial up to 240MHz	40MHz Texas Instruments DSP	RISC-CPU 64-bit	RISC-CPU 64-bit	Modular 32-bit microprocessor
CNC G codes support	Yes	Yes	Yes	Yes	Yes	Yes
Programming	C, C++, VisualBASIC, or LabVIEW	C, C++, or LabVIEW, etc	C/C++, Visual Basic or Delphi, LabVIEW On-board Motion	C, C++, VisualBASIC,	C language	C, C++, VisualBASIC,
Communication	IEEE 1394	USB2, Ethernet	PCI-bus	High speed optical network	Fanuc serial servo bus	RS232
Machine tools	Nanotech150AG	Nanotech350UPL Nanoform250 Nanoform300	N/A	N/A	Nanotech500FG Robonano	PicoAce

Control requirements in the micro realm are very different compared to the macro realm. In the micro realm, controllers have high speed, position counters with higher resolution capabilities, spline interpolation, higher order motion control and environmental control (Ehmann et al, 2005).

As a first example, for smoother interpolation, higher control speed is required. The smoother the interpolation, the better are the trajectories of the axes and this would result in smoother and accurate surface finish. Secondly, servoing at high resolution, the demand of encoder tracking is at a very high speed. These are examples of motion related control. Encoders are used for positioning feedback. In the micro realm, high resolution encoders are required. Typical encoder resolution is 5nm. Combining the drive system and the feedback system, obtaining high positioning and motion accuracy with high stiffness is achievable.

Apart from motion control requirements, process control is another element that must be monitored or controlled. All ultraprecision micromanufacturing machine tools must be thermally maintained at certain level. Thermal expansion would reduce the machine accuracy. Thermal sensors are normally installed within the machine enclosure for temperature monitoring. Other examples of non motion control related requirements are the control of coolant temperature, tool wear/breakage, etc. these are considered as the machine tool's auxiliary functions.

1.4. Aims and Objectives of the Research

1.4.1. Aims of Research

The aims of this research is to research, design and develop the control system for a functional 5-axis ultraprecision micromilling machine which has the characteristics of high speed, accuracy, smooth, robust and repeatable motion and high machining form accuracy. By developing this machine, the aim is to achieve the same or better performance level of current existing commercial machines in the market.

1.4.2. Objectives of the Research

The distinct objectives of the research are:

- To undertake in depth literature survey to understand the past, present and future industrial requirements of the ultraprecision machine tools, particularly on their control systems.
- To design, integrate and operate a functional 5-axis ultraprecision micromilling machine from the control system perspective.
- To design a control system for a 5-axis ultraprecision micrommiling machine that is capable of accuracies of less than 1µm over total, repeatabilities of less than 1 µm, produces finishes of less than 10 nm Ra, robust and fully autonomous.
- To develop an organized approach in machine tool control system design with the aid of scientific knowledge and analytical thinking equipped with relevant software tools.
- To implement the approach developed for integration and operation of the 5-axis ultraprecision micromilling machine.
- To investigate and evaluate the performance of the 5-axis ultraprecision micromilling machine from the control system design and requirements point of view.

1.5. Scope of the Thesis

This thesis is divided into nine chapters. The brief synopsis of each chapter is laid out as follows:

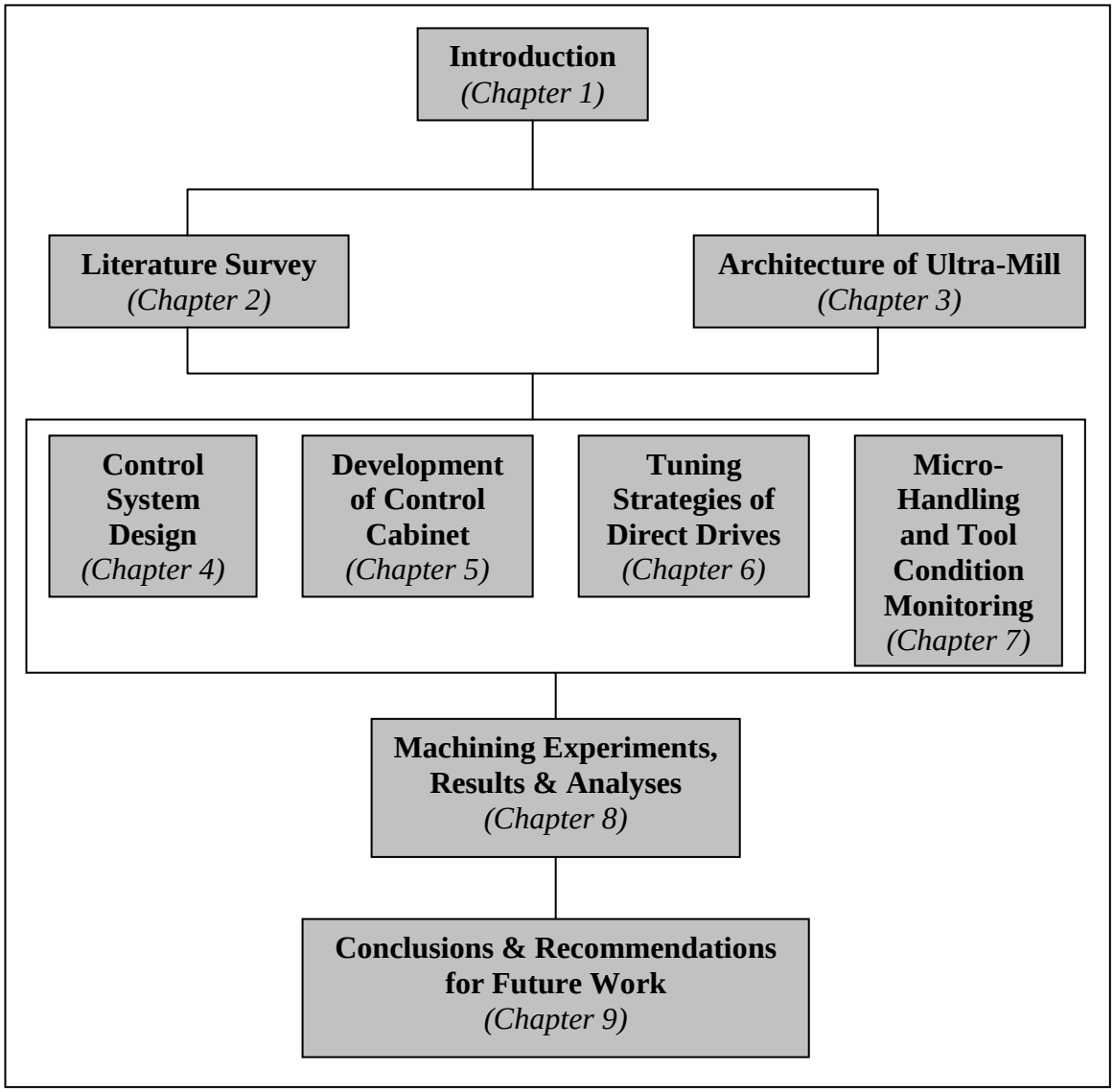

Fig. 1.6 Illustration of dissertation contents

Chapter 1 introduces the research background and a chronological history of CNC machine tools evolution. It also highlights the aims and objectives of this research and the structure of the thesis.

Chapter 2 provides a critical review to equip the author with the knowledge and understanding of past and current research stage. This literature study is responsible for the investigations of relevant and effective research to identify the related works that have been implemented in the area of 5-axis ultraprecision micromilling machine. This chapter includes a more in depth literature survey for ***Chapter 3*** to ***Chapter 8*** of this thesis.

Chapter 3 includes the brief description of the designed and integrated 5-axis ultraprecision micromilling machine. Here the specifications of the implemented technologies employed are discussed.

Chapter 4 describes and discusses the area of control system design for the machine tool. Here the control system requirements for ultraprecision machining are backed up with scientific reasoning.

Chapter 5 discusses the design and integration of the control cabinet for the 5-axis ultraprecision micromilling machine. In this chapter, the challenge of scaling down a machine tool is the main emphasize. This chapter highlights the design stage and the problems which had risen.

Chapter 6 includes the discussion on the performance of the direct drive systems being implemented in the 5-axis ultraprecision micromilling machine. Discussion is on achieving the best performance in minimal time.

Chapter 7 contains the topics of micro-handling and tool condition methods the 5-axis ultraprecision micromilling machine. This chapter will include the integration methods and the protocols used to establish the communication synchronization with the control system of the machine.

Chapter 8 includes the investigated case studies. In this chapter, the experiment details and the evaluation of the control system will be described. The performance of the control system is evaluated through the machined parts.

Chapter 9 summarizes the conclusions from the intense research work undertaken and makes further recommendations on improving this area of research in the future.

Chapter 2

Literature Review

2.1. Introduction

A thorough and effective assessment is undertaken so as to recognize work that have been carried out on ultraprecision machine tool control system design and technology trends. This is to critically review the state of the art of the research field. It comprises of theory formulation, product exploration and analysis, evaluation of concepts, research closest existing areas and uncovers research areas as illustrated in Figure 2.1. Associations of information are done through journals, textbooks, white papers, magazines, product related literature, etc.

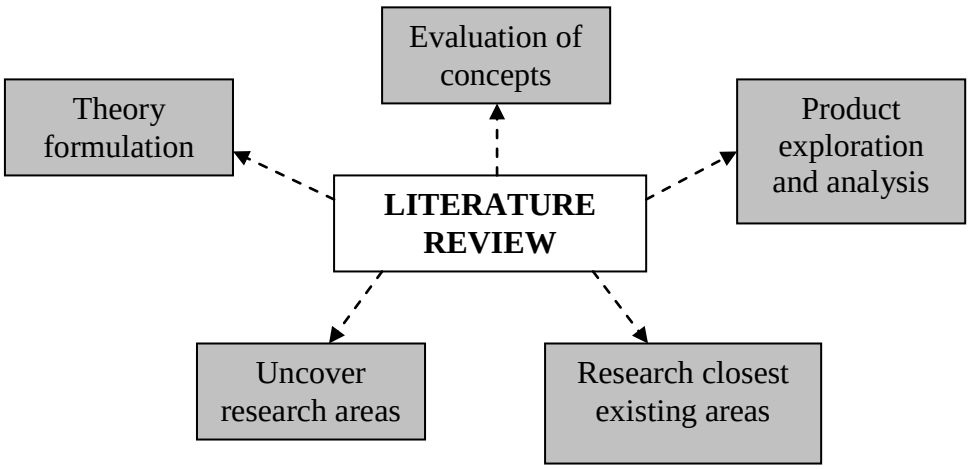

Fig. 2.1 Literature review components

The flow will be made in such a way that it will mirror the significance and relevance of the research phases. The key element is on the ultraprecision machine tool control system design and technology trends which will be implemented in the prototype machine and various analyses will be undertaken to study the performance of the prototype in the research.

2.2. Control System Architecture for Ultraprecision Machine Tools

The invention of Numerical Control (NC) machines was in the 1950s which led to the advancement to Computer Numerical Control (CNC) later in the 1970s (Liang et al.

2004). The architecture of CNC machine tool control system has evolved since then. The rapid movement in the computer industry has made the control system of machine tools more user friendly and most importantly more powerful.

2.2.1. Conventional CNC

The first NC machine was inspired and created by John T. Parsons at Massachusetts Institute of Technology (MIT) with collaboration with the Air Force. As quoted by Leatham-Jones (Leatham-Jones, 1986):

"Numerical Control (NC) is the technique of giving instructions to a machine in the form of a code which consists of numbers, letters of the alphabet, punctuation marks and certain other symbols. The machine responds to this coded information in a precise and ordered manner to carry out various machining functions."

After the emergence of NC, then comes the Computer Numerical Controller (CNC) in the 1970s. Compared to the NC, the CNC system utilizes computers to store and execute these NC codes. NC system utilized paper tapes (Luscombe et al, 1994).

CNCs were categorized as (Koren, 1983):

- Point to point only versus contouring and point to point.
- Incremental versus absolute.
- Open-loop versus closed loop control.
- NC or CNC.

Parts of the traditional CNC control system architecture still exist in modern day CNC machine tools. In the traditional CNC architecture, feedback information was only to be found at the servo level (Brien, 1995). The traditional CNC architecture is illustrated in Figure 2.2.

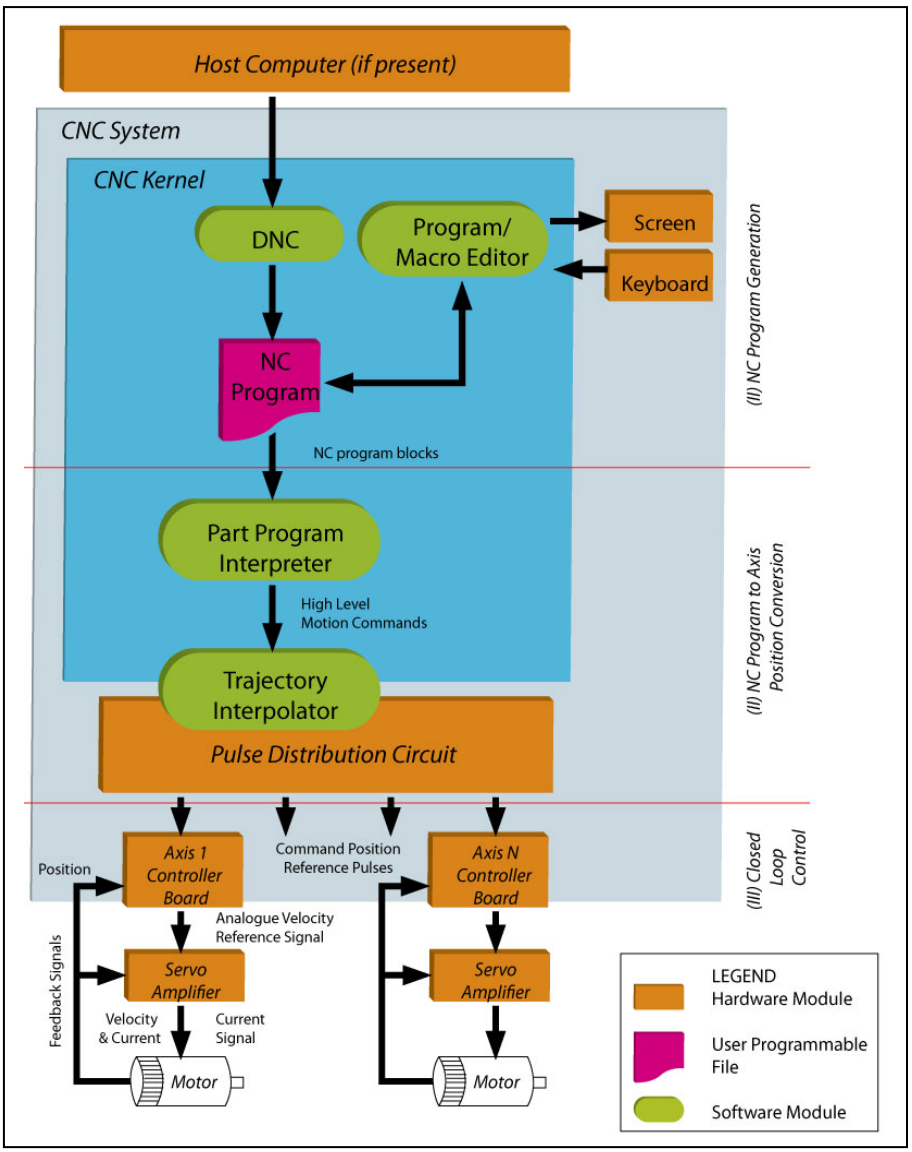

Fig. 2.2 The traditional CNC architecture (Brien, 1995)

This type of architecture is only suitable in conventional machine tools. In manufacturing process today, where machining is at the micro and nano realm or commonly now known as micro and nano machining, more sophisticated control system architecture is needed.

2.2.2. Ultraprecision CNC

Compared to more than twenty years ago, most machine tools being fabricated nowadays implement PC-based control system architecture. The revolution of PC-based control architecture for machine tools is inspired by the emergence of Open Architecture Controllers (OAC) (Alique and Haber, 2008; Nor et al, 2007). Even though

the general scheme of CNC architecture does not change entirely, utilizing a PC and open architecture controller has made CNC machine tool more user-friendly and powerful. Figure 2.3 illustrates the hierarchy of CNC controllers. Adaptive Control Optimization (ACO) and Adaptive Control Constraints are adaptive strategies to vary the machining variables in as machining progress to enhanced productivity (Koren, 1997). The Geometric Adaptive Compensation (GAC) applies real-time geometric error compensation techniques for impressions resulting from varying machining temperature, machine geometry, tool wear, etc. (Peklenik, 1970; Koren, 1997).

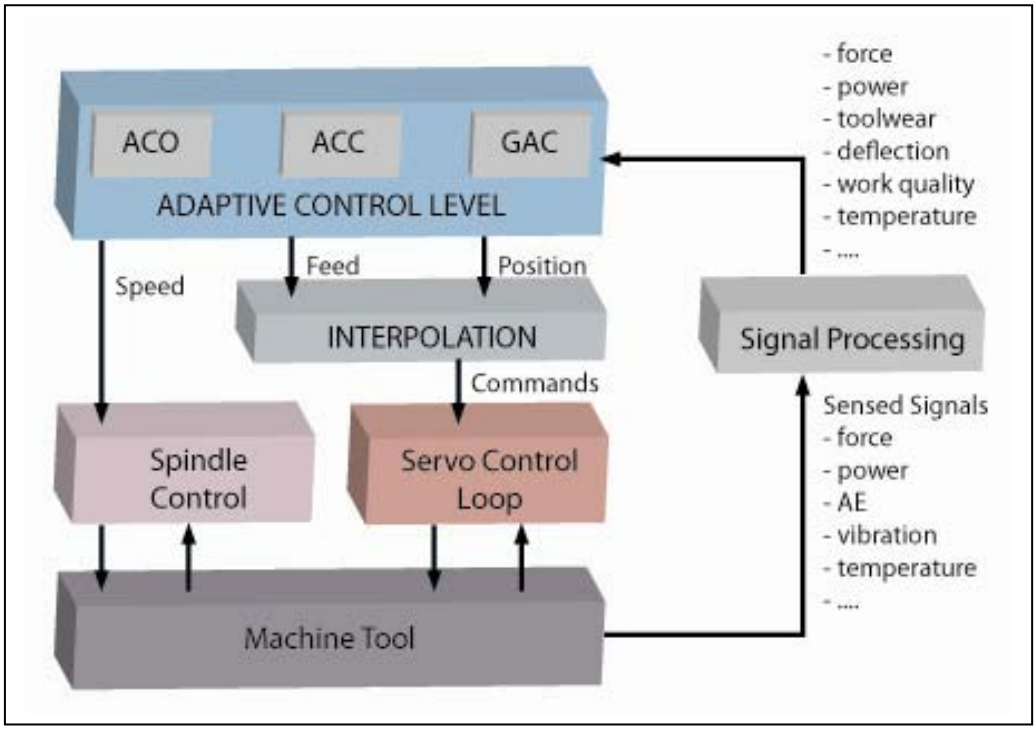

Fig. 2.3 Hierarchy of CNC controllers (Koren, 1997)

In advanced ultraprecision machine tools, multi-level hierarchical control system architecture is implemented. The multi-level hierarchical control architecture is shown in Figure 2.4.

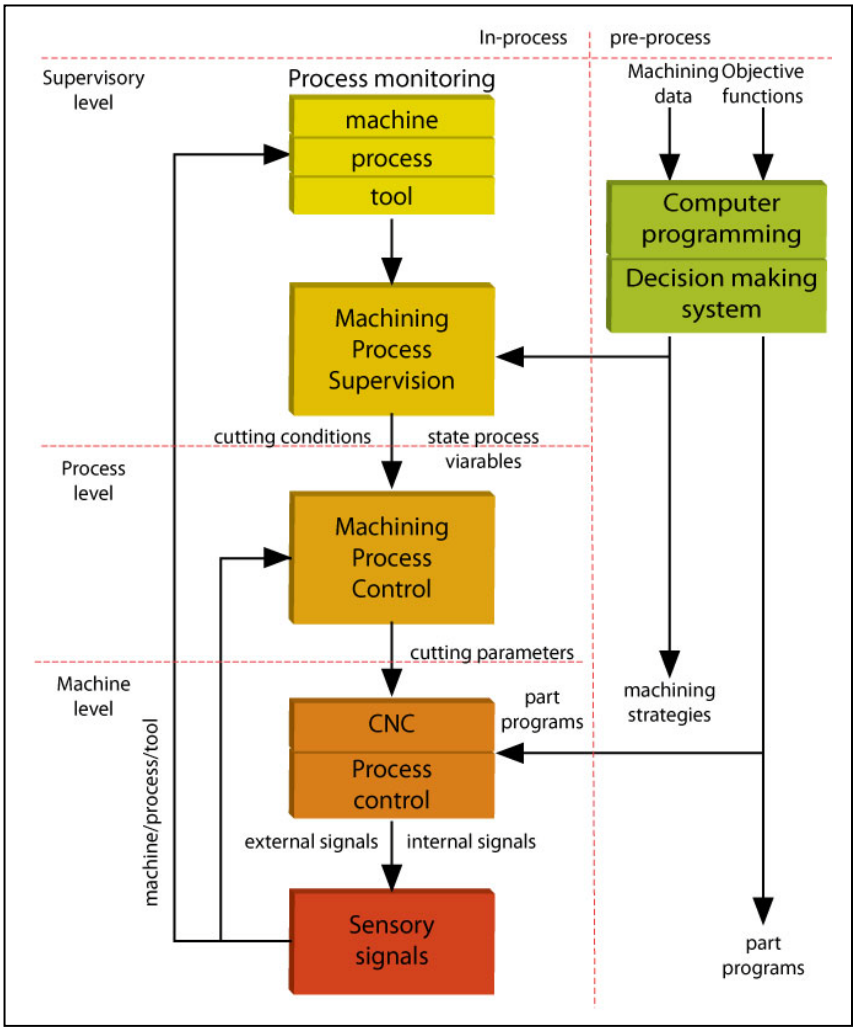

Fig. 2.4 The multi-level hierarchical control architecture (Alique and Haber, 2008)

The overall control system architecture of one ultraprecision to another does not have many differences. Differences could be found in (Koren, 1997; Srinivasan and Tsao, 1997; Suh et al, 2008):

- Servo or feed drive system control loops.
- Interpolation methods.
- Error compensation methods.

In ultraprecision machine tool control system, apart from the servo level, the emphasis is on the supervisory and process level.

2.2.3. PC-Based Control System

PC-based control system is continually employed by machine tool manufacturers to reduce cost and improve the performance of machine tools. PC-based control technology offers reliability and functionality. PC-based control system is influenced by the evolution of computer technologies (Proctor, 1998).

PC-based control system should have these characteristics (Gee, 2001):

- ***Must provide deterministic operation***- control must be treated as the highest priority and insure a predictable, repeatable response.
- ***Must survive a Windows crash***- machine control program should survive OS fault and resume normal operation.
- ***Must be isolated from poorly behaved Windows applications and drivers***- unstable applications or drivers cannot adversely affect control system.
- ***Must survive hard disk crash***- deterministic control should not be interrupted in the event of hard dish crash.
- ***Must be based on a proven real time engine***- control engine must have a proven record in mission critical applications.

2.2.4. Open Architecture Control (OAC)

The concept of Open Architecture Control (OAC) was proposed and introduced in the 1990s. There are many industrial research groups which do intensive research on OAC. These groups are:

- OSEC (Open System Environment for controller) from Japan (Fujita and Yoshida, 1996; Asato et al, 2002).
- OSACA (Open System Architecture for Controls within Automation Systems) from Europe (Lutz and Sperling, 1997; Asato et al, 2002).
- OMAC (Open Modular Architecture Controllers) from the USA (Asato et al, 2002).

These three controllers have similar fundamental architecture that include communication level, reference architecture and system configuration. The three groups mentioned above are motivated to develop new controllers for the area of industrial automation and machine tool communication and modernization. The OSACA

architecture is used mostly in the software area and whereas the OMAC and OSEC are frequently used in the industrial automation field (Asato et al, 2002).

.

With OAC, the machine tool controller should permit the integration of independent application program modules, control algorithms, sensor and computer hardware developed by various manufacturers (Pritschow et al, 1993; Wright et al, 1996; Schofield, 1996).

Apart from industrial research groups, there are also academic researches conducted on OAC. These academic research groups are:

- NGC (Next Generation Controller) sponsored by US Air Force which integrated CAD/CAM and sensor based machining (Pritschow and Lutz, 1993).
- MOSAIC (Machine Tool Open System Advanced Intelligent Controller) by University of California which operates in UNIX (Wright and Schofield, 1998; Wright and Wang, 1998).
- UMOAC (University of Michigan Open Architecture Controller) by University of Michigan which enables motion control reconfigurability (Koren, 1998).
- UBCOAC (University of British Columbia Open Architecture Controller) by University of British Columbia (Yellowley et al, 2001).

OAC is also the backbone of reconfigurable controllers which are modular, portable, customizable, reconfigurable at run-time and verifiable.

2.2.5 Common CNC Architectures

Alique and Haber have surveyed the most common commercially available CNC architectures that include (Alique and Haber, 2008):

- ***PC front-end –*** Incorporates a PC in a traditional CNC system. The PC is used to improve the interface with the operator even though all the control tasks remain rooted in the CNC.
- ***Motion control card with PC*** – Critical task (real-time functions) are carried out using digital signal processing (DSP) systems and PC regulates the non real-time tasks.

- ***Software based solution –*** All CNC functions are implemented using software running on a PC.
- ***Fully digital –*** All system components being interconnected to each other using digital interfaces where some cases involve the usage of standard fieldbus like SERCOS or CAN.

The above mentioned architecture is illustrated in Appendix II.

2.3. Ultraprecision Machine Design for Compactness

The current state of the art of machining micro components or products is using large conventional ultraprecision machines. With small complex and high quality finish products demands, the machine performance is very critical. This will of course increase the investment and operation costs and make it difficult for SME manufacturers to access the technology and thus the high value-added manufacturing business (Luo, 2003).

With parts or components size getting smaller, it is uneconomical to produce products using large conventional ultraprecision machines (Park, 2005; Hansen, 2006). Currently there are three categories of machine tools that are used to machine micro components and parts. There are:

- Conventional ultraprecision machine tools
- Microfactories
- Bench-top ultraprecision machine tools

2.3.1. Conventional Ultraprecision Machine Tools

The quality and size of the micro products depend on the properties of the machine tools which include the overall machine accuracy and dynamic performance (Park, 2005). Conventional or macro ultraprecision machine tools have several advantages including high rigidity, damping and the ability to actuate precisely using precision sensors and actuators (Takeuchi, 2000).

Conventional ultraprecision machine tools can provide very high accelerations and typical accuracy achievable is ± 1 µm (Rooks, 2004; Masuzawa, 2000; Kern, 2009).

Figure 2.5 illustrates some commercially available conventional ultraprecision machine tools and floor space requirements are compared in Table 2.1. Even though these companies provide the floor space requirements but in some cases, it has been found the floor space requirements only refer to the machine tool floor space requirements excluding the control cabinet and other auxiliary equipment. The dimensions in Table 2.1 only states the floor space required for the machine tool excluding the floor space required by other miscellaneous (control system and pneumatic) cabinets.

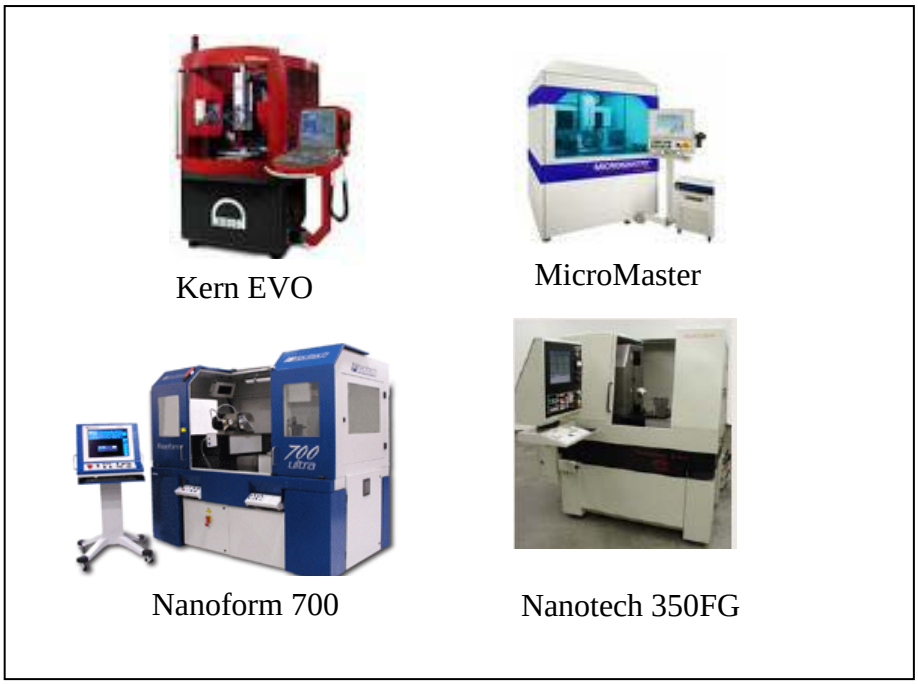

Fig. 2.5 Commercially available conventional ultraprecision machine tools

Table 2.1 Floor space requirement comparisons

Machine Model	**Floor Space Requirement** **w × d × h (m)**
Kern Evo [Kern, 2009]	2.80 × 2.50 × 2.20
Nanotech 350 FG [Nanotech, 2009]	1.93 × 1.80 × 2.00
Nanoform 700 Ultra [Precitech, 2009]	1.44 × 1.93 × 2.04
Micromaster [Kugler, 2009]	1.7 × 2.00 × 2.35

2.3.2. Microfactory

The microfactory which originated from Japan is a concept to design and develop miniaturized manufacturing systems to match the size of parts manufactured. Achieving the required precision machine tools do not need to be large (Okazaki et al, 2004). Since the parts machined are very small, research groups and companies are motivated to scale down the machine tools (Tanaka, 2001; Bang et al, 2004; Okazaki et al, 2004; Kussul et al, 2002; Kussul et al, 1996; Vogler, 2002).

The motivations behind the microfactory concept are:

- Portability with small footprint (Tanaka et al, 2001; Okazaki et al, 2004).
- Lower energy consumption (Park et al, 2005; Hansen et al., 2006).
- Space utilisation (Hansen et al, 2006; Okazaki et al, 2004).
- Increased structural loop stiffness and resonant frequency (Hansen et al, 2006).

Figure 2.6 shows examples of microfactory machine tools.

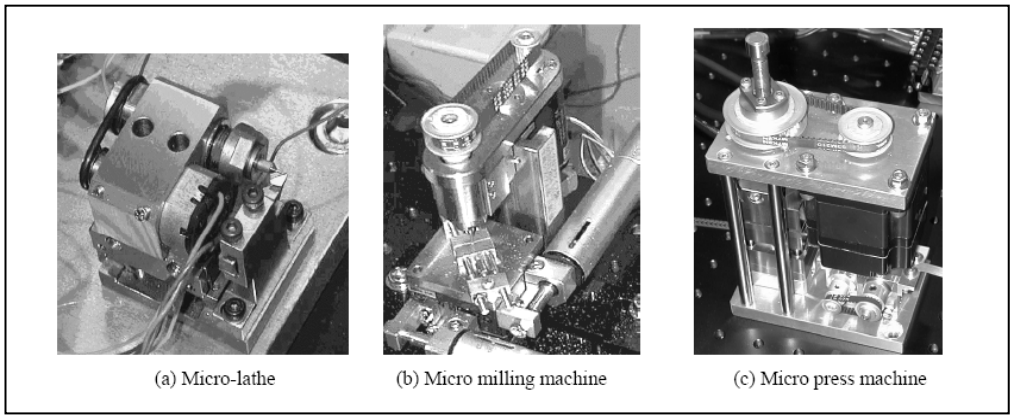

Fig. 2.6 Examples of microfactory (Okazaki et al, 2004)

2.3.3. Bench-Top Ultraprecision Machine Tools

The bench-top ultraprecision machine tool concept is relatively new. Surveying available literature through the Internet, the term bench-top ultraprecision machine tool produces many references to the 5-axis ultraprecision micromilling machine tool developed by the research group at Brunel University. This micromilling machine tool is called Ultra-Mill.

The concept of bench-top ultraprecision machine tool is a combination of the two concepts mentioned above. Comparing to the conventional ultraprecision machines,

bench-top machine tools benefit from cost saving production and operation, small space requirements, ease of localized environment control, etc. (Luo et al, 2005).

Compared to the commercially available ultraprecision machine tools mentioned in Section 2.3.1, the distinctive feature of the Ultra-Mill is the small floor space requirement (Ultra-Mill, 2009). This particular machine integrates everything into one small footprint, enabling optimum portability. Figure 2.7 shows the Ultra-Mill micromilling machine.

Fig. 2.7 5-axis benchtop micromilling machine (Ultra-Mill, 2009)

Comparing the conventional ultraprecision machine tools, microfactories and bench-top ultraprecision machine tools, the obvious difference is the size. Manufacturing micro or nano sized components on conventional ultraprecision machine tools is possible but is seen as uneconomical. Therefore from the survey, the bench-top ultraprecision machine tool is seen as a more economical method to manufacture micro or nano sized components as it possesses the precision requirements and portability characteristics.

2.4. Servo Drive Performance Requirements for Ultraprecision Machine Tools

2.4.1. Servo Drive Control

In the hierarchical levels in CNC controllers, the servo control layer is located at the lowest level as illustrated in Figure 2.2. The task of ensuring the output follows the reference signal as close as possible is performed by the servo control layer. Figure 2.8 illustrates a servo control system (Dorf and Bishop, 2001; Franklin et al, 2006).

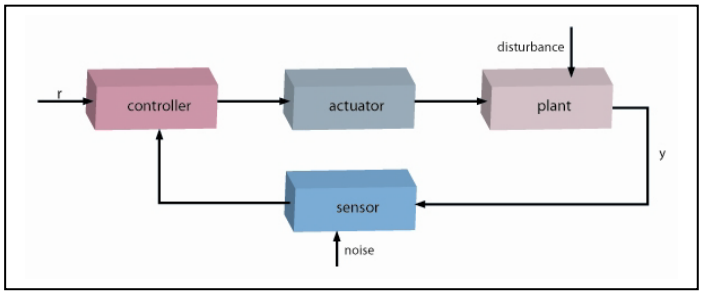

Fig. 2.8 Servo control loop (Dorf and Bishop, 2001; Franklin et al, 2006)

The general single axis control structure with an inner velocity and outer position loop in a cascaded form is illustrated in Figure 2.9. The control structure is designed so as to achieve a closed position loop bandwidth, steady state accuracy and disturbance rejections characteristics (Koren, 1997; Srinivasan and Tsao, 1997).

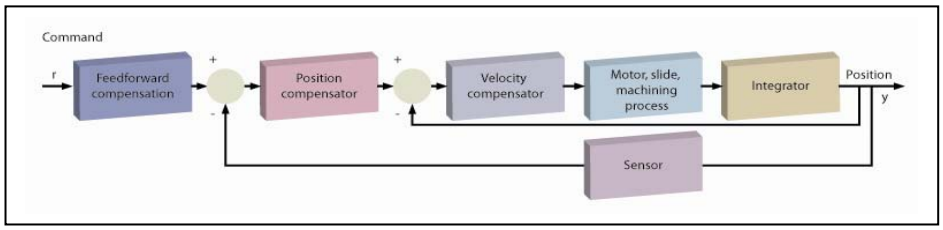

Fig. 2.9 Closed loop control structure (Koren, 1997; Srinivasan and Tsao, 1997)

In (Koren, 1997), the dynamics of machine tool axes are categorized as a second order system where well known feedback controllers can be applied, i.e. Proportional-Integral-Derivative (PID). In the PID controller, the integral part eradicates the steady state error in ramp tracking and so eliminates disturbances. The integral will cause significant overshoot. The adjustment signal of the controller is related to the proportional, integral and derivative of the position. Perturbations and model uncertainties could degrade the performance of PID controllers.

In order to improve tracking accuracy, feedforward controllers have been proposed by researchers (Koren, 1997; Srinivasan and Tsao, 1997). A feedforward controller forces the closed loop transfer function to approach unity by compensating the non-removable terms and delays in the axis dynamics. Improving overall axis performance, feedforward controllers are commonly combined with feedback controllers. The main aim of feedforward controllers is to reduce axis tracking errors.

The Zero Pole Error Tracking Controller (ZPETC) by Tomizuka (Tomizuka, 1987) was based on pole and zero cancellation. The advantage of the ZPETC is the ability to amplify closed-loop bandwidth and therefore reduces the tracking errors. A drawback of the ZPTEC is that with large disturbances the machining performance is poor.

In multi-axes machine tools, many servo control schemes have be introduced. One of the first and most famous bi-axis servo control schemes is the Cross Coupling Controller (CCC) proposed by Koren (Koren, 1980) as illustrated in Figure 2.10. The objective of the CCC is to construct a real time contour error model based on the feedback information from all axes. This is to identify an optimum compensating rule and then feed the correction back into the individual axes.

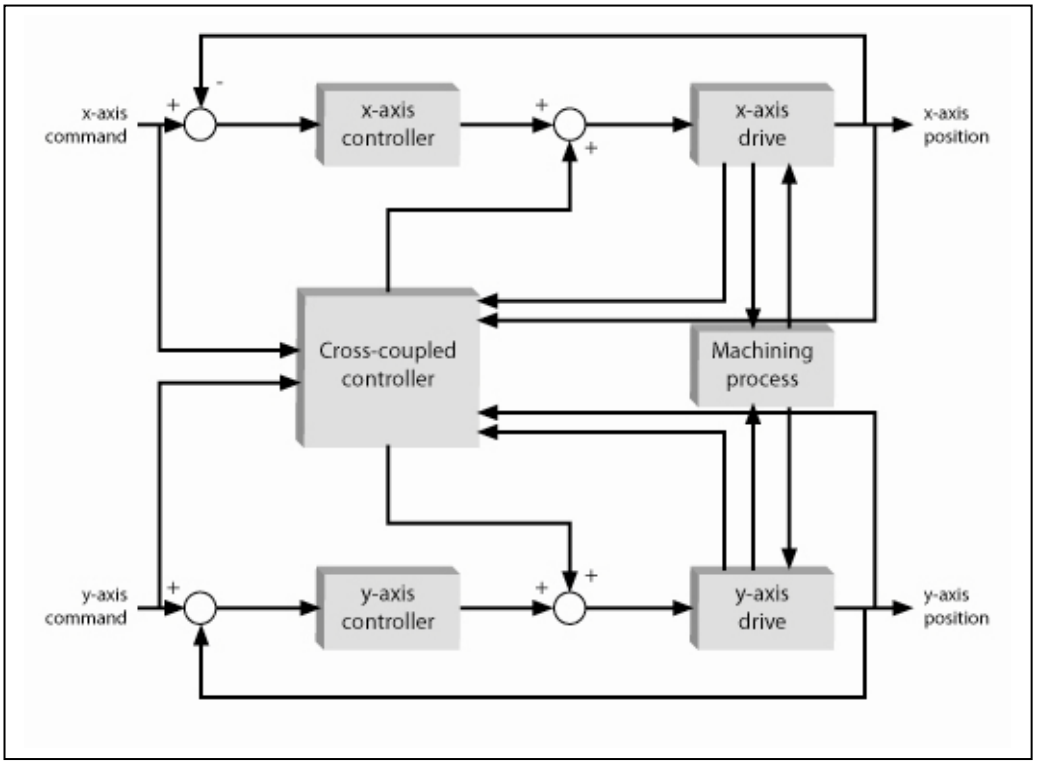

Fig. 2.10 CCC control scheme for bi-axis control

Apart from the above mentioned servo control schemes, there are many other schemes such as repetitive control (Tung et al, 1993; Koren and Lo, 1992), predictive control (Boucher et al, 1990; Boucher et al, 1993; Dumur and Boucher, 1994; Dumur et al, 1996), etc. A robust controller using quantitative feedback theory was created by Isaac Horowitz but is seldom found in servo control field (Houpis and Rasmussen, 1999). Even though there are many servo control schemes that come out of research, the most common control scheme used in industries is the PID controller (Wilson, 2004).

2.4.2. Servo Drive Performance

The servo or feed drives of the machine tool control the positioning and velocities of the axes. The positioning and velocities are calculated and generated by the CNC interpolators. Interpolators are generators of axis movement data from block data generated by the interpreter (Suh et al, 2008). The performances of feed drives include (Srinivasan and Tsao, 1997):

- Control over a wide range of speed.
- Precise control of position, desired accuracy of position control varying with application. Precision of position control during machining affects accuracy of part dimensions.
- Ability to withstand machining loads while maintaining accuracy of position control.
- Rapid response of drive system to command inputs from the machine tool CNC system.
- Precise coordination of the control of multi-axes of the machine tool in contouring operations.

Feed drive performance has benefited from the progress of drive actuation, sensing and drive control in real time. Feed drive performance is dependent on drive actuators, power electronics, power transmission devices, mechanical structures and sensors providing the feedback.

Since the introduction of direct drive feed drive systems such as linear motors, machine manufacturers have now implemented this technology as the most viable solution. Direct drive has taken the place of mechanical related transmission such as ball screw

system, belt and pulley, rack and pinion, etc. (Pritschow, 1998; Weidner et al, 1999). The benefits and advantages of direct drive systems are (Barrett et al, 2000):

- ***High speeds***- maximum speed of the linear motor is only limited by the bus voltage and the speed of the control electronics.
- ***High precision***- accuracy, resolution and repeatability of the linear motor direct drive are controlled by the feedback device.
- ***Fast response***- response rate of a linear motor driven device and its actuation can be over 100 times that of a mechanical transmission.
- ***Stiffness***- no mechanical linkage has increased the stiffness of the drive system.
- ***Zero backlash***- without mechanical transmission components and thus there is no backlash.
- ***Maintenance free***- being free of mechanical transmission, moving parts have no contact and thus no friction and wear.

Direct drive feed system is subjected to external disturbances during motion and machining. Lack of transmission element, the drive system is easily affected by friction, force ripple and machining or cutting force (Van Den Braembusshe et al, 1996; Srinivasan and Tsao, 1997). The performance of feed drive system is also affected by the type of bearings used in the drive systems (Slocum, 1992).

Compared to mechanical transmission drives, direct drive systems are vulnerable to external disturbances, these drive systems must be able to supply added disturbance rejections. To offer disturbance rejection, steps must be taken to budget the disturbance and then cancelling it (Ohnishi et al, 1996). Disturbance rejection methods have been reviewed exhaustively by Radke and Gao (Radke and Goa, 2006).

2.5. Microhandling in Micromilling Processes

Handling systems are widely employed in manufacturing systems. These are required in pick-and-place systems for loading and unloading of tools, workpieces, and components. The implementation of handling systems using robot systems are categorized widely for the flexible manufacturing system (FMS) realm (Rooks, 2003).

The term “machine tool tending” refers to the use of robot systems together with CNC machine tools (Rooks, 2003; Gardh, 2006). For machine tool tending in general, the size of the robot systems are big and the CNC machine tools involved are big as well.

At the moment, there has not been found any literatures that involves a robot system and a benchtop micro machine tool. Maekawa (Maekawa et al, 2001) has developed a micro transfer arm for a microfactory. The micro transfer arm satisfied these requirements (Maekawa et al, 2001):

- The arm is compact and compatible with the size of the microfactory.
- The arm has a large envelope to enable transfer.
- The arm has high mechanical stiffness to permit precise positioning.
- The arm must only access the workpiece from the top.
- The arm equipped with passive compliance and force sensor is capable of absorbing positional errors of the workpiece and detecting contact force.

The microhandling systems must be able to allow coarse and fine motion and positioning (Bleuler et al, 2000; Maekawa et al, 2001). The gripping force must be adaptable to suite the necessary workpiece or tool to avoid geometrical changes or surface damage.

From (Gardh, 2006, Maekawa et al, 2001), implementation of robot systems as handling systems at the moment is confined in two categories: production lines where large CNC machine tools are used and the microfactories.

2.6. Tool Condition Monitoring (TCM) in Micromilling

2.6.1. Tool Condition Monitoring in Macromachining

It is well known that the cutting force is correlated to tool wear (Lister, 1993; Dimla, 1999; Ko et al, 1994; Purushotthaman et al, 1994; Dornfeld, 1990). Tool wear contributes to diminished surface quality. There are many tool condition monitoring systems in the macromachining realm which has been explained by Dimla (Dimla, 2000):

- Acoustic emission (AE)

- Tool temperature.
- Cutting forces.
- Vibration signature.
- Other miscellaneous methods include ultrasonic and optical measurements, workpiece surface finish quality, workpiece dimensions, stress/strain analysis and spindle motor current.

The key element for a successful tool or process monitoring system is the sensor and the feedback signals (Jemielniak, 1995).

2.6.2. Tool Condition Monitoring in Micromachining

According to Tansel et al. (Tansel, et al. 1998), there are three types of breakage that occur in micromachning:

- Chip clogging when chips are not removed rapidly.
- Breakages resulting from tool wear.
- Excessive stress leading to breakage due to tool deflection.

In the micromachining realm, the tool condition monitoring systems have to be more accurate and operate at a higher bandwidth compared to those used in the macromachining realm (Malekian, et al. 2009).

Even though machining at the micro scale, some of the tool condition monitoring systems for macromachining could still be used. Acoustic emission Dornfeld et al, 2006), monitoring of cutting forces, vibration signature and motor current are systems which are also used in micromachining (Gandarias et al, 2005).

In micromilling, the cutting tools used are in the range between 0.1 to 0.5 mm in diameter. With tooling of this size in a misty machining surrounding, it is impossible for operators to visually detect breakage of cutters (Gandarias et al, 2005).

Some of the reasons as to, why tool condition monitoring systems are not fully accepted by industries are the installation position of the sensors and the working environment on the shop floor (Oliveira et al, 2008; O'Donnell et al, 2001; Lister, 1993). As an

example, the position of the sensor must be as close as possible to the tool in micromilling while the sensor must not be interfering with the machining process.

Recent reports have presented new methods in condition monitoring using the wireless method (Wang et al, 2006; Wright et al, 2008).

At the moment, there is no standard tool condition monitoring method available for industrial implementation. Different methods are still being experimented by various research groups.

2.6.3. Sensor Fusion

As mentioned earlier in by Jemielniak (Jemielniak, 1995), the key element for a successful tool or process monitoring system is the sensor. Sensor fusion is the implementation of many different types of sensors to increase confidence in tool or process monitoring (Dimla, 2000; Schofield, 1993).

Malekian (Malekian, 2009) experimented on tool wear monitoring in micromillimg operations. In his report, various types of sensors (dynamometer and AE sensors) were used to help detect tool wear. The best result according to Malekian was obtained from using both a dynamometer and AE sensors.

The decision as to which sensor or number of sensors to implement for tool condition monitoring system is not easy. One consideration is the cost of successfully tapping any chosen sensor signal. Another issue is the ease of obtaining the signal. When these two issues have straight forward solutions, choosing the best sensor will be easier. Care and consideration must be taken so that the sensor does not intervene with the machining process and at the same time keeping the monitoring cost down (Dimla, 2000).

2.7. Summary

This chapter has presented a review on the previous studies in the objective areas. This chapter has highlighted the state of the art of the technology involved in the development of machine tools from the past to present.

The literature survey has provided the understanding relating to the trends in micro and nano manufacturing system and process requirements. This includes the technological and scientific know-how that influences the requirements and engineering specifications to design and develop an ultraprecision mechatronics system.

The previous work presented are adapted and improved to produce a novel concept for the control system design and develop a functional prototype bench-top typed 5-axis micromilling machine. The realization of the research elements are carried out from hardware design and construction, software programming applications, algorithms manipulations and experimental results, analysis and discussions and are the subject matters of the chapters to follow in this thesis.

Chapter 3

Architecture of the 5-Axis Ultraprecision Micromilling Machine

3.1. Introduction

The configuration of the 5-axis ultraprecision micromilling machine named Ultra-Mill which was designed and constructed at Brunel University for a research project as illustrated in Figure 3.1.

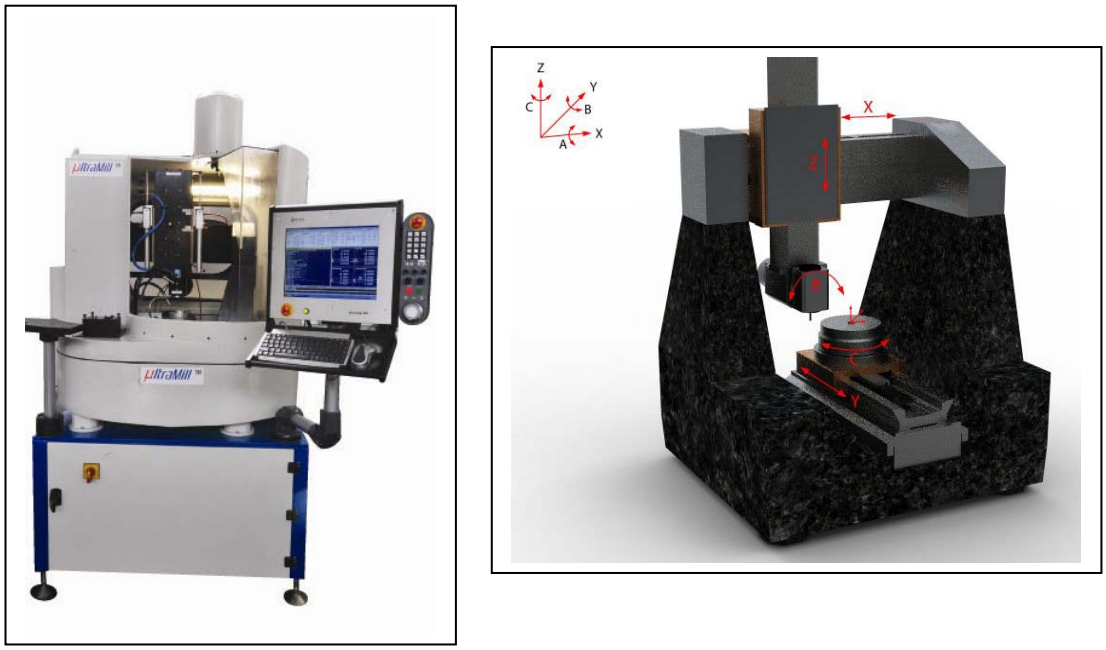

Fig. 3.1 5-axis micromilling machine (Ultra-Mill)

The machine was built in conjunction with the EU MASMICRO (Mass-Manufacture of Miniature/Micro Products) project. The main aim of the project is designing and constructing a 5-axis ultraprecision micromilling machine with the emphasis of finding a solution for manufacturing of micro and miniature components or products with higher surface quality and dimensional/form accuracy with high repeatability rate. Even though the main machining application for Ultra-Mill is the micromilling process, Ultra-Mill also has the abilities to provide micro-drilling, micro-grinding and micro-CMM processes. The machining envelope of Ultra-Mill is 150 mm x 150 mm x 80 mm and the overall floor space requirement is 1.1 m x 0.8 m x 2.1 m.

In the design stage, several possible 5-axis machine configurations were designed as illustrated in Figure 3.2 and analyzed to identify the best machine configuration for the purpose mentioned above and the feasibility in assembling the machine in terms of mechanical and electrical subsystems. As mentioned in Maj et al (2006), machine tool technology is a multi-discipline field which combined elements of mechanical and electronics engineering, in other words mechatronics engineering.

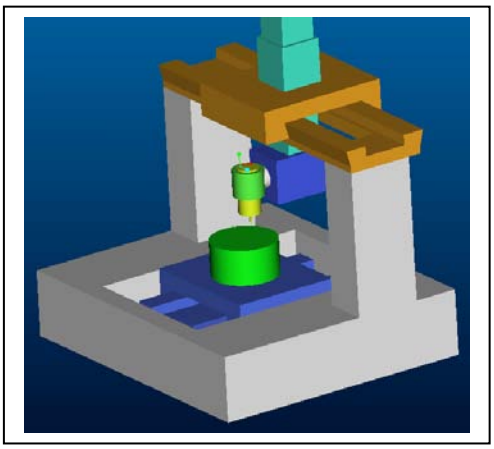

(a) Design 1

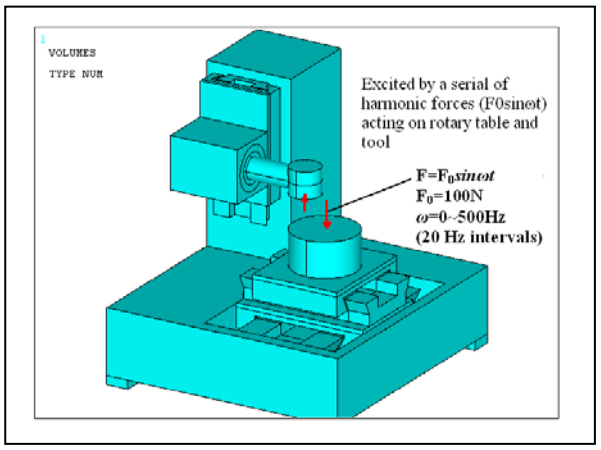

(b) Design 2

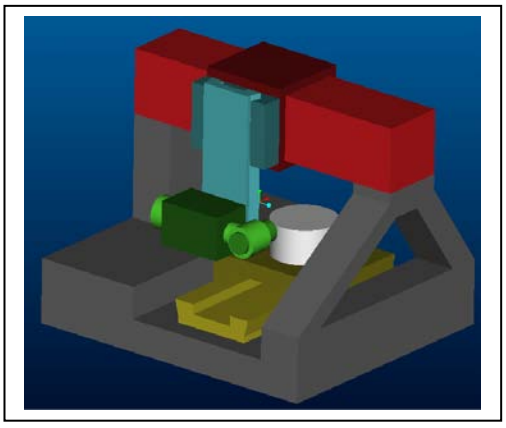

(c) Design 3

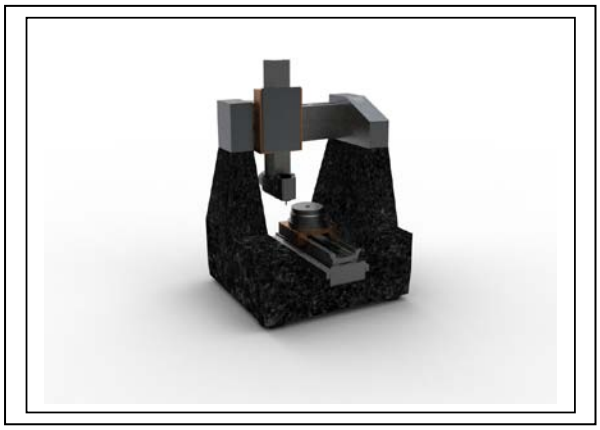

(d) Final design

Fig. 3.2 Conceptual and final designs of Ultra-Mill configuration

3.2. Mechanical Structure

In this section, the mechanical elements of the Ultra-Mill are briefly described. The machine base which all the axes are mounted on is made of granite. The granite structure has good wear resistance, high-stiffness and high thermal stability with good damping characteristics. These enable granite to become the common choice for

machine base for the ultraprecision machine tool industries (Luo et al, 2005). Figure 3.3 illustrates an exploded view of the Ultra-Mill.

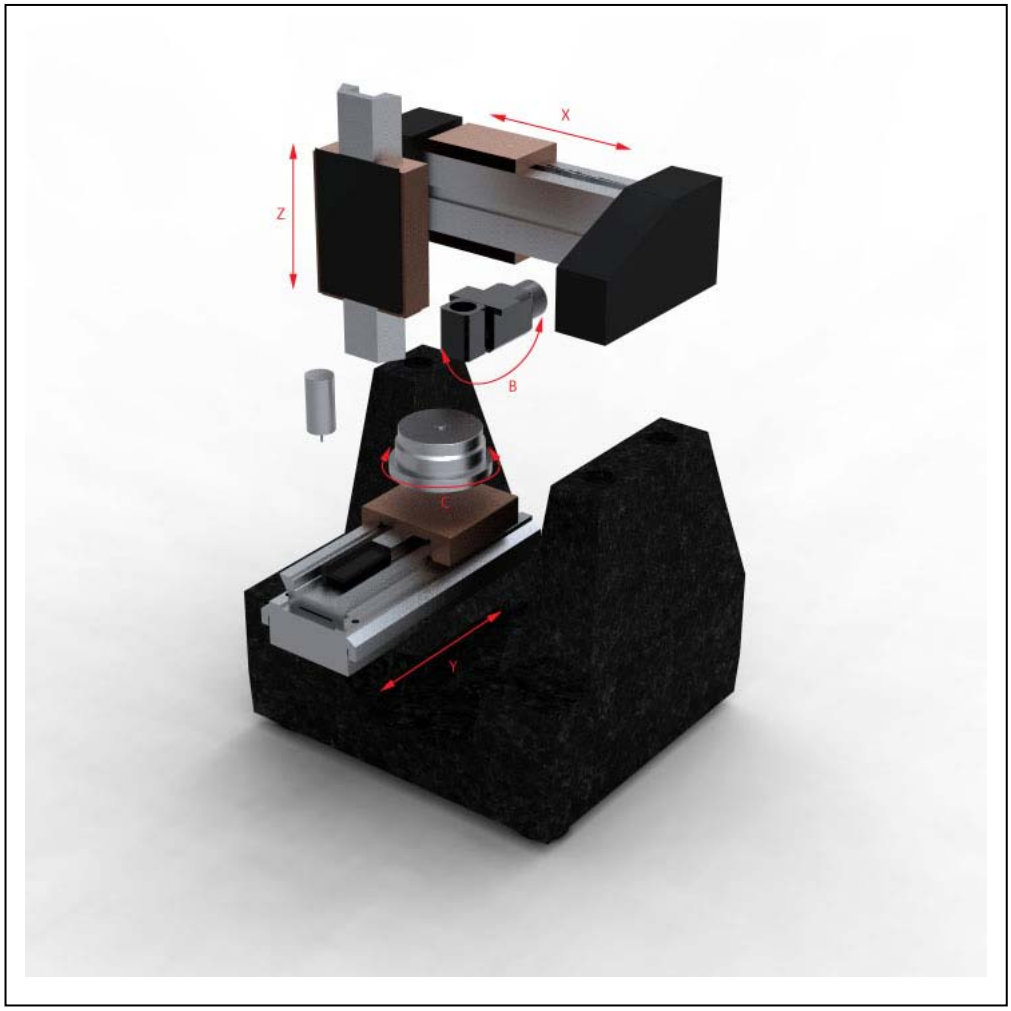

Fig. 3.3 Exploded view of the Ultra-Mill.

Luo also stated the machine design considerations include structural configuration, stiffness and damping, structural connectivity and interface and associated structural dynamics performance.

Cast iron is used for the linear axes (slideways), rotary axes and spindle. The overall machine performance depends on the material selection. As an example, it is common nowadays to employ polymer concretes for machine tool mechanical structure. The advantages of polymer concretes are that the machine tools would be light weight with high damping capacity and rigidity.

The dynamic of a system is embodied in its mechanical resonances. These phenomena are excited during motion which in turn could reduce the control system stability margin. The mechanical vibration and resonance have influence on the positioning and tracking accuracy.

For ultraprecision machine tools, the mechanical structure should have very low thermal expansion coefficient. Other than granite, super-invar, synthetic granite and Zerodur are types of materials which are commonly used for ultraprecision machine tool mechanical structure.

3.3. Drives and Actuation

In micromanufacturing, the ultraprecision machine tool axes must be friction free, without stick-slip, no backlash, smooth, easy maintenance and high acceleration capabilities to provide high accuracy motion and positioning at high or low machining speeds.

In all latest ultraprecision machine tools, direct drive systems are implemented. The usage of drive system which converts rotational movement into linear movement is not popular now. With direct drive systems, there is no more mechanical transmission which results in wear. Faster and accurate motion will be achieved using direct drive systems.

The bearings of the drives are equally important. Before, contact bearings such as roller bearings were widely implemented in machine tools. Roller bearings are no longer seen as suitable at high cutting speeds. Even oil lubricated bearings could not cope in high speed machining as there would be too much heat generated. Axes with air bearings are the best solution and becoming the norm in the latest commercial ultraprecision machine tools.

A new technique in air-bearings design is called the groove technique (Luo et al, 2005). This design merges aerostatic and aerodynamic design principles for ultra-high speed performance optimization. By feeding pressurized air through the orifice restrictors, aerostatic lift is generated (Stanev et al, 2004).

3.3.1. Linear Axes

As illustrated in Figure 3.3, the Y-axis slideway carries the rotary table (C-axis) and the X and Z axis slideways carry another rotary axis (B-axis) which houses the high speed spindle. The linear axes (X, Y, and Z) of the micromilling machine are equipped with aerostatic bearings fitted with squeeze film dampers to improve damping and eliminate friction and wear. Magnetic tracks are inserted to increase damping.

These linear axes or slideways manufactured by Loadpoint Bearings Limited are driven by three phase DC brushless linear motors. Optical linear encoders by Renishaw were used as feedback for the all linear axes with a resolution of 20 µm before digital interpolation and 5 nm after digital interpolation to provide motion accuracy of less than 1 µm over the total length of travel. Table 3.1 describes the linear axes specifications in more detail.

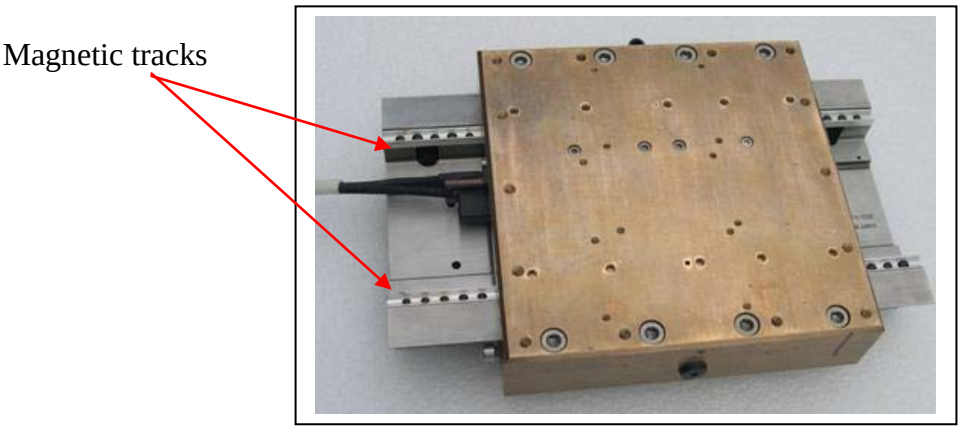

Fig. 3.4 Brushless DC linear motor driven aerostatic slideway

3.3.2. Rotary Axes

Ultra-Mill, as shown in Figure 3.5, has two rotary axes where the B-axis is the spindle swivelling axis and the C-axis is the workpiece rotary table. The B-axis is equipped with precision ball bearings. The workpiece rotary table (C-axis) is equipped with aerostatic bearings fitted with squeeze film dampers. Only the B-axis of the Ultra-Mill does not use aerostatic bearings.

The rotary axes or tables are manufactured from cast iron. Both the B and C axes are driven by three phase DC brushless torque motors and equipped with 0.02 arcsec resolution optical rotary encoders by Renishaw as feedback. Table 3.1 describes the rotary axes specifications in more detail.

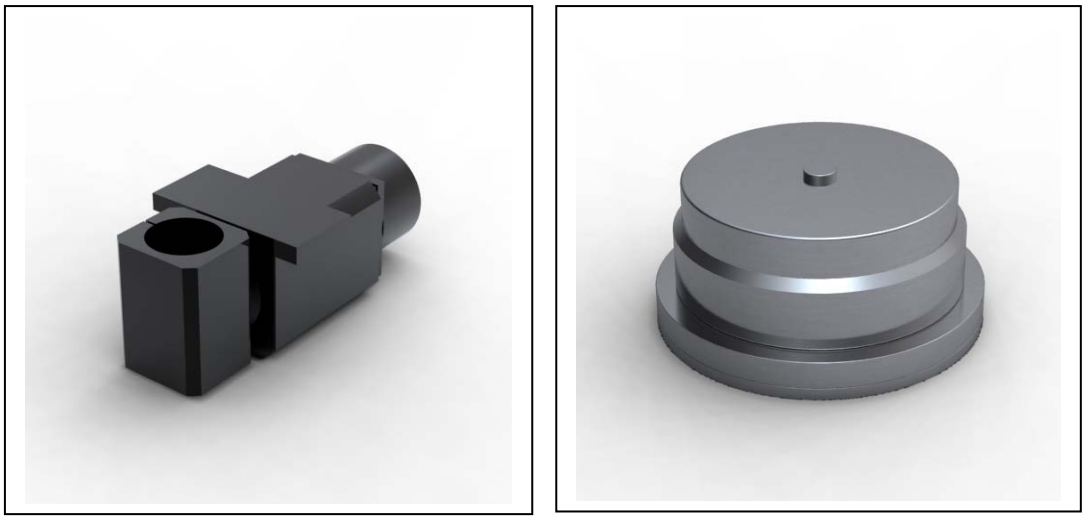

(a) B-axis (b) C-axis

Fig. 3.5 Rotary axes of Ultra-Mill

3.4. High-Speed Spindle

The micromilling machine is fitted with a high speed spindle supported on aerostatic bearings capable of achieving a maximum speed of 250,000 rpm. The spindle stiffness is 4 N/µm in the radial direction and 3 N/µm in the axial direction.

The high speed spindle is driven by a brushless DC motor. In the air bearing mechanisms, to improve the stability at high speeds, journal herringbone grooves were machined. This was manufactured by Loadpoint Bearings.

The high speed spindle does not have a feedback system. A chiller is needed to cool the high speed spindle when running. This is to avoid unwanted thermal expansion that would lead to eccentricity of the tool due to expansion of the spindle shaft. Table 3.1 describes the high speed spindle specifications in more detail.

Fig. 3.6 Brushless DC motor driven aerostatic high-speed spindle

Table 3.1 Ultra-Mill specifications

Linear Axes	**X**	**Y**	**Z**
Type	Air bearing slides fitted with squeeze film dampers		
Stroke	230 mm	225 mm	160 mm
Feedrate	0-3000 mm/min	0-3000 mm/min	0-3000 mm/min
Drive System	DC brushless linear motor	DC brushless linear motor	DC brushless linear motor
Feedback	Optical linear encoder	Optical linear encoder	Optical linear encoder
Resolution	5 nm	5 nm	5 nm
Motion Accuracy	<1.0 μm over total travel	<1.0 μm over total travel	<1.0 μm over total travel
Rotational Axes	**B (Spindle Swivelling)**		**C (Workpiece Rotary Table)**
Type	Precision ball bearing		Air bearing fitted with squeeze film dampers
Stroke	± 90°		360°
Rotational Speed	0-30 rpm		0-100 rpm
Drive System	DC brushless torque motor		DC brushless torque motor
Feedback	Optical rotary encoder		Optical rotary encoder
Resolution	0.026 arcsec		0.02 arcsec
Motion Accuracy	<1.0 μm over 180° in axial and radial direction		<0.1 μm in axial and radial direction
Machining Spindle	**Performance**		
Type	Water cooled aerostatic bearing		
Stiffness	Radial: 4N/μm; Axial: 3N/μm		
Maximum Speed	200,000 rpm		
Load Capacity	Radial: 55N at spindle nose; Axial: 45N		
Drive System	DC brushless motor		
Power	400 Watts at 200,000 rpm		
Motion Accuracy	<1.0 μm axial TIR and <2.0 μm radial TIR		
Tool Clamping	3 mm collet, manual or automatic (optional)		

3.5. Control System

In this section, the electrical subsystems of the micromilling machine will be discussed. The electrical subsystems include the controller, amplifiers, motors and sensors. Figure 3.7 illustrates the architecture of the servo loop of the micromilling machine.

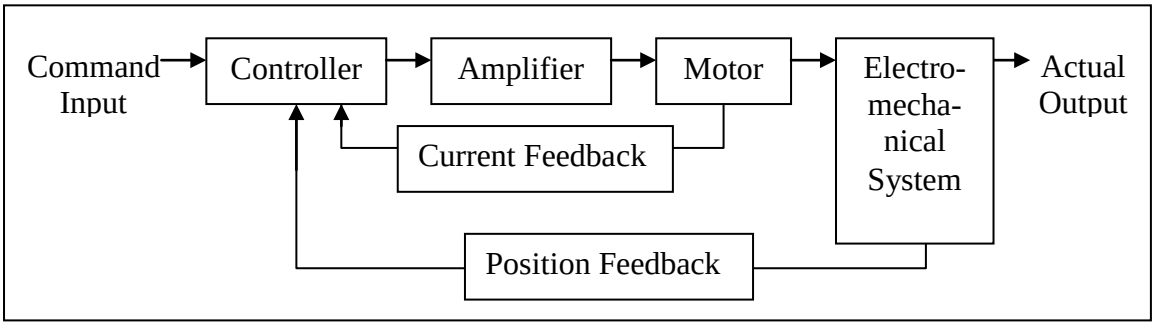

Fig.3.7 Servo loop architecture

3.5.1. Controller

The Universal Motion and Automation Controller (UMAC) by Delta Tau Data Systems Inc. is an open architecture controller (OAC) and is used as the machine control unit (MCU) of the micromilling machine. Currently, the controller has employed the most basic main processor which is the 80MHz DSP56303 CPU. Other processor speeds are available in (Delta Tau 2008f) and the selection of processor speed is dependent on the application to be driven.

The UMAC controller does all the interpretation, interpolation, servo loop computation, position control, etc. The controller could also be called Numerical Control unit. The UMAC has interfaces for amplifiers (drives) and feedback from encoders and would make the system a closed loop system. There are input and output (I/O) interfaces on the controller which are used to drive or obtain signal feedback for auxiliary equipment or functions which are controlled by PLC programs. In the controller, lie the servo algorithms (PID plus feedforward).

3.5.2. Amplifier

The Ultra-Mill employs pulse width modulation (PWM) amplifiers for all the linear and rotary axes. The PWM amplifiers are products from Delta Tau Data Systems Inc. Each amplifier has two channels, which makes it possible to drive two motors with one amplifier. PWM amplifiers are used instead of linear amplifier due to the fact that linear amplifiers consume more power and PWM amplifiers are able to meet the motors performance requirements.

The high speed spindle is driven by an amplifier supplied from Kavo. This amplifier is also a PWM typed amplifier. This amplifier is able to drive the spindle up to a maximum speed of 250,000 rpm.

3.5.3. Motor

All the motors (direct drive systems) used in the micromilling machine are DC brushless motors. The linear motors are from Anorad and the rotary motors are from Micromech. The high speed spindle is also equipped with a DC brushless motor.

3.5.4. Sensor

The feedbacks used for all axes apart from the high speed spindle are optical glass encoders by Renishaw. The feedbacks are connected directly to the controller unit. All optical encoders have 20 µm resolution. After digital interpolation by the controller, the resolution is 5 nm.

The Ultra-Mill is equipped with several sensors such as:

- ***Pressure switch sensor***- to monitor the pneumatic supply.
- ***Proximity sensor***- to monitor open/close machine guard status.
- ***Non-contact tool monitoring system***- to measure tool height, diameter and breakage.
- ***Position switches***- to detect axes position (positive or negative end limits, home position).

3.6. CNC Control and Software Subsystem

There are several programs and software packages used to set up and drive the micromilling machine. The programs that were used to set up the machine configuration are from Delta Tau Data Systems Inc. Listed below are the programs that were used to set up the micromilling machine:-

- ***Turbo Set Up***- Program to set up electrical drives parameters and feedback registers.
- ***Pewin Pro*** (Delta Tau 2008a) - Monitoring motor status online. Parameters or variables could be adjusted in this program. Motion and PLC programs are written within this environment.

- ***PMAC Tuning Pro*** (Delta Tau 2008e) - This program is used to tune the servo and current loop of each axis. Tuning of the PID plus feedforward can be done with the aid of step and sinusoidal moves.
- ***PMAC Plot*** (Delta Tau 2008d) - The program is capable of recording or gathering motor current, command or actual position of motors, etc. data for monitoring and analyzing purposes.
- ***PMAC HMI*** (Delta Tau 2008b) - A Visual Basic based package to enable the customization of the Human Machine Interface (HMI). This package enables the programmer to add extra or remove existing features.
- ***NC Pro Runtime*** (Delta Tau 2008c) - a Visual Basic based interface which displays the information such as part number, distance to go, current position, etc. to the machine operator.

Apart from these programs from Delta Tau Data Systems, a Computer Aided Manufacturing (CAM) package has been added and integrated as part of the Ultra-Mill. The CAM package is PowerMill 8 by Delcam. This CAM package has the ability to generate machine codes (G-codes) for simultaneous 5-axis machining.

Prior to the decision of opting for PowerMill, CAM packages such as DepoCam and Cimatron were researched and evaluated to determine the suitability for all the machining processes the Ultra-Mill is capable of. Decisions were made by evaluating the advantages and disadvantages of each CAM package.

The selection of the CAM software was based on:

- ***User interface –*** ease to navigate, obtaining critical information, integration of user interface into third party program, etc.
- ***CAD flexibility*** – ability to read most common CAD data files (iges, sat, etc.)
- ***CAM functionality*** – cutting strategies optimization, feeds and speeds scheduling, collision detection capabilities, etc.
- ***NC program generation*** – types of post-processor, types of NC program to suite machine tool controller, easy NC program editing, etc.

3.7. In-Process Inspection and Monitoring System

Enhancing the functionality, reliability, sensitivity and accuracy of ultraprecision machine tools for micromanufacturing require high bandwidth sensors and fast signal processing capabilities. This category falls in the intelligent and smart machine tools where the goal is to minimize human interventions.

In micromanufacturing, the machining processes involve machining of small parts or features using small diameter tools. With these, the energy emission during tool and workpiece engagement or the cutting forces involved are very minute compared to macromachining. As an example, operators are not able to determine if the micro-tool used is already broken due to the size of the tool and various machining condition. Therefore, it is required that the existence of the tool is determined by measuring system.

Combination of various types of sensors is the key for in-process inspection and monitoring of machining and machine tool condition. The execution of the in-process inspection and monitoring system program are done using Programmable Logic Control (PLC) method.

3.8. Summary

In this chapter, the key components and supporting technologies of the micromilling machine tool have been discussed and elaborated. The characteristics of each subsystem were fully explored, analyzed and experimented individually before integration.

Key technological characteristics of each subsystem have been discussed in this chapter.

Chapter 4

Control System Design for the 5-Axis Ultraprecision Micromilling Machine

4.1. Introduction

Manufacturing of high precision components or parts with sizes varying between a few hundred microns to a few millimetres or surface features in submicron and nanometre level are increasingly in demands for various industries, such as aerospace, biotechnology, optics, etc. The demands for ultraprecision machines have increased due the demands to meet the accuracy, surface finish and geometrical complexity of components and parts. Typical manufacturing requirements are high dimensional accuracy being better than 1 micron, flatness and roundness better than 50 nm and surface finish ranging between 10 and 50 nm. Manufacture of high precision components and parts requires very intricate material removal procedure.

There are five main elements, namely machine tool, cutting tool, material properties and operating conditions and environmental conditions, which are conducive to good quality components and parts. The attributes of the five mentioned elements are illustrated in Figure 4.1. End users evaluate the performance of a machine tool based on the dimensional accuracy and surface quality of machined parts including the machining time.

The control of multi-axis precision systems with high-speed and high-accuracy motions and positioning are desirable to manufacture products with high accuracy, complex features, increase productivity, maintain machine stability, etc. The evolution of nanoscale technology manufacturing has raised the requirements for fast, accurate and robust positioning at the machine system design stage. Apart from the mechanical design, the performance of the entire precision systems is much dependent on various electrical and electronics subsystems, controllers, drive instruments, feedback devices, inspection and monitoring system and software. On the other hand, understanding the machining processes is a necessity. There are some variables that dynamically alter the system behaviour and sensitivity to disturbance that could be ignorable in conventional

machines or machining processes but will be disastrous in micro and nano machining, which then is directly reflected on the components.

This chapter emphasizes in the designing and development of the control systems for an ultraprecision machine tool, Ultra-Mill. In the design stage, the ultraprecision machine performance specifications are arranged in the precedence order. The issues that are highlighted in the design stage are motion accuracy, dynamic stiffness and thermal robustness. As shown in Figure 4.1, the mechanical and electronics elements constitute to the overall achievable machine performance.

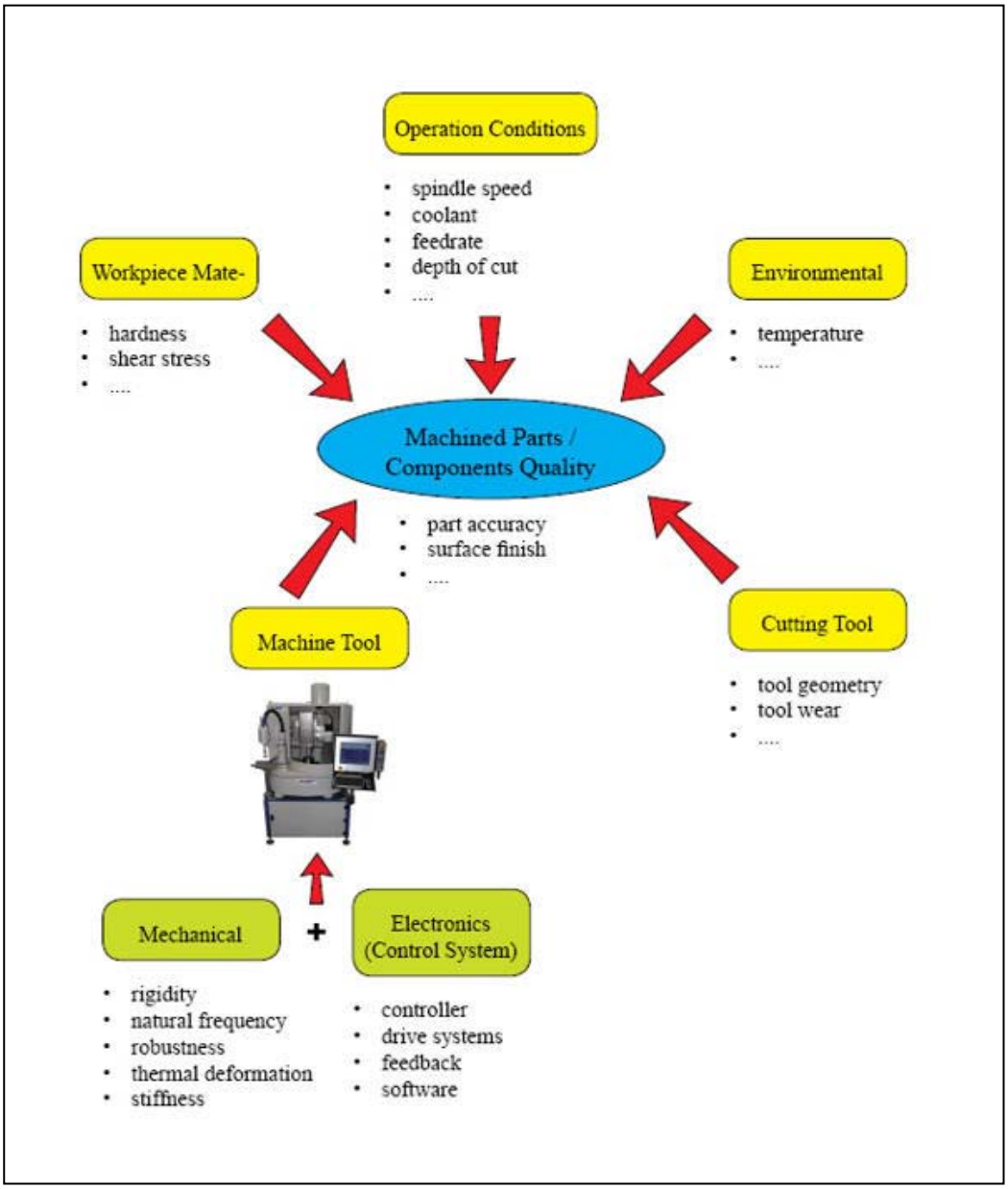

Fig. 4.1 Machined parts qualities factors

Having this in mind, the design and construction of the Ultra-Mill involves complex and complicated design know-how for a mechatronics system. Mechatronics is a multidisciplinary engineering field which integrates electrical, control, software and mechanical elements. Machine specialization during the design stage helps to reduce the risk of misimplementation of technologies which in turn could be expensive. In this thesis, the main topic is the control system design and development for the Ultra-Mill. The mechanical design may be touched on slightly but will not be elaborated in depth as this is not the main aim. In the Ultra-Mill, the vital subsystems are the mechanical structure, spindle, drive and actuation, controller, feedback, monitoring and inspection systems and software.

From the mechatronics point of view, the control system comprises of controllers, drives and actuators, sensors and software. In an ultraprecision machine tool control system structure, there are a number of controlled subsystems. These are the motion control, process control and control of other auxiliary functions. Motion control concentrates in moving the mechanical element, process control observes the real time condition and auxiliary functions enhance the overall machine functionality. Figure 4.2 illustrates the ultraprecision machine tool mechatronics design constitutions.

The control system must provide the three elements, motion accuracy, dynamic stiffness and thermal robustness, of the Ultra-Mill so as to have high stiffness, low thermal distortion and low motion errors. Since this chapter will concentrate on the control system design of the Ultra-Mill, the next few subtopics will be focusing in the controller dynamics, drive and actuation dynamics, feedback dynamics and software dynamics.

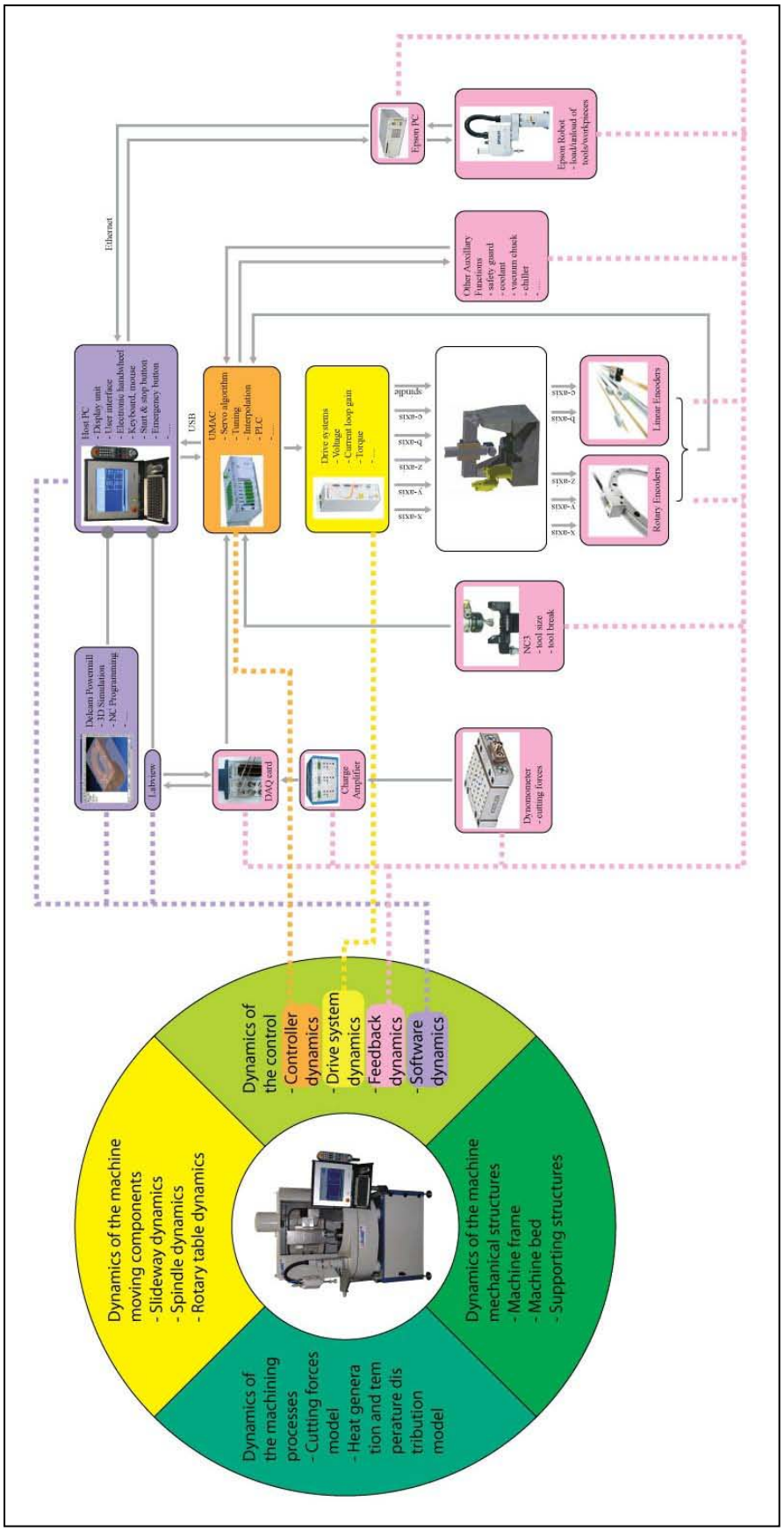

Fig. 4.2 Ultraprecision machine tool design constitutions

4.2. Control System Requirements and Characteristics

As mentioned in Section 4.1, the control susbsystems consist of the controller, drive and actuation system, feedback, monitoring and inspection systems and software. These subsystems could be classified as machine level and monitoring level. These subsystems determined the speed, accuracy, etc. of the machine tool, monitors the changes in machine tool for anomalies and responsible in rectifying any problems raised. An ultraprecision machine tool must be able to quickly fault detect, fault determinate and fault correct.

After conducting a survey, it has been decided that Ultra-Mill will be implementing PC-based control system with open architecture as this architecture is dimensionally open ended. PC-based control system provides the freedom and expansion based on the flexibility it offers. Aside from that, the architecture is able to provide flexibility, precision, computational power, customization and is cost effective. This is also contributed to the fact that this is a research project and potential future modifications of the Ultra-Mill are possible. The control system dynamics for Ultra-Mill is illustrated in Figure 4.3.

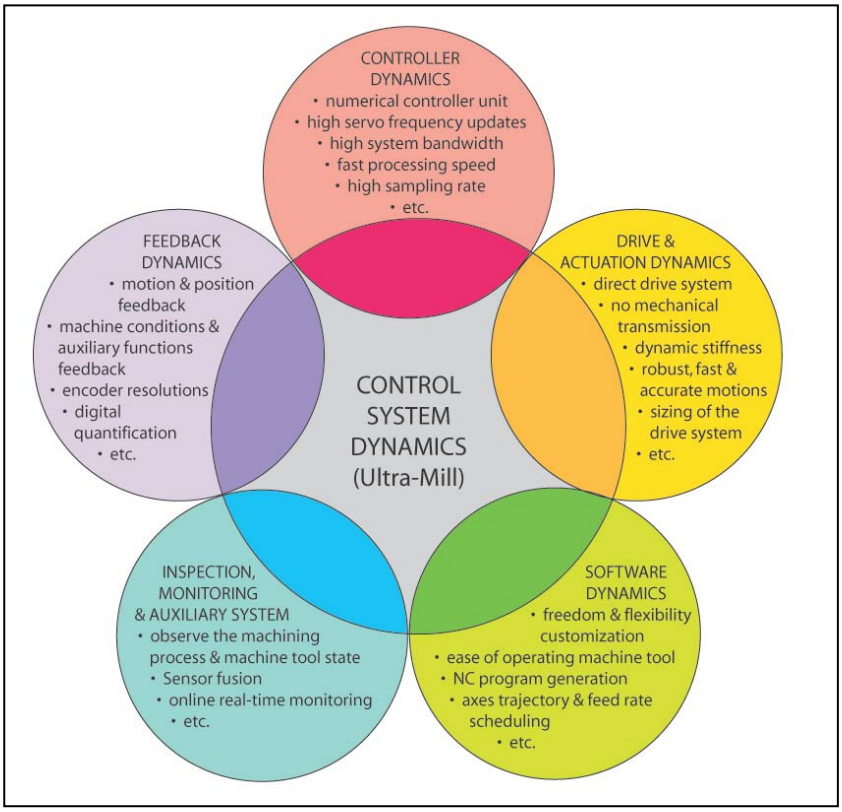

Fig. 4.3 Control system dynamics for Ultra-Mill

Combination of PC-based control with the latest measuring and operational system has led to a rise in both user time and precision, with the resulting decrease in down time and repairs and an increase in both quality and quantity of parts produced per measured unit of time (Alique and Haber 2008).

In the next sections, the dynamics or characteristics elaboration of each control subsystem will be discussed. Figure 4.4 shows the control system architecture of the Ultra-Mill.

Figure 4.6 illustrates the machining process framework and the location of the control system is highlighted in blue within that framework.

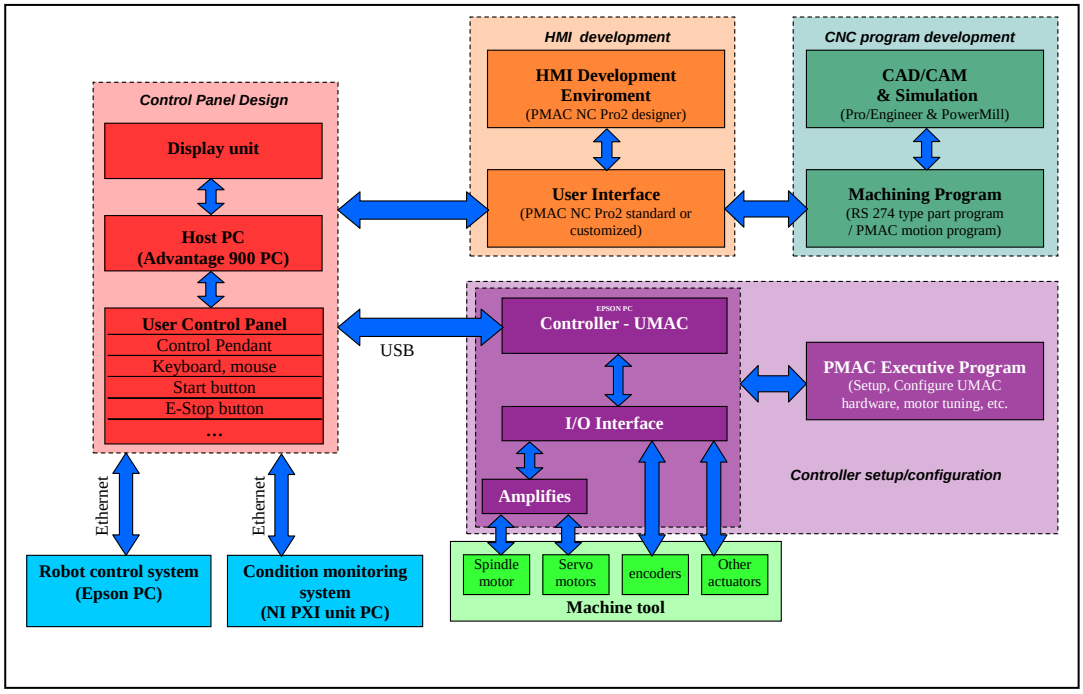

Fig. 4.4 Control system architecture of Ultra-Mill

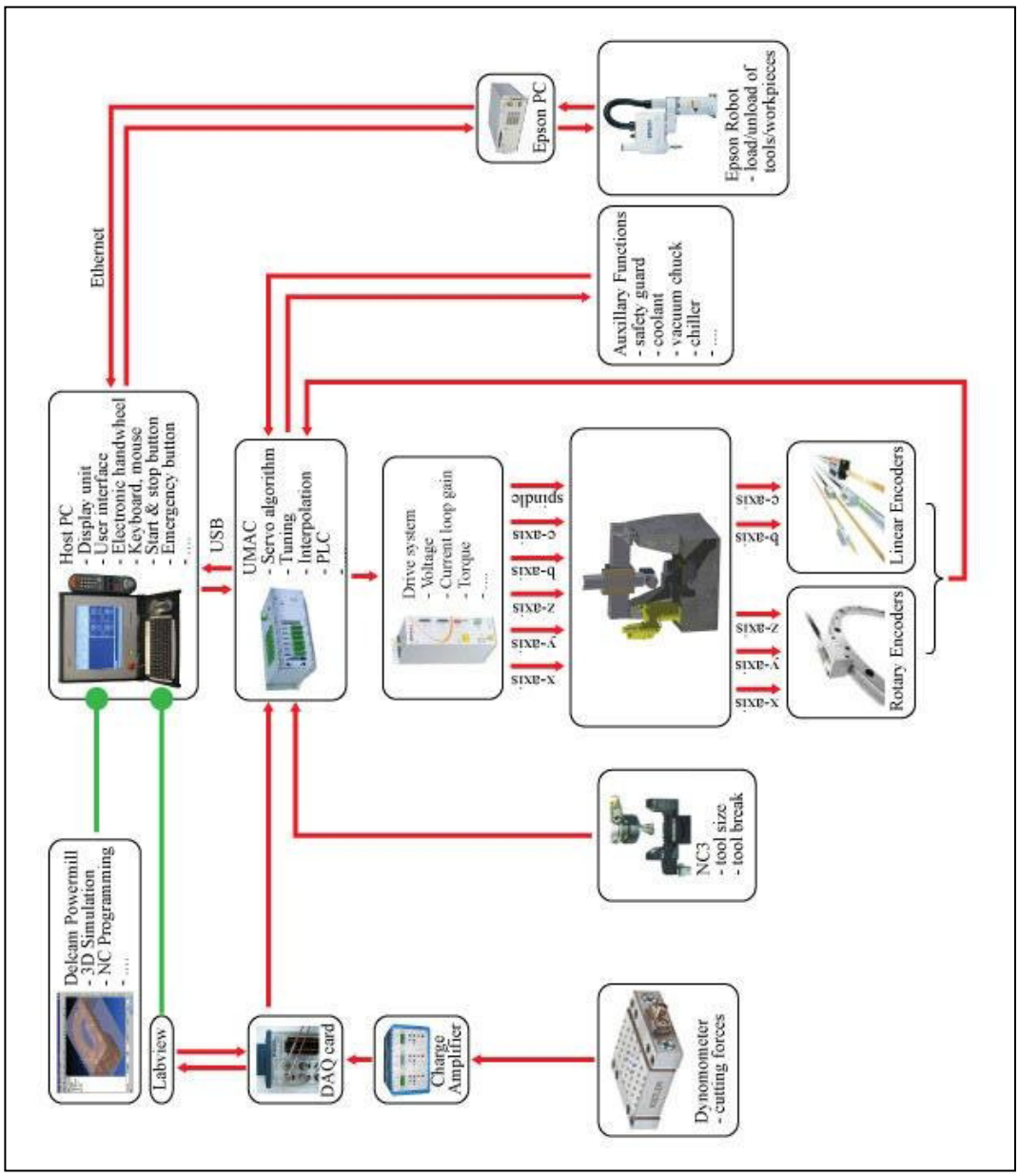

Fig. 4.5 Control system architecture with attributes

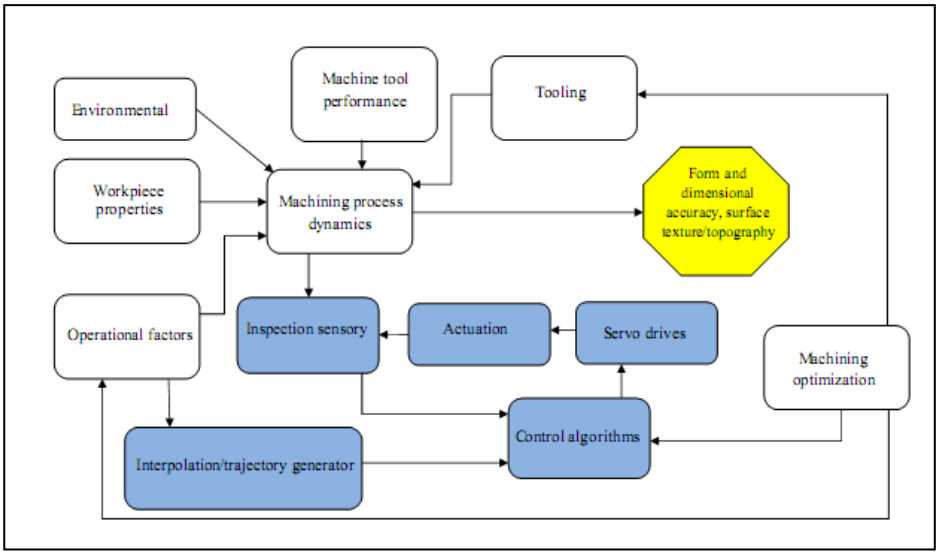

Fig. 4.6 Machining process framework

4.2.1. Controller Dynamics

As stated by Ikawa (Ikawa et al, 1991), high speed multi-axis CNC controllers are essential not only for the efficient control of, servo drives in high precision loop synchronism for contouring but also for the thermal and geometrical error compensation optimized tool setting and direct entry of shapes. The controller is the most important subsystem of the Ultra-Mill as the controller acts as the numerical controller unit which incorporates the interpreter, interpolator, position controller and servo computation functions. Apart from being the numerical controller, the controller observes and monitors the operational logic of the machine tool as a whole system.

The stiffness of the axes refers to the ability to resist any external force that could cause a minor displacement or deformation. The servo algorithm which is embedded in the controller could lead to high servo stiffness which in turn will provide overall machine accuracy and sensitivity.

The servo stiffness is not only dependent on the controller but is dependent on the combination of the controller with the drive and actuation system and the feedback system which also include some software parameter settings. In this section, the dynamics or characteristics of the controller will be discussed. These characteristics were understood in the design stage of the control system development.

In micromilling process, it is required that the cutting tool trajectory will involve micron level movements and positioning. The control system must be able to provide micron level movements and positioning in a fast, accurate, repeatable and robust manner. The controller must have high servo frequency updates and high system bandwidth. These provide the servo stiffness required and in a case where the servo frequency update is low, the servo system will be less sensitive which in turn will diminish the disturbance rejection ability.

High controller processing speed is required so as to avoid any delay in data transfer between the PC and the controller. The processing speed must be high enough to complete the servo cycle and sustain the computational rate of the controller. From experience, low processing speed has resulted in the servo loop cycle being incomplete. This has resulted in motion error whereby the axes of the machine tool ceased to function.

Figure 4.7 describes the characteristics of various types of processing chips for motion control. The selection of motion control processors are based on processing speed and power, programming time and ease of programming.

The sampling rate of the entire system is important in minimizing contour errors. In multi-axis simultaneous machining, the controller sampling rate must be adequate so as to provide overall system stiffness. Some controllers lack sufficient capability: as the number of axes increases, the slower is the sampling rate.

As mentioned earlier in this section, the servo stiffness is not only dependent on the controller. The servo algorithm is embedded in the controller. To obtain good response and stiffness of the motors, the servo algorithm must be tuned. For the Ultra-Mill, the servo algorithm is a proportional, integral and derivative plus velocity and acceleration

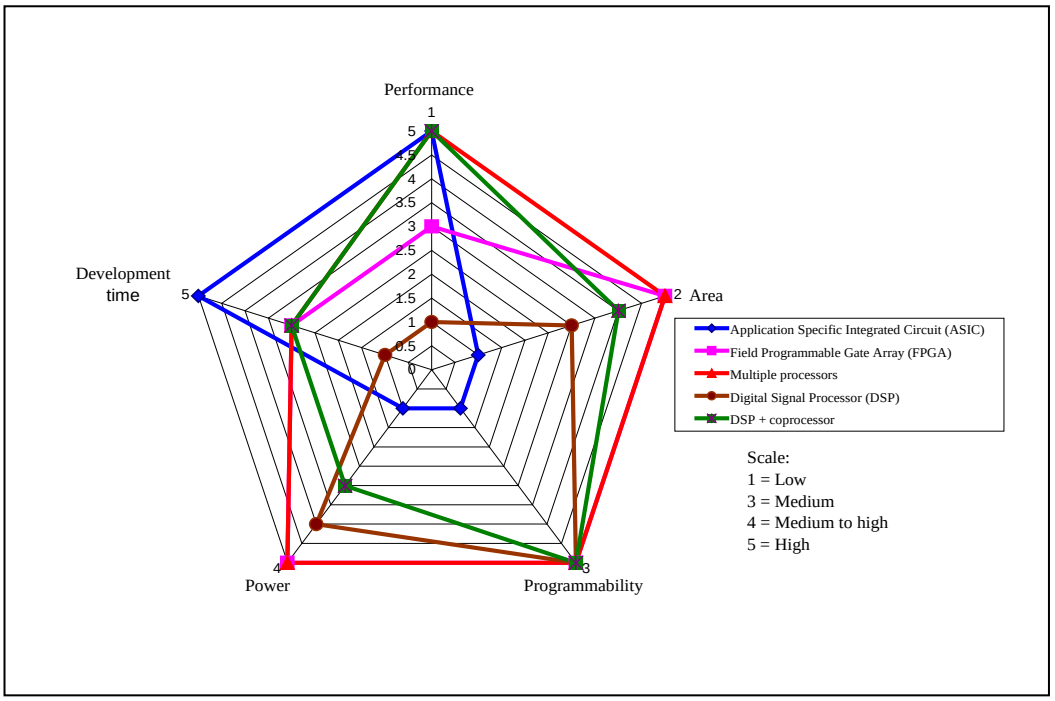

Fig.4.7 Characteristics of various types of motion control processors

feedforward controller. The tuning of the servo loop will be discussed more thoroughly in Chapter 6.

In the case of Ultra-Mill, the DSP chip will execute the real-time motion control functions whereas the PC's CPU acts as a host which executes the non-real time event processing and the human machine interface (HMI). DSP supplies optimal processing for feedback regulation, notch filtering, velocity estimation, motor commutation, running fast tool servos, etc. and will increase performances in terms of speed, precision, surface finish, machining cycle times, improving reliability and robustness.

4.2.2. Drive and Actuation Dynamics

As mentioned before, the Ultra-Mill uses direct drive systems with aerostatic bearings. Here no mechanical transmission is involved. During machining, disturbances impact directly on the axes. The disturbances come in the form of cutting force. Compared to screw-based systems, the direct drive system with aerostatic bearings are not as stiff. On the other hand, the screw-based systems have backlash, friction, etc. which would lead to wear.

The stiffness of the direct drive systems with aerostatic bearings is dependent on the control system, motor, amplifier and encoder. In micromilling, the cutting forces are considered minute compared to macromilling forces. These have been observed through experiments which will be elaborated in Chapter 7. These forces can be random as it could be a combination of effects due to machine vibration, chatters, etc.

Direct drive systems have higher natural frequencies and higher stiffness than ball screw drives, because there is no elastic deformation involved in the drive system (Weidner et al, 1999). Other characteristics that influence the decision of implementing direct drive systems in the Ultra-Mill are described in Section 2.4.2.

The dynamic stiffness of the servo loop is vital so as to achieve high performance micromilling characteristics. The stiffness will impact on how well the loop will react when disturbance is injected into the loop during machining. To predict the stiffness of the loop, modelling using a computer aided control engineering package (i.e. Matlab/Simulink) is used. This section will elaborate on the modelling on the servo loop of the direct drive system. Chapter 6 will explain more in depth of the simulation and modelling of the drive system.

The Ultra-Mill adopts the proportional, integral and derivative (PID) plus velocity and acceleration feedforward servo algorithm. The feedforward scheme helps to reduce the following error. The command output of the UMAC controller is shown in Equation (4.1).

$$DAC_{out} = 2^{-19} K_p \left[K_{sp} \left(FE + \frac{K_{vff} CV + K_{aff} CA}{128} + \frac{K_i IE}{2^{23}} \right) - \frac{K_d K_{sv} AV}{128} \right] \tag{4.1}$$

DAC_{out}, K_p, K_{sp}, FE, K_{vff}, CV, K_{aff}, CA, K_i, IE, K_d, K_{sv} and AV represent the 16-bit servo cycle output command, proportional gain, internal position scaling term, following error, velocity feedforward gain, servo cycle commanded velocity, acceleration feedforward, servo cycle commanded acceleration, integral gain, servo cycle integrated following error, derivative gain, internal scaling position scaling term and servo cycle actual velocity. The output is in the form of voltage signal. This voltage

will then be converted into current signal so as to provide the thrust force for the motors. The thrust force is provided by the PWM amplifier and is proportional to the input current.

Achieving robust, fast and accurate motions also depends on the hardware and software of the control system. Taking stiffness as an example, achieving high stiffness depends on the motor peak force, current available and the encoder resolution for hardware side. In the software paradigm, it depends on how well the servo loop is tuned. Most ultraprecision machine tools apply the simple PID (proportional, integral and derivative) with feedforward algorithms, although the research community are always developing newer advanced servo algorithms so as to accomplish enhanced motion performance. In ultraprecision machine tools, greater care is taken in their mechanical design in order to obtain higher stiffness and eliminate non-linearites such as friction and motor torque ripple, rather than improving the control system (Wilson, 2004).

In the design stage for the drive systems, accomplishing overall excellent drive system performances in terms of speed, accuracy, etc. for motion and positioning, the drive systems must have these characteristics:

- Sufficient voltage and current loop gain so as to achieve maximum speed.
- Adequate force/torque to resist disturbance forces (i.e. cutting force, frictional force, etc.) and to accelerate the axis load.

Sizing of the drive system is a part of the design. Mathematical formulas were used to calculate the correct motor size to provide maximum and adequate performance. Attention is given to motor power and stiffness requirements. These equations are as shown below. During the sizing stage, a few key motor behaviours must be established, i.e. peak speed, accelerating rate, length of travel, accelerating load, etc.:

$$PeakCurrent(I_p) = \frac{f_p}{K_t} \tag{4.2}$$

$$ContCurrent(I_{rms}) = \frac{f_{rms}}{K_t} \tag{4.3}$$

$$V_{D\min} = (I_p \times R_c) + (v \times B_{emf}) \tag{4.4}$$

$$V = \frac{V_{amp\max bus} - (I_p \times R_c)}{B_{emf}} \tag{4.5}$$

$$f_{rms} = \sqrt{\frac{t_1 f_1^{\,2} + t_2 f_2^{\,2} + t_3 f_3^{\,2} + \ldots + t_n f_n^{\,2}}{t_1 + t_2 + t_3 + \ldots + t_n + t_{dwell}}} \tag{4.6}$$

I_p, f_p, I_{rms}, f_{rms}, K_t, V_{Dmin}, R_c, v, B_{emf}, V, $V_{ampmaxbus}$, t and f represent parameters for peak current, peak force, continuous current, continuous force, motor force constant, minimum drive voltage, coil resistance, velocity, back EMF, maximum speed, amplifier maximum bus voltage, time and force respectively.

It is worthwhile to oversize the drive system during the design stage. Having more power will lead to motors running cooler, therefore will decrease thermal errors. In the Ultra-Mill, the mechanical structure (linear and rotary axes) is not as big and heavy compared to conventional machine tools. With big masses, the structure behaves like a low pass filter.

Once the motor sizing has been completed, the next step is choosing the amplifiers to drive these motors. For this application, an PWM amplifier was chosen. The PWM amplifier was chosen instead of, for example linear amplifier, is due to the fact the PWM amplifier is powerful and is of lower cost compared to a linear amplifier. Other considerations that were taken into account during the selection of the amplifiers are the gain, bandwidth, efficiency, linearity, noise, output dynamic range, slew rate, etc. The biggest advantage of PWM amplifier is the efficiency. The operating temperature of PWM amplifiers is much lower than that of linear amplifiers.

However there is a limit to improving the machine dynamics and performance merely based on mechanical enhancement. Direct feed drive systems deliver a new dimension

for improving ultraprecision performance particularly in the framework of undertaking nano/micro machining.

4.2.3. Feedback Dynamics

In any mechatronics system, the feedback system is extremely important and the speed of detecting and fault correction is also essential. The feedback system is divided into two sections, (1) feedback for motion and (2) feedback for machine conditions and auxiliary functions. In-process conditions must be monitored in real time constantly to ensure no machine degradation and not forgetting to ensure the machine safety as well. The feedback signals are sent back to the machine controller for interpretation.

For the axes motion and positioning feedback, encoders are able to provide the actual position reading. The velocity feedback is derived from position feedback. In the design specification for motion and positioning accuracy, the Ultra-Mill required a 5 nm encoder resolution. The encoder scales that were used have 20 μm gratings. To obtain 5 nm resolution from 20 μm gratings, electronics multiplication is implemented. With 4,096 digital quantification of the physical resolution, 4.88 nm resolution is attained. The increase in the resolution will directly increase the axes stiffness provided the controller could digitally close the servo loop at a high frequency. Here, the combination of hardware and software is unavoidable so as to enhance overall system performance.

The other type of feedback as mentioned earlier is for machine conditions and auxiliary functions. These sensory systems normally using limit switches, pressure switches, thermocouples, etc., operate by supplying a high or low signal to the controller for status changes.

In ultraprecision micromilling machine, feedback systems are very important and when feasible, many feedback systems should be implemented so as to making the system more autonomous but at the same time keeping the cost of implementation low. As an example, many research groups use dynamometers to measure cutting forces so as to detect tool wear or tool breakage. The dynamometer is not a feasible instrument that machine tool manufacturers will consider implementing in all production machines as the dynamometer is very expensive.

As machining process involves small or miniature parts and components, microtools, microforces, micromovements and micropositioning, motion feedback, machine conditions and in-process monitoring systems must be implemented to increase the quality and productivity.

4.2.4. Inspection, Monitoring and Auxiliary System

Inspection and monitoring systems are required for high precision systems. These systems will monitor the machine and machining processes in real-time with the aid of sensor fusion to increase the functionality, consistency, sensitivity and precision. In micromachining processes the amount of energy and cutting forces are minute compared to macromachining. In addition, thermally induced error must be eliminated.

The inspection and monitoring system is to observe the machining process and machine tool state. Sensory systems, normally electronic latches, limit switches, pressure switches, thermocouples, etc., for auxiliary functions operate by supplying a high or low signal to the controller for status changes. With these, machine conditions can be monitored in real time constantly. The operation of this feedback is governed through programmable logic controller (PLC) programs.

Other than these auxiliary functions for monitoring the machine status or state, tool condition inspection and monitoring is very crucial. The microtool cannot be seen clearly with the naked eye and therefore making it very difficult for tool setting and inspection. For the Ultra-Mill, a non-contact laser tool setting system and a vision system using a camera are adopted. The non-contact laser tool setting system is used to inspect the condition of the microtools (i.e. tool height, diameter, and wear/breakage) before, during and after machining. In Chapter 7, tool condition monitoring is discussed in more detail.

The Ultra-Mill has integrated a 3-axis SCARA robot from Epson for loading and unloading of tools and workpieces. The communication between the Ultra-Mill and the robotic arm is established via Ethernet using the client (Ultra-Mill) and server (robotic arm) program framework. The communication enables the Ultra-Mill to select the usage of the robotic arm. Acknowledgements are sent and received between Ultra-Mill and the robotic before and after each completed task. This is so as to avoid any possible

collision between the robotic arm and the mechanical parts of the Ultra-Mill. There is a customized layout of the handlings system function incorporated into the HMI.

4.2.5. Software Dynamics

Software plays a vital role in the setting up and operating of the Ultra-Mill. The setting up part will not be discussed here. However this section will concentrate on the operational part. Operating the Ultra-Mill requires a human machine interface (HMI) to display information for operators. The interface allows the operator to input NC programs for machining. The interface displays information such as axes position, feedrate, spindle speed, etc.

Under software dynamics, the concentration is on the computer aided manufacturing (CAM) packages characteristics. The CAM is considered as a part of the control system due to the fact the CAM generates the axes trajectory and coordination for machining. Within the CAM, there are many machining strategies to choose from. Apart from choosing the best strategies, parameters such as step over, step down, etc. also need to be configured. Fluent in operating the CAM alone does not guarantee high quality parts. It is also down to experience in choosing the correct cutting parameters, tooling, material, etc.

It is understood that machining at the micro and nano realm involves a thorough optimal tool path and machining parameters planning. The strategies applied in macromachining are rarely applicable in micromachining. Delcam's Powermill has been selected to be the CAM package for the Ultra-Mill. This package is integrated into the human machine interface. The integration allows the operator to generate NC programs and edit them when necessary. When preparing an NC program using the CAM package, five considerations must be observed in the selection of the tool path strategies (Korn, 2006):

- Selection of optimal and appropriate tool path strategies.
- Tool path selections must take parts size and complexity into consideration.
- Roughing and finishing operations may need to merge when appropriate.
- Cutting forces (dependent on spindle speed, feedrate, depth of cut, etc.) must be maintained throughout the process so as to produce repeatable accuracy.

- Awareness of CAD/CAM translation errors which could affect machining accuracy.

In the design stage, as part of the CAM specification, the CAM must be able to accommodate simultaneous multi-axis machining. This required the machine to produce much more accurate components or parts finishing and minimize machining time and cost. Another point is the feedrate scheduling. Optimized feedrate scheduling increases parts finish accuracy and minimized tool wear and breakage.

Since the parts machined are small, good 3D simulation functions of the tool trajectories are required to evaluate the chosen strategies before actually machine the parts. This will assist in understanding and optimizing the tool path selection. The 3D simulation of the actual trajectory during execution is beneficial to indicate how much material has been removed and the current position in the machining sequence. A CAM package with 3D simulation abilities and collision avoidance system is able to minimize the frequency of the tool running into vices and avoids any possible damage to the machine structure.

Software dynamics is considered important as this is part of the motion control system.

4.3. Ultra-Mill Control System Implementations

This section will describe how the control system implementations were done. Selected subsystem implementation will be discussed.

4.3.1. Servo Loop Setting Up

Adequately setting up the servo loop is very vital to guarantee the desired performance. In the setup, parameters such as the PWM frequency, servo frequency, maximum voltage, maximum current, etc. are required so as to obtain the best performance and at the same time protect the motors.

Figure 4.8 describes the step by step servo loop set up through a flowchart. The servo loop set up consists of three elements, namely controller settings, drive and actuation settings and feedback settings. All these are set up using the Turbo Setup package by Delta Tau.

In the controller settings, setting the PWM and servo frequencies adequately is very critical. These frequencies must be set within specific range for every drive or amplifiers. These frequencies must not be set too large as this could lead to excessive heating in drives or amplifiers. Setting them very low will result in low response, excess acoustic noise, vibration and motor overheating.

The next procedure is related to settings of drive and actuation settings. These are set using the data sheet for each drives and motors to ensure the highest performance achievable and motor protection.

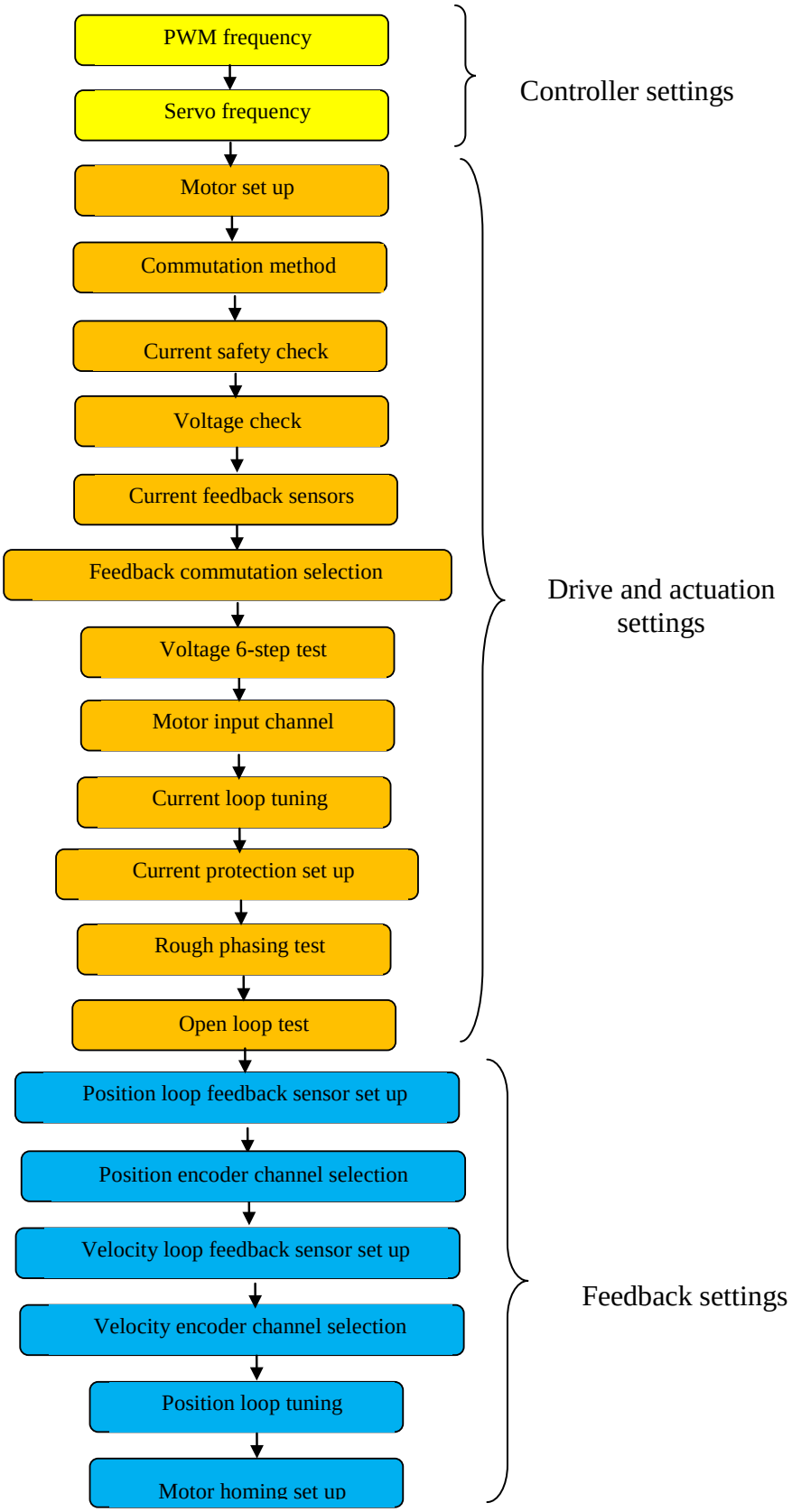

Fig. 4.8 Servo loop set up

The last step in the servo loop set up is to complete the feedback loop. The correct encoder channels must be known correctly for each drives. Selection of encoder type, encoder resolution, numbers of poles, markers for end limit or homing, feedback type, etc. are done in the feedback set up.

Once the servo loop is adequately set up, the next is to perform the PID plus velocity and acceleration feedforward parameters to obtain servo performance with high robustness, responsive, low following error, etc. These are explained thoroughly in Chapter 6.

4.3.2. Human Machine Interface (HMI)

The HMI is the medium that supplies the operators with information regarding the machine statuses and conditions and machining parameters. The interface accommodates functionalities such as part program editing, various machine parameters setting, machine diagnostics, etc. for the benefit of the machine operator.

The interface customisation was intended so as to ensure less adaptation of the operator to the system and design the interface to make machine operations and tasks management simpler and less complicated. The customisation involves making the interface having clear and readable display, include familiar features (i.e. mimicking Windows layout), easy manoeuvring to locate certain functions, information, etc.

This section will describe the customization that was implemented for the Ultra-Mill interface. In the HMI design, several design principles were used to ensure the effectiveness of the elements (interface layout, colours, fonts, etc.) selected. The task of the HMI is to assist operators and making the job of operating the machine much simpler. In the design stage, design principles such as human factors engineering (HFE) and ergonomics and user-centred design were combined and simplified to that shown in Figure 4.9.

The design and customisation of the HMI was executed in Visual Basic. Appendix IV includes part of the HMI programming codes.

4.3.2.1. HFE and Ergonomics

Human factors engineering (HFE) and ergonomics are sometimes defined as the science of fitting the work to the user instead of forcing the user to fit the work. This is however, a more primary principle rather than a definition. In the design stage, the designer has to weigh up and decide which approach would improve the performance of the user and the interaction between the user and the system. Any stressors a user may encounter when interacting with the system should be considered and evaluated if they could be minimized or eliminated.

The main idea of this principle is products and tasks comfortable and efficient for the user.

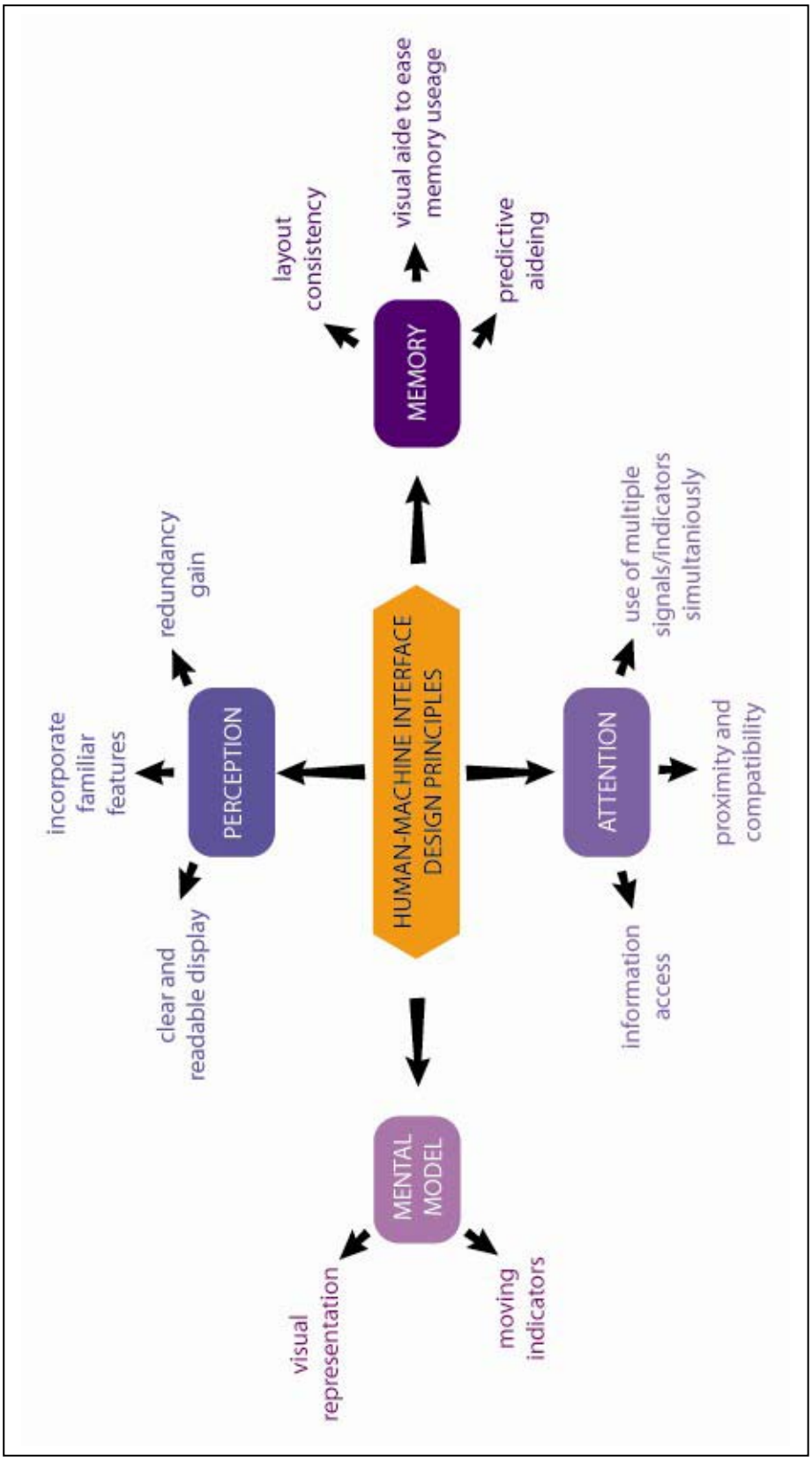

Fig 4.9 HMI design principles

4.3.2.2. User Centred Design

User centred design involves how information is relayed to the user or machine operators. This information includes machine status, motor status, coolant level, warning alarm, etc. There are many ways to relay the information to user or operator. In the design stage, it is critical to highlight that the interface task is to aid the operator's task.

Here are some good design elements examples that were considered:

- Clear and readable display- utilizing screen friendly fonts and using the correct colours for backgrounds, texts and function buttons.
- Incorporate familiar features- to incorporate features used by Windows on its interface.
- Redundancy gain- present statuses or alarms more than once with alternative physical forms.
- Visual representation- variables should be represented in an obvious visual way whenever possible e.g. high and low feed rates are indicated using an indicator moving along a triangular slider.
- Information access- minimizing the steps taken to access any information (frequently accessed sources to be located at the nearest possible position, drop down menus, etc.).

Figure 4.10 illustrates the customizable interface for the Ultra-Mill.

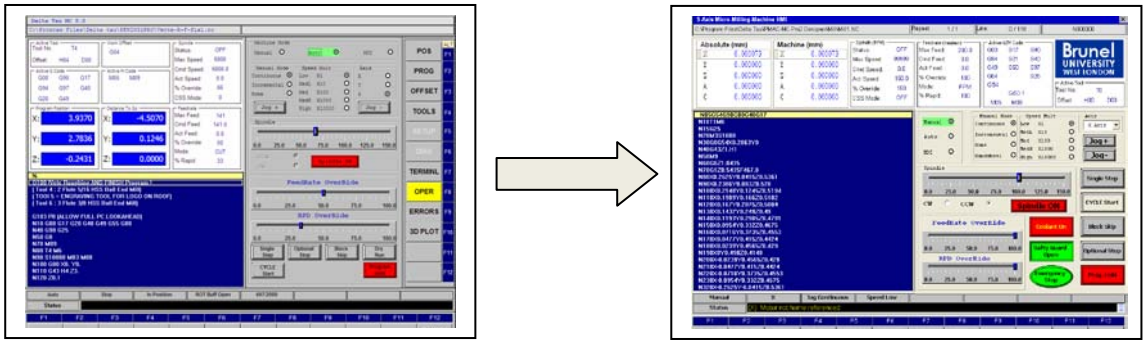

Fig. 4.10 Customization of HMI design

4.3.2.3. Auxiliary Functions

Ultra-Mill has several auxiliary functions that are fitted as part of the control system. These auxiliary functions are divided into three groups:

- Miscellaneous equipment: coolant, vacuum chuck, automatic spindle collet system, machine guard and pressure switch.
- Handling system: 3-axis SCARA robotic arm for tool and workpiece loading and unloading.
- Tool monitoring system: tool diameter and height measurement, tool breakage, tool wear, etc.

These functions are required to reduce human intervention and make machine operations safer. All the auxiliary functions are connected to Ultra-Mill controller via the input-output board (I/O) board or Ethernet connection.

The auxiliary functions are controlled through programmable logic controller (PLC) programs. PLC programs are relatively easy to construct and protocols controlled require a high or low signal to or from the I/O board. In the case of the Ultra-Mill, miscellaneous equipment and the tool monitoring system are connected to controller via the I/O board and the handling system utilises the Ethernet connection.

Chapter 7 will discuss further the design, development and implementations of the handling system and the tool monitoring system. Figure 4.11 describes the Ultra-Mill operating flowchart.

Appendix IV illustrates some examples of the PLC programs.

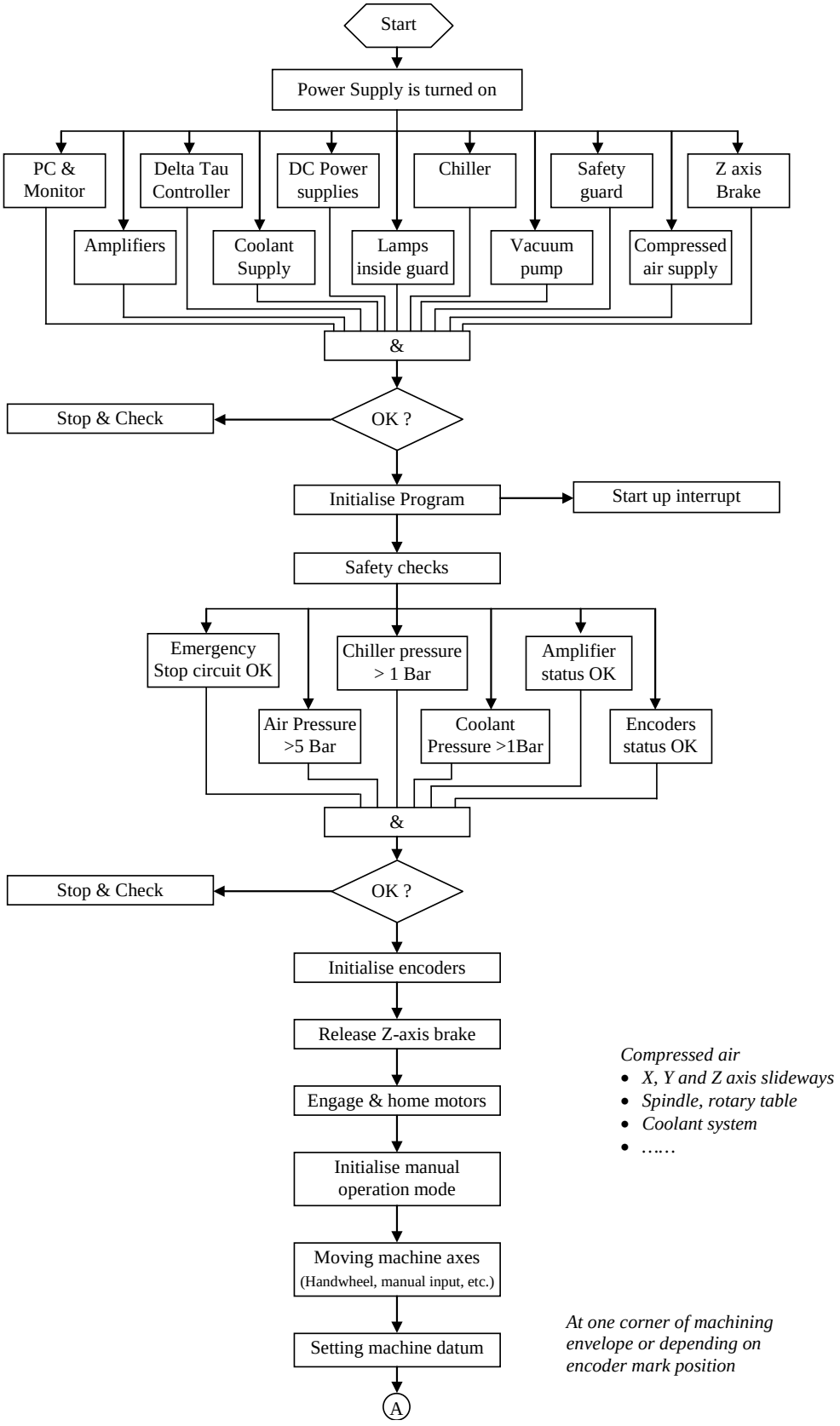
Start
Power Supply is turned on
PC & Monitor
Delta Tau Controller
DC Power supplies
Chiller
Safety guard
Z axis Brake
Amplifiers
Coolant Supply
Lamps inside guard
Vacuum pump
Compressed air supply
&
Stop & Check
OK ?
Initialise Program
Start up interrupt
Safety checks
Emergency Stop circuit OK
Chiller pressure > 1 Bar
Amplifier status OK
Air Pressure >5 Bar
Coolant Pressure >1Bar
Encoders status OK
&
Stop & Check
OK ?
Initialise encoders
Release Z-axis brake
Engage & home motors
Initialise manual operation mode
Moving machine axes
(Handwheel, manual input, etc.)
Setting machine datum
A
Compressed air
X, Y and Z axis slideways
Spindle, rotary table
Coolant system
……
At one corner of machining envelope or depending on encoder mark position

(a)

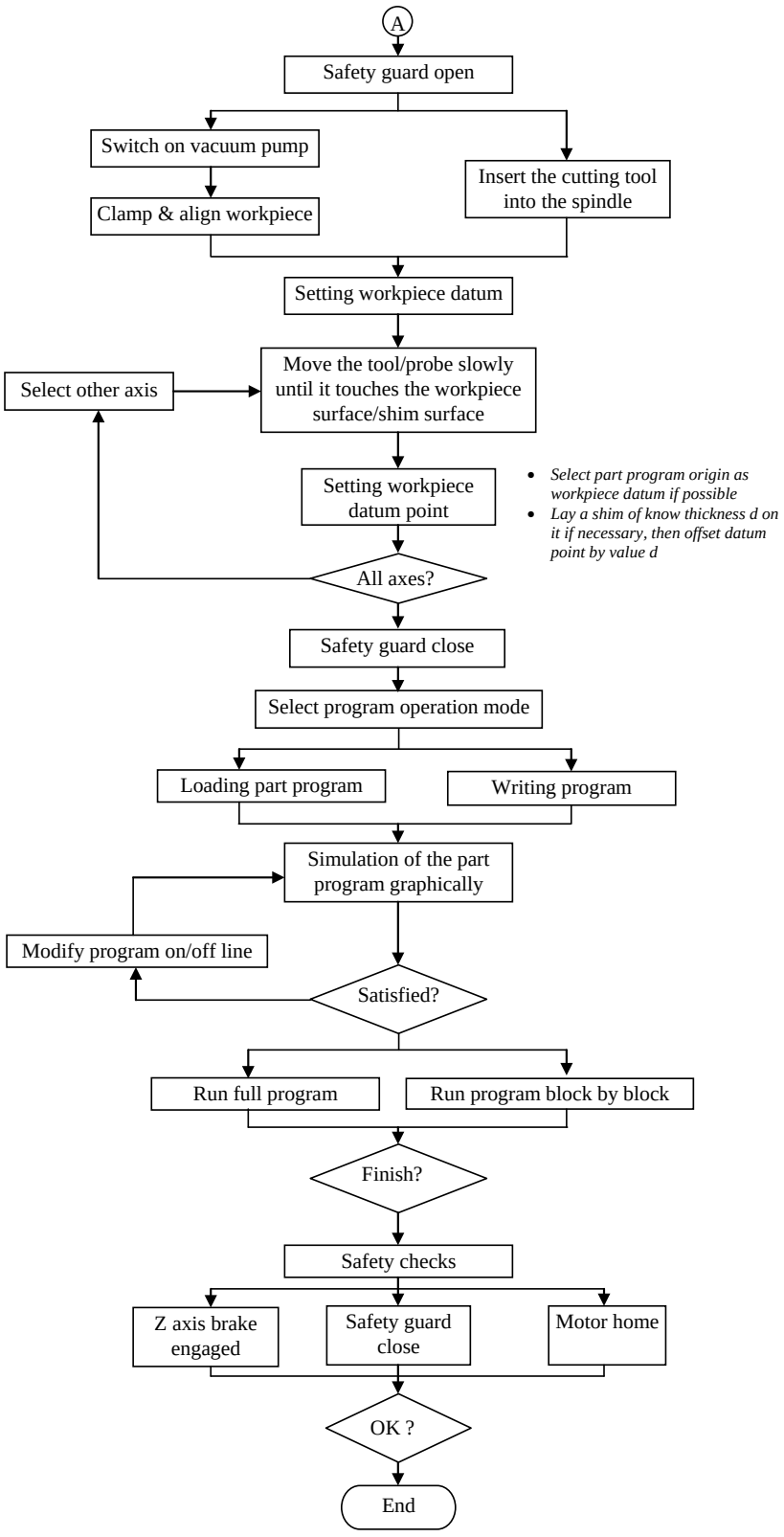

(b)

Fig. 4.11 Ultra-Mill operating flowchart

4.4. Summary

This chapter has described the design and development of the control system for the Ultra-Mill. In this design framework, theory is formulated in design requirements to meet crucial performance specifications.

Firstly, the dynamics of the servo loop must be designed to ensure high dynamic stiffness to reject external disturbance without sacrificing the sensitivity, precision, speed, etc. for motion and positioning. This is all related to the motion control design and requirements.

Secondly, the precision system and the processes must be monitored in real-time as long as the machine is executing any given task. Sensor fusion is required to obtain different signals for different change in conditions to provide confidence for problems identification. This is crucial especially in area of micromachining processes. The speed of fault detection and rectification is very important to avoid wastage of manufacturing resources.

Thirdly, software manipulation is required to ensure the aimed performance is achieved. In terms of motion control for tool trajectory, a CAM package is required to generate the toolpath. Selection of suitable CAM package must ensure the suitability for micromachining.

From here, it is known that, in achieving the best overall machine and machining process performance, the combination of hardware and software is required. This is to compensate the weakness or enhance any subsystem so as to manufacture products with high accuracy, complex features, increase productivity, maintain machine stability, etc.

Chapter 5

Development of the Control Cabinet

5.1. Introduction

In the field of micromachining, the machines that are used to produce the parts or components are relatively large in size. Machining in the micro or nano meter scale is not economical by utilizing these large machines. Common precision machines would have key modules such as mechanical structure, control cabinet working with a control system, drives and actuation systems, tooling and fixturing and inspection system, etc. For the Ultra-Mill, the idea is to build and integrate these modules into one machine configuration which in turn will minimize the overall floor space and reduces the footprint of the machine tool. Table 5.1 illustrates the floor space requirements for various commercial machine tools compared to the Ultra-Mill.

Table 5.1 Floor space requirements comparisons

Machine Model	**Floor Space Requirement w × d × h (m)**
Kern Evo [Kern, 2009]	2.80 × 2.50 × 2.20
Nanotech 350 FG [Nanotech, 2009]	1.93 × 1.80 × 2.00
Nanoform 700 Ultra [Precitech, 2009]	1.44 × 1.93 × 2.04
Micromaster [Kugler, 2009]	1.7 × 2.00 × 2.35
Ultra-Mill [Ultra-Mill, 2009]	*1.1 × 0.80 × 2.10*

Apart from minimizing the floor space, there are other reasons or motivations which are pushing machine builders and research groups to develop machines with small footprints.

Motivations for miniaturization include:

- Lower energy consumption, lower material cost and compactness (Chae et al, 2006; Fukuda et al, 1998).
- Decrease of heat deformation of the machine tools (Kussul et al, 2004).

- Vibration amplitudes of small machine tools are lower than large machine tools (Kussul et al, 2004).

5.2. Design Issues

In this chapter, the design issues section will cover only the development of the control cabinet for the Ultra-Mill which includes the design and implementation perspectives. Discussions on the miniaturization of the mechanical elements will not be discussed in this thesis.

Designing the cabinet for Electromagnetic Compatibility (EMC) and thermal management is a not straight forward. In the design stage, contradictions between EMC and thermal management were observed. A small fraction of the design principles is dependent on each other. For example, thermal management design requires the apertures on the cabinet to be large to allow sufficient airflow for cooling but on the other hand, EMC management design requires the apertures to be as small as possible to avoid a decrease in the shielding effectiveness.

In the design stage, EMC and thermal budgeting is done to obtain the best design layout. In the budgeting, enclosure sizing, airflow rate, etc. were taken into account. In the EMC management design stage, manufacturer guidelines and normal practiced standards (BSI and ISO) were observed. For the thermal management design, a Computational Fluid Dynamics (CFD) study was conducted.

The control cabinet of the Ultra-Mill consists of CNC control unit, electrical control units (circuit breakers, contactors, etc.), filter, amplifiers, encoder interfaces, cables, etc. the installation of this equipment must comply with the manufacturers' recommendation which complies with certified standards, e.g. BSI or ISO. Apart from design according to the recommendations, designing for easy maintenance is very crucial if there is a need for upgrading or repairing of equipment in the later stages. Complication arises when contradictions amongst standards, manufacturer installation guidelines and available mounting surface occurs.

Typical electrical cabinets have the equipment mounted on the back wall of the cabinet. Also for machine tool control cabinet, the normal location of the cabinet is standing next to the machine tool.

The electrical cabinet for Ultra-Mill is custom fabricated to suit the machine base. The cabinet is fabricated so as to be able to fit nicely underneath the machine enclosure. The cabinet is fitted with a roller on two sides which enables it to operate like a drawer system as shown in Figure 5.1.

Fig. 5.1 The control cabinet drawn out

The dimension of the cabinet is 1020 mm × 480 mm × 790 mm ($l \times h \times d$) and is in horizontal position. For this type of enclosure, the height is a problem as it must accommodate the highest equipment with the height of 338 mm. mounting of cableways on top and below the equipment is essential for cable management and the minimum separation distance between the cableways and the equipment must be obeyed.

According to manufacturer guidelines, the equipment must be mounted in the vertical position and this has resulted in the equipment being mounted on all vertical surfaces of the electrical cabinet as illustrated in Figure 5.2 and the complete cabinet layout is presented in Appendix V. The equipment is mounted on aluminium plates to allow for good grounding.

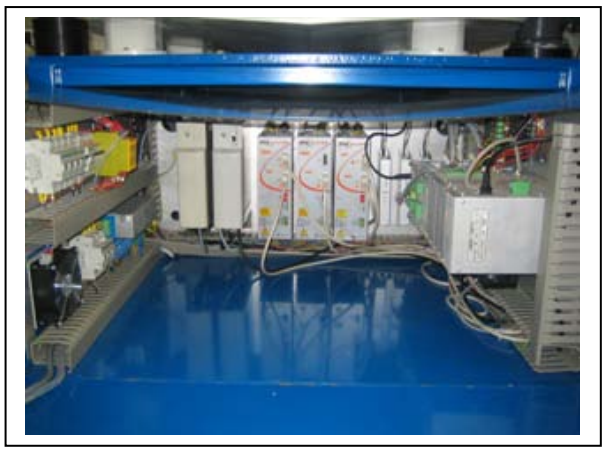

Fig. 5.2 Internal layout of the control cabinet

5.2.1. EMC Issues

In this section, design for EMC management will be discussed. EMC is a crucial design stage for any electrical or electronics design. Excellent EMC design will enable products to:

- Operate without interfering with other systems.
- Operate without interfering with itself.

The design for EMC for this cabinet begins not at the components level but at the systems level. A checklist is important for excellent EMC design and must be obeyed when permissible. A few key points of good EMC design would be to:

- Identify sensitive and noisy equipment.
- Select suitable components.
- Have good equipment and wiring layout.
- Have grounding and filtering.

The design for good EMC has been discussed in many standards and literature and therefore in this section, only certain parts of EMC design will be touched on as they were the issues which arose during the installation of equipment in the electrical cabinet. The European Conformity (CE) markcertifies a product has met the consumer safety, health and environmental requirements (Wikipedia, 2009c). Typical thinking of control panel builders and system integrators on “CE + CE = CE” unfortunately does not apply (Armstrong, 2001). Figure 5.3 illustrates the design considerations for EMC management design.

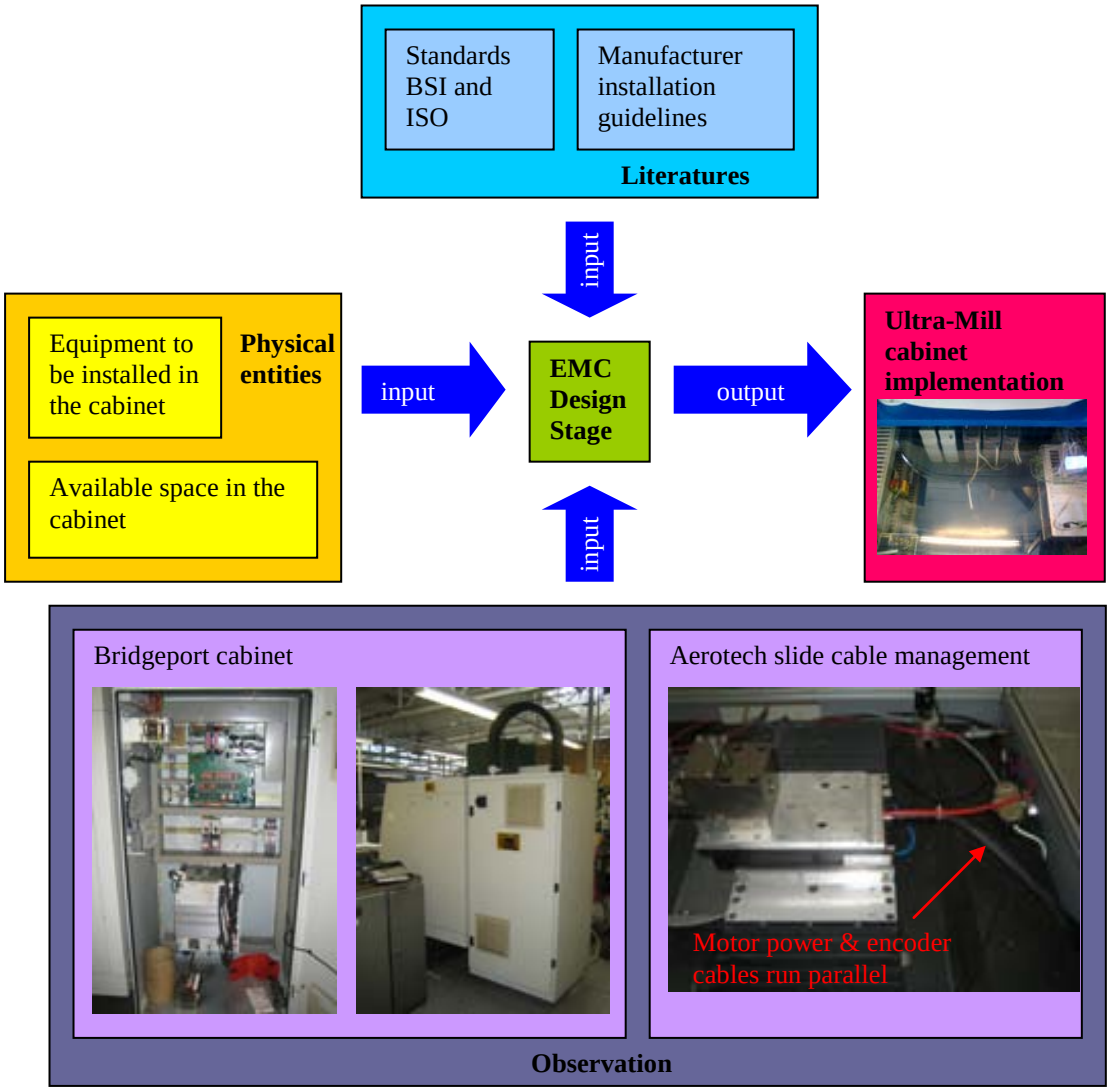

Fig. 5.3 EMC design process

This section will discuss and concentrate on the area of equipment layout, cable segregation and vents or apertures. These areas were the issues that arose while designing and integrating the electrical cabinet. The major contributor to these issues came from the limited mounting space for the equipment. Ideally the electrical cabinet should be placed in an anechoic chamber for electromagnetic interference (EMI) testing. The usage of the anechoic chamber is to attenuate the electromagnetic energy

5.2.1.1. Equipment Layout

The most important element in equipment layout is to obey the manufacturer installation guidelines. These guidelines include the minimum separation distance required between

two pieces of equipment. The minimum distance requirement could be for thermal management. The guidelines also indicate how the equipment should be mounted in an enclosed or not enclosed area. Standards require the equipment of different types (sensitive and noisy equipment) to be separated with a minimum separation distance (Schneider, 2007; Moore, 2003, Armstrong, 2001; Armstrong, 2000; Williams, 2000). The equipment in the electrical cabinet of the Ultra-Mill was arranged according to the equipment category and minimum separation between equipment of same category and different category were observed when permissible. Some minimum separation distances were unable to be followed accurately due to lack of mounting space. All equipment was mounted on aluminium plates which act as local RF reference for good grounding.

5.2.1.2. Cable Management

Cable management is an important element in the design stage of the electrical cabinet. The cables must be segregated according to the cable classes or types. Cable segregation is more or less the same with the arrangement of the equipment as there are the noisy and sensitive cables. In this case, the sensitive cables would be those carrying feedback signals from the encoders of the machine tool and the noisy cables are related to the motor power cables and the mains power supply. All the cables that were used in the electrical cabinet are shielded cables where some of them are twisted shielded cables.

The cables are categorized according to their types and are placed within plastic cableways. These cableways are mounted on the aluminum plates. Plastic cableways were implemented so as to reduce the cost and mimicking another CNC machine electrical cabinet within the university premises. The cables are arranged so as to obey the minimum separation distance, i.e. minimum separation distance between encoder and power cables is 1 m, which are recommend and described in (Schneider, 2007; Armstrong, 2001; Armstrong, 2000; Williams, 2000). Cables with dissimilar classes should only cross over each other at right angles.

As stated earlier, the space limitation is the biggest constraint in obtaining the best optimal cabinet design layout. Therefore this has resulted in some cables of different classes unable to be kept separated at recommended distances. The recommended guidelines are there to ensure safety. These compromises do not directly indicate that

the cabinet is not susceptible and emits interference to other equipment in the vicinity. Other than using shielded cables, these cables were correctly bonded and terminated at both ends as per recommendations of the EMC practice.

Making partitions in the cableways to separate the different cable classes is another method of cable management for EMC. From observing another CNC machine electrical cabinet within the university premises and motor manufacturers, motor power cables and encoder cables were made to run parallel in the cableways.

Once the control cabinet was completed, it was checked and certified to be powered on by an in-house electrical technician. Upon powering the Ultra-Mill, it was observed that it did not interfere with other equipment operations and it did not interfere with itself.

5.2.1.3. Apertures

Allowing adequate air flow in and out of a control cabinet, apertures or vents are required. Shielding effectiveness would be compromised if the apertures or vents are too big (Johns, 2002). This would make any cable that runs near an aperture acting as an antenna. In a typical cabinet design, honeycomb shaped cavities are implemented for good air flow and yet maintain high shielding effectiveness.

The designed cabinet has two holes that are used to pass the cables to the machine tool. At each hole, there is an energy chain connected to it. The cables are placed in the energy chains for tidiness as shown in Figure 5.4. These cables are placed in the energy chains due to the fact the cabinet operates like a drawer system. No honeycomb type vents were implemented in this electrical cabinet due to the high fabrication cost.

Fig. 5.4 Energy chain connected to the electrical cabinet

5.3. EMC Analysis of the Cabinet

A 3D electromagnetic simulation called Microstripes by CST was used to perform the EMC analysis of the electrical cabinet of the Ultra-Mill. The tool uses the time domain Transmission Line Matrix (TLM) method for solving the simulated analysis. For a thorough EMC analysis, the electric and magnetic fields source are required. The field source comes directly from the board level. In the case of the Ultra-Mill, no board level information was in hand. To obtain the board level information, all the PCB circuitry of each equipment must be constructed and then analysed. This is a time consuming task and is not the purpose of this research.

In order to make the analysis easier and meaningful, simulation and analysis of the shielding effectiveness of the electrical cabinet was only considered. Shielding effectiveness means the ratio between the field strength without the barrier in position or to that when present. Shielding effectiveness (SE) is the summation of reflection, absorption and the re-reflection.

$$SE\ (dB) = R\ (dB) + A\ (dB) + b\ (dB) \tag{5.1}$$

The electrical cabinet of the Ultra-Mill has five steel surfaces and a Perspex cover used as the sixth surface. The Perspex cover provides a viewing window inside the cabinet. The Perspex cover, from EMC point of view, provides no shielding. This has weakened the shielding effectiveness of the cabinet. As mentioned earlier the cabinet is placed underneath the machine enclosure. By placing the cabinet in the steel frame of the machine enclosure, the shielding effectiveness now is at an accepted value. Now the cabinet has steel surfaces all around whereas initially it only had five steel surfaces.

5.3.1. EMC Analysis

This section will elaborate on the EMC analysis that was conducted. The first analysis is on the SE on the electrical cabinet alone. The second analysis is the SE when the cabinet is placed underneath the machine enclosure.

Two types of simulated condition were conducted, these are:

- Applying an electrical pulse outside the cabinet and measuring from inside the cabinet.

- Applying an electrical pulse within the cabinet and measuring from outside the cabinet.

The simulated condition is a similar method to a Hammer test (test for mechanical structure). The idea is to observe how the signal influences the structure and the duration taken for the signal to decay. For the EMC analysis, the observe signal is how much of the pulse enters or exits the cabinet. The less the pulse enters or exits indicates good shielding effectiveness. Shielding effectiveness is dependent on the material and the thickness of the cabinet.

5.3.1.1. Analysed Models Results

Stated are the analysed models:

Model 1: Electrical cabinet only with five steel surfaces and Perspex cover.

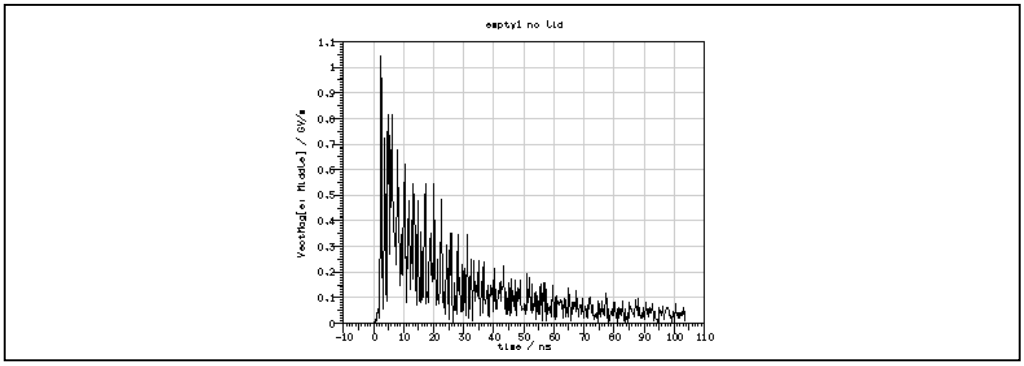

(a) Pulse in voltage in time domain

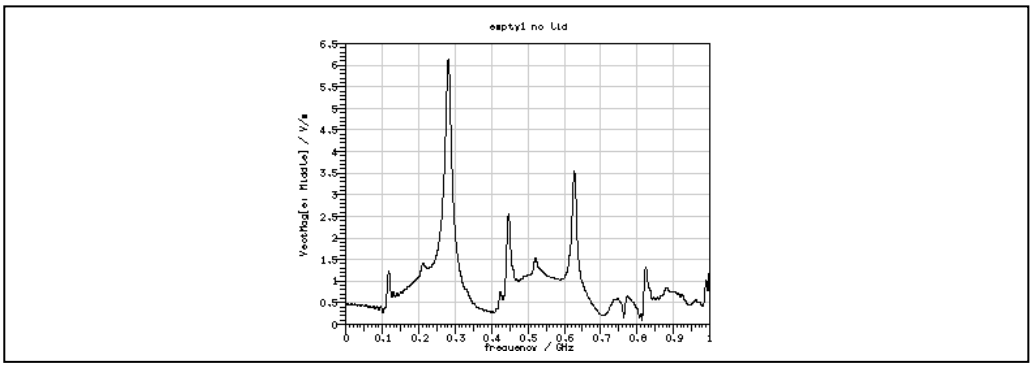

(b) Pulse in voltage in frequency domain

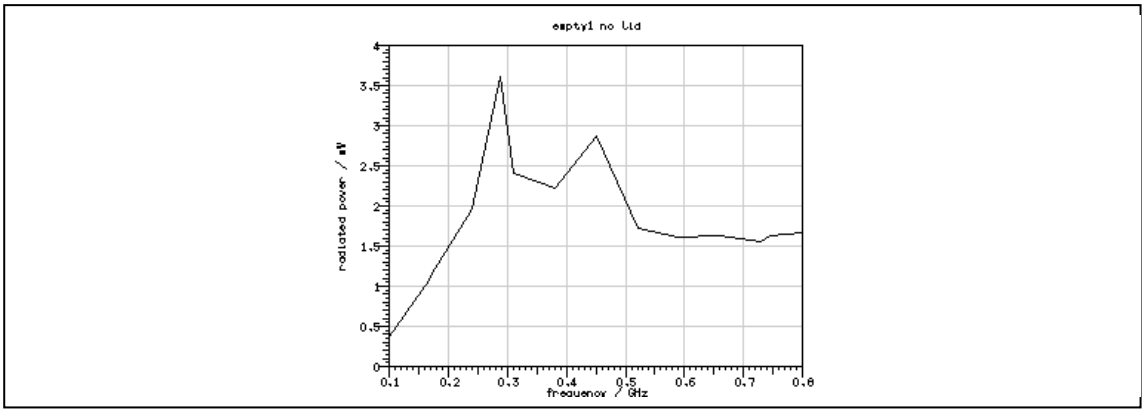

(c) Radiated power in frequency domain

Fig. 5.5 Results of electrical cabinet only with five steel surfaces and Perspex cover

Model 2: Electrical cabinet only with six steel surfaces.

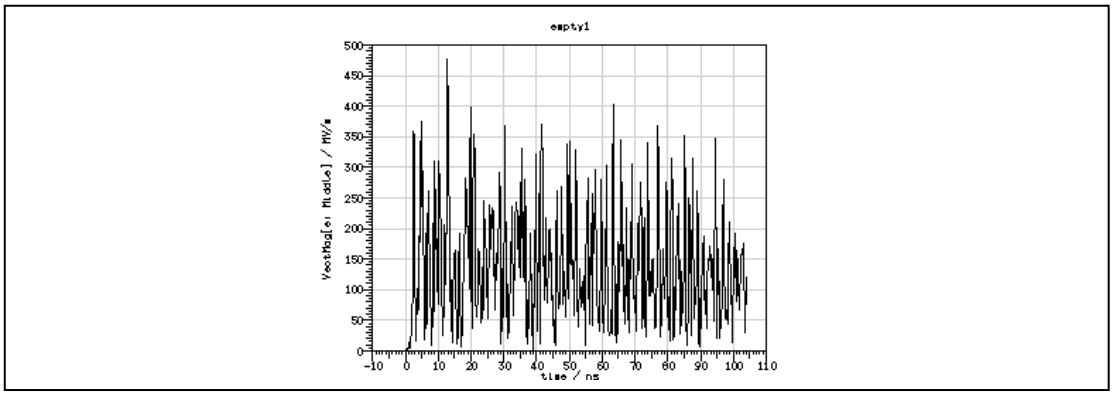

(a) Pulse in voltage in time domain

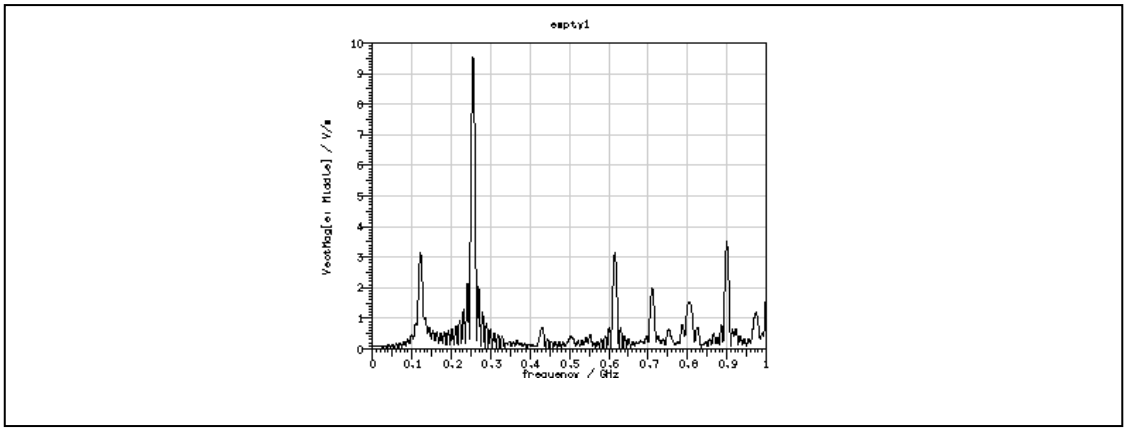

(b) Pulse in voltage in frequency domain

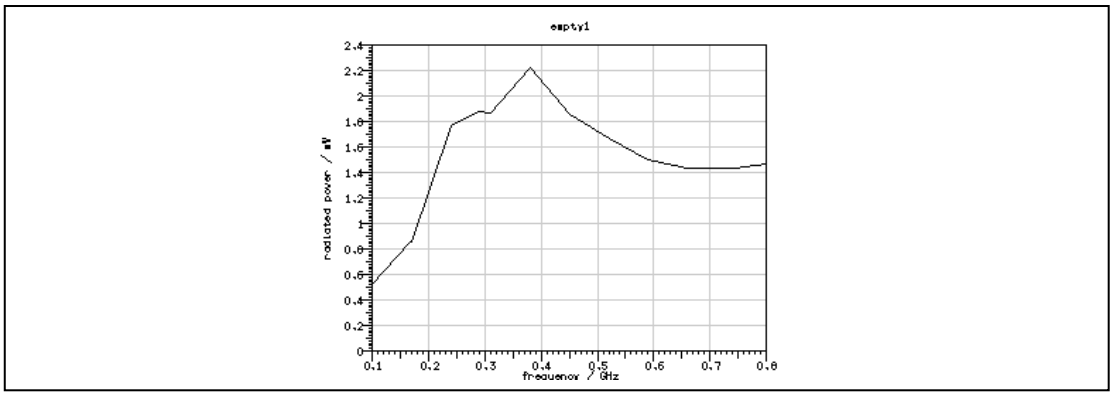

(c) Radiated power in frequency domain

Fig. 5.6 Results of Electrical cabinet only with six steel surfaces

Here are the comparisons between Model 1 and Model 2.

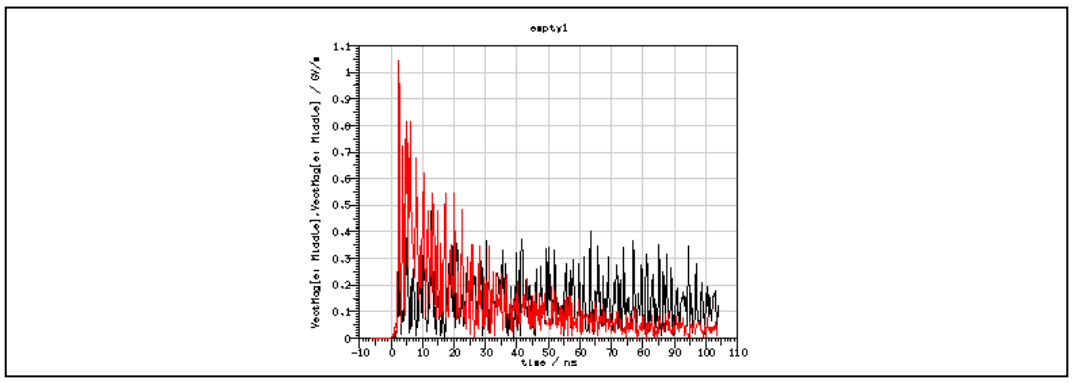

(a) Comparisons of pulse in voltage in time domain

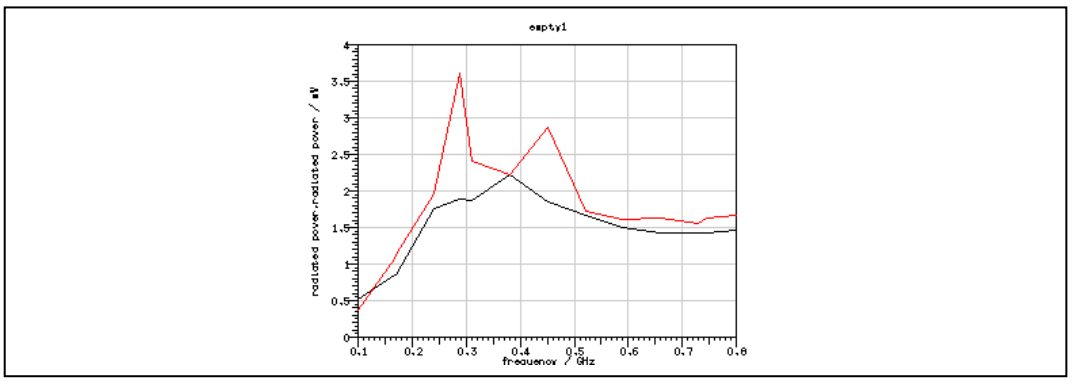

(b) Comparisons of radiated power in frequency domain

Fig. 5.7 Comparisons of results Model 1 and Model 2

From the simulated results, it is observed that having Perspex cover has reduced the shielding effectiveness tremendously. In Figure 5.7, the red signal is that of with Perspex cover and the black signal is with a steel cover instead.

Model 3: Model 1 placed within machine enclosure.

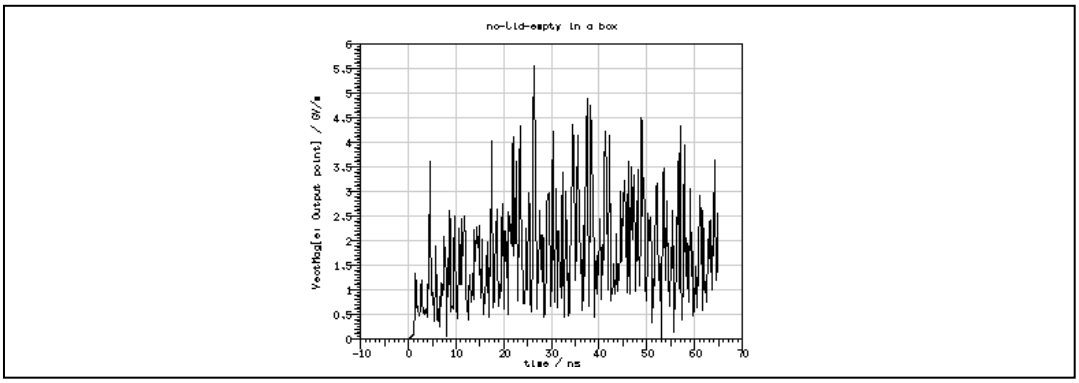

(a) Pulse in voltage in time domain

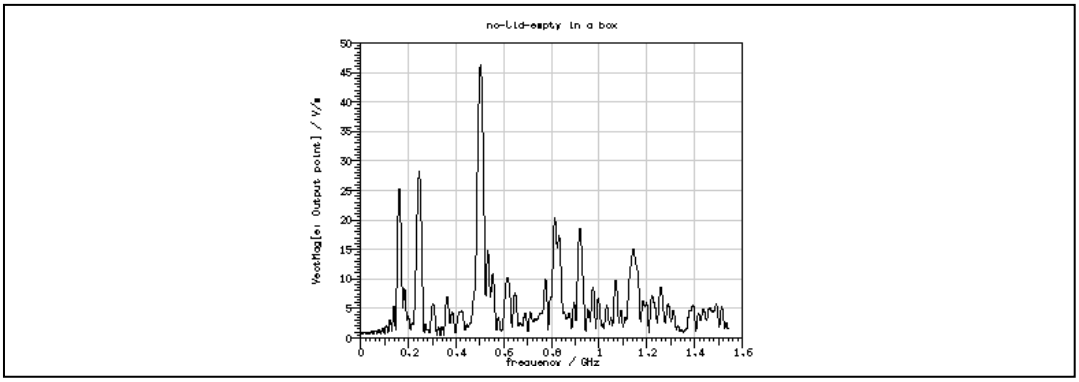

(b) Pulse in voltage in frequency domain

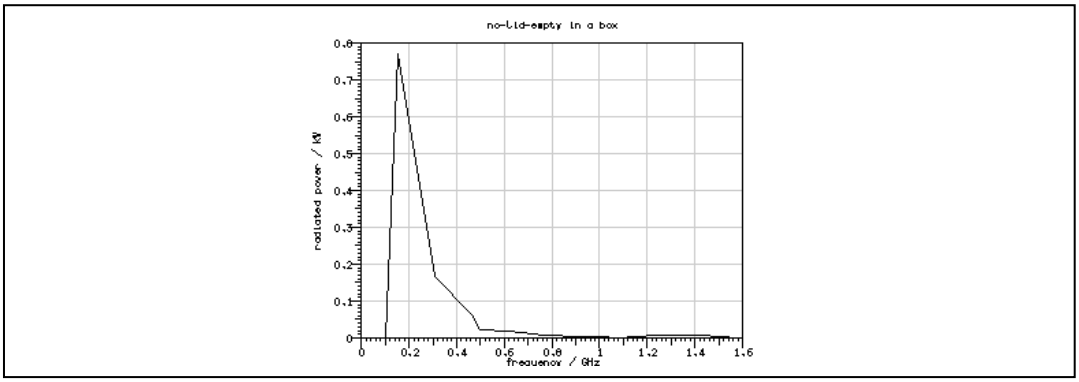

(c) Radiated power in frequency domain

Fig. 5.8 Results of Model 3 within machine enclosure

Model 4: Model 2 placed within machine enclosure.

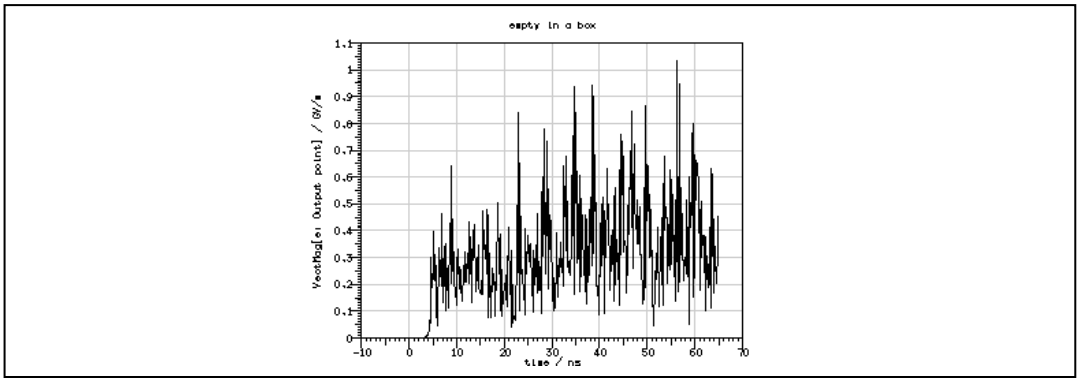

(a) Pulse in voltage in time domain

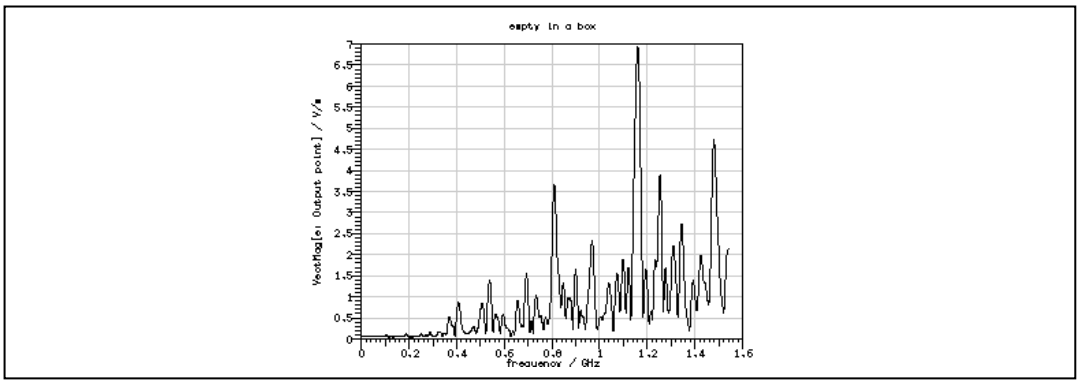

(b) Pulse in voltage in frequency domain

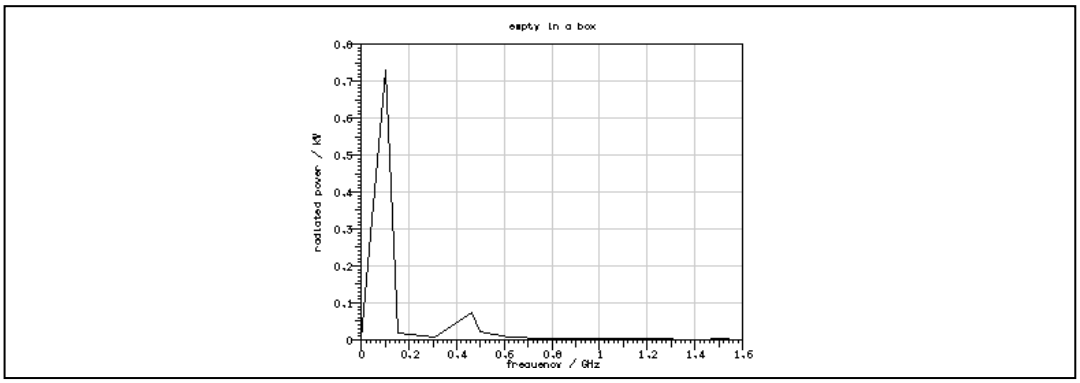

(c) Radiated power in frequency domain

Fig. 5.9 Results of Model 4 within machine enclosure

Here are the comparisons between Model 3 and Model 4.

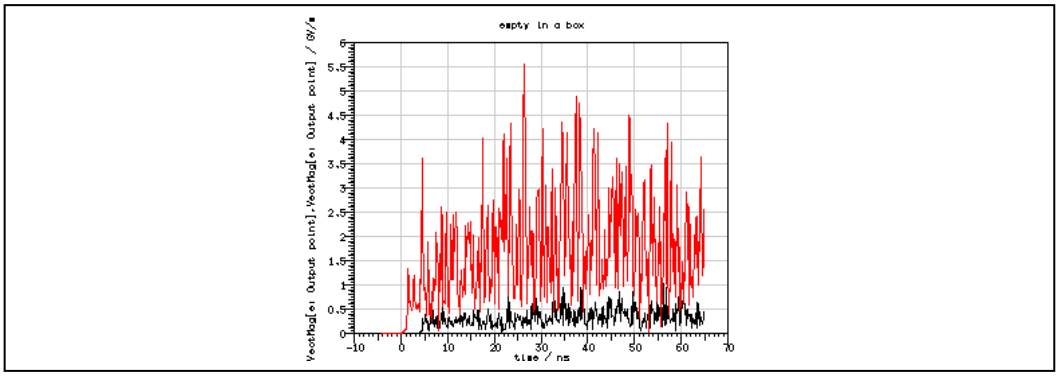

(a) Comparisons of pulse in voltage in time domain

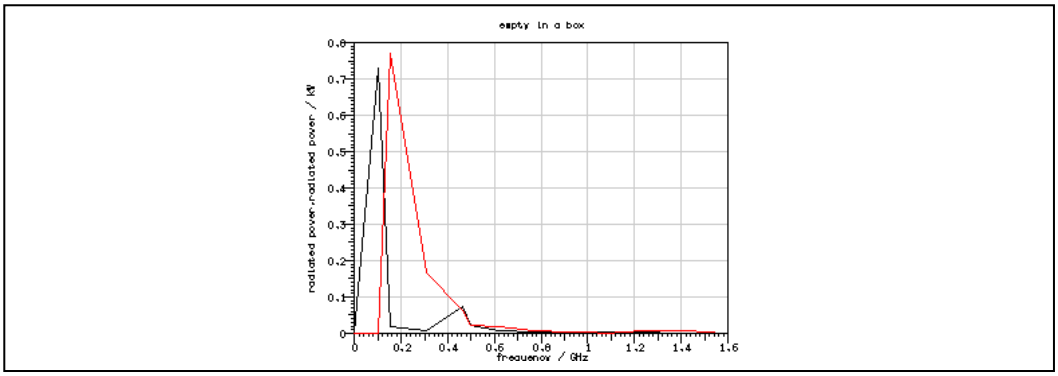

(b) Comparisons of radiated power in frequency domain

Fig. 5.10 Comparisons of results for Model 3 and Model 4

From the simulated results, the shielding effectiveness of Model 1 and Model 2 have increased by placing them in the machine enclosure. In Figure 5.8, the red signal is that of Model 3 and the black signal is for Model 4.

5.4. Thermal Issues

Thermal analysis was done based on the designed arrangements of the equipment as mentioned above. Each equipment that is placed in the electrical cabinet has a recommended ambient operating temperature. Excellent ventilation and cooling system must be implemented to maintain the ambient temperature within the cabinet below the limit.

As mentioned in the Section 5.2.1.3, shielding effectiveness would be compromised if the apertures or vents are too big. The only two big apertures within the cabinet are those to pass through the cables to machine tool. Two additional apertures were created for placement of outlet and inlet fans for cooling.

5.4.1. Thermal Analysis of the Cabinet

A series of thermal analyses were conducted for electrical cabinet. These analyses were conducted with aid of a Computational Fluid Dynamics (CFD) package called EFD Pro8 by Flomerics. This package operates within the Pro Engineer environment.

In the thermal analyses, three parameters will be observed. These parameters are:

- Solid temperature (equipment).
- Fluid flow.
- Fluid temperature.

Several conceptual designs for best cooling and ventilation method will be presented in the next section. With these thermal analyses, fluid temperature, solid temperature, hot spots, etc. could be identified. An important criterion in thermal design is to ensure the air temperature is above dew point so as to avoid condensation (Schulter, 2002).

5.4.2. Conceptual Designs

Three conceptual designs were analyzed. The three ventilation designs are:

- One inlet and one outlet fans with no vents (Type A).
- Two outlet fans with no vents (Type B).
- Two top outlet fans with honeycomb vents (Type C).

The fans' position of the Type A and Type B are the same apart from having one inlet and one outlet fan or two outlet fans. The Type C design has a chimney effect style flow. Figure 5.11 illustrates the three ventilation designs.

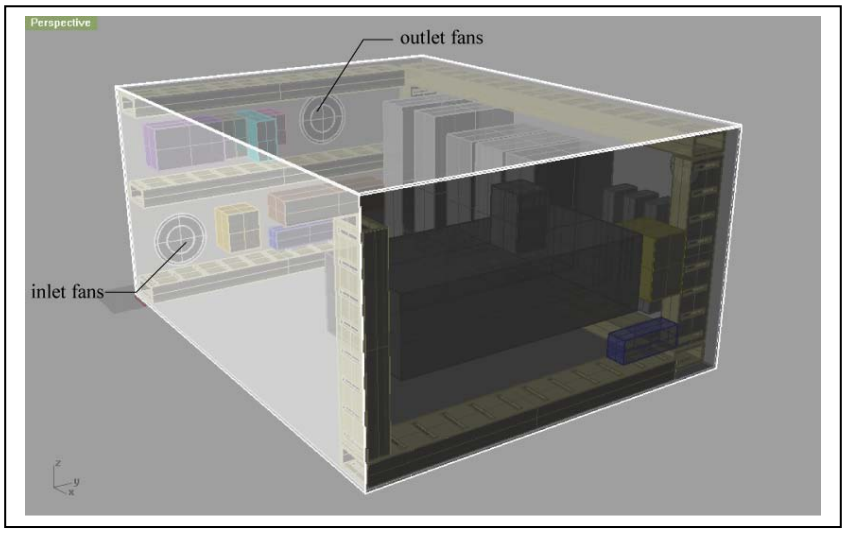

(a) One inlet and one outlet fans with no vents (Type A)

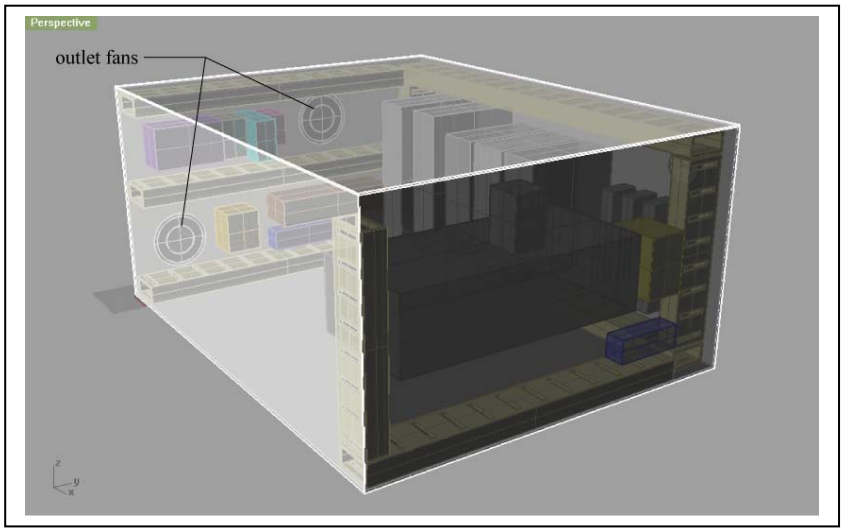

(b) Two outlet fans with no vents (Type B)

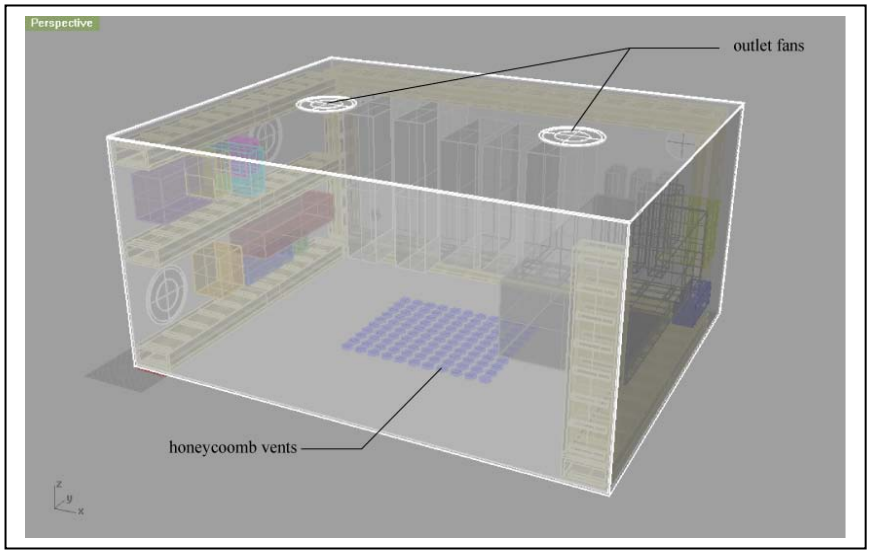

(c) Two top outlet fans with honeycomb vents (Type C)

Fig. 5.11 Three ventilation design of the electrical cabinet

5.4.3. Analysis and Results of the Conceptual Designs

Through the thermal analyses, the fluid temperature, solid temperature and hot spots within the three designs were identified. The hot spots are identified to be at the back position of the cabinet. Here all the motor amplifiers are mounted. These amplifiers generate the most heat compared to the other equipment. In the analyses, the emphasize is to find the best cooling solution especially for the back plate where the amplifiers are located. Table 5.2 illustrates the results from the thermal analyses:

Table 5.2 Thermal analysis results

Design	**Fluid temperature/Celsius**			**Solid Temperature (Back)/Celsius**			**Solid Temperature (Other)/Celsius**		
	min	**avg**	**max**	**min**	**avg**	**max**	**min**	**avg**	**max**
(A)	30.11	35.88	39.56	32.15	36.77	39.67	29.52	31.06	33.89
(B)	43.56	49.84	52.81	43.56	49.84	52.81	34.39	40.03	42.91
(C)	28.07	28.79	30.18	23.942	24.33	25.85	23.77	24.18	24.85

The implemented cooling design was selected based on the lowest temperature for solid and air, good air flow and cost. From the analyses, it was found that Type C has the best cooling design but due to fabrication cost, this design could not be implemented. This

indicates that Type A design will be the next best viable option. Figure 5.12 shows the fluid flow with temperature and equipment temperature for the Type A design.

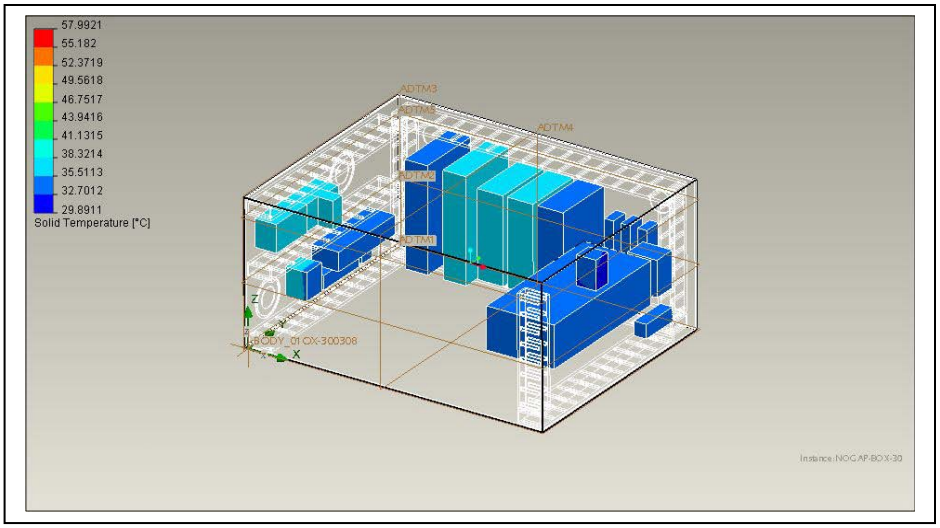

(a) Solid or equipment temperature

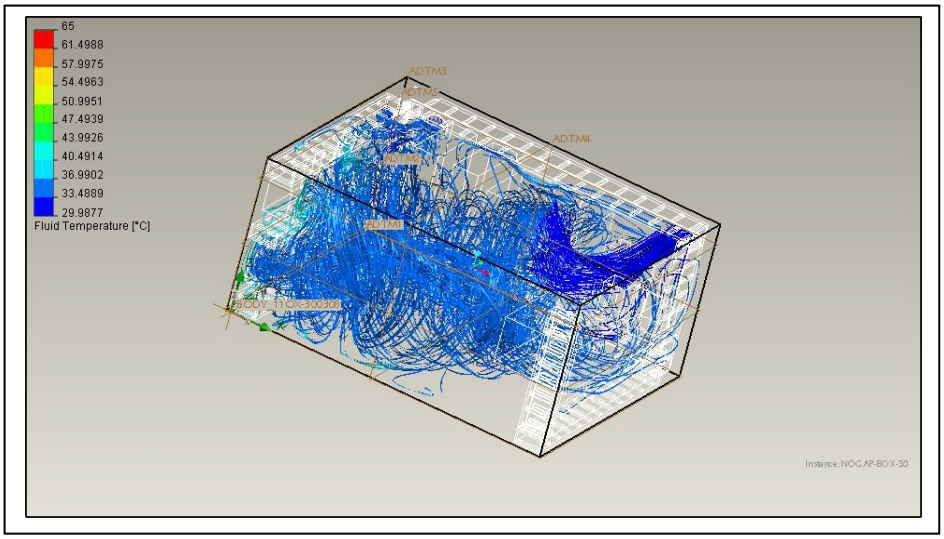

(b) Fluid flow with temperature

Fig. 5.12 Thermal analysis results of design Type A

Validation of the simulated results for Design A was conducted using a digital thermometer. The digital thermometer was placed inside the cabinet and the temperature measured was between 33 ºC to 36 ºC. This coincides with the value obtained from simulation.

5.5. Summary

This chapter has discussed the development and design of control cabinet from the EMC and thermal management viewpoint. The biggest design constraint for this particular cabinet was the size of the cabinet.

From the EMC management point of view, the machine tool did not interfere with other operating equipment in the vicinity. This indicates that even though not all recommendations were follow accurately, the machine tool has observed the design outcome for good EMC management. The simulated results showed the Perspex cover used for the cabinet has decreased the shielding effectiveness.

With the aid of a CFD package, the best cooling option was determined. Thermal analyses could be done accurately in a short time. Although, the best cooling design (with honeycomb vents) option was not selected, the implemented cooling design is sufficient to maintain the machine performance.

Chapter 6

Tuning Strategies for the Direct Drives

6.1. Introduction

In this chapter, the methods of tuning the direct drives will be elaborated. The direct drives that are implemented in the Ultra-Mill are DC brushless motors with air bearings. With aerostatic bearings, these axes are frictionless which would not result in any wear and tear during motion. For the Ultra-Mill, all electromechanical drive systems for each axis are the same. The only differences in the axis are the type of the motors, for example linear or rotary motor, motor electrical characteristics and the load (mass) each motor is accommodating. Figure 6.1 shows the simplified drive system loop that is applied to all the axes.

Proper tuning of the axes ensures high stiffness and excellent disturbance rejection capabilities. Achieving robust, fast and accurate linear motions also depends on the control system involving both hardware and software. Taking stiffness as an example, achieving high stiffness depends on the motor peak force, current available and the feedback resolution in the hardware section. From the software point of view, it depends on the tuning parameters of the servo control algorithms. The aim is high servo stiffness and excellent disturbance rejection capabilities, the axes that hold the cutting tool and workpiece should have minimal positioning error or no deflection of workpiece and cutting tool during engagement.

As stated in (Smith, 2008), the term servo lag is the difference between actual and commanded position. By tuning the motor adequately, the following error is minimized, motor stiffness is increased and directly decreases the servo lag. In multi-axis machine, individual axis error will contribute to the overall machining contouring error and volumetric errors. By ensuring the minimum following error of each individual axis, the contouring and volumetric errors of the machined parts will be therefore reduced and better surface finish obtained.

6.2. Electromechanical Modelling

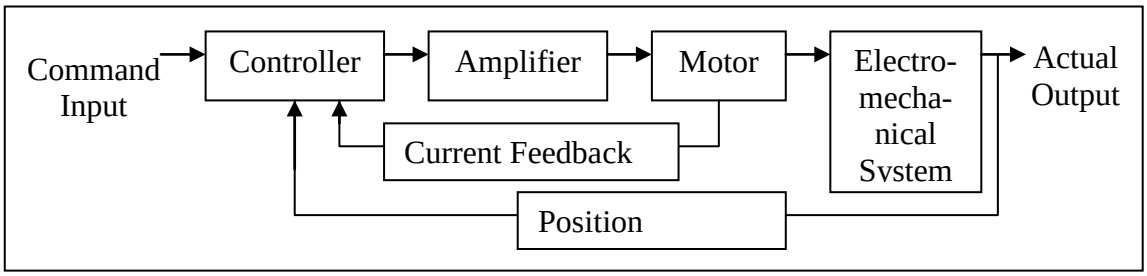

Fig. 6.1 Servo loop of the electromechanical system

The UMAC controller implements a Proportional-Integral-Derivative (PID) plus Feedforward with notch filters servo algorithms for all axes. These axes have a closed loop structure apart from the high speed spindle. Figure 6.2 elaborates the servo algorithms structure and equation 6.1 explains the mathematics of the servo algorithms.

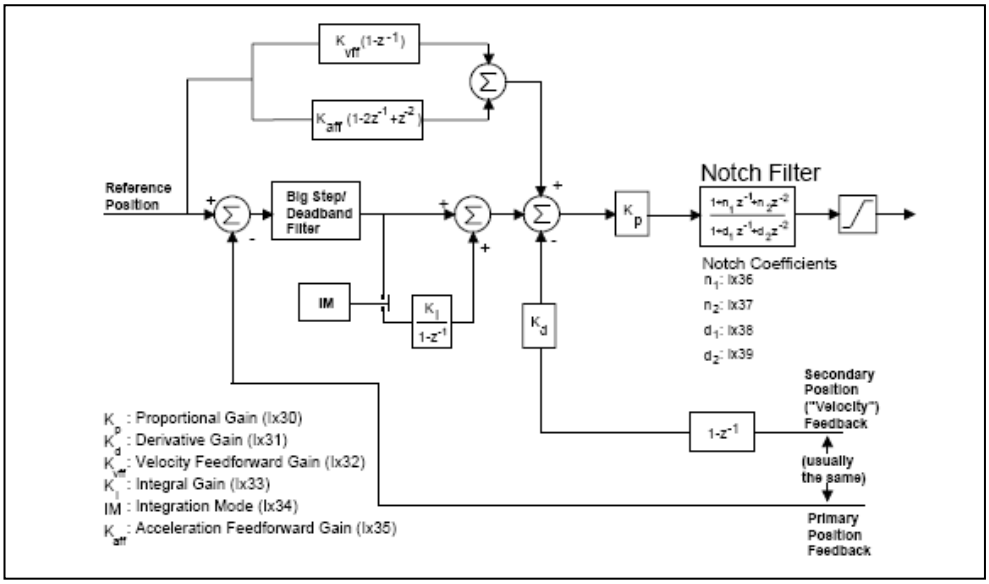

Fig. 6.2 UMAC servo algorithms (Delta Tau, 2008f)

$$CMDout(n) = 2^{-19} * Ixx30 * [\{Ixx08 * [FE(n)+(Ixx32*CV(n)+Ixx35*CA(n))/128 + Ixx33 * IE(n)/2^{23}]\} - Ixx31 * Ixx09 * AV(n)/128] \quad (6\text{-}1)$$

From the equation 6-1, the definition of the constants are listed below (Delta Tau, 2008f):

CMDout(n) is the 16-bit output command in servo cycle n.

Ixx30 is the proportional gain value motor xx.

Ixx08 is an internal position scaling term for motor xx.

FE(n) is the following error in counts in servo cycle n, which is the difference between the commanded position and actual position for the cycle.

Ixx32 is the derivative gain value for motor xx.

CV(n) is the commanded velocity in servo cycle n.

Ixx35 is the acceleration feedforward gain value for motor xx.

CA(n) is the commanded acceleration in servo cycle n.

Ixx33 is the integral gain value for motor xx.

IE(n) is the integrated following error in servo cycle n.

Ixx31 is the velocity feedforward gain value for motor xx.

Ixx09 is an internal position scaling term for motor xx.

AV(n) is the actual velocity in servo cycle n.

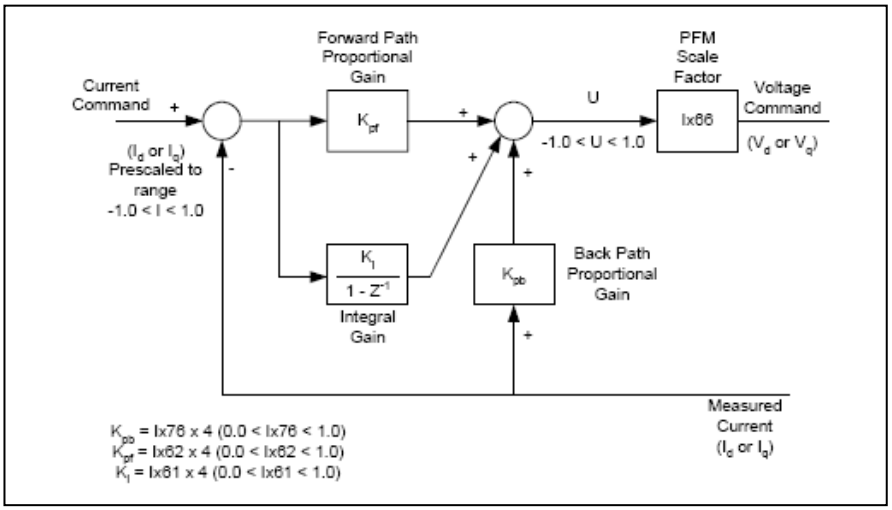

Fig. 6.3 UMAC digital current loop structure (Delta Tau, 2008f)

This would indicate that the electromechanical drive systems would have the identical mathematical model structure for system identification. In the case of Ultra-Mill, all linear axes have the same electrical characteristics apart from the load they are driving and the two rotary axes have different electrical characteristics.

6.2.1. Mathematical Modelling

As mentioned in Chapter 3, the direct drive systems are equipped with aerostatic bearings. By adopting the aerostatic bearings with direct drive system technologies, the electromechanical system has very low or no damping at all (Schmidt, 1997; Schmidt et al, 1999) and is friction free. For the mathematical model, the electromechanical system is modelled as a lump of mass. As mentioned in (Slocum, 1992), aerostatic bearings have absolutely zero static friction and dynamic friction forces are negligible at low speeds (less than 2 m/s).

With the absence of mechanical transmissions, the disturbance (i.e. friction forces, cutting forces, etc.) affects immediately the electromechanical system. For the Ultra-Mill, there are no friction forces acting on the moving parts apart from cutting forces. The primary equation of motion for the drive systems is:

$$K_{Amp} I_M = F_T = M\tilde{v} + Bv + F_d \tag{6-2}$$

K_{Amp}, I_M, F_T, M, $\tilde{v}$, B, υ and F_d represent amplifier gain, current, motor force, mass, acceleration, friction coefficient, feedrate and disturbance force. The motor force is a product of the motor force constant (N/A) and motor current (A_{rms}). Since B = 0, the equation becomes:

$$F_T = M\tilde{v} + F_d \tag{6-3}$$

For DC brushless rotary motor with air bearings provided the term M for mass is changed with J which represents the total inertia. Now the equation should be:

$$T = J\tilde{\omega} + B\omega + F_d \tag{6-4}$$

T, J, $\tilde{\omega}$, B, ω and F_d represent motor torque, total inertia, acceleration, friction coefficient, feedrate and disturbance force. The motor torque is a product of the motor force constant (N/A) and motor current (A_{rms}). Since B = 0, the equation becomes:

$$T = J\tilde{\omega} + F_d \tag{6-5}$$

Figure 6.4 illustrates the mathematical model of servo loop of the direct drive system. This is derived from Figure 6.2 and 6.3.

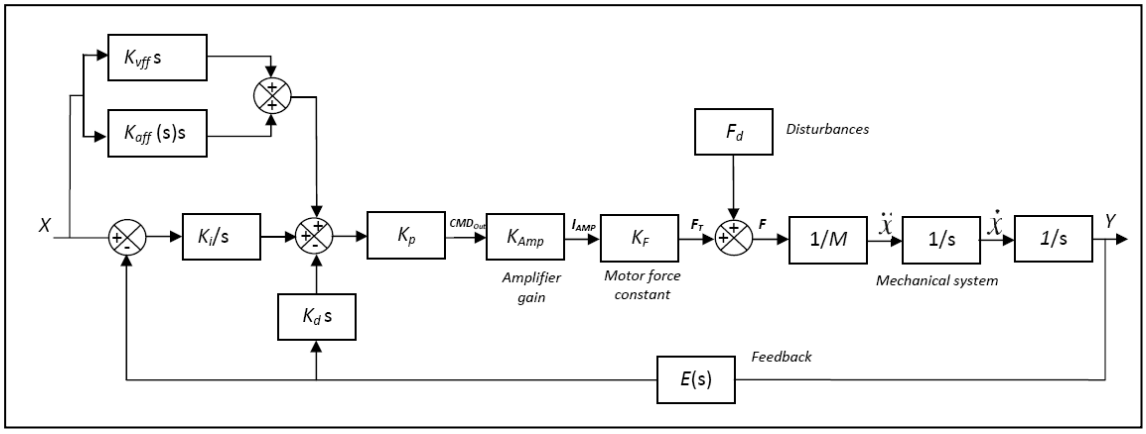

Fig. 6.4 Mathematical model of the servo loop

From Figure 6.4, transfer functions with feedforward controller and without feedforward controller could be derived. The feedforward controller consists of the velocity feedforward and acceleration feedforward controllers.

(a) Mathematical transfer functions with feedforward controller.

Let $K_{vff}\,s + K_{aff}(s)s = G_{FF}(s)$

$$\frac{Y(s)}{X(s)} = \frac{(K_i + G_{FF}s(s))K_pK_{Amp}K_F}{Ms^3 + (K_i + K_ds^2)K_pK_{Amp}K_FE(s)} \tag{6-6}$$

$$\frac{Y(s)}{F_d(s)} = \frac{s}{Ms^3 + K_iK_pK_{Amp}K_F\left(1 + \frac{K_d}{K_i}\right)E(s)} \tag{6-7}$$

(b) Mathematical transfer functions without feedforward controller.

$$\frac{Y(s)}{X(s)} = \frac{K_iK_pK_{Amp}K_F}{Ms^3 + (K_i + K_ds^2)K_pK_{Amp}K_FE(s)} \tag{6-8}$$

$$\frac{Y(s)}{F_d(s)} = \frac{s}{Ms^3 + (K_i + K_ds^2)K_pK_{Amp}K_FE(s)} \tag{6-9}$$

G_{FF}, K_p, K_i, K_d, K_{vff}, K_{aff}, K_{Amp}, K_F, CMD_{Out}, I_{Amp}, F_T, F_d, M, and $E(s)$ represent gains for feedforward, proportional, integral, derivative, velocity feedforward, acceleration feedforward, amplifier, motor force constant, controller command output, amplifier current, thrust force, disturbance force, mass of moving part and feedback. Equation 6.7 and 6.9 represents the servo stiffness.

6.2.2. Electromechanical Modelling in Matlab/Simulink

The mathematical model that was derived from the previous sections is now converted into Matlab/Simulink in the form of block diagrams for simulation purposes. The simulation is used to assess how the servo loop performs.

The model uses discrete Z-transformation with the sampling period equal to the real servo interrupt frequency.

Figure 6.5 illustrates the electromechanical drive system servo loop modelled in Matlab's Simulink environment.

In Figure 6.6, "PID Discrete" block represents the controller which contains the PID plus feedforward structure. The "Plant" block represents the electromechanical drive system including the current loop in described in Figure 6.6.

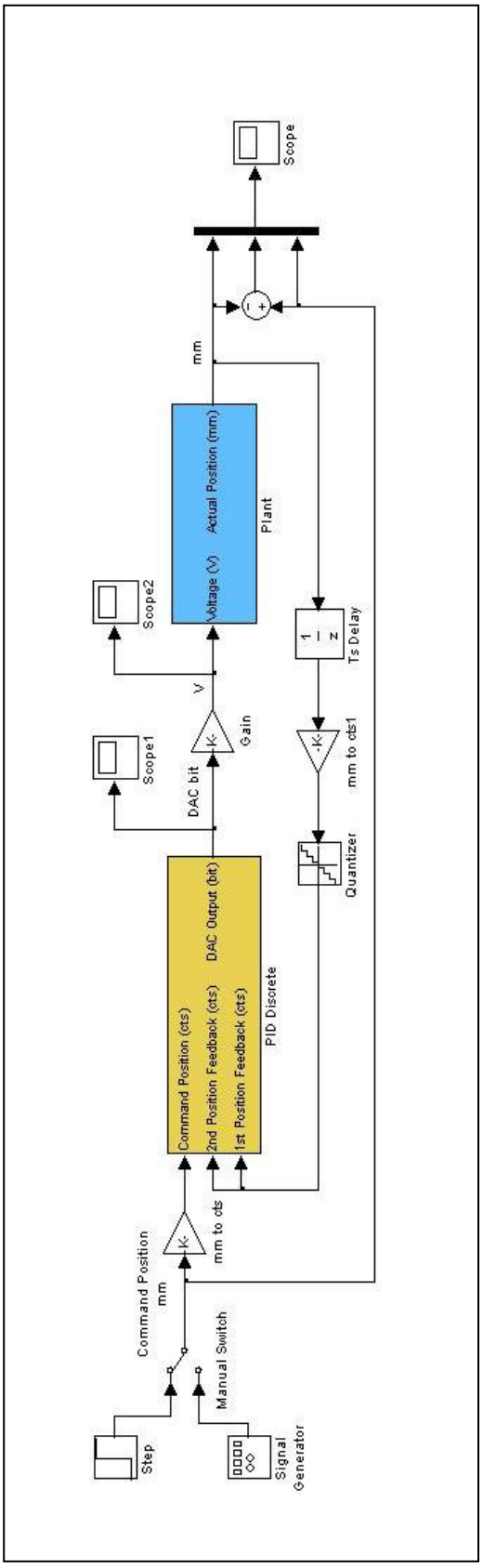

Fig. 6.5 Simplified model of the electromechanical drive system in Simulink environment

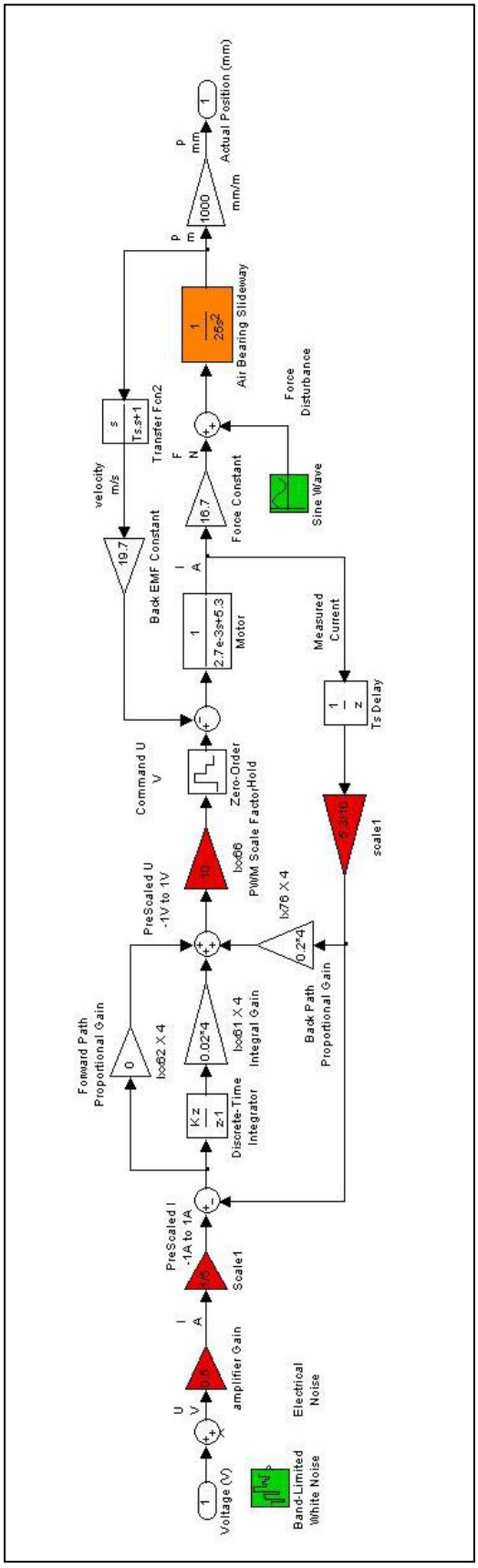

Fig. 6.6 Model of the current loop and the electromechanical drive system

6.3. Tuning Procedures

There are steps in tuning the UMAC's PID plus feedforward servo algorithms. Most controllers used in machine tools currently have an auto-tuning function. Most engineers would utilize the auto-tuning utility initially. Auto-tuning is frequently seen as a means to formulate servo tuning more scientific and repeatable but in the real world, this is hardly ever the situation. The automatic tuning utility does not provide the best tuning parameters but it provides the starting parameters. To obtain the best parameters, manually tuning the servo algorithms is needed but this is time consuming. Figure 6.7 illustrates the tuning procedures. During the tuning procedures, for the step response, the key parameters observed are rise time, overshoot and settling time and for the parabolic response, the key parameter of concerned is the maximum following error.

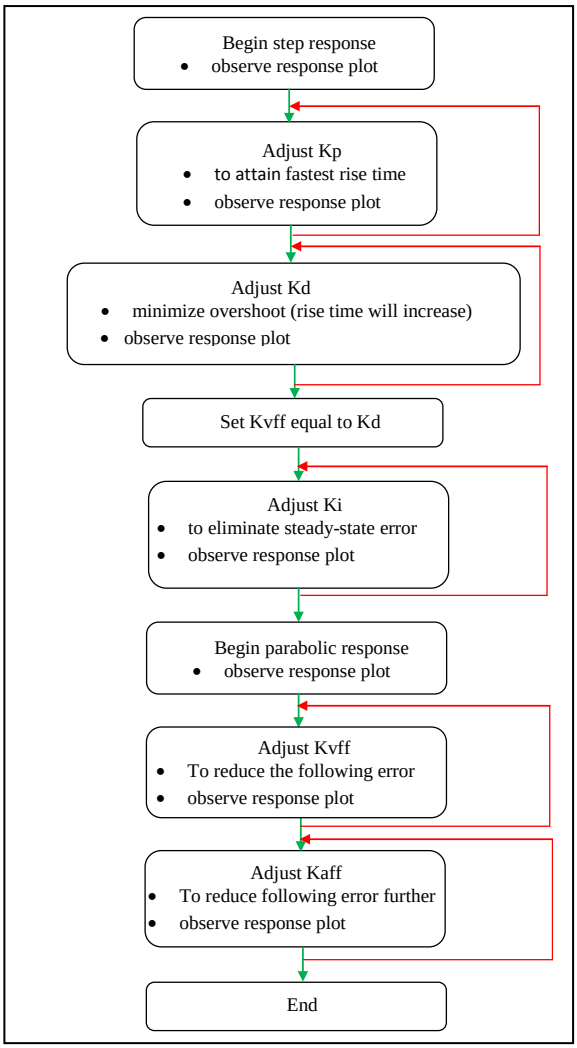

Fig. 6.7 Tuning steps

In the step response tuning, the variables K_p, K_i and K_d are tuned so as to achieving fastest response time, minimal overshoot and eliminating steady-state error. Decreasing the overshoot will result in rise in response time. Once the K_p and K_d parameters are fixed, the dynamic response of the system has been taken care of. By adjusting the K_i will make the system more responsive but overshoot will reappear but the dynamic response will not be disturbed.

In the parabolic response tuning, the variables K_{vff} and K_{aff} are tuned so as to minimizing the following error the correlation between the velocity and acceleration. If the velocity correlation is minimized, the acceleration correlation will increase. If the acceleration correlation is minimized, the velocity correlation will increase. Even though this happens, the following error will still be small.

6.4. PID Tuning

In the tuning sections, discussion will concentrate on the tuning of the linear axis. The tuning method is the same for all five axes and therefore this discussion will be based on tuning for just one direct drive system. The tuning principles and aims of the tuning are identical for all five axes.

Firstly, tuning with a step move will be done using the model in the Simulink environment shown in the earlier sections. In this section, tuning of PID algorithm will be elaborated.

Here the P, I and D tuning parameters are involved. The best combinations of these parameters are selected based on rise time, overshoot, settling time, etc. from the response of the step move input for the axis. From the step move input, tuning the P, I and D parameters so as to the axis is sensitive, high disturbance rejection, non-sluggish, low tracking error etc. in terms of motion and positioning performance.

After the step move, parabolic move was used to observe the tracking error of the axis. When undergoing parabolic move test, if the tracking error is still unacceptable, the tuning process must be repeated until good motion and position performance is achieved.

6.4.1. Performance Evaluation

Based on the tuned parameters, the best combination of parameters was selected based on the tracking error performance. The smaller the following error (FE), the stiffer the axis is and hence provides excellent disturbance rejection abilities.

Table 6.1 Performance with parabolic move

P gain	I gain	D gain	Max. FE/counts	Max. FE/um
26258	16380	20958	93.4707	14.60479688
50000	20000	30000	109.9496	17.179625
60000	50000	20000	36.2467	5.663546875
60000	100000	20000	21.929	3.42640625
100000	100000	6000	7.7207	1.206359375
200000	100000	5000	5.2227	0.816046875
300000	100000	4000	4.8184	0.752875
300000	100000	6000	4.9691	0.776421875
400000	100000	4000	4.1445	0.647578125
500000	100000	3000	error	#VALUE!

From Table 6.1, the blue region contains the gains that were obtained from autotuning. The yellow region indicates the best tuning gains accepted. The red region shows where the instability of the motor occurs. Figure 6.8 and Figure 6.9 illustrate the following error from autotuning and the accepted tuning gains.

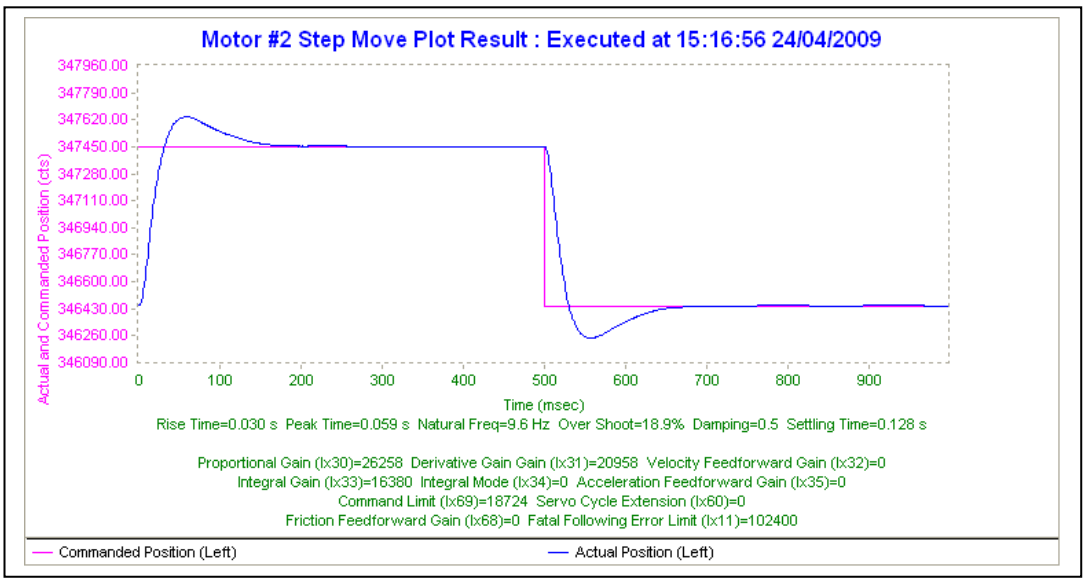

(a) Step move

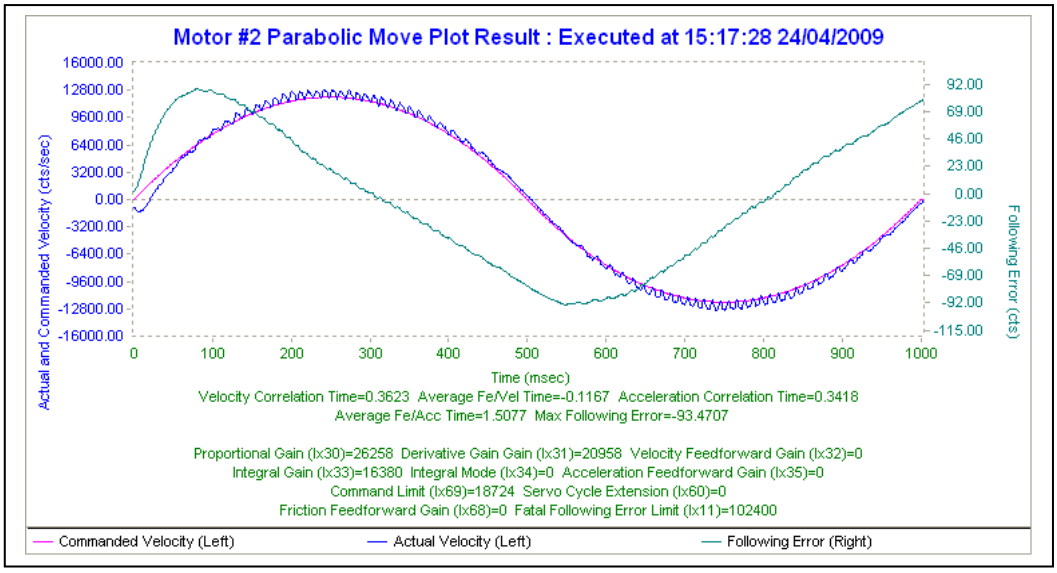

(b) Parabolic move

Fig. 6.8 Following error from autotuning gains

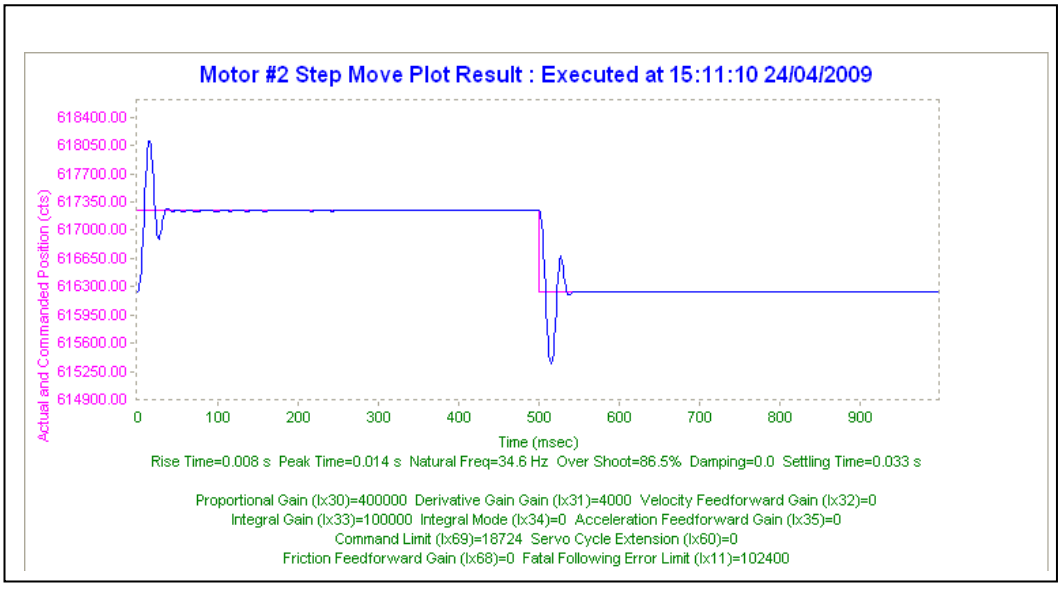

(a) Step move

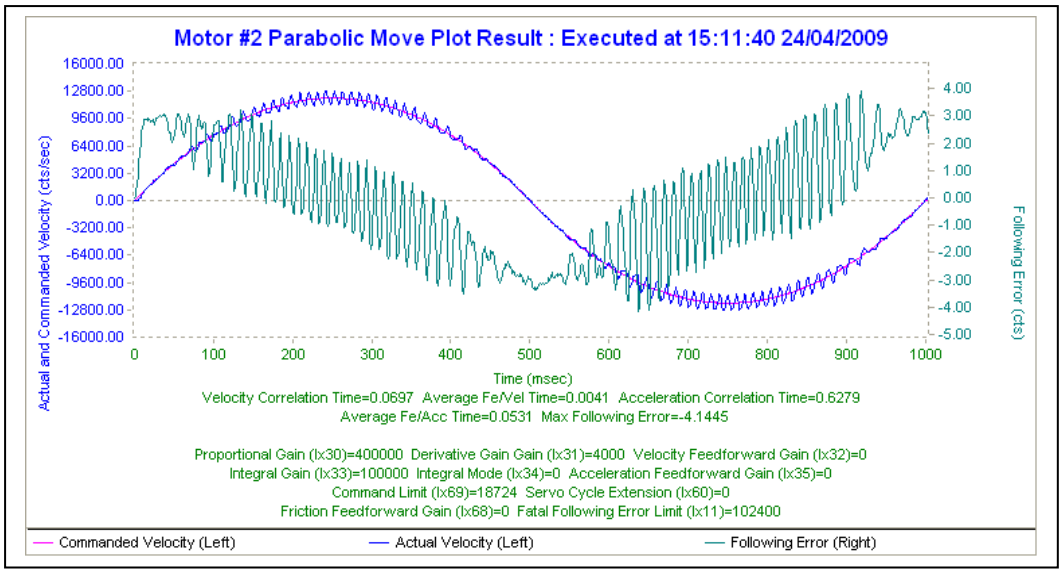

(b) Parabolic move

Fig. 6.9 Following error from accepted tuning gains

6.5. PID plus Feedforward Tuning

Secondly, tuning with a step move will be done using the model in the Simulink environment shown in the earlier sections. In this section, tuning of PID plus feedforward algorithm will be elaborated.

Here the P, I, D, Vff and Aff tuning parameters are of concerned. The best combinations of these parameters are selected based on rise time, overshoot, settling time, etc. from the response of the step move input for the axis. From the step move input, the tuning purpose is exactly the same with tuning the P, I and D parameters. The feedforward parameters will help to decrease the tracking error of the axis.

After the step move, parabolic move was used to observe the tracking error of the axis. When undergoing parabolic move test, if the tracking error is still unacceptable, the tuning process must be repeated until good motion and position performance is achieved.

6.5.1. Performance Evaluation

Based on the tuned parameters, the best combination of parameters was selected based on the tracking error performance. The smaller the following error, the stiffer the axis is and hence provides excellent disturbance rejection abilities.

Table 6.2 Performance with parabolic move

P gain	I gain	D gain	Vff gain	Aff gain	Max. FE/counts	Max. FE/um
30000	100000	6000	1000	10000	4.4141	0.689703125
30000	100000	6000	2000	20000	4.2191	0.659234375
30000	100000	6000	3000	30000	3.9105	0.611015625
30000	100000	6000	4000	40000	3.8652	0.6039375
30000	100000	6000	5000	50000	3.8079	0.594984375
30000	100000	6000	6000	60000	3.5215	0.550234375
30000	100000	6000	500	5000	4.7936	0.749
30000	100000	6000	700	7000	4.5941	0.717828125
30000	100000	6000	800	8000	4.4105	0.689140625
30000	100000	6000	900	9000	4.2344	0.661625

Table 6.2 shows the tuning gains used to evaluate the motor performance. The gains in the yellow region are implemented in the motor based on the smallest following error obtained. Figure 6.10 illustrates following error from the implemented tuning gains.

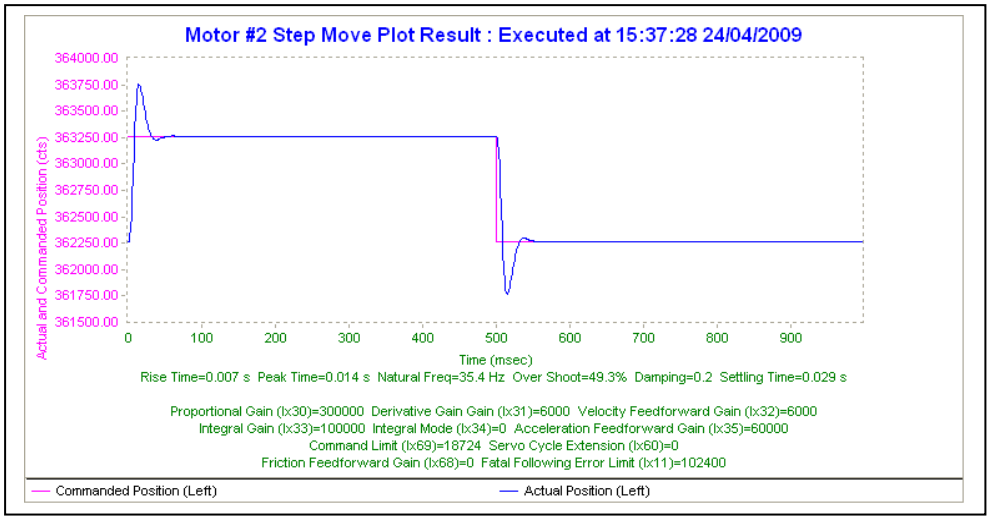

(a) Step Move

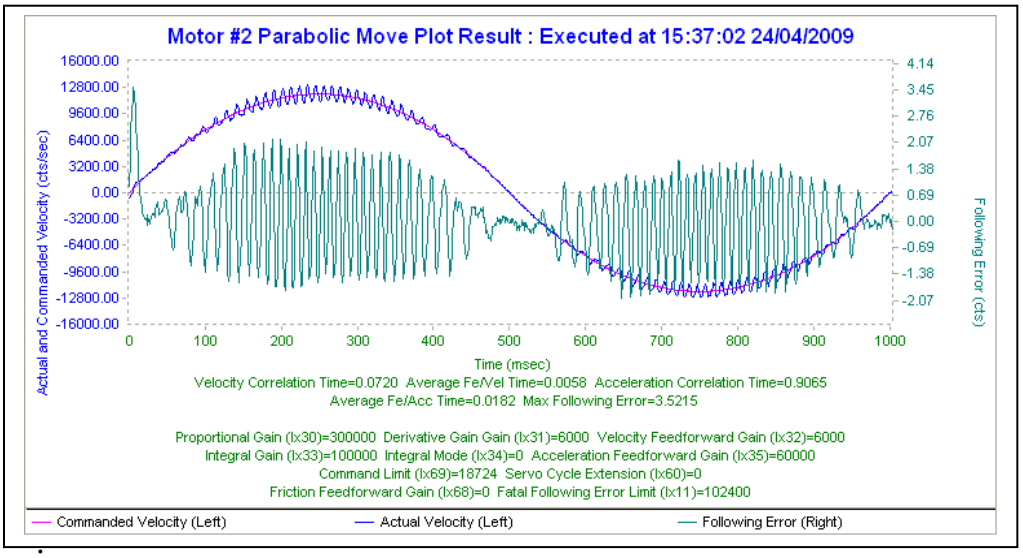

(b) Parabolic move

Fig. 6.10 Following error from the implemented tuning gains

6.6. Proposed Tuning Method

In this section, a fast method of servo tuning is discussed. The proposed tuning method uses Matlab's Simulink Design Optimization which includes the Parameter Estimation and Response Optimization toolboxes.

Firstly the Parameter Estimation toolbox will be used to aid estimate any unknown model parameters. Unknown parameters are estimated using measured data from real setup and data generated by the Simulink model itself. This toolbox is able to approximate model parameters or initial conditions of any single or multiple models using transient data (Matlab, 2009a).

Secondly, Parameter Optimization toolbox will be employed to help obtained best parameters based on the constraint set on the desired responses. This toolbox optimizes parameters for a time domain design characteristics (i.e. step response behaviour, lower or upper bound signals, reference signal, etc.) (Matlab, 2009a). Here the toolbox formulates the time-domain characteristics as constrained optimization problems. In the optimization process, the toolbox simulates the simulink model and compares the simulated data with constrained objectives.

6.6.1. Modeling Optimization

In order to get the modeling as accurate as possible, the Parameter Estimation tool was firstly used. The model of the controller is assumed as accurate as the model was constructed based on the mathematical equation representing the controller (Delta Tau, 2008f). For the plant, we could not assume the model is accurate as there are some modelling uncertainties

Enhancing the accuracy of the plant model, data were collected by running a couple of tuning procedures on the physical setup. Step move and parabolic move were conducted on the actual system and the data from the move were acquired. A flow chart of the optimization procedures is shown in Figure. 6.11.

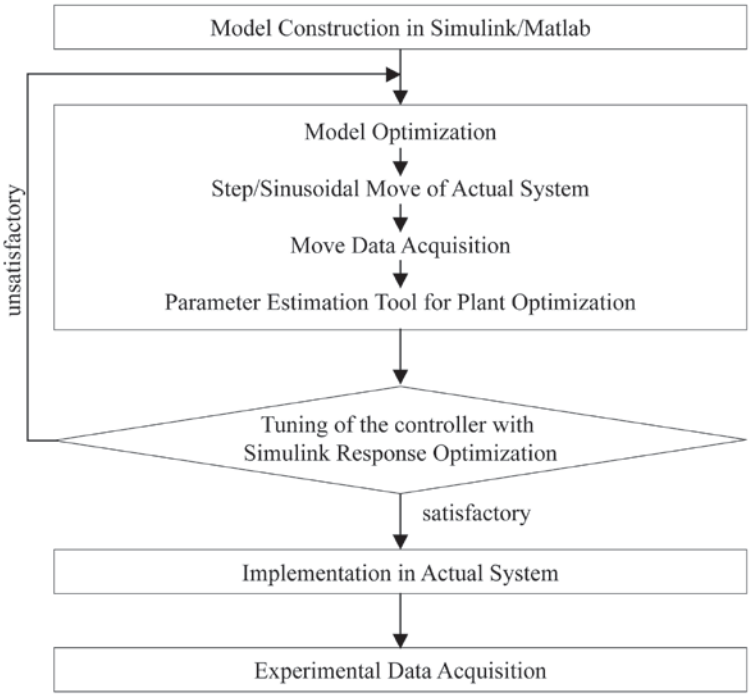

Fig. 6.11 Optimization flowchart

In the system identification stage, the plant is treated as a grey box. The grey box (includes the current loop and the electromechanical drive system) consists of the plant transfer function with unknown constants which would be identified using the Parameter Estimation tool. The collected data are the input and output signals of the plant. These data would help to identify the parameters within the plant transfer function. These unknown constants that would be obtained using the Parameter

Estimation tool must match each other for the step and parabolic moves input into the plant. Figure 6.12 illustrates the procedure in identifying the unknown constants. Identification of the plant constants is essential. Once the plant constants are known, the next stage would be tuning the controller.

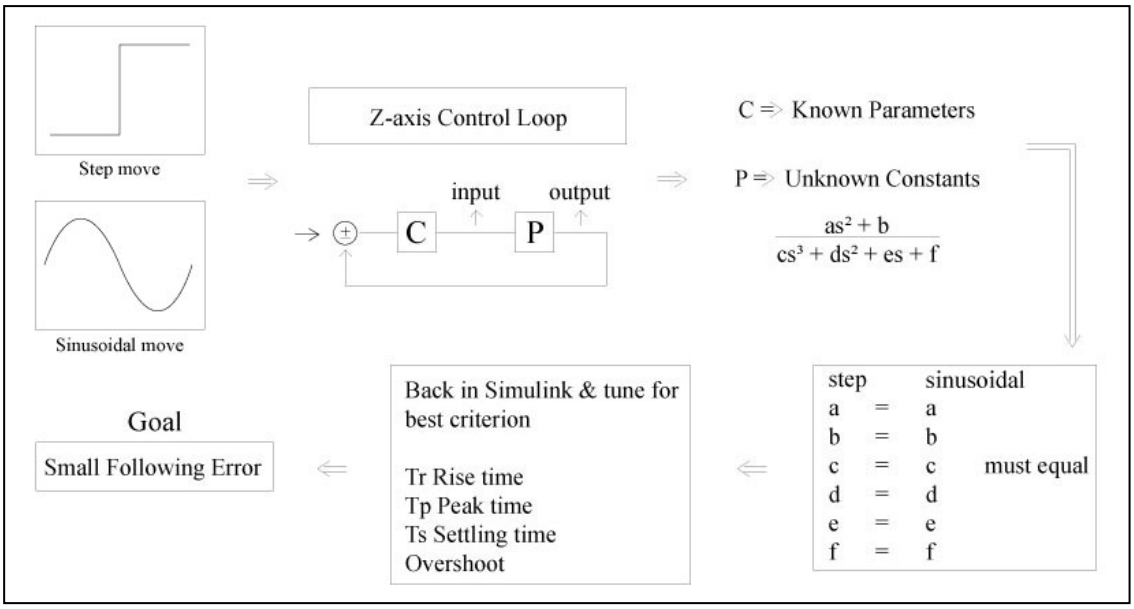

Fig. 6.12 The identification process for unknown plant constants

6.6.2. Controller Tuning using Parameter Optimization Toolbox

The controller is tuned using the Signal Constraint block under Simulink's Parameter Optimization toolbox. As stated in section 6.6, the signal constraint module helps to identify the parameters within the controller based on the design requirements i.e. rise time and overshoot, etc. The signal function used to tune these parameters is the step input function. Figure 6.13 illustrates the controller tuning using the Signal Constraint block.

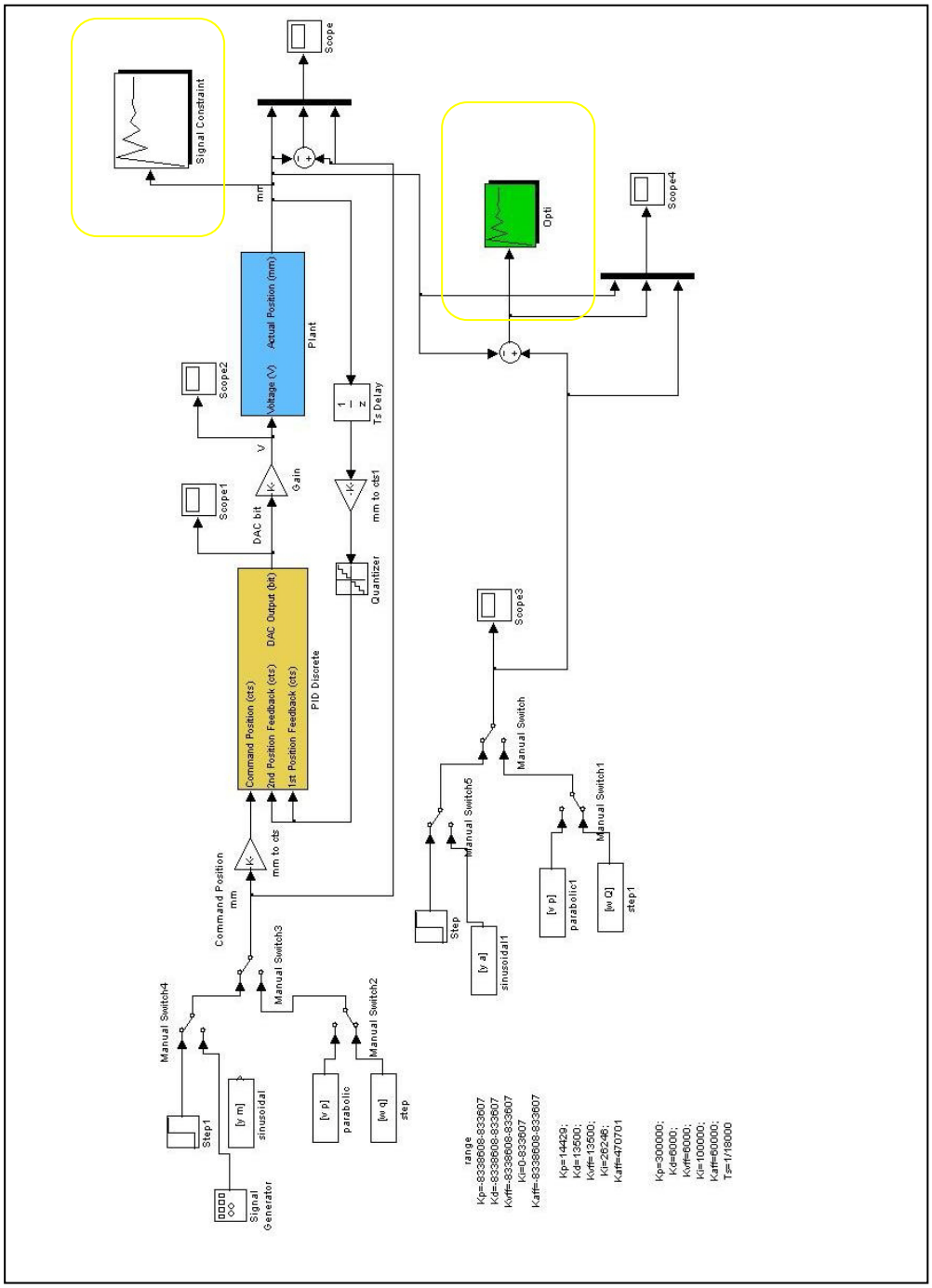

Fig. 6.13 Controller tuning using the signal constraint block

The Signal Constraint block or Parameter Optimization toolbox have different optimizing algorithms to tune the parameters based on the constraint set. Various algorithms have been tested to optimize the tuned parameters and genetic algorithm (GA) has been chosen as best results have been achieved compared to the other algorithms. Another important point in this optimization part is the number of iterations. The bigger the iteration, the better tuned parameters will be obtained. The acceptable PID plus feedfoward parameters must not exceed the permitted values limited by the controller of the actual physical system.

The PID with the feed forward parameters is tuned to achieve the smallest possible following error. As stated in (Smith, 2008), the term servo lag is the difference between actual and commanded position. By tuning the motor adequately, the following error is minimized, motor stiffness is increased and directly decreases the servo lag. In multi-axis machine, individual axis error will contribute to the overall machining contouring error and volumetric errors. By ensuring the minimum following error of each individual axis, the contouring and volumetric errors of the machining will be therefore reduced and better surface finish obtained.

6.6.3. Performance Assessments

Experiments of the proposed method are conducted on linear axis of 3-axis diamond turning machine as shown in Figure 6.14. The linear axis is identical to that of the linear axes of Ultra-Mill, DC brushless with air bearings. During the cutting experiments, face cutting of aluminium component is carried out through well-designed cutting protocols. As part of the assessment protocol, three cutting trial (face cutting) were conducted. Three face cutting experiments conducted:

- **Cutting Trial 1**: Parameters obtained from the auto-tuning function of the controller.
- **Cutting Trial 2**: Parameters obtained by manually tuning the controller after using the auto-tuning function.
- **Cutting Trial 3**: Parameters obtained using the proposed method.

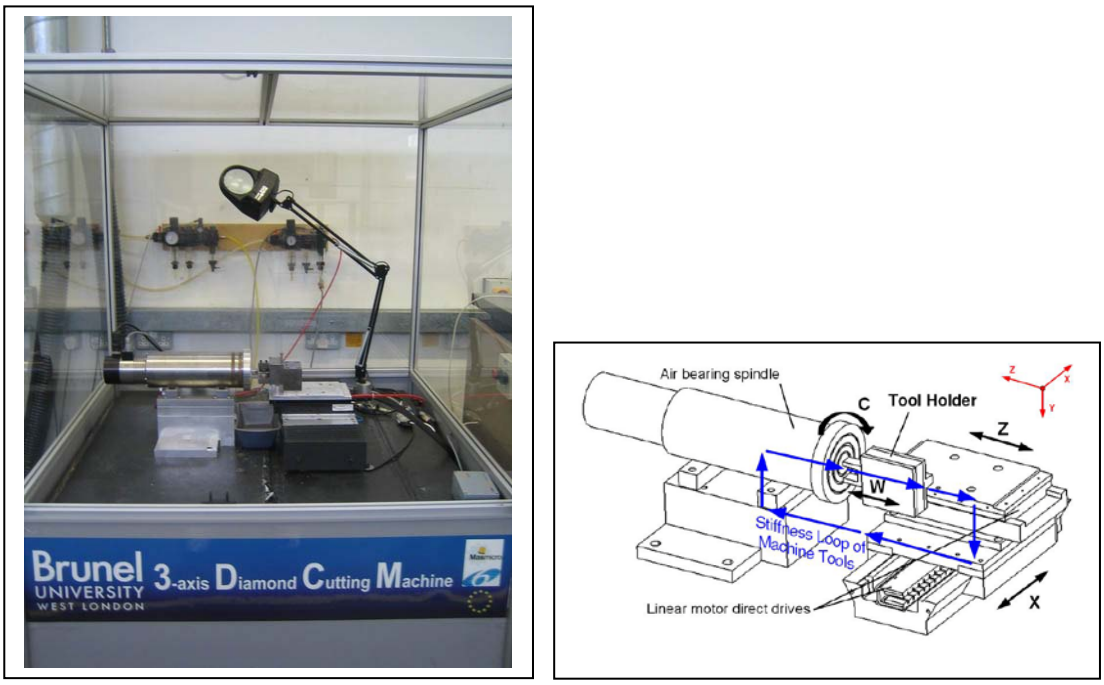

(a) The 3-axis diamond turning machine developed at Brunel

(b) Illustration of the linear motor direct drives on the machine.

Fig. 6.14 3-axis diamond turning machine

The reasons why the performance assessments were conducted on the 3-axis diamond turning machine are:

- 3-axis diamond turning was setup as a testbed to understand the subsystems.
- This testbed was completed well before the Ultra-Mill.
- Linear axes used in 3-axis diamond turning machine are identical to that of linear axes of Ultra-Mill apart for the load each slide is accommodating.

For these three cutting experiments, all the machining conditions are the same with the depth of cut, feed rate and spindle speed being 5 µm, 10 µm/rev and 3,000 rpm except for the parameters applied in the PID with feed-forward algorithms.

For assessments of the selected tuning parameters, a 50 nm and 100 nm step move was conducted to observe the following errors. Figure 6.15 illustrates the step moves.

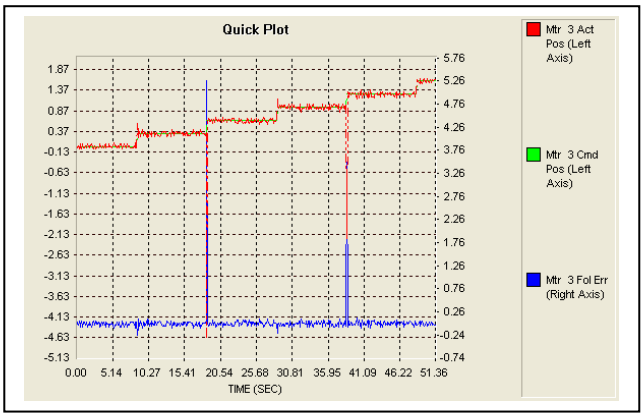

(a) 50 nm step move

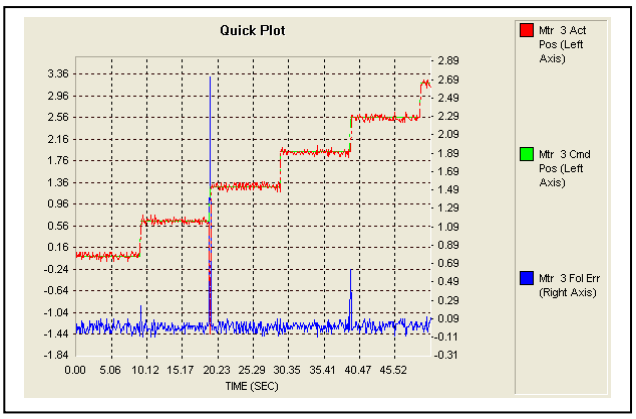

(b) 100 nm step move

Fig. 6.15 Step move of 50 nm and 100 nm

In Figure 6.15, red signal represents actual position, green signal represents commanded position and blue signal represents following error. The green signal is not really visible in the graph due to the small deviation between the actual and commanded position. From these step moves, the following error obtained is ±15.625 nm.

6.6.4. Surface Roughness Machined

Figure 6.16 shows the surface roughness on the three face-turned components, measured by using a Zygo 3D Surface Profiler. The measured surface roughnesses on the three components are 15 nm, 9 nm and 6 nm Ra respectively. The lowest surface roughness (6 nm Ra) obtained is through using the proposed tuning method. The 15 nm Ra and 9 nm Ra surface roughness is achieved using parameters obtained by auto-tuning method only and manually tuning the controller after using the auto-tuning function.

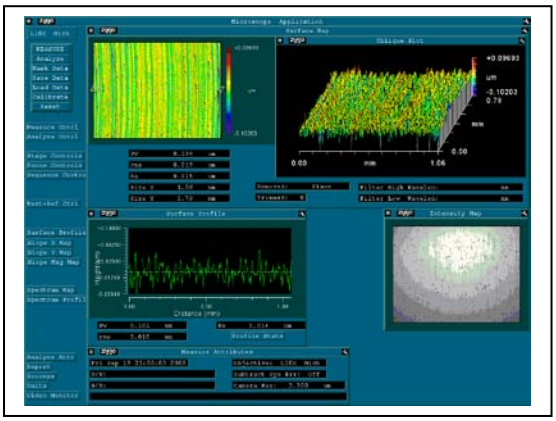

(a) 15 nm Ra

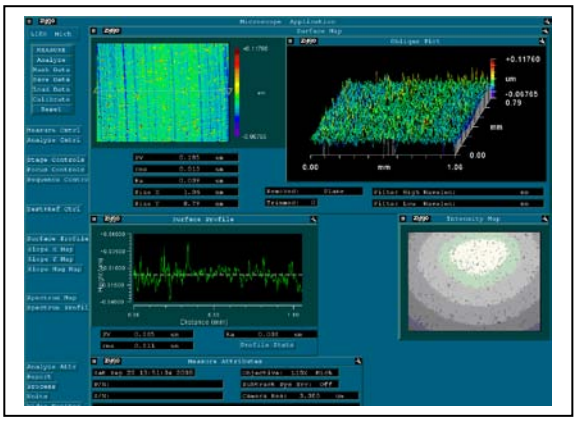

(b) 9 nm Ra

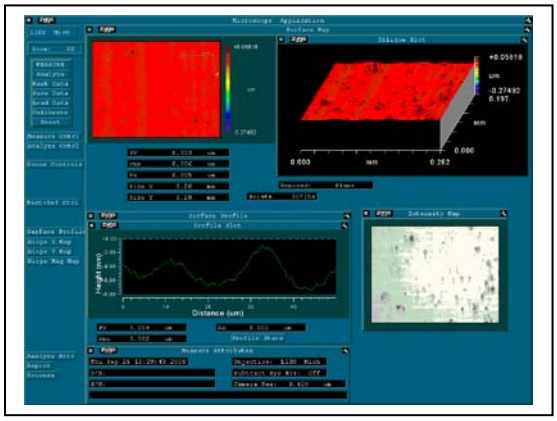

(c) 6 nm Ra

Fig. 6.16 Component surface roughness measured by a Zygo 3D Surface Profiler

6.7. Summary

This chapter has described the requirements of adequate servo loop tuning. The performance of the servo loop tuning is reflected directly in the accuracies and surface finishes of workpieces. As mentioned earlier, servo tuning is a time consuming process even for the experts.

This chapter has also showed the possibilities of making the servo tuning task slightly simpler and faster using a Computer Aided Control Engineering tool such as Matlab. In adopting this method, the hope of obtaining the best tuning parameters that are relevant and useable in the actual physical system lies in how well the electromechanical system is modelled.

This proposed method was validated via well structured experimental setup. The results

obtained were encouraging. Even though the experiments were conducted on the 3-axis diamond turning machine, as mentioned earlier, all the slide systems are identical to that of the Ultra-Mill and therefore this method is directly applicable to it.

Although there might be some overshoot in the system, this does not mean the system is inadequate or unstable. In reality, some overshoot does exist in systems and at times making it more stable and more responsive.

Chapter 7

Control for Microhandling and Tool Condition Monitoring

7.1. Introduction

This chapter will discuss further the design and implementation of the two topics, microhandling and tool condition monitoring systems. The first discussion in this chapter is on microhandling and the second discussion will be on tool conditioning monitoring systems. Ultra-Mill machines miniature parts or components using microtools**.** These tools have diameters less than 1 mm. In a typical machine tool, there is an automatic tool changing (ATC) system and the tools are inserted into a toolholder. This enables the tool changing process to be done automatically and fast.

Ultra-Mill does not have a tool changing system and the tool is directly inserted into the high spindle collet system manually. The tool changing system was not included in design specification of the machine. To assist with tool changing, the decision of implementing a SCARA robot was taken. The SCARA robot is needed to load and unload cutting tools and workpieces to the machine tool. A tool magazine is placed outside the machine guard.

Furthermore the SCARA robot is utilized for loading and unloading of workpieces in the machining envelope to and from the workpiece magazine which is also located. Handling miniature components or parts by hand is strictly avoided as this could damage the machined parts. The SCARA robot is able to maintain constant gripping forces throughout the process of loading and unloading.

Tool condition monitoring (TCM) system is very important to assure the quality of parts produced. The tool condition monitoring system tracks the tool wear and tool failure or breakage. The monitoring of tool wear or tool breakage could reduce the cost of machining parts with bad surface finish or the time spent continuing air cutting when the tool is already broken. The tools used on Ultra-Mill are not easily inspected or judged with the naked eye. When using coolant in machining, it makes it even more difficult for the operator to detect tool breakage.

There are two kinds, online and offline, of tool monitoring systems. In this thesis, monitoring the tool using a non-contact tool setting and detection system is categorized as an offline method. Even though the tool checking sequence is included in the NC program, the checking of the tool is done away from machining process while the tool and the workpiece are not in contact. The online method is more preferable. This enables the system to monitor for tool wear or tool breakage continuously during machining. The differences will be discussed in depth later in this chapter. Comparison tests were conducted to evaluate the best implementation solution.

7.2. Microhandling System

The microhandling system was designed by Carinthian Tech Research AG (CTR) from Austria and the system was implemented by Brunel on the Ultra-Mill with the help of Carinthian Tech Research AG (CTR) from Austria. This company was a partner in the Masmicro research project in developing the Ultra-Mill. The microhandling system consists of a SCARA robot from EPSON. The task of the robotic arm is to load and unload the tools and workpieces to and from the Ultra-Mill.

Microhandling system using a robotic arm is normally categorized as a flexible manufacturing system (FMS). Industries implement robot handling systems mainly in production lines of large factory shopfloor (i.e. pharmaceutical, food, etc.).

This section will discuss the design and implementation of the robotic arm as the handling system of the Ultra-Mill. The robotic arm and Ultra-Mill merged into one system. Figure 7.1 shows the handling system mounted on the Ultra-Mill

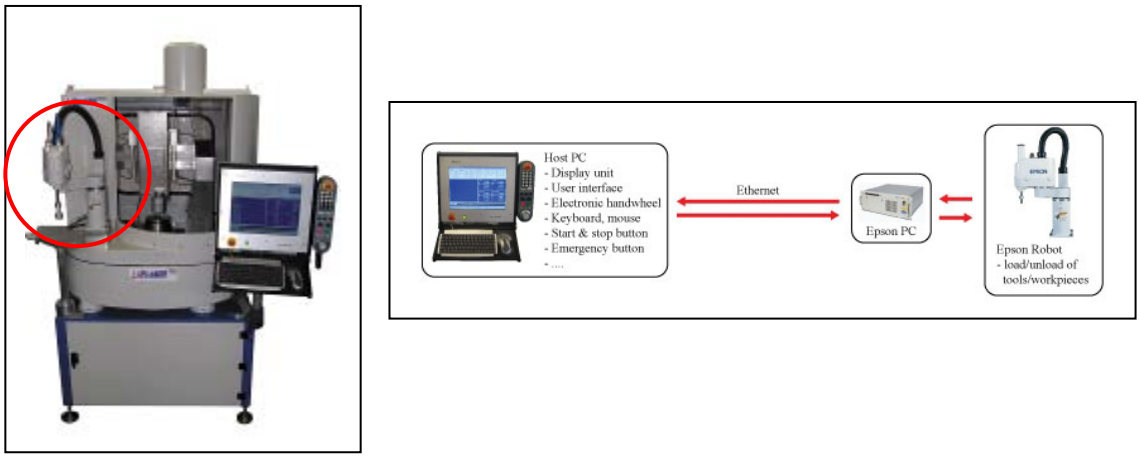

Fig. 7.1 Handling system mounted on Ultra-Mill

7.2.1. Microhandling System Description

The handling system comes with an independent control system. The customization of the robot control system is done with help of CTR. The handling system itself comes with two robot systems. The first robot system is the Epson SCARA robot and the second is the minirobot fitted with a microgripper and a vision system. These two robots make the handling system.

The Epson robot could also work independently of the minirobot. The end effector of the Epson robot could be its own macrogripper or the minirobot with the microgripper as shown in Figure 7.2. The selection of the end effector is dependent on the size of tools or workpieces. The Ultra-Mill uses small tools which are less than 1 mm in diameter with 3 mm shank diameter.

(a) Macro gripper (b) Minirobot with microgripper

Fig. 7.2 Two different end effectors

For loading and unloading of tools with 3 mm shank diameter, the handling system will use only the Epson robot with the macrogripper. In this operation, the visions system is not required. Workpieces with dimensions smaller than 3 mm are transported between the Ultra-Mill and workpiece pallet using the Epson robot equipped with the minirobot.

Working with minirobot, a visions system is needed to allow the handling system to know the location of the workpieces. This is required so as to ensure the minirobot grips the workpiece correctly relative to workpiece central point.

7.2.2. Communication and Control Protocol

In this section the communication protocol between the handling system and Ultra-Mill is discussed. As mentioned earlier, the handling system and the Ultra-Mill have independent control system. For ensuring good performance characteristics, these two control systems must merge to become one. Both control systems are PC-based control system.

7.2.2.1. Communication Protocol

The communication connection between the handling system and Ultra-Mill is done via the Ethernet connection. Using the Ethernet connection, a static internet protocol (IP) address will be set up on both systems. This means that one of these systems would be a server and the other would be a client.

The selection as to which control system should be the server or client is based on two reasons. The first step is deciding which control system is the primary system. The second is establishing which control system controls the other. The Ultra-Mill control system is considered to be the primary control system which in turn is the client system. This is because the operation or activity of the handling system is dictated by Ultra-Mill. Therefore upon powering on the system, the handling system will be in a listening mode. The handling system will wait for Ultra-Mill to establish the communication.

The client and server program was programmed using the function libraries in Visual Basic. Both control systems use Visual Basic as a means for customization. Figure 7.3 illustrates the communication protocol between the handling system and Ultra-Mill.

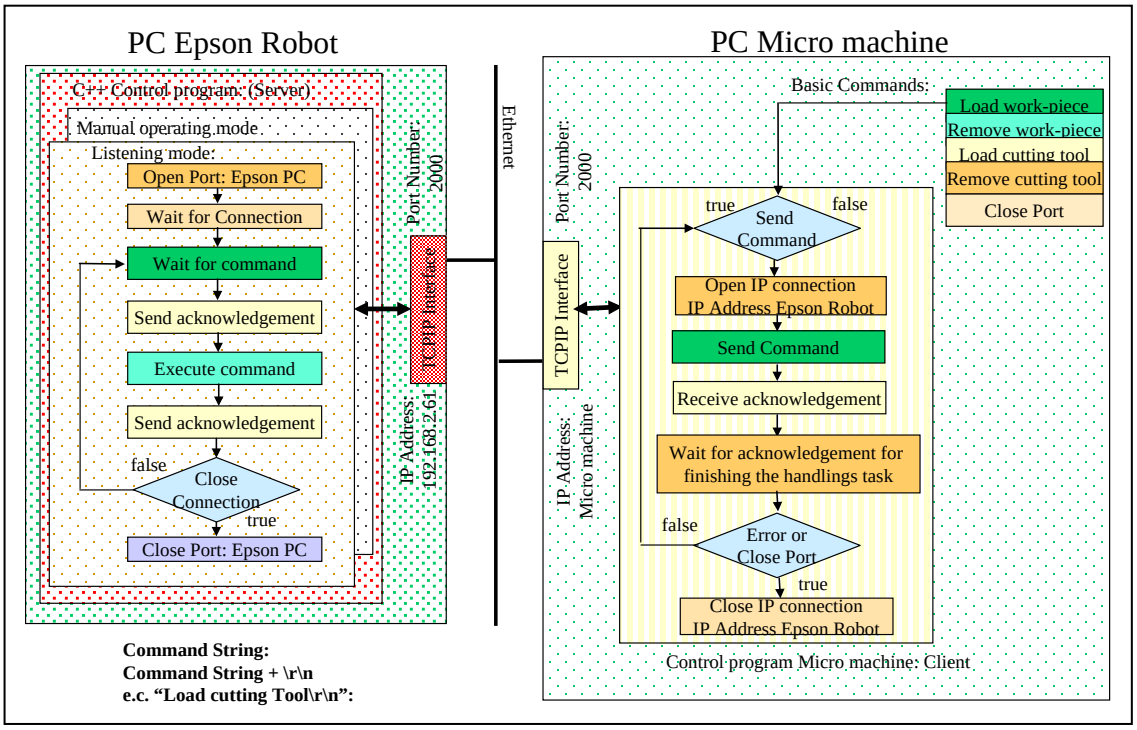

Fig. 7.3 Communication protocol between handling system and Ultra-Mill

7.2.2.2. Control Protocol

A synchronized control protocol between the handling system and Ultra-Mill must be designed and established so as the entire system is free from errors. Errors in the control protocol will most likely damage one or more physical elements of the entire system (i.e. collision between the handling system with the machine guard, spindle collet system, etc.) during the loading and unloading tasks.

Ensuring no errors occur during loading and unloading tasks, a thorough design of the protocol must be done. Here the protocols are designed by establishing the precedence order of the motion. To keep things simple, there should not be more that two movements occurring at one time. For example, the Ultra-Mill axes should already be in paused mode and ready in position waiting for the task of the handling system. In order to ensure safest working environment, acknowledgements are sent between the handling system and Ultra-Mill upon complementing a task. Before proceeding to the next task, acknowledgements must be sent and accepted between the two systems. Table 7.1 below shows the tasks which require acknowledgements. The tasks of the robot are also displayed as part of the HMI of the Ultra-Mill as described in Figure 7.4.

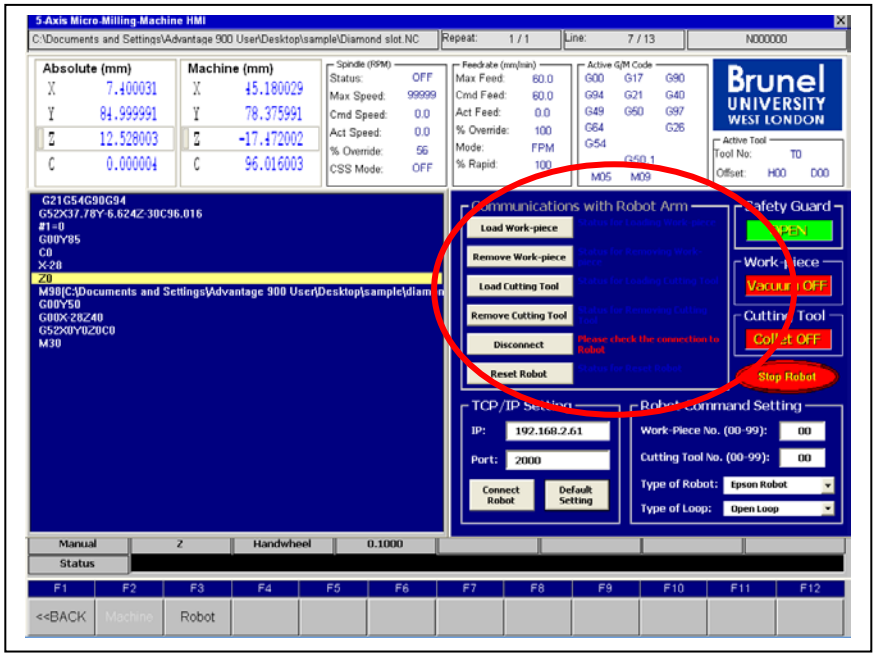

Fig. 7.4 Displayed handling system tasks on the HMI

Table 7.1 List of tasks and acknowledgments

Task	Acknowledgements
Robot initialized	0
Robot received the command “Load work-piece”	1.0
Tweezers is in Position for “Load work-piece”	1.1
Robot received “Vacuum ON for Load work-piece”	1.2
Robot finished the “Load work-piece” process	1.3
Robot receive thed command "Remove work-piece"	2.0
Tweezers is in Position and Griped for “Remove work-piece”	2.1
Robot received “Vacuum OFF for Remove work-piece”	2.2
Robot finished the "Remove work-piece" process	2.3
Robot received the command "Load cutting tool"	3.0
Tweezers is in Position for “Load cutting tool”	3.1
Robot received “Vacuum ON for Load cutting tool”	3.2
Robot finished the "Load cutting tool" process	3.3
Robot receive the command "Remove cutting tool"	4.0
Tweezers is in Position and Griped for “Remove cutting tool”	4.1
Robot received “Vacuum OFF for Remove cutting tool”	4.2
Robot finished the "Remove cutting tool" process	4.3
Reference Position not found	20
Tweezers not found	30
Work-piece on tweezers not found	40
Work-piece Reference Position not found	50
Work-piece not found	60

The flowchart shown in Figure 7.5 illustrates the operation protocol between the handling system and Ultra-Mill.

To maximize the usage of these protocols in a production situation, the protocols involving loading and unloading is written as M-codes in the form of PLC programs. As

an example, for a proper manufacturing cycle of at least two job cycles without operator's intervention, full automatic sequences must be implemented. These protocols would be a part of the NC program.

The NC program example for machining process will have this structure:

1. *M-codes to open machine guard, load workpiece and close machine guard*
2. *Run NC part program*
3. *M-codes to open machine guard and unload workpiece*
4. *M-codes to load workpiece*
5. *M-codes to close machine guard*
6. *Run NC part program*
7. *M-codes to open machine guard and unload workpiece*

The NC program structure above is just an example for two jobs or cycles. For more jobs, the NC program will be running in loops. In the NC program example above, loading and unloading of tool is not considered. The loading and unloading tool protocol is implemented as M-codes, similar to loading and unloading of workpieces.

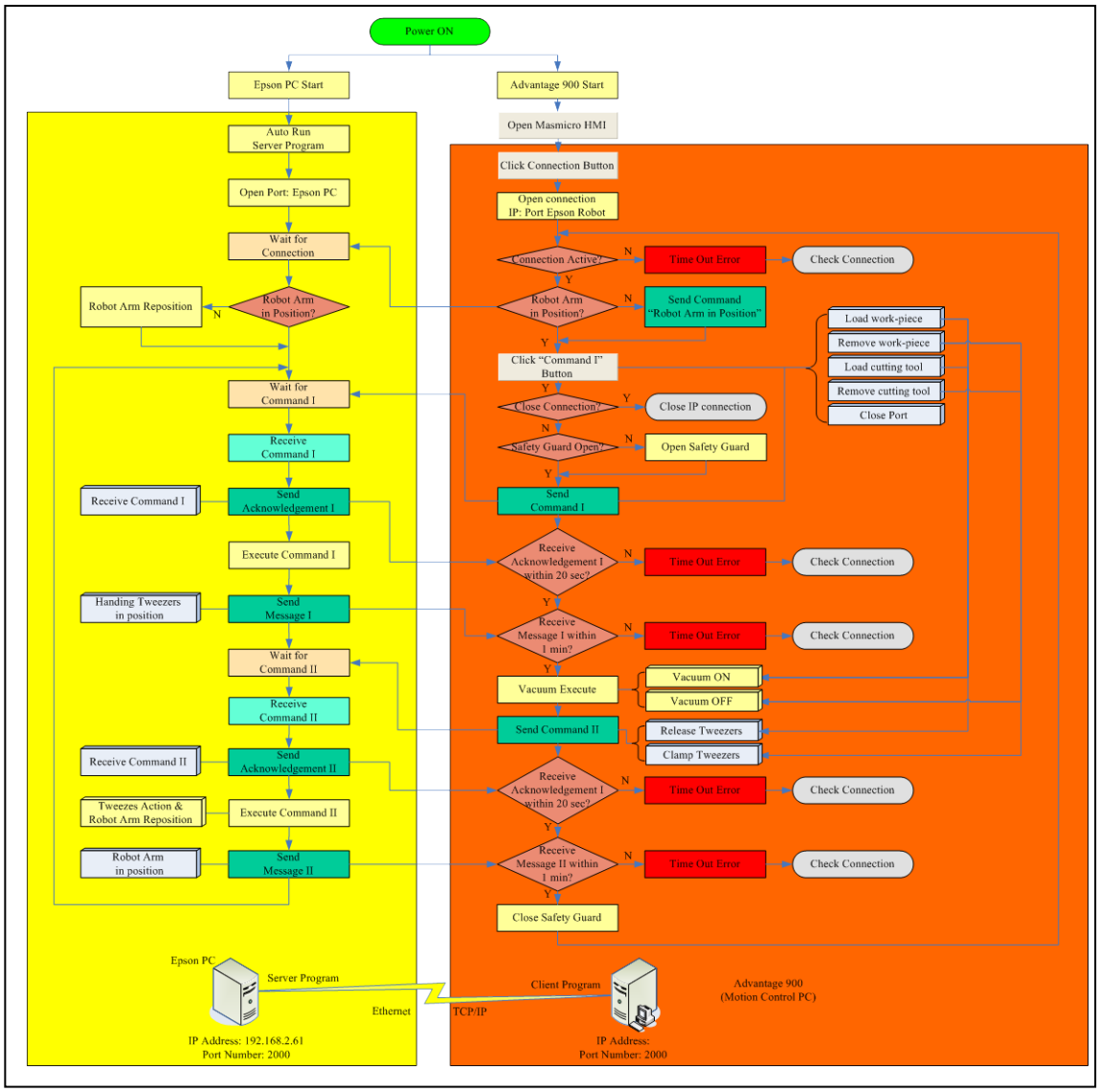

Fig. 7.5 Operation protocol between handling system and Ultra-Mill

7.2.3. Sub-system Performance Evaluation

The performance evaluation of the handling system is qualitatively evaluated. The performance is rated through how well the operational protocol functions and number of errors that happen. While assessing the protocol, some problems did occur which almost resulted in collision on the robotic arm with the machine guard. This problem was however rectified and further testing displayed no possible collision would occur.

Test runs using NC programs with the M-codes corresponding to handling system tasks were conducted to evaluate the success of the implementation. Machining cycles were conducted and the loading and unloading of workpieces was according to operation

protocol. It is therefore safe to conclude that the synchronization between the two control systems was designed and implemented accurately.

7.3. Tool Condition Monitoring System

The tool condition monitoring (TCM) system design was initially the task of Patras University from Greece who was another Masmicro group partner. During the course of the Masmicro project, Patras University did not successfully design and implement an overall functional tool condition monitoring (TCM) system that is suitable for Ultra-Mill.

The initial proposed tool condition monitoring method was using the acoustic emission (AE) method. Acoustic emission is a naturally occurring phenomenon whereby external stimuli generate sources of waves when a small surface displacement of a material is removed. The waves are produced when there is a rapid release of energy (Wikipedia, 2009b). Monitoring the tool using AE is an online method whereby the tool is monitored during the cutting process.

Tests conducted by Patras University used only tools with 3 mm diameter. Tooling with diameter of less than 1 mm was never experimented. The system that Patras University proposed used an acoustic emission sensor mounted close to the tool and a data acquisition system using a PXI system from National Instruments (NI).

Since Patras was unsuccessful to fulfil this requirement, the author decided to experiment two possible tool monitoring methods as solution for the Ultra-Mill.

7.3.1. Assessed Tool Condition Monitoring Method for the Ultra-Mill

Two tool condition monitoring methods were tested prior to implementation for the Ultra-Mill. The first method was using a 3-axis Dynamometer from Kistler and the second method was a non-contact laser-based tool system by Renishaw. These two methods must be able to detect these conditions as displayed in Figure 7.6.

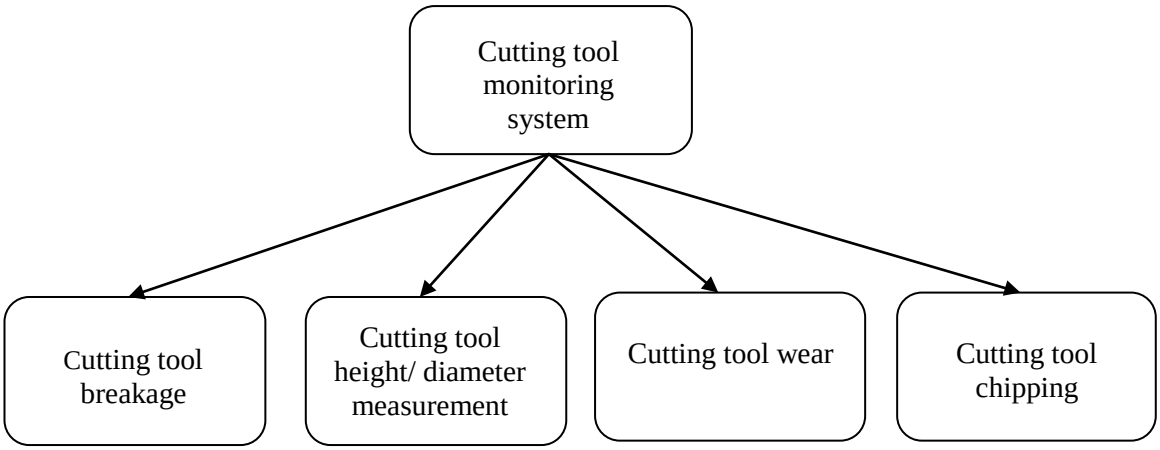

Fig. 7.6 Tool monitoring system functions

7.3.1.1. 3-Axis Dynamometer

A 3-axis dynamometer is able to detect forces in tri-directional (X, Y, Z). The dynamometer has the capacity to identify small dynamic changes when acted by big forces. In the assessment stage, the MiniDyn 9256C by Kistler as illustrated in Figure 7.7 was used to measure cutting forces for slot cutting.

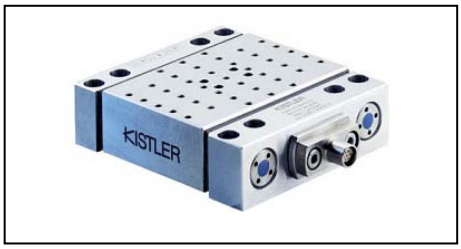

Fig. 7.7 Kistler's MiniDyn 9256C

The construction and operating principle of the dynamometer are explained in depth in (Kistler Minidyn 2008). The dynamometer is connected to a three channel charge amplifier which is then relayed to the PC for data acquisition. Dynoware by Kistler, was used to analyse data. As the function of the dynamometer is force detection, Figure 7.8 illustrates the elements that influence the cutting forces during micro milling process.

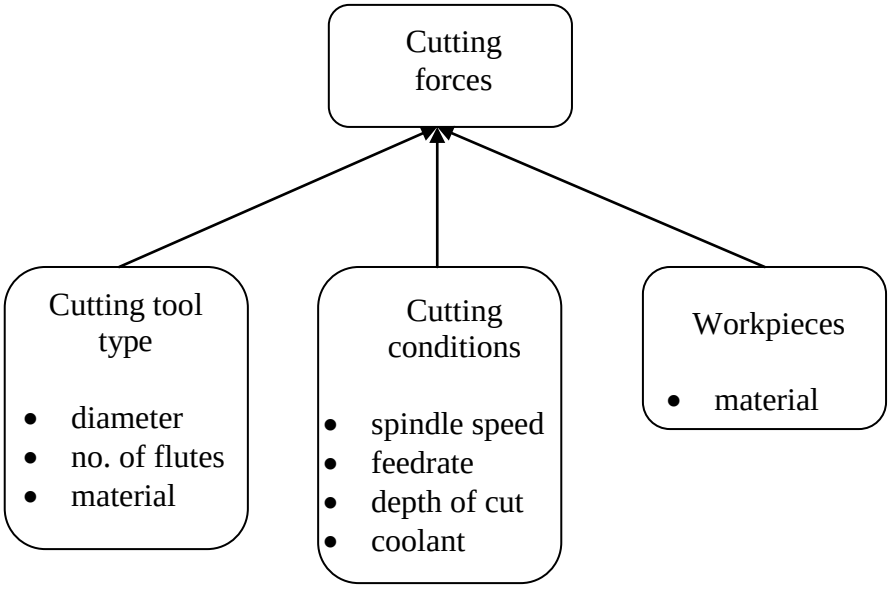

Fig. 7.8 Cutting forces influences

7.3.1.1.1. Control Method using Dynamometer

At this stage the TCM with dynamometer is itself a subsystem. This subsystem is required to detect tool failure, interpret the cutting forces on the fly and relay this information to the Ultra-Mill control system for decision making, therefore making this method an online method. The Ultra-Mill control system only accepts a high or low signal from this subsystem as inputs for the PLCs. Figure 7.9 shows the cutting force signal flow for fault detection and decision making.

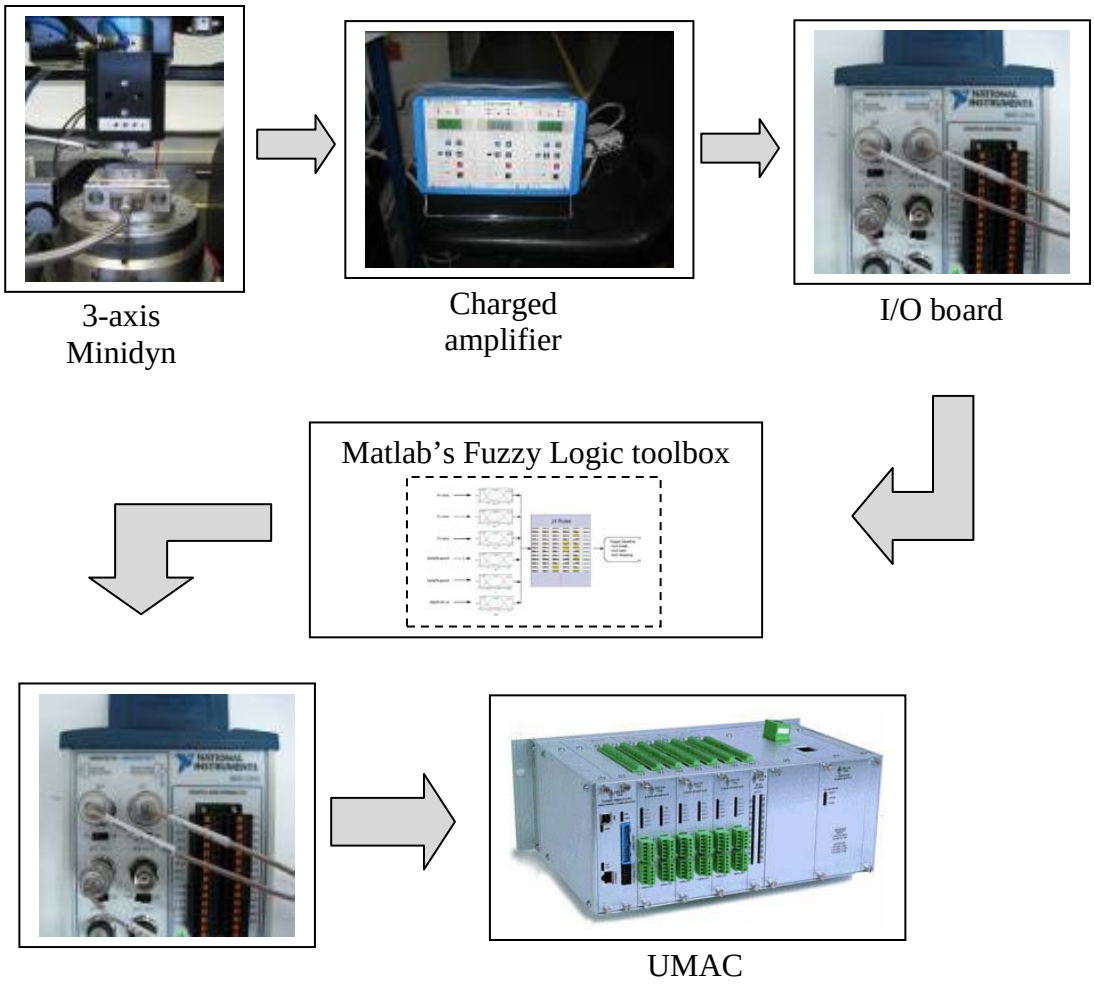

Fig. 7.9 Cutting force signal flow

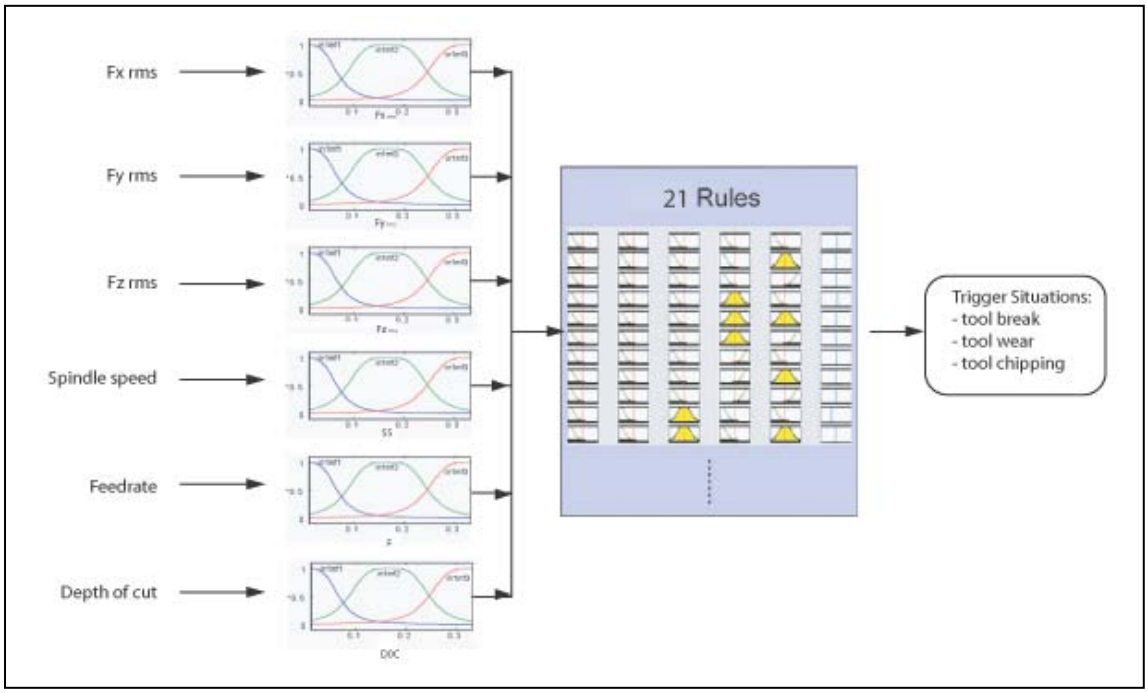

Fig. 7.10 Fuzzy inference system (FIS) for tool monitoring system

Figure 7.10 describes the fuzzy inference system (FIS) for the tool monitoring system. Inputs used are the three-direction cutting forces (F_{xrms}, $F_{yrms,}$ $F_{zrms)}$ and cutting parameters (spindle speed, feedrate and depth of cut) which are used as membership functions. Each function has its own level indicator (low, middle, high, etc.). For example spindle speed of 10,000 rpm is low, 50,000 rpm is middle and 100,000 rpm is high. The level of the inputs cannot be specifically determined in which have led to the use of fuzzy-logic toolbox. Fuzzy-logic is defined as it is all about the relative importance of precision which would lead to how important it is to be exactly right when a rough answer will be sufficient (Matlab, 2009b).

Then a rule table must be constructed to obtain the output (tool condition) based on the input conditions. Figure 7.11 illustrates the rule-based table that was constructed. From experiments, 21 rules have been constructed based on inputs mentioned above. Tool condition which is the output has been categorized into three level (good, average, bad). Shown in Figure 7.11 is the rule table.

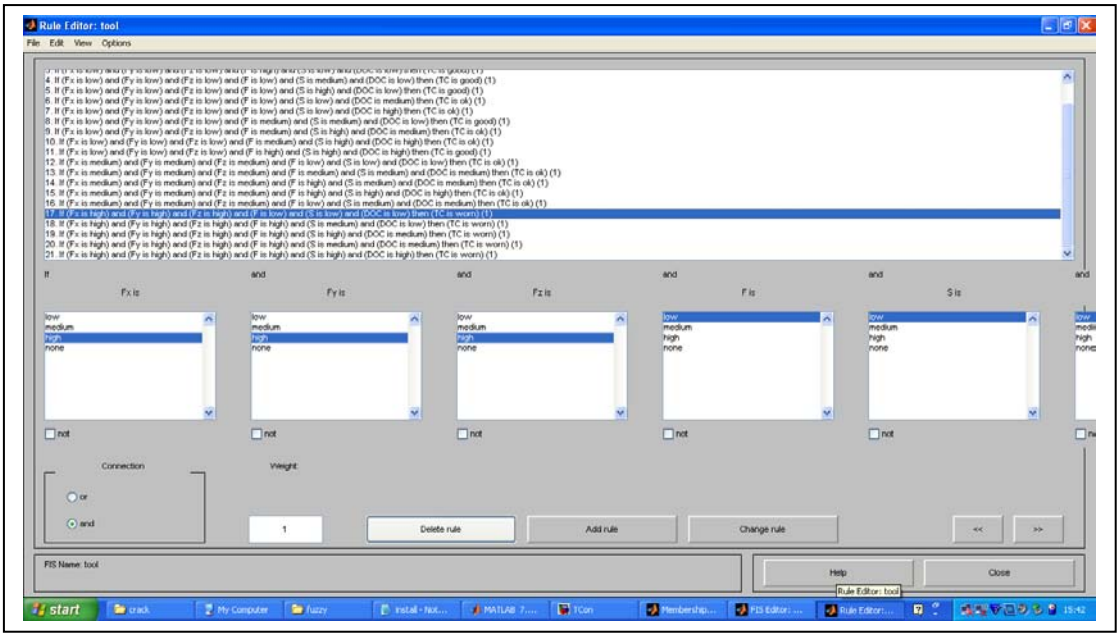

Fig. 7.11 Rule table

Listed below are some examples of the rules:

- *If (Fx is low) and (Fy is low) and (Fz is low) and (F is low) and (S is low) and (DOC is low) then (TC is good) (1)*
- *If (Fx is low) and (Fy is low) and (Fz is low) and (F is medium) and (S is medium) and (DOC is low) then (TC is good) (1)*
- *If (Fx is medium) and (Fy is medium) and (Fz is medium) and (F is low) and (S is low) and (DOC is low) then (TC is ok) (1)*
- *If (Fx is high) and (Fy is high) and (Fz is high) and (F is high) and (S is medium) and (DOC is low) then (TC is worn) (1)*
- *If (Fx is high) and (Fy is high) and (Fz is high) and (F is high) and (S is high) and (DOC is high) then (TC is worn) (1)*

Simulations were run to determine the effectiveness of the fuzzy-logic based model. Inputs from another set experiment were used as inputs (F_{xrms}, $F_{yrms,}$ $F_{zrms,}$ spindle speed, feedrate and depth of cut) and the output obtained did manage to provide the tool condition.

In order to develop the tool failure detection and the ability to interpret cutting forces on the fly, many experiments must be done and a lot of signal processing tasks must be conducted using the data collected from the experiments. The signal processing and interpretation is done with aid of Matlab's fuzzy logic toolbox. Signal processing using the experimental data and interpretation of behaviour associating cutting parameters and

cutting forces is required so as to understand when tool failure is achieved and to predict possible tool failure before actually failing.

This subsystem development is limited only to fundamental design and has not fully achieved actual implementation for the Ultra-Mill as designing and researching of TCM is a different research on its own.

7.3.1.1.2. Performance Assessments using Dynamometer

As part of the performance assessment of the dynamometer, slot cutting experiments with aluminium and copper workpieces were conducted. In the experiments different combination of cutting parameters (i.e. feedrate, depth of cut, coolant on/off, spindle speed) using ball end tungsten carbide tools with 200 µm diameter.

The experiments were designed using DOE (Design on Experiments) with three cutting parameters have different levels. The selected parameters are 70,000 rpm, 80,000 rpm and 90,000 rpm for spindle speed, 20 mm/min, 30 mm/min, and 40 mm/min for feedrate and 50 µm, 70 µm and 100 µm for depth of cut. Table 7.2 shows the cutting forces in X, Y and Z direction with respect to different cutting parameters.

Table 7.2 Cutting forces in X, Y and Z direction

Run	Factor 1	Factor 2	Factor 3			
	Spindle speed	Feedrate	DOC	Fx rms	Fy rms	Fz rms
	rpm	mm/min	µm	N	N	N
1	70,000	20	50	0.03	0.39	0.08
2	80,000	40	75	0.14	1.46	0.02
3	90,000	20	50	0.12	1.39	0.04
4	80,000	40	50	0.07	1.14	0.26
5	70,000	30	100	0.1	1.07	0.1
6	70,000	40	75	0.15	1.24	0.02
7	90,000	40	50	0	0.41	0.1
8	90,000	30	50	0.09	0.19	0.12
9	80,000	40	100	0.17	0.36	0.07
10	70,000	40	50	0.18	0.38	0.09
11	80,000	20	50	0.06	1.1	0.16
12	80,000	30	50	0.18	0.91	0
13	80,000	30	75	0.06	0.19	0.03
14	70,000	20	100	0.19	0.05	0.7
15	90,000	20	100	0.14	0.78	0.02
16	90,000	30	75	0.07	0.05	0.04
17	90,000	30	100	0.26	0.34	0.09
18	70,000	40	100	0.24	0.4	0.22
19	70,000	30	75	0.17	0.14	0.03
20	80,000	20	75	0.18	0.62	0.17
21	90,000	40	75	0.2	1.22	0.07
22	80,000	20	100	0.09	0.06	0.06
23	80,000	30	100	0.23	0.37	0.09
24	70,000	30	50	0.24	0.04	0.05
25	70,000	20	75	0.04	0.01	0.03
26	90,000	20	75	0.22	0.04	0.18
27	90,000	40	100	0.22	0.13	0.18

The results for other cutting experiments are in Appendix VII. Figure 7.12 illustrates the magnitude of cutting forces against number of test run. Figure 7.13 describes the finishing of the slots. The cutting forces are dominant in the Y-direction as this was the cutting direction.

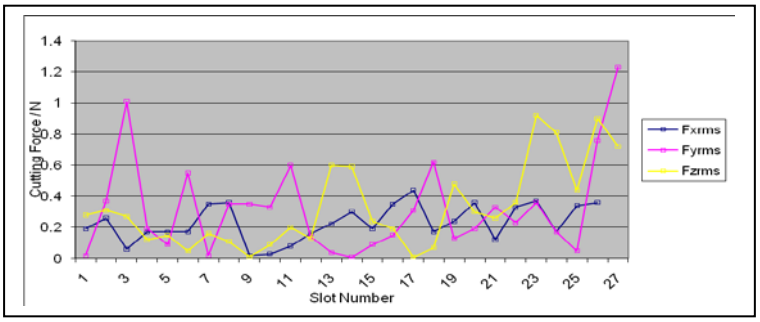

(a) Fx_{rms}, Fy_{rms} and Fz_{rms} for copper

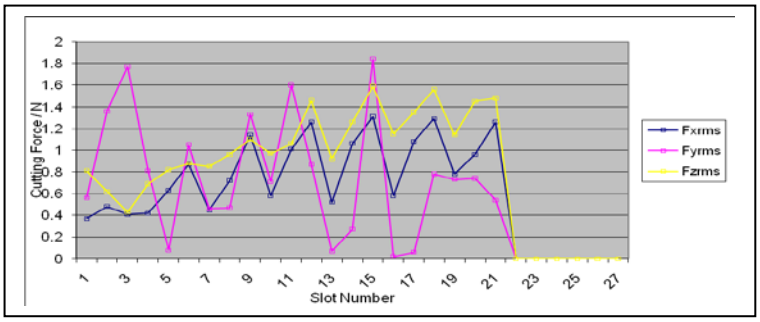

(b) Fx_{rms}, Fy_{rms} and Fz_{rms} for copper

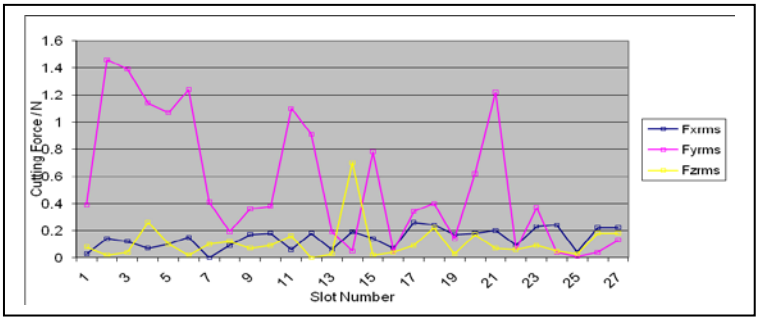

(c) Fx_{rms}, Fy_{rms} and Fz_{rms} for aluminum

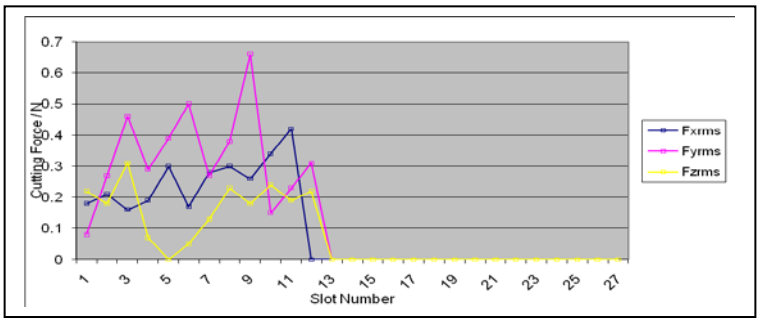

(d) Fx_{rms}, Fy_{rms} and Fz_{rms} for aluminium without coolant

Fig. 7.12 X, Y and Z cutting forces for copper and aluminium

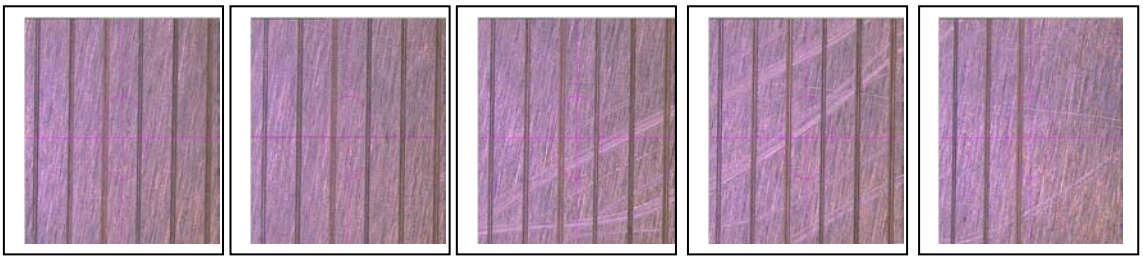

(a) Completed 27 slots on copper

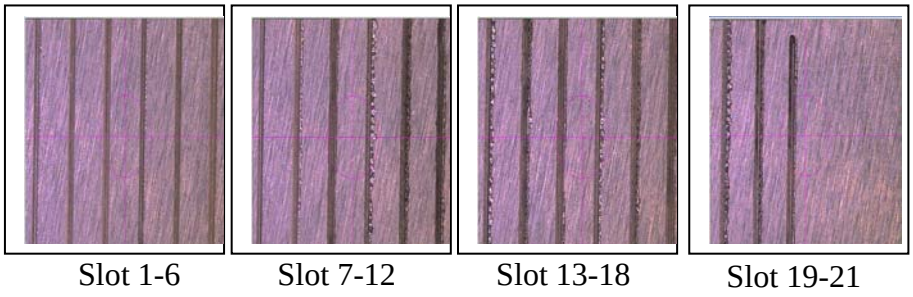

(b) Incomplete, 21 slots only due to tool breakage on copper

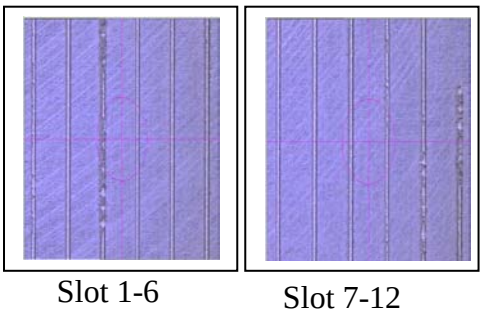

(c) Incomplete, 12 slots only due to tool breakage on aluminium without coolant

Fig. 7.13 Slot finishing

Figure 7.13 shows the finishes on the slots cut. Comparing Figure 7.13(a) and (b), the tool wear is clearly seen. For the experiment shown in Figure 7.13(b), the tool breakage was evident at slot 21. Whereas Figure 7.13(c) illustrates the finishes of the slot and the tool only completed 12 slots as this experiment was conducted without coolant.

From these figures, it is clear that as the tool wears, the finish becomes worse and the tool eventually fails. Running a finger on the slots from the first to the last slot, the roughness of the slots could be felt increasingly as there exist many burrs. Use of coolant could prolong the tool life.

7.3.1.2. Non-Contact Laser-Based Tool System

As mentioned earlier, the second method tested was using a non-contact laser-based tool system. The system used was the NC4+ (modular setup) by Renishaw. This system has a modular setup so as to accommodate the machine configurations. The NC4+ is able to provide fast tool setting and tool breakage detection. Using this system, the dimensions of the tool is the input. Figure 7.14 shows the NC4+ system and Table 7.3 describes the specifications of the system. Since the smallest tool diameter used on the Ultra-Mill at the moment is 200µm, the NC4+ is a suitable candidate for integration with the Ultra-Mill.

Fig. 7.14 NC4+ by Renishaw (Renishaw, 2009)

The advantages of implementing this system are:

- Detection of tools with minimum diameter of 0.03 mm.
- Compact but modular system to suit machine tool with small machining envelope.
- Accurate and precise tool length and diameter measurement and setup.
- Controlled using standard M-code.

Table 7.3 NC4+ specifications (Renishaw 2009)

Specification	NC4	NC4+
Laser type	Class 2, Visible red light < 1 mW 670 nm	Same
Laser beam alignment	Adjuster pack	Optional mounting brackets
Electrical connection	Hard-wired cable on end of unit. Other options available on request.	Hard-wired cable on underside of unit.
Repeatability of trigger points (2 sigma)	±1.0 µm at 1 m separation	Same
Minimum tool diameter for measurement	Ø0.03 mm (0.001 in) or larger, depending on separation and set-up	Ø0.3 mm at 0.5 m separation Ø1 mm at 5 m separation
Minimum tool diameter for breakage detection	Ø0.03 mm (0.001 in) or larger, depending on separation and set-up	Ø0.1 mm at 0.5 m separation Ø0.3 mm at 5 m separation
Air protection system	Supply pressure greater than 3 bar. Air usage 8 litres / min.	Same
Power supply	120 mA @ 12 V, 70 mA @ 30 V	Same
Temperature limit	Operating: +5 °C to + 50 °C Storage: -10 °C to + 70 °C	Same
Dimensions	Refer to data sheet	Ø30 mm x 35 mm long
Separations available	F300 - 225 mm air gap F230 - 170 mm air gap F115 - 55 mm air gap F95 - 23 mm air gap	0.5 m to 0.8 m 0.8 m to 1.5 m 1.5 m to 2 m 2 m to 3 m 3 m to 5 m Other options available on request.
Sealing	IP X8	Same
Mounting	Single M10 / M12 fixing. Alternative fixing arrangement available.	Fixing for M3 screws.
Compatible interface	NCi-5	NCi-5

7.3.1.2.1. Control Method using NC4+

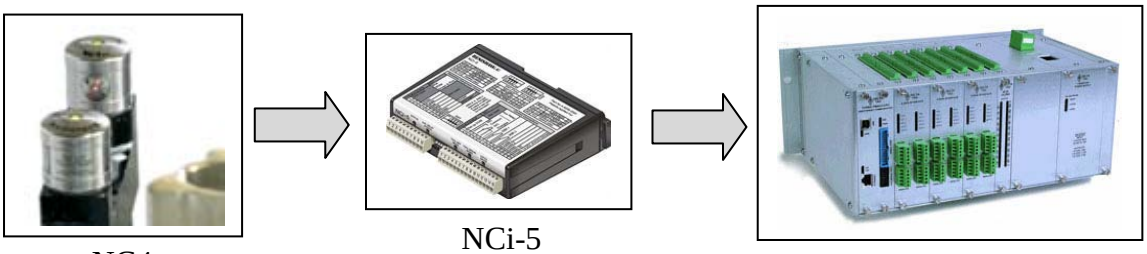

Fig. 7.15 Signal flow using the NC4+

This section describes the control method for tool monitoring system using the NC4+. The status signal of the laser will be relayed to UMAC via the NCi-5 interface. This interface processes signals from theNC4+ and then convert the signals into a high or low signal (1 or 0).

As mentioned earlier the non-contact tool setting system can determine the height and diameter of tools, cutting edge detection and tool breakage detection. All these are done by running the tool into the laser beam of the NC4+. Statuses will be determined by cutting or interruption in the laser direction.

To ensure the tool could be detected by the laser, spindle speed and feederate are critical for detection. The spindle must be running and federate must low enough to for detection when the tool is moving through the laser beam.

The tool measuring and fault detection are implemented via PLC programs. These macros are written to instruct the Ultra-Mill to follow the selected task. The macros appear as M-codes and are included within the NC program. These tool measuring and detection cycles are placed within the NC programs at carefully spaced intervals. It is not wise to run the these sequences too frequently as this would increase the machining time; on the other hand, running these sequences infrequently is problematic. The tool might have broken just after the last checking cycle and therefore wasting time until the next checking cycle is called.

The PLC programs for the macros use the output signal from the NCi-5 interface as inputs to I/O board of the UMAC. The I/O board addresses are then used in the PLC

programs for the macros of the M-codes. Some sections of the programming macros is described in Appendix VII.

Once tool change is required, Ultra-Mill will then use the robotic arm for loading and unloading task as explained in the Section 7.2.2.

7.3.1.2.2. Performance Assessments using Non-Contact System

As part of the performance evaluation, qualitative testing of this subsystem is conducted. The test initially involves the detection of the tool using the laser system. From there, test for tool measuring and tool detection procedures are then tested. The tests conducted displayed the reliably of the laser beam in detecting the beam.

Tests were conducted with the 200 µm tungsten carbide tool. At first, a few issues were noted. Detection was difficult and adjustments were made to the spindle speed and feedrate for the motion through the laser beam. Another difficulty was detecting the tooltip. The laser was cut by the tool neck not the tooltip. Cutting the laser with the tooltip will eventually give false measurements of the tool height and diameter. This could also lead to tool breakage not detected as the tool neck is there but tooltip might have broken or chipped off.

After few trial and error steps, the balance for spindle speed and feedrate was eventually found and tooltip detection was possible.

7.4. Summary

Chapter 7 has described the development of two subsystems. Both subsystems are very critical to the Ultra-Mill as support systems. The advantages of each subsystem have been highlighted in the earlier sections of this chapter.

As mentioned earlier, the robotic arm is required for tool loading and unloading purposes. This is used as a substitute for the ATC module. The subsystem functions really well in accommodating tool and workpiece loading and unloading.

The second subsystem that was discussed in this chapter was the TCM. TCM is required especially for micromachining machine tools. As the tools get smaller, the

more difficult it is to monitoring. Two sets of systems were tested, dynamometer and non-contact laser system, and evaluated. The dynamometer has advantages of monitoring the tool condition online and whereas the non-contact laser system checks the tool at selected intervals during the machining cycle.

Even though the dynamometer is a better solution but it is not industrially possible due to the high cost. Therefore machine builders will not spend so much on this subsystem. The high cost is not only related to cost of the dynamometer itself but also the cost of conducting experiments and processing and interpreting the signals behaviour which will be regarded as software development. On the other hand, the non-contact laser system is easy to implement and minimal software programming required compared to the dynamometer. This has led to the Ultra-Mill adopting the non-contact laser system as the tool inspection and monitoring system.

Chapter 8

Machining Experiments, Results and Analyses

8.1. Machining Trials

Machining trials were conducted on the Ultra-Mill with two different machine configurations. The first configuration is a 4-axis configuration with the spindle parallel in the Y-axis. The second configuration is the standard 5-axis configuration with the spindle parallel to the Z-axis and two rotary axes (B and C-axis). Figure 8.1 shows the two configurations on the Ultra-Mill.

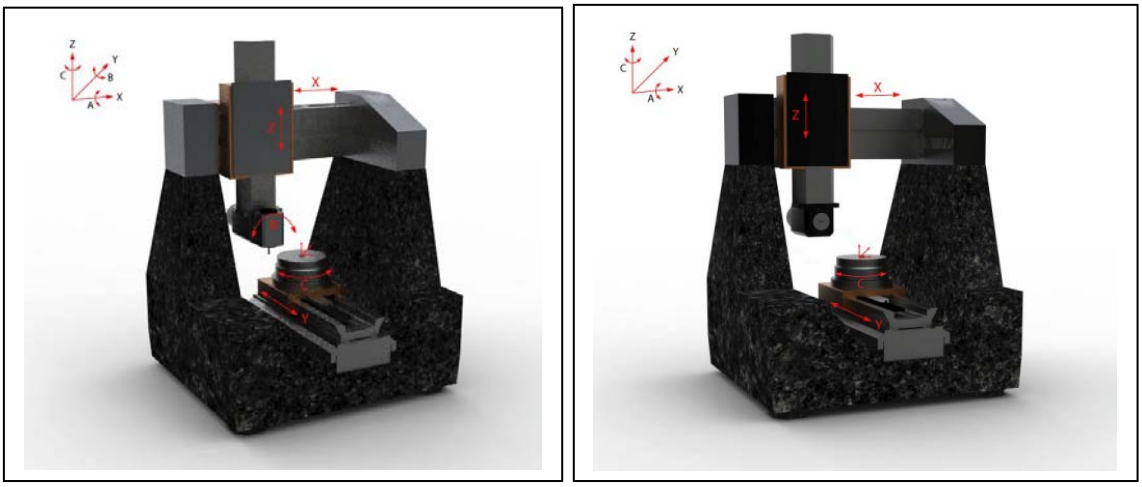

(a) 5-axis configuration (b) 4-axis configuration

Fig. 8.1 Two possible configurations for Ultra-Mill

Both machining trials displayed the flexibility of Ultra-Mill depending on the job required to machine. Although the first configuration is not standard, the parts were machined with high accuracy and repeatability. In this chapter, machining trials, result and analyses from two case studies will be discussed.

8.1.1. Case Study 1: Aplix Components

In this case study, the objective is to produce tooling for velcro (hook-and-loop fasteners) manufacturing as illustrated in Figure 8.2. This job is conducted with the assistance of a French company, Aplix, who required the tooling to be manufactured on the Ultra-Mill.

Fig. 8.2 Hooks (left) and loops (right)

The manufacturing process for the tooling is done by plunge milling using standard ball-nose tungsten carbide milling tools (diameter of 200 µm) and bespoke tapered ball-nose tungsten carbide milling tools. Another conducted machining trial was machining with a bespoke diamond cutting tool. Figure 8.3 illustrates the brass rings and milling tools used.

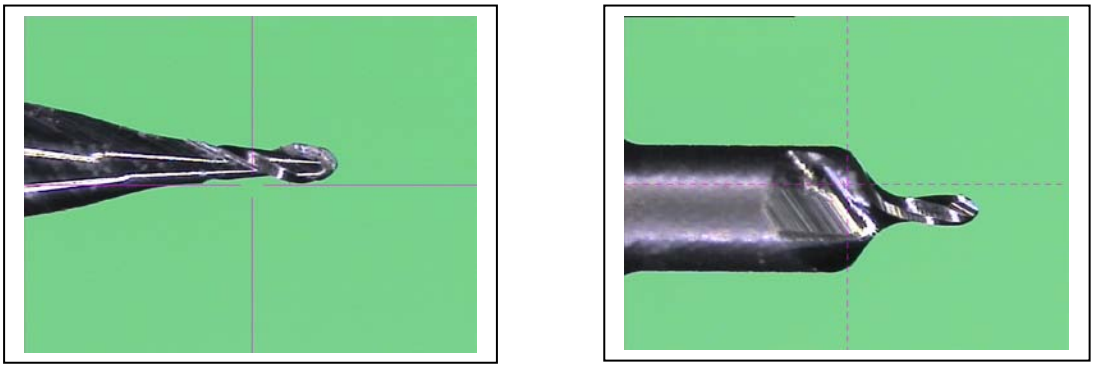

(a) (b)

(c)

Fig. 8.3 a) Standard ball-nose tungsten carbide milling tool, b) Bespoke tapered ball nose tungsten carbide milling tool, c) Brass ring

The raw material used for the velcro tooling is brass rings with outer diameter of 236 mm, inner diameter of 200 mm and thickness of 0.5 mm. On the outer diameter of the ring, 1376 cavities are required to be machined. The separations between two cavities required are 0.2616 degrees. The rings required both top and bottom to be machined. Each side took 105 minutes to complete the 1376 cavities.

8.1.1.1. Experiment 1

Machining trials were conducted with the milling tools mentioned above with the same cutting parameters. Table 8.1 illustrates the cutting parameters that were implemented for machining trials.

These cutting trials were conducted in Aplix's presence. Before these formal cutting trials, preliminary cutting trials were conducted using both the standard ball-nose tungsten carbide and bespoke tapered ball-nose tungsten carbide. These preliminary trials were conducted to understand the machining process and to find out the tool life with different cutting parameters in order to build machining confidence before moving on using the bespoke diamond cutting tools. No preliminary trials were done using the bespoke diamond cutting tools.

Table 8.1 Cutting parameters

Tool Type	**Tool Diameter (μm)**	**Feedrate (mm/min)**	**Depth of Cut (mm)**	**Spindle Speed (krpm)**
standard ball-nose tungsten carbide	200	20	0.5	70
bespoke tapered ball-nose tungsten carbide	N/A	20	0.4	70
bespoke diamond cutting tool	N/A	1	~ ½ of tool radius	80

During the preliminary trials, different spindle speeds and feedrate were implemented in the machining process. The depth of cut was kept constant according to the machined part specifications. From these trials, burrs built up by the edge of the cavities are significant with increased feedrate. The spindle speed was kept constant initially at 70,000 rpm with different feedrate, burrs built up were significant. The burrs built up were also significant with increased spindle speed. From these preliminary trials, it is understood that burrs built up is dominantly related to the feedrate. The size of the cavities is the same. This implies that there is no thermal growth in the high speed spindle and if tool runout exists, this tool runout is constant. Mist coolant was used in all machining trials. No dry cutting was conducted as this would definitely result in worse finish and shorter tool life.

Using a TESA V-200 vision system, the cavities were inspected. These cavities were machined with the cutting parameters displayed in Table 8.1. Table 8.2 describes the dimensions of the cavities. The cavities are measured at every 90º indexing of the rotary table. The depth of the cavities machined using bespoke tools was difficult to measure using the TESA V-200 vision system.

The inconsistency of the readings is related to how sharp the focus point is defined using the vision system operated by the operator and dependent on the operator's judgements. Chips and burrs on the surface made it difficult to find a good clear edge for measurements to be taken. From the measurements taken, the machined cavities were within the tolerance of the product specification. The figures of these cavities with the burrs built up are shown in Appendix VIII. Figure 8.4 illustrates a 3D imaging of the cavities measured using VHX-600 Generation 2 digital microscope from Keyence.

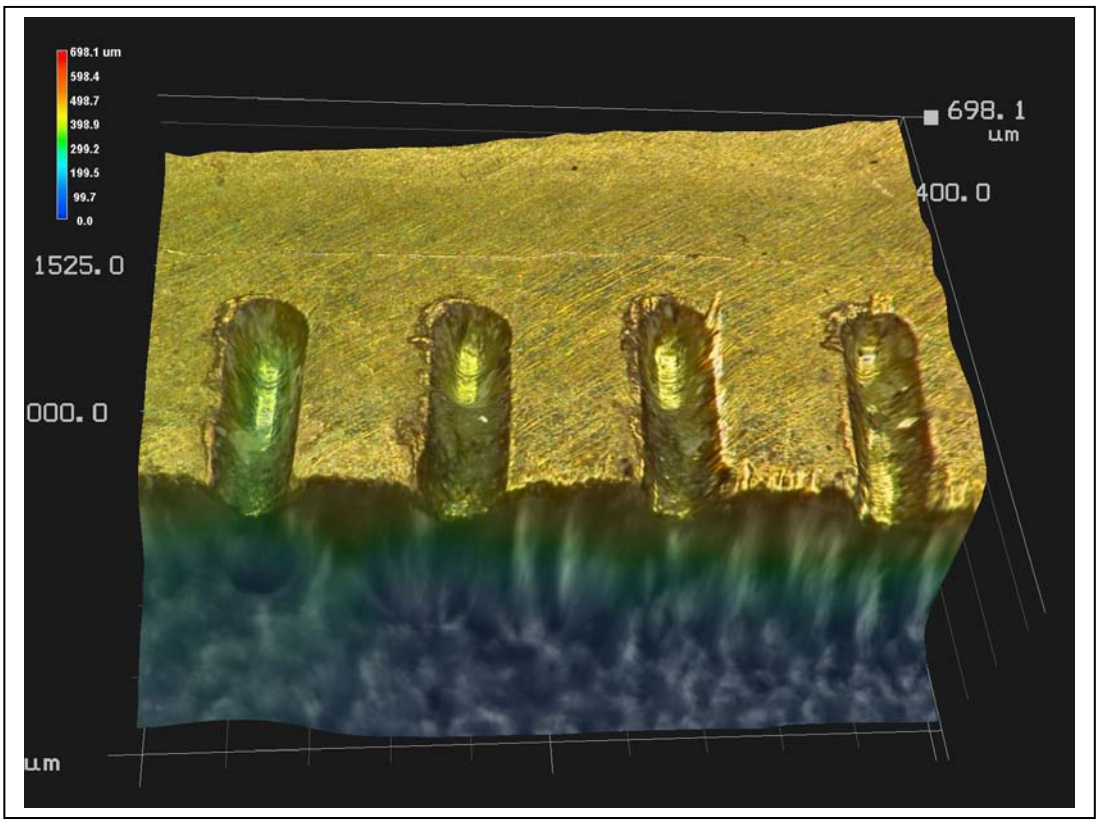

Fig. 8.4 3D imaging of the cavities

Table 8.2 Slots dimensions taken at every 90 degrees

Cutter type	Ring marks	Side	Slots position	Measuring parameters		
				Length (μm)	Width (μm)	Depth (μm)
Standard	One-side (1 of 3)	top	first slot (0°)	551.3	219.8	93.5
			90°	536.8	223	95.6
			180°	581.8	221.9	93.5
			270°	552.2	216.7	93.6
			last slot	553.4	218.9	87.3
	Double-side (2 of 3)	top	first slot (0°)	547.9	223	101.5
			90°	533.6	221.7	95.3
			180°	580.9	219.7	100.4
			270°	544.8	222.7	98.2
			last slot	545	219.8	92.5
		under	first slot (0°)	548.1	226.4	93.5
			90°	543.5	219	111
			180°	585.1	218.1	84.1
			270°	557.5	222.5	96.4
			last slot	553.4	223.6	91.4
	One-side (3 of 3)	top	first slot (0°)	549.8	208.7	98.6
			90°	557	212.8	91.7
			180°	575.9	212.5	97.6
			270°	531.8	212.2	93.9
			last slot	547.3	211.9	93
Bespoke	One-side (1 of 3)	top	first slot (0°)	552.3	170.5	N/A
			90°	547	169.4	N/A
			180°	581.4	174.1	N/A
			270°	566.5	164.5	N/A
			last slot	551.9	166.4	N/A
	Double-side (2 of 3)	top	first slot (0°)	546.3	166.4	N/A
			90°	549.4	165.2	N/A
			180°	585	169.1	N/A
			270°	551.3	168	N/A
			last slot	548.4	166.4	N/A
		under	first slot (0°)	552.9	170.5	N/A
			90°	547	162	N/A
			180°	585.3	169	N/A
			270°	561.4	165.5	N/A
			last slot	542.6	163.6	N/A
	One-side (3 of 3)	top	first slot (0°)	554.7	179.6	N/A
			90°	538.1	180	N/A
			180°	581.7	176.8	N/A
			270°	551.9	177.7	N/A
			last slot	547	172.5	N/A
Diamond	One-side	top	first slot	394.4	187.2	83.8
			third slot	397.4	183.7	84.7
			fifth slot(last slot)	395.1	185.2	52.9(cutter broken)

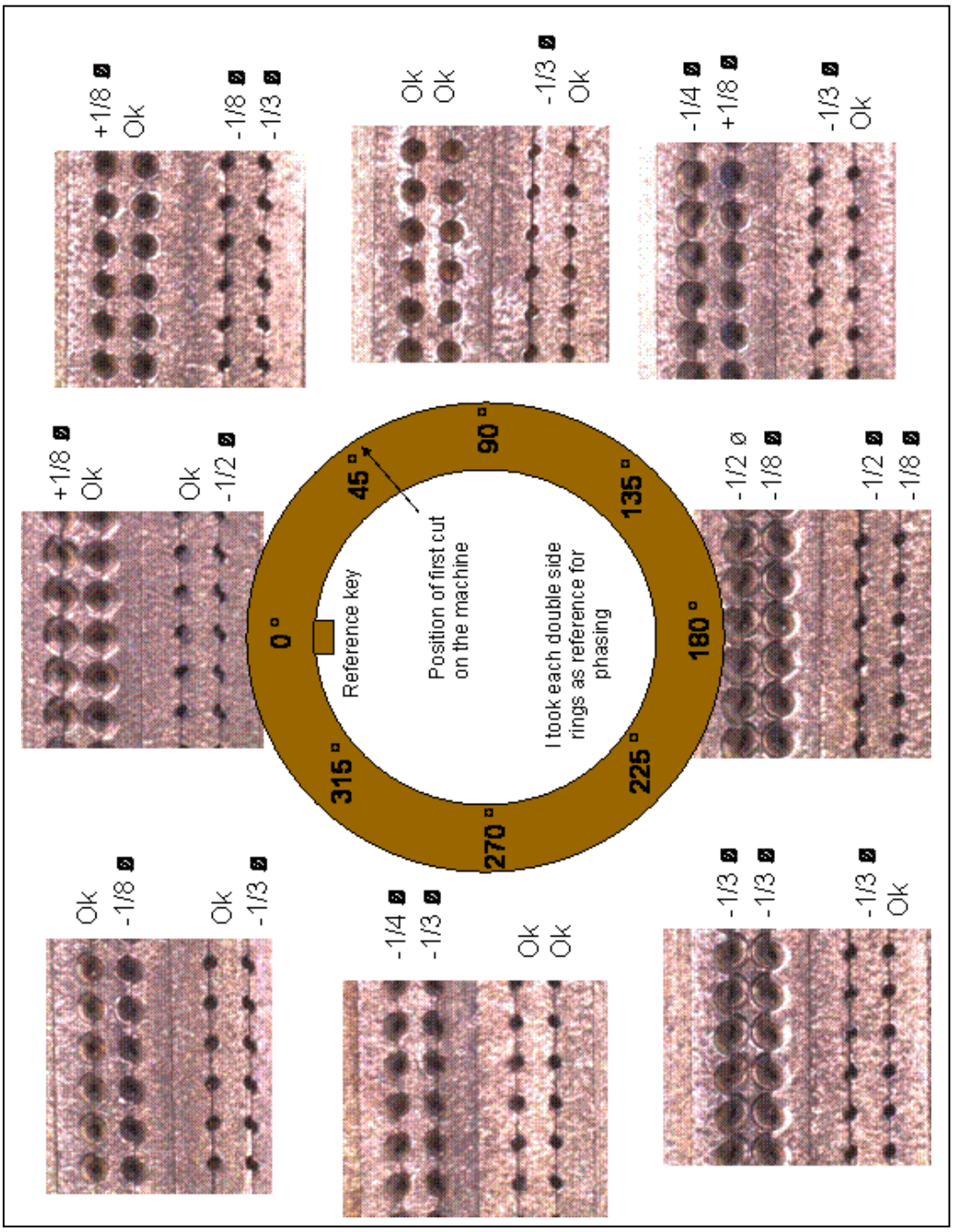

Fig. 8.5 Cavities phase measurements

The cavities were manufactured on circular rings with 200mm diameter. On each ring, there is a reference key for fixing the ring to fixture on the rotary table. Once machining have completed, the rings are placed on top of each other to observe the cavity positions. It was found that some position of the gear teeth on one ring is out of phase with another ring. Figure 8.5 describes the machined cavities. Some phasing error was detected.

When measuring the distance between each cavity on all rings separately, it was found the separation distance is within the tolerance of cavities specifications. Since the rings were manufactured individually, the phasing errors came from the fixturing and have resulted in mechanical induced errors. When observed closely, the reference key on the rings are able to move once fixed onto the fixture and have resulted in the phasing errors between rings.

8.1.1.2. Experiment 2

Experiments were also conducted on this Aplix application to identify the cutting forces applied during machining. Tests were conducted using a dynamometer, MiniDyn provided by Kistler. The model of the dynamometer is MiniDyn 9256C2 and is connected to three charge amplifiers model 5011. The MiniDyn could output three axis force readings (X, Y and Z directions). A software package called Dynoware by Kistler was used for data acquisition. Figure 8.6 shows the dynamometer setup in the machine tool.

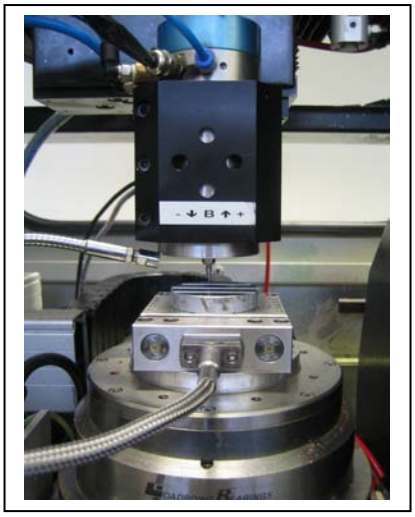

Fig. 8.6 Dynamometer set up on Ultra-Mill

In the experiments for the Aplix application using only the standard ball-nose tungsten carbide milling tools (diameter of 200 um), forces only in the Z-axis direction were observed. The forces in the Z-axis direction are most significant based on the motion for the machining process (plunge milling). Experiments were conducted with the same tool and workpiece used in the Aplix application. In the experiments, depth of cavities is kept constant according to the product requirements. However, the machining parameters which were changed were spindle speed and feedrate.

These experiments were conducted to identify the best machining parameters with the emphasis of minimizing machining time and reduce the burrs of the slots. At the same, to view the cutting forces effects on the machine axes robustness. Table 8.3 shows the machining parameters with the cutting force in the Z-axis direction.

Table 8.3 Machining parameters with Z-axis forces

Experiment	Spindle Speed (krpm)	Feedrate (mm/min)	Cutting Force (N)
1	70	20	0.75
2	80	20	0.7
3	90	20	0.6
4	100	20	0.5
5	70	30	0.55
6	80	30	0.45
7	90	30	0.43
8	100	30	0.47
9	70	40	0.55
10	80	40	0.56
11	90	40	0.5
12	100	40	0.5

In the experiments, it was observed that machining forces in the Z-axis direction did not exceed 1 N. During the machining process, the biggest force observed was between 1 to 1.4 N. These big forces are due to the tool touch or engagement with the workpiece. These peaks were observed consistently for every touch or engagement and reduce significantly when cutting process has started. Once the cutting process begins, the cutting forces are as illustrated in Table 8.3. Figure 8.7 illustrates forces during tool and wokpiece engagement.

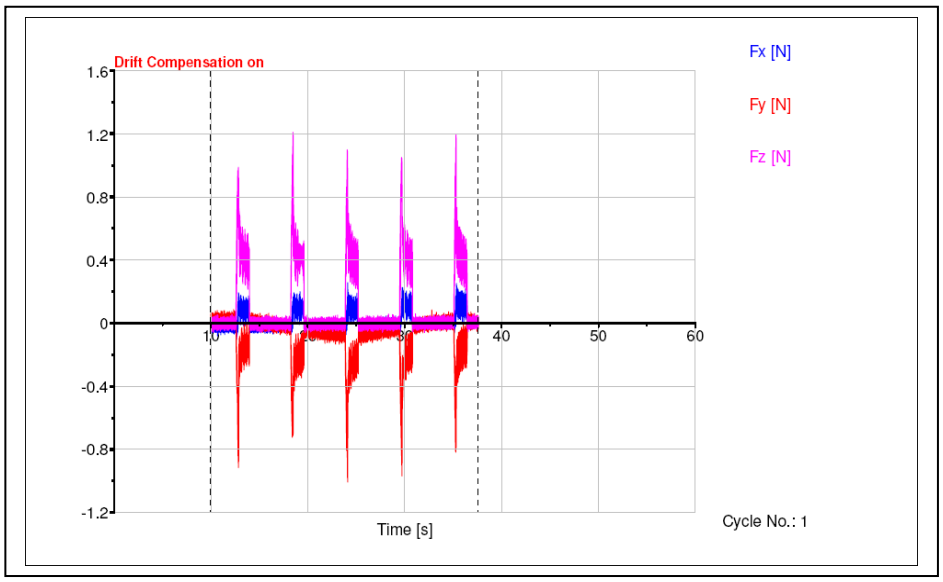

(a) Cutting forces of Experiment 3

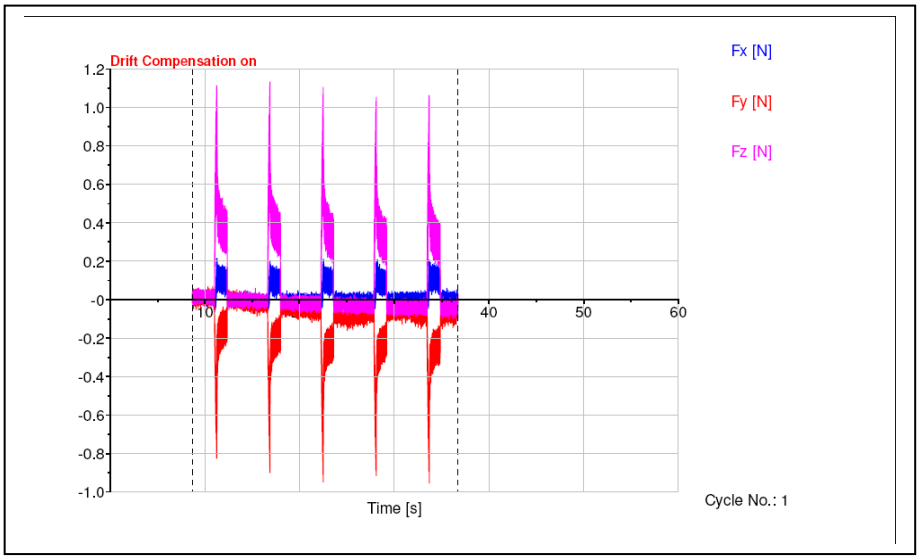

(b) Cutting forces of Experiment 5

Fig. 8.7 Tool workpiece engagement forces

For these experiments, the axis motion error in the Z direction is smaller than 1μm. this indicates the Z-axis is complying with the design specifications. The force which was exerted in the Z direction was too small and hence very insignificant when compared to Z-axis slide. With these experiments, the increase in feedrate in Z direction has resulted in burrs problems. Better finish was observed at slower feedrates (between 20 to 30 mm/min).

8.1.2. Case Study 2: Bespoke L-Shaped Test Workpiece

Case study 2 is conducted to evaluate the geometric accuracies. This test could determine the geometrical errors of the workpiece are influenced by mechanical errors or control system errors. Errors induced are normally associated with the manufacturing error or assembly error of the mechanical structures.

The test part is machined out of aluminium using a 2 mm diameter tungsten carbide tools. The test is to evaluate the straightness, squareness, parallelism, etc. of the machined surfaces. The 3D model of the testpiece is presented in Figure 8.8.

The workpiece consist of two parts. The first is a horizontal flat pyramid which will be machined in the XY plane and the second is a vertical flat pyramid which will be machined in the YZ plane. There are also microsteps which will be machined on the flat part of the pyramid as shown in Figure 8.8 and 8.9. The relationship (straightness, squareness, parallelism, etc.) between the XY and YZ planes is the objective of this test. Figure 8.9 illustrates the L-shaped workpiece on the Ultra-Mill.

Once machined, the testpiece is sent to the National Physics Laboratory (NPL) for measurements using the F25 micro-CMM by Carl Zeiss.

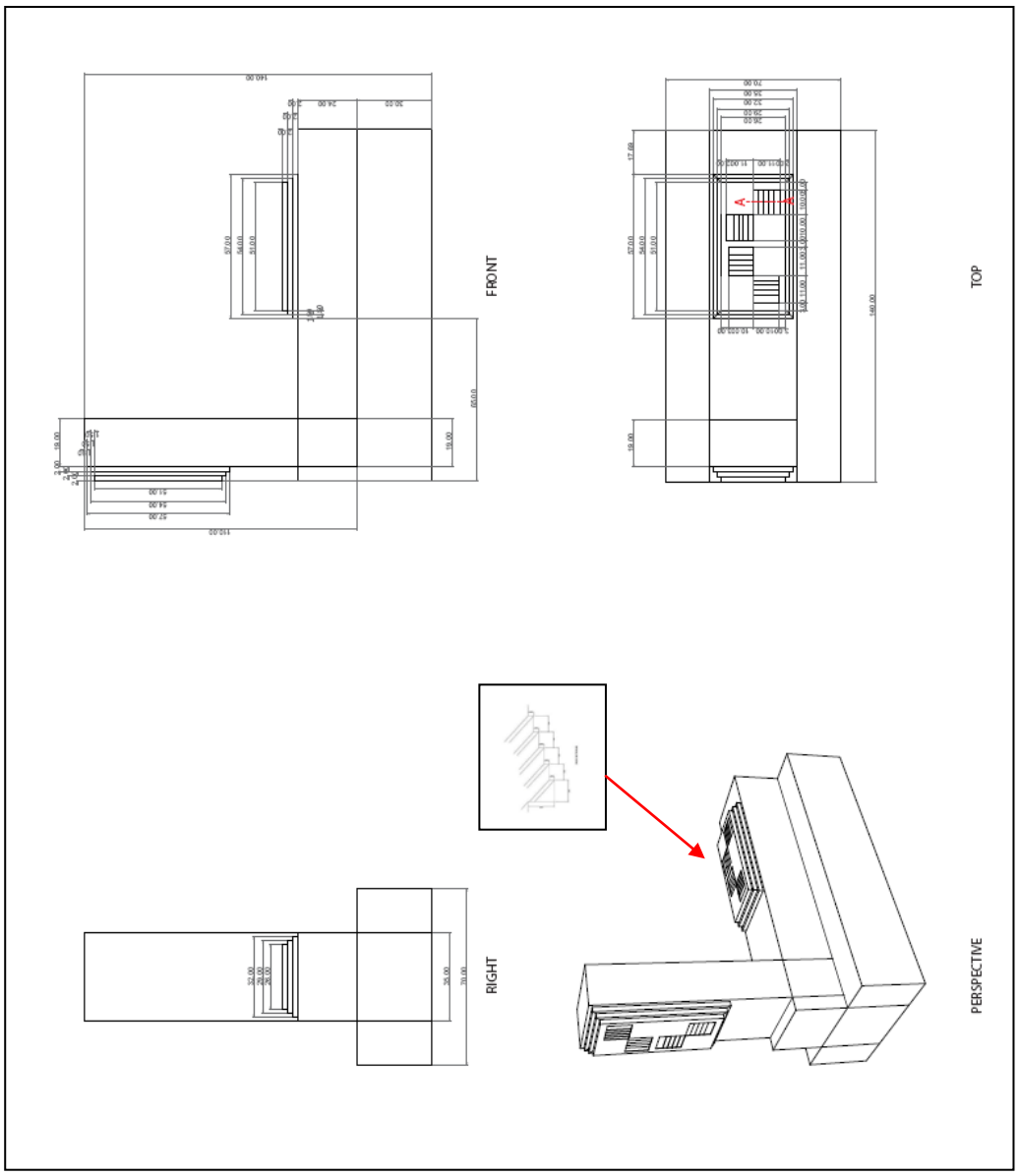

Fig. 8.8 Machined L- shaped test workpiece

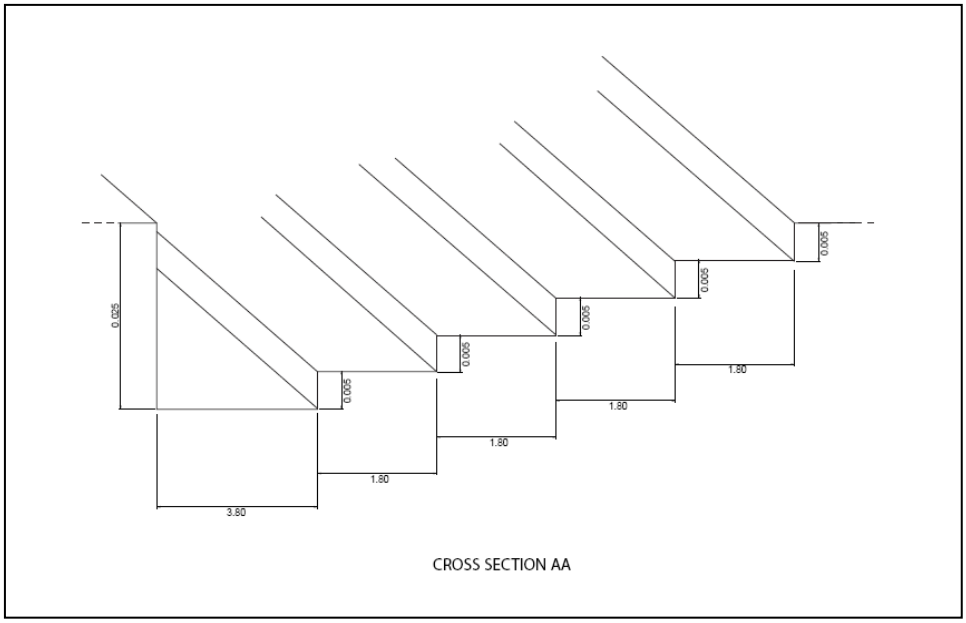

Fig. 8.9 Micro step features

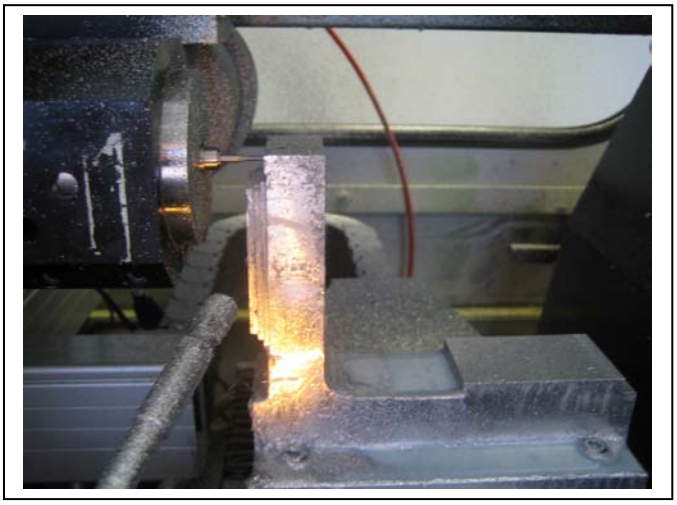

Fig. 8.10 Machined testpiece on Ultra-Mill

8.1.2.1. Assessment and Results

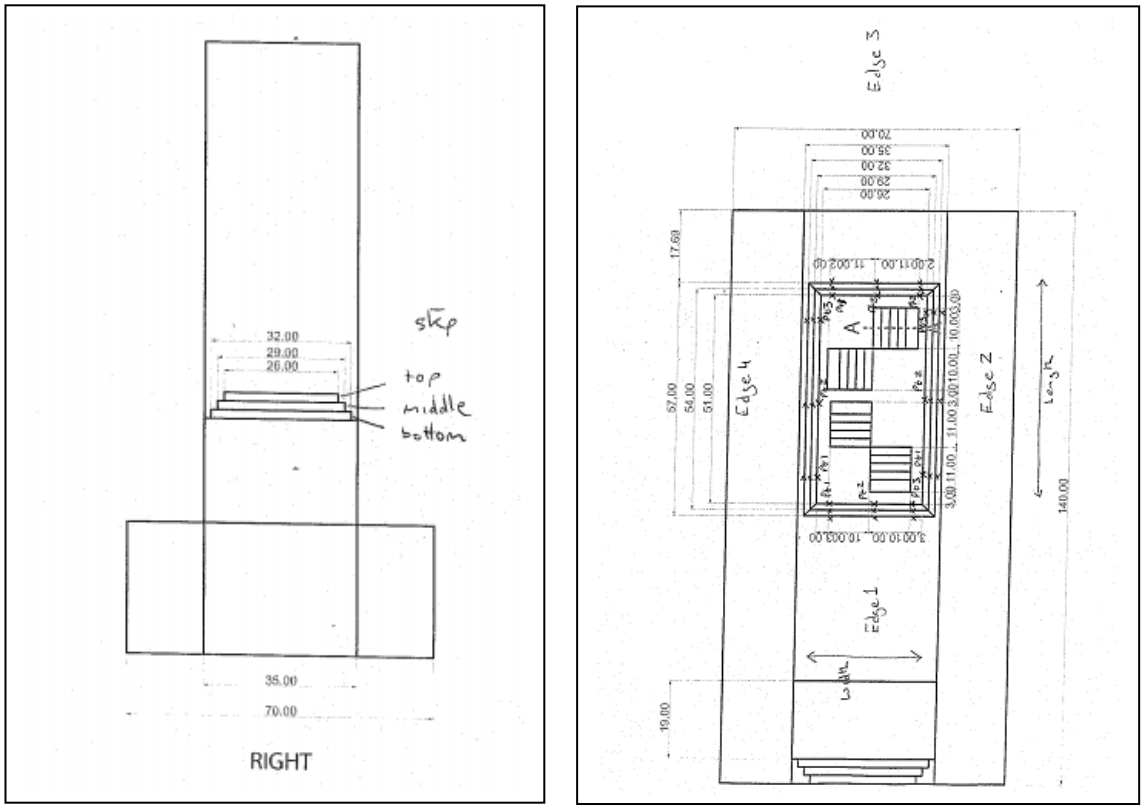

(a) (b)

Fig. 8.11 Workpiece measurements identifier

Figure 8.11 shows the measuring identifier with reference to 3D model to clearly understand the following measurement tables below.

Table 8.4 Straightness readings of the horizontal pyramid

Straightness					
	Top z = -1.0		Middle z = -3.0		Bottom z = -5.0
Edge 1	0.001044	Edge 1	0.001661	Edge 1	0.001047
Edge 2	0.001308	Edge 2	0.001810	Edge 2	0.002235
Edge 3	0.001832	Edge 3	0.000449	Edge 3	0.000947
Edge 4	0.001388	Edge 4	0.001131	Edge 4	0.001802

Table 8.5 Parallelism readings of the horizontal pyramid

Parallelism					
Top		Middle		Bottom	
Edge 1 & edge 3	0.001925	Edge 1 & edge 3	0.001006	Edge 1 & edge 3	0.001324
Edge 2 & edge 4	0.002141	Edge 2 & edge 4	0.005177	Edge 2 & edge 4	0.003735
Top & middle		Top & bottom			
Edge 4	0.002414		0.002173		

Table 8.6 Perpendicular readings of the horizontal pyramid

Perpendicularity					
Top		Middle		Bottom	
Edge 1	0.001130	Edge 1	0.001796	Edge 1	0.001079
Edge 3	0.002061	Edge 3	0.000900	Edge 3	0.001330

Table 8.7 Angles measurements of the horizontal pyramid

Angles					
Top		Middle		Bottom	
Edge 1 to Edge 2	89.999085	Edge 1 to Edge 2	89.995699	Edge 1 to Edge 2	89.997783
Edge 2 to Edge 3	89.999772	Edge 2 to Edge 3	90.002554	Edge 2 to Edge 3	90.000837
Edge 3 to Edge 4	90.002586	Edge 3 to Edge 4	90.003286	Edge 3 to Edge 4	90.002940
Edge 4 to Edge 1	89.998557	Edge 4 to Edge 1	89.998461	Edge 4 to Edge 1	89.998440

Table 8.8: Length measurements of the horizontal pyramid

Length					
	Top nominal = 51.00 mm		Middle nominal = 54.00 mm		Bottom nominal = 57.00 mm
Pt 1	50.991875	Pt 1	53.984635	Pt 1	56.984762
Pt 2	50.990394	Pt 2	53.984571	Pt 2	56.983854
Pt 3	50.991835	Pt 3	53.984514	Pt 3	56.984028

Table 8.9 Width measurements of the horizontal pyramid

Width					
Top nominal = 26.00 mm		Middle nominal = 29.00 mm		Bottom nominal = 32.00 mm	
Pt 1	25.993312	Pt 1	28.986900	Pt 1	31.986544
Pt 2	25.991640	Pt 2	28.982597	Pt 2	31.985697
Pt 3	25.990759	Pt 3	29.006350	Pt 3	31.983858

Table 8.10 Height measurement of the horizontal pyramid

Height			
Top to step 1 nominal = 2.00 mm		Top to step 2 nominal = 4.00 mm	
Pt 1	1.979254	Pt 1	3.976226
Pt 2	2.012438	Pt 2	4.010168
Pt 3	2.020126	Pt 3	4.020810
Pt 4	1.998121	Pt 4	3.996811

Table 8.11 Step width measurements of the horizontal pyramid

Step width							
Top edge to step 1 edge nominal = 1.50 mm							
Edge 1		Edge 2		Edge 3		Edge 4	
Pt 1	1.499722	Pt 1	1.496372	Pt 1	1.493038	Pt 1	1.497217
Pt 2	1.500358	Pt 2	1.495244	Pt 2	1.493819	Pt 2	1.495713
Pt 3	1.499698	Pt 3	1.493831	Pt 3	1.492982	Pt 3	1.521760
Top edge to step 2 edge nominal = 3.00 mm							
Edge 1		Edge 2		Edge 3		Edge 4	
Pt 1	3.001104	Pt 1	2.995762	Pt 1	2.991784	Pt 1	2.997470
Pt 2	3.001261	Pt 2	2.997044	Pt 2	2.992199	Pt 2	2.997013
Pt 3	3.000922	Pt 3	2.994576	Pt 3	2.991271	Pt 3	2.998523

Table 8.12 Flatness measurements of the horizontal pyramid

Flatness	
step 1	0.001029
step 2	0.004410

Table 8.13: Planes parallelism measurements of the horizontal pyramid

Parallelism (planes)	
Top to step 1	0.080910
step 1 to step 2	0.005664

The results shown are for the horizontal flat pyramid and the results of the vertical pyramid are shown in Appendix VIII. After measuring using the F25 at NPL, these were found:

- The surface quality is not too bad.
- It does provide clear indication that Ultra-Mill is working pretty well.
- Some absolute accuracy does lie outside the specifications and ideally should be smaller than 5 μm.

Looking at the absolute accuracy, this could be influenced by:

- Tooling quality (toolwear, actual size, etc.).
- Top surface of workpiece was not ground properly.
- Tool runout.

Results for the vertical flat pyramid are illustrated in Appendix VIII.

Unfortunately the relationship between the XY and YZ is yet to be confirmed. This is the limitation of sending out testpieces for measurements as it is still at NPL waiting to be determined.

Other various machined components are described in Appendix VIII.

8.2. Control System Performance Evaluation Based on Machining Trials

Through the two studies discussed in the earlier sections, the results obtained have proven in terms of control system performance is concerned, the control system is operating relatively well.

Some results obtained may included some deviation compared to designed specifications and these have been categorized more as mechanically induced errors. Setting up, fixturing, tool quality, etc. are the key elements which could enhance the mechanical induced errors.

8.2.1. Machine Dynamic Performance

In terms of machining dynamics performance, various machining processes were conducted on the Ultra-Mill and have found the all the axes have sufficient or more than enough dynamic stiffness to reject disturbances injected into the direct drive systems.

This was displayed on the axes tracking and following errors. During machining, the axes are able to have following or tracking errors of less than 1 µm. The cutting forces were not large enough to overcome the axes stiffness.

The stiffness of the axes was supplied through excellent tuning of the servo loop.

8.2.2. Volumetric Errors

Machine tools with significant volumetric errors would produce workpieces having these errors embedded in the part accuracy, surface quality and form. These errors are influence by geometric, thermal and dynamic errors. These errors would provide an error signature which is related to the machine directly. Volumetric errors of a machine tool could be reduced with properly setting up the axes with emphasize of minimizing the straightness, squareness, parallelism and circularity errors of the axes and through software compensation.

Stated in (ISO 230-6, 2002), volumetric performance is the ability of machine tool to perform the intended multi-axes functions anywhere within the working volume or a smaller volume as agreed between manufacturer and user. The correct definition of 3D

volumetric positioning error is the root mean square of the three linear axes displacement errors (Wang, 2009).

8.2.2.1. Ultra-Mill 5-Axis Error Analysis

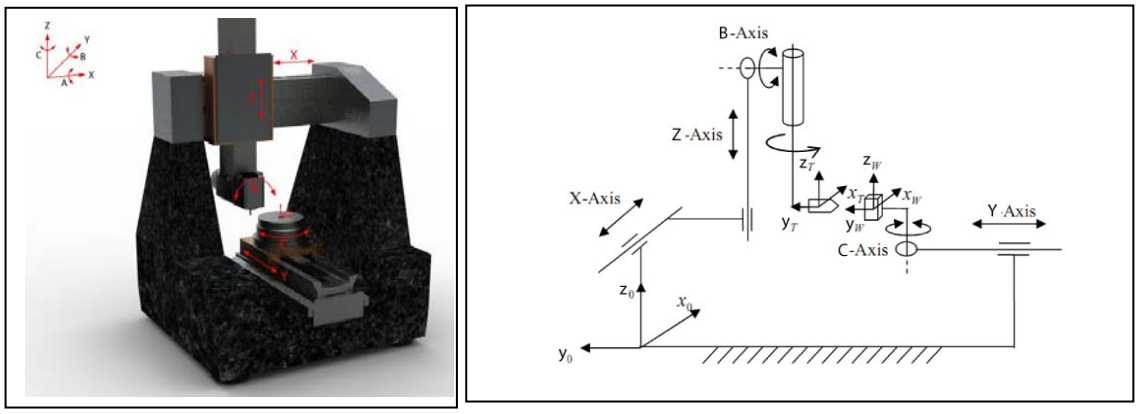

(a) Schematic of Ultra-Mill

(b) Diagrammatic sketch of Ultra-Mill structures

Fig. 8.12 Ultra-Mill schematic and diagrammatic sketch

Figure 8.12 describes the schematic and diagrammatic sketch of the Ultra-Mill for error analysis. Homogeneous transformation matrices (HTM) are adopted to derive the relative position of a rigid body in 3D space relative to designated coordinate system. Determining the geometrical errors for a machine tool, the relationship between the tooltip must be defined in a common reference coordinate system (Slocum 1992).

The six degrees of a rigid body HTMs are represented as:

$$T_X = \begin{bmatrix} 1 & 0 & 0 & A \\ 0 & 1 & 0 & 0 \\ 0 & 0 & 1 & 0 \\ 0 & 0 & 0 & 1 \end{bmatrix} \quad (8.1) \qquad T_Y = \begin{bmatrix} 1 & 0 & 0 & 0 \\ 0 & 1 & 0 & B \\ 0 & 0 & 1 & 0 \\ 0 & 0 & 0 & 1 \end{bmatrix} \quad (8.2) \qquad T_Z = \begin{bmatrix} 1 & 0 & 0 & 0 \\ 0 & 1 & 0 & 0 \\ 0 & 0 & 1 & C \\ 0 & 0 & 0 & 1 \end{bmatrix} \quad (8.3)$$

$$T_A = \begin{bmatrix} 1 & 0 & 0 & 0 \\ 0 & \cos\alpha_X & -\sin\alpha_X & 0 \\ 0 & \sin\alpha_X & \cos\alpha_X & 0 \\ 0 & 0 & 0 & 1 \end{bmatrix} \quad (8.4) \qquad T_B = \begin{bmatrix} \cos\alpha_Y & 0 & \sin\alpha_Y & 0 \\ 0 & 1 & 0 & 0 \\ -\sin\alpha_Y & 0 & \cos\alpha_Y & 0 \\ 0 & 0 & 0 & 1 \end{bmatrix} \quad (8.5)$$

$$T_C = \begin{bmatrix} \cos\alpha_Z & -\sin\alpha_Z & 0 & 0 \\ \sin\alpha_Z & \cos\alpha_Z & 0 & 0 \\ 0 & 0 & 1 & 0 \\ 0 & 0 & 0 & 1 \end{bmatrix} \tag{8.6}$$

A, B and C represent translations and α_X, α_Y, and α_Z represent rotational in the X, Y and Z axes.

Combination of the six individual HTMs is described as:

$$T = T_X T_Y T_Z T_A T_B T_C = \begin{bmatrix} \cos\alpha_Y \cos\alpha_Z & -\cos\alpha_Y \sin\alpha_Z & \sin\alpha_Y & A \\ \sin\alpha_X \cos\alpha_Z \sin\alpha_Y + \sin\alpha_Z \cos\alpha_X & -\sin\alpha_X \sin\alpha_Z \sin\alpha_Y + \cos\alpha_Z \cos\alpha_X & -\cos\alpha_Y \sin\alpha_X & B \\ \cos\alpha_Z \cos\alpha_X \sin\alpha_Y + \sin\alpha_Z \sin\alpha_X & -\cos\alpha_X \sin\alpha_Z \sin\alpha_Y + \cos\alpha_Z \sin\alpha_X & \cos\alpha_Y \cos_X & C \\ 0 & 0 & 0 & 1 \end{bmatrix} \tag{8.7}$$

A rigid body consists of translational errors (δ_X, δ_Y and δ_Z) and rotational errors (ε_X, ε_Y and ε_Z) associated with motion which is used in Equation 8.7, therefore error in linear motion is represented as:

$$T_\varepsilon = \begin{bmatrix} 1 & -\varepsilon_Z & \varepsilon_Y & A+\delta X \\ \varepsilon_Z & 1 & -\varepsilon_X & B+\delta Y \\ -\varepsilon_Y & \varepsilon_X & 1 & C+\delta Z \\ 0 & 0 & 0 & 1 \end{bmatrix} \tag{8.8}$$

Errors in rotational axes (A, B and C) are represented as:

$$T_{A\varepsilon} = \begin{bmatrix} 1 & -\varepsilon_Z & \varepsilon_Y & \delta_X \\ \varepsilon_Y \sin\alpha_X + \varepsilon_Z \cos\alpha_X & \cos\alpha_X & -\sin\alpha_X & \delta_Y \\ \varepsilon_Y \cos\alpha_X + \varepsilon_Z \sin\alpha_X & \sin\alpha_X & \cos\alpha_X & \delta_Z \\ 0 & 0 & 0 & 1 \end{bmatrix} \tag{8.9}$$

$$T_{B\varepsilon} = \begin{bmatrix} \cos\alpha_Y & -\varepsilon_Z \cos\alpha_Y & \sin\alpha_Y & \delta_X \\ \varepsilon_X \sin\alpha_Y + \varepsilon_Z & 1 & -\varepsilon_X \cos\alpha_Y & \delta_Y \\ -\sin\alpha_Y & \varepsilon_Z \sin\alpha_X + \varepsilon_X & \cos\alpha_Y & \delta_Z \\ 0 & 0 & 0 & 1 \end{bmatrix} \tag{8.10}$$

$$T_{C\varepsilon} = \begin{bmatrix} \cos\alpha_Z & -\sin\alpha_Z & \varepsilon_Z & \delta_X \\ \varepsilon_X \sin\alpha_Y + \varepsilon_Z & \cos\alpha_Z & -\varepsilon_X & \delta_Y \\ \varepsilon_X \sin\alpha_Z - \varepsilon_Y \cos\alpha_Z & \varepsilon_X \cos\alpha_Z + \varepsilon_Y \sin\alpha_Z & 1 & \delta_Z \\ 0 & 0 & 0 & 1 \end{bmatrix} \tag{8.11}$$

From the general HTM, the HTM for the Ultra-Mill is derived. Axes notations are illustrated in Figure 8.12(a).

In Equation 8.12, the left hand side represents the workpiece-machine base chain and the right hand side represents the tool-machine base chain. The individual transformation is represented in equations 8.13, 8.14, 8.15, 8.16 and 8.17.

$${}^{f}T_{Y}{}^{Y}T_{C} \begin{bmatrix} X_A \\ Y_A \\ Z_A \\ 1 \end{bmatrix} = {}^{f}T_{X}{}^{X}T_{Z}{}^{Z}T_{B} \begin{bmatrix} X_t \\ Y_t \\ Z_t \\ 1 \end{bmatrix} \tag{8.12}$$

$${}^{f}T_{Y} = \begin{bmatrix} 1 & -\varepsilon_Z(Y) & \varepsilon_Y(Y) & \delta_X(Y) \\ \varepsilon_Z(Y) & 1 & -\varepsilon_X(Y) & -Y - \delta_Y(Y) \\ -\varepsilon_Y(Y) & \varepsilon_X(Y) & 1 & \delta_Z(Y) \\ 0 & 0 & 0 & 1 \end{bmatrix} \tag{8.13}$$

$${}^{Y}T_{C} = \begin{bmatrix} \cos\alpha_Z & -\sin\alpha_Z & \varepsilon_Y(C) & \delta_X(C) \\ \sin\alpha_Z & \cos\alpha_Z & -\varepsilon_X(C) & \delta_Y(C) \\ \varepsilon_X(C)\sin\alpha_Z - \varepsilon_Y(C)\cos\alpha_Z & \varepsilon_X(C)\cos\alpha_Z + \varepsilon_Y(C)\sin\alpha_Z & 1 & \delta_Z(Y) \\ 0 & 0 & 0 & 1 \end{bmatrix} \tag{8.14}$$

$$ {}^{f}T_{X} = \begin{bmatrix} 1 & -\varepsilon_{Z}(X) & \varepsilon_{Y}(X) & X+\delta_{X}(X) \\ \varepsilon_{X}(X) & 1 & -\varepsilon_{X}(X) & \delta_{Y}(X)-\chi X \\ -\varepsilon_{Y}(X) & \varepsilon_{X}(X) & 1 & \delta_{Z}(X) \\ 0 & 0 & 0 & 1 \end{bmatrix} \tag{8.15} $$

$$ {}^{X}T_{Z} = \begin{bmatrix} 1 & -\varepsilon_{Z}(Z) & \varepsilon_{Y}(Z) & \delta_{X}(Z)-\beta_{1}Z \\ \varepsilon(Z) & 1 & -\varepsilon_{X}(Z) & \delta_{Y}(Z)-\beta_{2}Z \\ -\varepsilon_{Y}(Z) & \varepsilon_{X}(Z) & 1 & Z+\delta_{Z}(Z) \\ 0 & 0 & 0 & 1 \end{bmatrix} \tag{8.16} $$

$$ {}^{Z}T_{B} = \begin{bmatrix} \cos(-\alpha_{Y}) & -\varepsilon_{Z}(B)\cos(-\alpha_{Y}) & \sin(-\alpha_{Y}) & \delta_{X}(B) \\ \varepsilon_{X}(B)\sin(-\alpha_{Y})+\varepsilon_{Z}(B) & 1 & -\varepsilon_{X}(B)\cos(-\alpha_{Y}) & \delta_{Y}(B) \\ -\sin(-\alpha_{Y}) & \varepsilon_{Z}(B)\sin(-\alpha_{Y})+\varepsilon_{X}(B) & \cos(-\alpha_{Y}) & \delta_{Z}(B) \\ 0 & 0 & 0 & 1 \end{bmatrix} \tag{8.17} $$

Notations of the equations as shown above are:

- The positional errors in X, Y and Z directions are $\delta_X(X)$, $\delta_Y(Y)$ and $\delta_Z(Z)$.
- The radial and axial errors when the rotational axis is around X-axis of the reference coordinate frame are $\delta_X(B)$, $\delta_Y(B)$ and $\delta_Z(B)$.
- The radial and axial errors when the rotational axis is around X-axis of the reference coordinate frame are $\delta_X(C)$, $\delta_Y(C)$ and $\delta_Z(C)$.
- The straightness errors of X-axis in Y and Z directions are $\delta_Y(X)$ and $\delta_Z(X)$.
- The straightness errors of Y-axis in X and Z directions are $\delta_Y(X)$ and $\delta_Y(Z)$.
- The straightness errors of Z-axis in X and Y directions are $\delta_Z(X)$ and $\delta_Z(Y)$.
- The rotational errors of X-axis about X, Y and Z directions are $\varepsilon_X(X)$, $\varepsilon_Y(X)$ and $\varepsilon_Z(X)$.
- The rotational errors of Y-axis about X, Y and Z directions are $\varepsilon_X(Y)$, $\varepsilon_Y(Y)$ and $\varepsilon_Z(Y)$.
- The rotational errors of Z-axis about X, Y and Z directions are $\varepsilon_X(Z)$, $\varepsilon_Y(Z)$ and $\varepsilon_Z(Z)$.
- The rotational errors of rotational axes about the Y-axis of the reference coordinate frame are $\varepsilon_X(B)$ and, $\varepsilon_Z(B)$.

- The rotational errors of rotational axes about the Z-axis of the reference coordinate frame are $\varepsilon_X(C)$ and, $\varepsilon_Y(C)$.
- Squareness errors between the XY, XZ and YZ planes are α, β_1 and β_2.

The difference between the tooltip actual location and nominal location is defined as the volumetric errors. Substituting all error components with zero in Equation 8.12, the nominal tooltip location is defined as:

$$\begin{cases} X_n = \cos\alpha_Z (X + X_t \cos\alpha_Y + Z_t \sin\alpha_Y) + \sin\alpha_Z (Y_t + Y) \\ Y_n = -\sin\alpha_Z (X + X_t \cos\alpha_Y + Z_t \sin\alpha_Y) + \cos\alpha_Z (Y_t + Y) \\ Z_n = Z - X_t \sin\alpha_Y + Z_t \cos\alpha_Y \end{cases} \tag{8.18}$$

Hence, the final errors $(\Delta X, \Delta Y, \Delta Z,)^T$ could be defined as:

$$\begin{cases} \Delta X = X_A - X_n = X_A - \left[\cos\alpha_Z (X + X_t \cos\alpha_Y + Z_t \sin\alpha_Y) + \sin\alpha_Z (Y_t + Y)\right] \\ \Delta Y = Y_A - Y_n = Y_A - \left[\sin\alpha_Z (X + X_t \sin\alpha_Y + Z_t \sin\alpha_Y) + \cos\alpha_Z (Y_t + Y)\right] \\ \Delta Z = Z_A - Z_n = Z_A - Z + X_t \cos\alpha_Y \end{cases} \tag{8.19}$$

The Ultra-Mill mechanical structure was set up using a straight edge, a clock and experience of the technicians. Laser inferometers were unavailable to use during the set up. Laser inferometers are nowadays regarded as the standard equipment used for machine tool setting up. According to (ISO 230-1, 1996; ISO 230-6, 2002), the measuring instruments that are needed for setting up are laser inferometers or other measuring systems with comparable accuracy may be used. With the method implemented while setting up the Ultra-Mill, tests must be made to identify the errors and these errors would be identified through the machined parts.

Validating the HTM derived for Ultra-Mill requires data from the machining error assembly. These data will put into the HTM and then compared with error date of machined parts. Unfortunately at Brunel University, there is no such equipment that could be used to obtain these data in order to compare with the error from the machined part and the error calculated mathematically.

8.3. Summary

This chapter has elaborated the experiments conducted to evaluate the performance of the Ultra-Mill. From the selected case studies in this chapter, it is correct to say that performance of the Ultra-Mill satisfies with its design specifications in terms of form and geometrical accuracies, motion and positioning accuracies and achievable surface finish.

Through the cutting trials, the errors obtained are not related to the control system but are related to mechanical induced errors. These were found through careful analysis to eliminate the factors influencing these errors. Technically, these could easily be reduced by modifying the method of fixturing.

Aside from errors caused by fixturing, the assembly errors or manufacturing errors could be compensated using software compensation method. In making this feasible, suitable measuring equipment must be used to determine these errors as these errors are very minute. Combination of these minute errors will cause a large error machining at the micro and nano scale.

This chapter also described the types of errors involved with are related to the machined parts quality. The geometrical axes analysis for the Ultra-Mill has been derived using the HTM method. This mathematical formulation has provided the understanding on how small errors will lead to large errors.

Chapter 9

Conclusions and Recommendations for Future Work

9.1. Conclusions

Referring to the discussions discussed and elaborated in the chapters of this thesis and supported by validations through simulated and experimental results, these conclusions are drawn:

1) History of machine tools have been understood which is then used as understanding of the importance of machine tool used for manufacturing process. With the current requirements of 3D micro and nano products specifications, ultraprecision machine tools are the instrument to be used.
2) The current state of art of machine tool control systems have been surveyed in Chapter 2 to keep abreast with current requirements of ultraprecision multi-axis machine tools to produce the highest level of performance in terms of motion control system and the control system of the whole mechatronics system.
3) With the knowledge through the literature review, the design and development of the control system for the 5-axis ultraprecision micromilling machine, Ultra-Mill, is constructed. The design framework includes and elaborated all the important elements so as to identify the requirements for each subsystem.
4) Evaluation of the control system performance in terms of EMC and thermal effects have been simulated and validated to conclude that both the simulation values and real world values coincide. EMC and thermal have big influence in the control system in terms of electrical and electronics whereby these two elements could increase the potential of machine degradation.
5) Understanding the requirements of servo loop performances have been highlighted in Chapter 6. The Ultra-Mill implements direct drive system with aerostatic bearings where the external disturbance will affect directly the axes motion and position. Requirements of servo tuning are understood to increase axis dynamic stiffness, sensitivity and responsiveness.
6) The Ultra-Mill uses microtool with diameter less than 1mm and handling of the tools is critical since no ATC is present. An automated system was implemented by adopting a 3-axis SCARA robot for loading and unloading between the

spindle and tool magazine. The design of the communication between the Ultra-Mill control system and the 3-axis SCARA robot is fully presented.

7) Knowledge of tool monitoring is investigated in Chapter 7. Here the influences of tool wear and breakage were evaluated. A 3-axis dynamometer was used to measure the cutting forces during cutting trials and found that the cutting forces are minute. Tool condition monitoring was implemented using a non-contact laser system as this is the easiest solution and most importantly it is industrially feasible.
8) The Ultra-Mill performance was tested through various types of machining trials ranging from the ultraprecision level and conventional level. Geometrical errors were evaluated through machining trials as well. Errors found from the geometrical error experiments were influenced by mechanical and assembly errors of the machine structure and not the control system. Software compensation is required to compensate for these errors.
9) The research objectives highlighted in Section 1.4.2 have been achieved, analyzed and validated through experiment results.

9.2. Contribution to Knowledge

The innovation and contribution to knowledge from this research lie in:

1) Proposing the approach and concept of designing the control systems for a multi-axis micromilling ultraprecision machine tool which could be adopted as fundamental design protocol for other precision machine systems.
2) Undertaking orderly evaluation and validation of the implemented control system design through structured design of experiments.
3) Providing a framework for the relationship between control system design/requirements and machined components characteristics.
4) Implementation of servo loop tuning using Simulink Design Optimization toolbox.

9.3. Recommendations for Future Work

As recommendations for future work, these are suggested:

1) Re-evaluate the existing control system subsystems with comparison to existing commercial available ultraprecision machine tools for optimal overall performance.

2) Development of different types of servo algorithms.
3) Design and implementation of more cost effective monitoring systems.
4) Investigate the potential of simultaneous multi-axis servo loop tuning.
5) Further research on thermal effects compensation through the control systems.

References

Aerotech, n.d. [online]. Available at: http://www.aerotech.com/products/controllers /motion_controllers.html (Accessed on 9th September 2009).

Alique, J. R. and Haber, R., 2008. 'Advanced controls for new machining processes'. Machine tool for high performance machining, Springer-Verlag, pp. 159-218.

Alting, L., Kimura, F., Hansen, H. N., Bissacco, G., 2003. 'Micro engineering'. CIRP Annals-Manufacturing Technology, Vol. 52(2), pp. 635-658.

Altintas, Y., 2000. 'Manufacturing Automation: Metal Cutting Mechanics, Machine Tool Vibrations and CNC Design'. Cambridge University Press, London.

Armstrong, K., 2000. [online]. 'EMC for systems and installation: part 3'. Available at: www.compliance-club.com (Accessed on 2nd January 2009).

Armstrong, K. 2001. [online]. 'EMC for systems and installation: part 6'. Available at: www.compliance-club.com (Accessed on 5th January 2009).

Asato, O.L., Karo, E.R.R. and Porto, R.Y.V., 2002. 'Analysis of open CNC architecture for machine tools'. Journal of the Brazilian Society Mechanical Sciences, Vol. 24(3), pp. 208-212.

Bang, Y. B., Liee, K., and Oh, S., 2004. '5-axis micromilling machine for machining micro parts'. International Journal of Advanced Manufacturing Technology, Vol. 25, pp. 888-894.

Barrett, J., Harned, T. and Monnich, J., 2000. [online]. 'Linear motor basics'. Available at: http://www.parkermotion.com/whitepages/linearmotorarticle.pdf (Accessed on 2nd February 2008).

Bishop, R., 2008. 'Mechatronic System Control, Logic and Data Acquisition', CRC Press, New York.

Boucher, P., Dumur, D. and Ehrlinger, A., 1990. 'Generalized predictive cascade control (GPCC) for machine tools drives'. CIRP Annals-Manufacturing Technology, Vol. 39, pp 357-360.

Boucher, P., Dumur, D. and Kurzweil, H. P., 1993. 'Polynomial-predictive functional control (PPFC) for motor drive'. CIRP Annals-Manufacturing Technology, Vol. 42(1), pp. 453-456.

Brien, G. C., 1995. 'A natural kinematic and soft-axis architecture for open systems CNC'. Phd Dissertation, Swinburne University of Technology.

Byrne, G., Dornfeld, D. and Denkena, B., 2003. 'Advancing cutting technology'. CIRP Annals-Manufacturing Technology, Vol. 52(2), pp. 483-507.

Chae, J., Park, S. S. and Freiheit, T., 2006. 'Investigation of micro-cutting operations'. International Journal of Machine Tools and Manufacture, Vol. 46, pg. 313-332.

Cheng, K., 2008. 'Machining Dynamics: Fundamentals, Applications and Practices'. Springer Verlag, London.

Delta Tau Data Systems Inc., 2008a. 'Pewin Pro2 Software Manual'. Delta Tau Data Systems Inc. California.

Delta Tau Data Systems Inc., 2008b. 'PMAC HMI Software Manual'. Delta Tau Data Systems Inc. California.

Delta Tau Data Systems Inc., 2008c. 'PMAC NC Pro2 Software Manual'. Delta Tau Data Systems Inc. California.

Delta Tau Data Systems Inc., 2008d. 'PMAC Plot Software Manual'. Delta Tau Data Systems Inc. California.

Delta Tau Data Systems Inc., 2008e. 'PMAC Tuning Pro Software Manual'. Delta Tau Data Systems Inc. California.

Delta Tau Data Systems Inc., 2008f. 'UMAC Turbo CPU/Communications Board Hardware Manual'. Delta Tau Data Systems Inc. California.

Delta Tau Data Systems Inc., 2008g. 'Turbo PMAC user manual'. Delta Tau Data Systems Inc. California.

Delta Tau Data Systems Inc., n.d. [online]. Available at: http://www.deltatau.com (Accessed on 18th July2009).

Dimla, D. E., 1999. 'Tool wear monitoring using cutting force measurements'. Proceedings of the 15th NCMR: Advances in Manufacturing Technology, pp. 33-37.

Dimla, D. E., 2000. 'Sensor signals for tool-wear monitoring in metal cutting operations- a review of methods'. International Journal of Machine Tools and Manufacture, Vol. 40, pp. 1073-1098.

Dorf, R. C. and Bishop, R. H., 2001. 'Modern Control Systems'. Upper Saddle River, NJ, Prentice Hall, USA.

Dornfeld, D. A., 1990. 'Neural network sensor fusion for tool condition monitoring'. CIRP Annals-Manufacturing Technology, Vol. 39(1), pp. 101-105.

Dornfeld, D. A., Lee, D. E., Hwang, I., Valente, C. M. O. and Oliveira, J. F. G., 2006. 'Precision manufacturing process monitoring with acoustic emission'. International Journal of Machine Tools and Manufacture, Vol. 46, pp. 176-188.

Dumur, D. and Boucher, P., 1994. 'New predictive solutions to very high speed machining'. CIRP Annals-Manufacturing Technology, Vol. 43(1), pp. 363-366.

Dumur, D., Boucher, P. and Ehrlinger, A., 1996. 'Constrained predictive control for motor drives'. CIRP Annals- Manufacturing Technology, Vol. 45(1), pp. 355-358.

Fanuc, n.d. [online]. Available at: http://www.fanuc.co.jp/en/product/cnc/15i150i/ (Accessed on 18th July2009).

Franklin, G. F., Powell, J. D. and Naeini, A. E., 2006. 'Feedback Control Systems of Dynamic Systems'. Prentice Hall, USA.

Fujita, S. and Yoshida, T., 1996. 'OSE: open system environment for controller'. Proceedings of the 7th International Machine Tool Engineers Conference, pp. 234-243.

Fukuda, T. and Menz, W., 1998. 'Micro Mechanical Systems: Principles and Technology'. Elsevier Science B. V., The Netherlands.

Gandarias, E., Dimov, S., Pham, D. T., Ivanov, A., Popov, K., Lizarralde, R. and Arrazola, P. J., 2005. 'New methods for tool failure detection in micromilling'. Proceeding of IMechE, Part B: Journal of Engineering Manufacture, Vol. 220(2), pp. 137-144.

Gee, D., 2001. 'The how's and why's of pc based control'. Proceedings of Pulp and Paper Industry Technical Conference, pp. 67-74.

Gordon, S. and Hillery, M. T., 2005. 'Development of a high-speed CNC cutting machine using linear motors'. Journal of Materials Processing Technology, Vol. 166, pp. 321-329.

Hansen, H.N., Eriksson, T., Arentoft, M. and Paldan, N., 2006. 'Design rules for microfactory solutions'. Proceedings. of 5th Int. Workshop on Microfactories, Besancon, France.

Heidenhain, 2007. [online]. 'Uniformly digital: technical information'. Available at: www.heidenhain.com (Accessed on 12th February 2009).

Houpis, C. S. and Rasmussen, S. J., 1999. 'Quantitative Feedback Theory: Fundamentals and Applications'. Marcel Dekker Inc.

ISO 230-1, 1996. 'Test code for machine tools - Part 1: Geometric accuracy of machines operating under no-load or finishing conditions'. International Organization for Standardization.

ISO 230-6, 2002. 'Test code for machine tools - Part 6: Determination of positioning accuracy on body and surface diagonals (diagonal displacement tests)'. International Organization for Standardization.

Jemielniak, K., 1995. 'Commercial tool condition monitoring system based on power and acoustic emission sensors'. International Journal of Advanced Manufacturing Technology, Vol. 15, pp. 711-721.

Johns, D. P., Francois-Saint-Cyr, A. and German, F., 2002 [online]. 'EMC and thermal design conflicts in a PC'. Flomerics, Inc. Available at: http://electronics-cooling.com/articles/2002/2002_november_a1.php (Accessed on 24th November 2008).

Kern Evo Product Brochure, 2009. [online]. Available at: www.kern-microtechnic.com (Accessed on 2nd February 2009).

Kistler, 2005. DynoWare Type 2825A-02: Instruction Manual. Kistler Instrumente AG, Germany.

Kistler, 2008. 'MiniDyn Multicomponent Dynamometer Type 9256C: Instruction Manual'. Kistler Instrumente AG, Germany.

Ko. T. J., and Cho, D. W., 1994. 'Cutting state monitoring in milling by a neural network'. International Journal of Machine Tool and Manufacture, Vol. 34(3), pp. 625-631.

Koren, Y., 1980. 'Cross-coupled biaxial computer control for manufacturing systems'. Transaction of the ASME: Journal of Dynamic Systems, Measurement and Control, Vol. 102(4), pp. 265-272.

Koren, Y., 1983. 'Computer Control of Manufacturing Systems'. McGraw-Hill Inc, New York, USA.

Koren, Y., 1997. 'Control of machine tools'. Transactions of the ASME: Journal of Manufacturing Science and Engineering, Vol. 119(4(B)), pp 749-755.

Koren, Y., 1998. 'Open architecture controllers for manufacturing systems'. Open Architecture Control System, ITIA Series.

Koren, Y. and Lo, C. C., 1992. 'Advanced controllers for feed drives'. CIRP Annals-Manufacturing Technology, Vol. 41(2), pp. 689-698.

Korn, D., 2006. [online]. 'CAD/CAM considerations for micromilling'. Modern Machine Shop. Available at: http://www.mmsonline.com/articles/cadcam-considerations-for-micromilling.aspx# (Accessed on 1st January 2009).

Kugler Micromaster Product Brochure, 2009 [online]. Available at: www.kugler-precision.com/innovations.html (Accessed on 2nd February 2009).

Kussul, E. M., Huerta, L. R., Ruiz, A. C., Kasatkina, A. M., Kasatkina, L. M., Baidyk, T. N. and Velasco, G., 2004. 'CNC machine tools for low cost micro devices manufacturing'. Journal of Applied Research and Technology, Vol. 2, pp. 76-91.

Kussul, E., Baidyk, T., Ruiz-Huerta, L., Caballero-Ruiz, A., Velasco, G. and Kasatkina, L., 2002. 'Development of micromachine tool prototypes for microfactories'. Journal of Micromechanics and Microengineering, Vol. 12, pp. 795-812.

Kussul, E., Baidyk, T., Ruiz-Huerta, L., Caballero-Ruiz, A., Velasco, G. and Kasatkina, L., 1996. 'Micromechanical engineering: a basis of the low-cost manufacturing of mechanical micro devices using micro equipment'. Journal of Micromechanics and Microengineering, Vol. 6, pp. 410-425.

Kyura, N. and Oho, H., 1996. 'Mechatronics: an industrial perspective'. IEEE/ASME Transactions on Mechatronics, Vol. 1, pp. 10-15.

Leatham-Jones, B., 1986. ‘Introduction to Computer Numerical Control’. Pitman Publishing Limited, London.

Liang, S. Y., Hecker, R. L. and Landers, R. G., 2004. ‘Machining process monitoring and control: the state of the art’. Transaction on the ASME: Journal of Manufacturing Science and Engineering, Vol. 126(2), pp. 296-310.

Lister, P.M., 1993. ‘On-line measurement of tool wear’. Phd Dissertation, University of Manchester Institute of Technology.

Luo X., Cheng, K., Webb, D. and Wardle, F., 2005. ‘Design of ultraprecision machine tools with applications to manufacture of miniature and micro components’. Journal of Materials Processing Technology, Vol. 167, issues 2-3, pp. 515-528.

Luscombe, A. M., Toncich, D. J., Thompson, W. and Dluzniak, R., 1994. ‘A new type of machine control system to replace traditional CNC’. International Journal of Advanced Manufacturing Technology, Vol. 9, pp. 369-374.

Lutz, P. and Sperling, W., 1997. ‘OSACA - the vendor neutral control architecture’. Proc. of the European Conference on Integration in Manufacturing, Dresden, Germany.

Madou, M. J., 1997. ‘Fundamentals of Microfabrication’, CRC Press, Boca Ranton, USA.

Maekawa, H. and Komoriya, K., 2001. ‘Development of a micro transfer arm for a microfactory’. Proceeding of the 2001 IEEE International Conference on Robotics and Automation, Seoul, Korea, May 21-26, pp. 1444-1451.

Maj. R, Modica, F. and Bianchi, G., 2006. ‘Machine tool mechatronic analysis’. Proceedings of the IMECHE part B: Journal of Engineering Manufacture, Vol. 220(3), pp. 345-353.

Malekian, M., Park, S. S. and Jun, B. G., 2009. 'Tool wear monitoring of micro-milling fusion operation'. Journal of Materials Processing Technology, Vol. 209(10), pp. 4903-4914.

Masuzawa, T., 2000. 'State of art of micromachining'. CIRP Annals- Manufacturing Technology, Vol. 49(2), pp. 473-488.

Matlab, 2009a. [online]. Available at: http://www.mathworks.com/access/helddesk /help/pdf_doc/sldo/sldo_gs.pdf (Accessed on 1st October 2008).

Matlab, 2009b. [online]. Available at: http://www.mathworks.com/access/helpdesk /help/pdf_doc/fuzzy/fuzzy.pdf (Accessed on 18th June 2009).

Mihalik, N. P., 2006. 'Micromanufcaturing and Nanotechnology'. Springer-Verlag Berlin Heidelberg.

Mitsubishi, n.d. [online]. Available at: http://www.mitsubishielectric.com/ (Accessed on 18th July2009).

Moore, G., 2003. 'Development, implementation and management of a system level EMC design mitigation plan'. IEEE International Symposium on Electromagnetic Compatibility, Vol. 1, pp 173- 176.

Moriwaki, T., 2008. 'Multi-functional machine tool'. CIRP Annals - Manufacturing Technology, Vol. 57(2), pp. 736-749.

Nanotech 350 FG Product Brochure, 2009 [online]. Available at: www.nanotechsys.com (Accessed on 2nd February 2009).

Nor, M. K. M., Huo, D. and Cheng, K., 2007. 'A PC-based control system for multiple-axis micro/nano machining: control architecture and implementations'. In: 8th International Conference on Laser Metrology, CMM and Machine Tool Performance. Cardiff, 26th -28th June 2007, pp. 289-298.

O'Donnell, G. E., Young, P., Kelly, K. and Bryne, G., 2001. 'Towards the improvement of tool condition monitoring systems in the manufacturing environment'. Journal of Material Process Technology, Vol.119, pp.133-139.

Ohnishi, K., Shibata, M. and Murakami, T., 1996. 'Motion control for advanced mechatronics'. IEEE/ASME Transactions on Mechatronics, Vol. 1(1), pp. 56-67.

Okazaki, Y., Mishima, N. and Ashida, K., 2004. 'Microfactory - concept, history and developments'. Journal of Manufacturing Science and Engineering, Vol. 126, pp. 837-844.

Oliveira, J. F. G., Junior, F. F., Coelho, R. T. and Silva, E. J., 2008. 'Architecture for machining process and production monitoring based in open computer numerical control'. Proceedings of the Institution of Mechanical Engineers, Part B: Journal of Engineering Manufacture, Vol. 222 (12), pp. 1605-1612.

Park, S. S., Chae, J. and Freiheit, T., 2005. 'Investigation of micro-cutting operations'. International Journal of Machine Tools and Manufacture, Vol. 46, pp. 313-332.

Peklenik, J., 1970. 'Geometric adaptive control of manufacturing systems'. CIRP Annals – Manufacturing Technology, Vol. 18(1), pp. 265-272.

PMC, n.d. [online]. Available at: http://www.pmccorp.com/ (Accessed on 18th July 2009)

Precitech Nanoform 700 Ultra Product Brochure, 2009 [online]. Available at: www.precitech.com (Accessed on 2nd February 2009).

Pritschow G., 1998. 'Comparisons of linear and conventional electromechanical drives'. CIRP Annals - Manufacturing Technology, Vol. 47(2), pp. 541-548.

Pritschow, G., Daniel, C. H., Juchans, G. and Sperling, W., 1993. 'Open system controllers - a challenge for the future machine tools industry'. CIRP Annals-Manufacturing Technology, Vol. 42(1), pp. 449-452.

Proctor, F., 1998. ‘Practical architecture controllers for manufacturing applications’. Open Architecture Control System, ITIA Series.

Purushotthaman, S. and Srinivasa, Y. G., 1994. ‘A back-propagation algorithm applied to tool wear monitoring’. International Journal of Machine Tool and Manufacture, Vol. 34(3), pp. 341-350.

Radke, A. and Gao, Z., 2006. ‘A survey of state and disturbance observers for pratictioners’. Institute of Electrical and Electronics Engineers Inc.

Renishaw, 2002. [online]. ‘NC1 non-contact tool setting system’. Available at: www.renishaw.com (Accessed on 1st January 2009).

Renishaw, 2009. [online]. Available at: http://www.renishaw.com/en/nc4-non-contact-laser-tool-setter--6099 (Accessed on 3rd march 2009).

Rooks, B., 2004. ‘The shrinking sizes in micro manufacturing’. Assembly Automation, Vol. 24(4), pp. 353-356.

Schmidt, C., 1997. ‘A comparion of control strategies for feed-drive system of ultraprecision machine tools – effects of frictionless air bearings’. Proceedings of International Conference on Power Electronics and Drive Systems, Vol. 1, pp. 262-269.

Schmidt, C., Heinzl, J. and Brandenburg, G., 1999. ‘Control approaches for high-precision machine tools with air bearings’. IEEE Transactions on Industrial Electronics, vol. 6, No. 5, pp. 979-989.

Schneider Electric, 2007. Electrical Installation Guide 2007: Part Q - EMC guidelines. Schneider Electric, UK.

Schofield, S., 1993. ‘Open architecture controller for advanced machine tools’. PhD Dissertation, University of California.

Schulter, B., 2002. [online]. 'Controlling the temperature inside equipment racks'. White Paper by Middle Atlantic Products, Inc. Available at: http://repnet.middleatlantic.com/COMPANY/MarketingFiles/TempInsideRacks/Thermal%20 Management%203-04.pdf (Accessed on 24th November 2008).

Siemens, n.d. [online]. Available at: http://www.siemens.com (Accessed on 18th July2009).

Slocum, A. H., 1992. 'Precision Machine Design'. Society of Manufacturing Engineers, USA.

Smith, G. T., 2008. **'**Cutting Tool Technology Industrial Handbook'. Springer-Verlag London Limited.

Srinivasan K. and Tsao, T. C., 1997. 'Machine tool feed drives and their control- a survey of the state of the art'. Transaction of the ASME: Journal of Manufacturing Science and Engineering, Vol. 19(4(B)), pp. 743-748.

Stanev, P. T., Wardle, F. And Corbett, J., 2004 'Investigation of grooved hybrid air bearing performance'. Proceedings of the Institution of Mechanical Engineers, Part K: Journal of Multi-body Dynamics, Vol. 218(2), pp. 95-106.

Suh, Suk-Hwan, Kang, S. K., Chung, D. K. and Stroud, I., 2008. 'Theory and Design of CNC Systems'. Springer-Verlag London.

Takeuchi, Y., Sakaida, Y. and Sata, T., 2000. 'Development of a 5-axis control ultra precision milling machine for micromachining based on non-friction servomechanisms'. CIRP Annals- Manufacturing Technology, Vol. 49, pp. 295-298.

Tanaka, M., 2001. 'Development of desktop machining microfactory'. Riken Review, (34), pp. 46-49.

Tomizuka, M., 1987. ‘Zero phase error tracking algorithm for digital control’. Transaction of the ASME: Journal of Dynamic Systems, Measurement and Control, Vol. 109(1), pp. 65-68.

Tung, E. D., Anwar, G. and Tomizuka, M., 1993. ‘Low velocity compensation and feedforward solution based on repetitive control’. Transaction of the ASME: Journal of Dynamic Systems, Measurement and Control, Vol. 115(2A), pp. 279-284.

Ultra-Mill Product Brochure, 2009. Brunel University, UK.

.

Van Den Braembusshe, P., Swevers, J., Brussel, H. V. and Wanheck, P., 1996. ‘Accurate tracking control of linear synchronous motor machine tool axes’. Mechatronics, Vol. 6(5), pp. 507-521.

Vogler, M. P., Liu, X., Kapoor, S. G., Devor, R. E. and Ehmann, K. F., 2002. ‘Development of meso-scale machine tool (mMT) systems’. Society of Manufacturing Engineers, MS MS02-181, pp. 1-9.

Wang, C., 2009. [online]. 'Machine Tool Calibration: Standards and Methods'. Available: http://www.americanmachinist.com/304/Issue/Article/False/83523/Issue (Ac cessed on18th July 2009).

Wang, W., Lee, K., Woo, I., Park, I. and Yang, S., 2006. ‘Optimal design on SAW sensor for wireless pressure measurement based on reflective delay line’. Sensors and Actuators, Vol. 139, pp. 2-6.

Weck, M., Fischer, S. and Vos, M., 1997. ‘Fabrication of micro components using ultra precision machine tools’. Nanotechnology, Vol. 8, pp. 145-148.

Weidner, C. and Quickel, D., 1999. ‘High speed machining with linear motors’. Manufacturing Engineering, Vol. 122(3), pp. 80-87.

Wikipedia, 2009a. [online]. Available at: http://en.wikipedia.org/wiki/Open_system_ (computing) (Accessed on 18th February 2009).

Wikipedia, 2009b. [online]. Available at: http://en.wikipedia.org/wiki/Acoustic_ emission (Accessed on 26th May 2009).

Wikipedia, 2009c. [online]. Available at http://en.wikipedia.org/wiki/CE_mark (Accessed on 28th June 2009).

Williams, T., 2000. 'EMC for Product Designers'. Butterworth-Heinemann, UK.

Wilson, C., 2004. [online]. 'Control requirement for high-precision, high-speed machining'. White paper from DeltaTau Data Systems, Inc. Available at: http:// www.deltatau.com/common/support/whitepapers/High-Precision%20Controls.pdf. (Accessed on 1st January 2009).

Wilson, C., 2004. [online]. 'Controller requirements for high speed motion applications.' Available at: http://www.deltatau.com/common/support/whitepapers/ High-Precision%20Controls.pdf, (Accessed on 1st January 2009).

Wright, P. and Wang, F. C., 1998. 'Open architecture controllers for machine tools, Part 2: A real-time quintic spline interpolator'. Journal of Manufacturing Science and Engineering (120), pp. 425-432.

Wright, P., Schofield, S. and Wang, F. C., 1996. 'Open architecture control for machine tools'. Integrated Manufacturing Laboratory, University of California.

Wright, P. and Schofield, S., 1998. 'Open architecture controllers for machine tools, Part 1: Design principles'. Journal of Manufacturing Science and Engineering, Vol. 120, pp. 417-424.

Wright, P., Dornfeld, D. and Ota, N., 2008. 'Condition monitoring in end-milling using wireless sensor networks (WSNs) '. Transaction of NAMRI/SME, Vol. 36, pp. 177-183.

Yellowley, I. and Oldknow, K. D., 2001. 'Design, implementation and validation of a system for the dynamic reconfiguration of open architecture machine tool controls'. International Journal of Machine Tools and Manufacture, Vol. 41, pp. 795-808.

Yonglin, C., 2005. ‘An evaluation space for open architecture controllers’. International Journal of Advanced Manufacturing Technology, Vol. 26, pp. 351-358.

Appendices

Appendix I

- **List of Publications Arising from this Research**

List of publications arising from this research

1. M. K. M. Nor, D. Huo and K. Cheng. A pc-based control system for multiple-axis micro/nano machining: control architecture and implementations. 8th International Conference on Laser Metrology, CMM and Machine Tool Performance. Cardiff, UK, 26th -28th June 2007, pp. 289-298.

2. M. K. M. Nor, D. Huo, K. Cheng and F. Wardle. Design of a 5-Axis ultraprecision micro milling machine (ultra-mill) and its key enabling technologies. Proceedings of the Euspen International Conference- San Sebastian, Spain, 2nd – 5th June 2009, pp. 204-207.

3. M. K. M. Nor and K. Cheng. Development of the pc-based control system for a 5-axis ultraprecision micromilling machine – ultra-mill and its performance assessment. Proceedings of the IMechE, Part B: Journal of Engineering Manufacture, (In press).

4. M. K. M. Nor and K. Cheng. An industrial feasible approach for assessing the performance of a 5-axis micromilling machine. Proceedings of the 10th Euspen International Conference, Delft, Holland, 1st – 4th June 2010, (In press).

Appendix II

- **CNC Architectures**

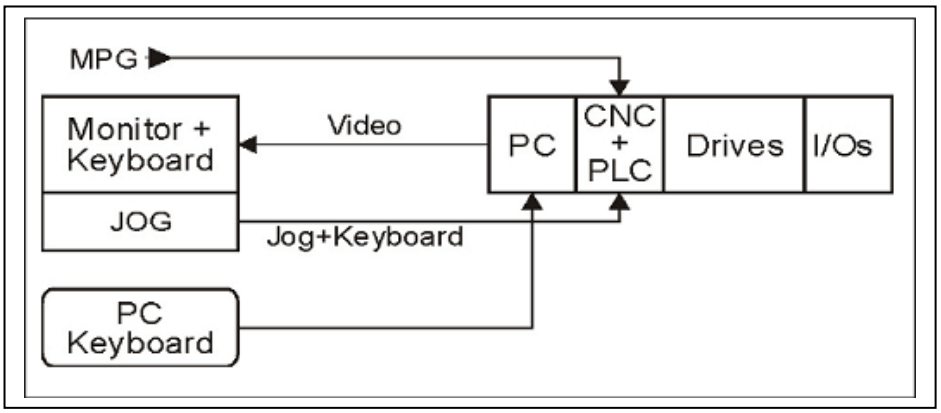

(a) Architecture 1

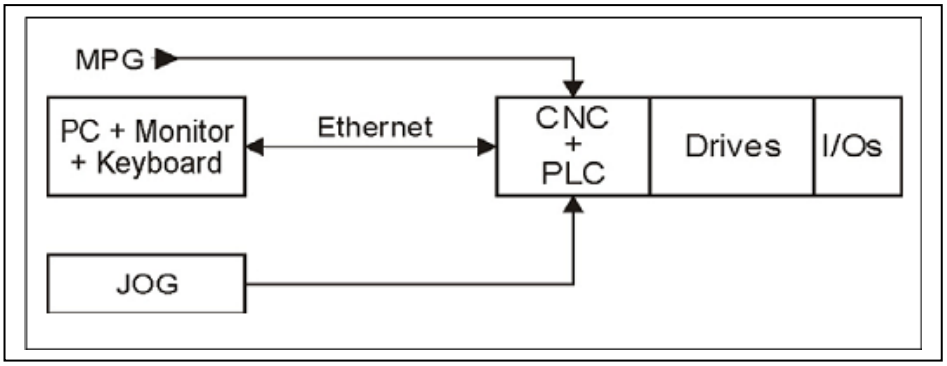

(b) Architecture 2

Fig. A-2.1 PC front-end architecture (Alique and Haber, 2008)

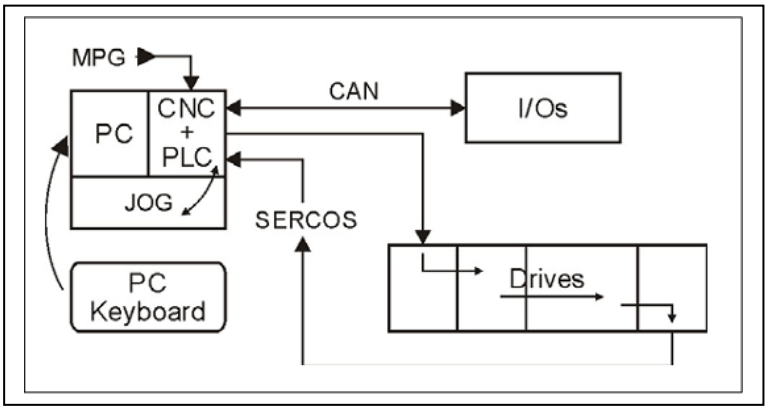

Fig. A-2.2 Architecture for software-based (Alique and Haber, 2008)

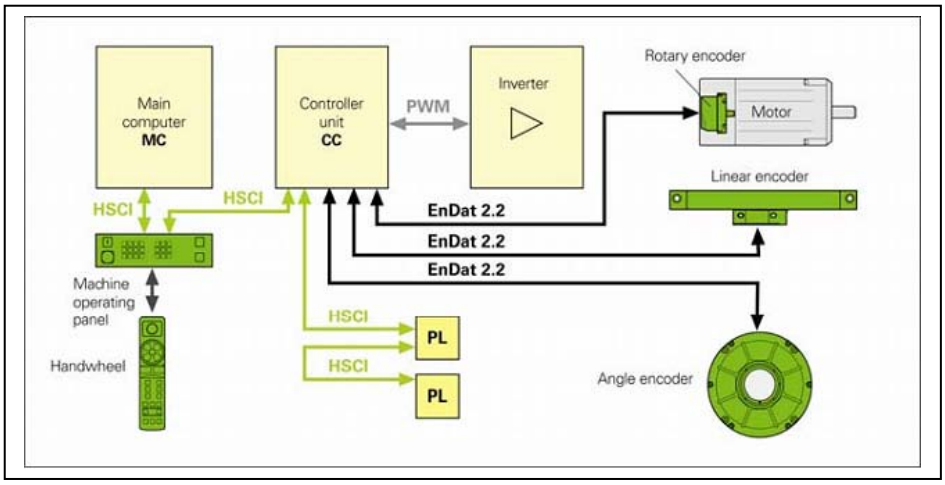

Fig. A-2.3 Fully digital architecture (Heidenhain, 2007)

Appendix III

- **Ultra-Mill Brochure with Specifications**

Brunel UNIVERSITY WEST LONDON

upm ltd

µltraMill™

5-axis Ultraprecision Bench-Top Micro Milling Machine

Machine Features & Capabilities

- Micro milling, drilling and grinding of fine surface features
- Machining of ferrous and nonferrous metals, plastics and crystals
- Aerostatic bearings incorporating squeeze film dampers and direct drives motors on all linear and one rotational axis so as to achieve smooth motion with exceptional accuracy and excellent dynamic performance
- High speed aerostatic spindle capable of 200,000 rpm offers the highest machining efficiency for micro machining
- Natural granite base provides excellent thermal stability and damping capacity
- PC based CNC control system with Windows platform and customizable HMI
- Optional extras include a robot-based tool/workpiece change and inspection subsystem and a condition monitoring subsystem

Specification

The μltraMill ™ is an ultraprecision bench-top 5-axis CNC controlled milling machine specially designed for manufacture of 3 dimensional miniature mechanical components and micro-featured surfaces in a wide range of engineering materials. The μltraMill ™ is compact and has a resource/energy efficient design giving submicron precision and nanometric surface finishes.

General	Description
System Configuration	Ultra-precision 5-axis bench-top micro milling machine with gantry frame
Base Material	Natural granite
Machining Envelope	150 mm x 150 mm x 80 mm (vertical)
Workpiece Material	Ferrous or nonferrous metal, plastics and crystals
Control System	Delta Tau PC-based multi-axis CNC motion controller (UMAC), in a Windows environment; Compact control enclosure - drawer cabinet mounted underneath the machine base to minimise overall machine footprint.
CNC Front-End	Delta Tau Advantage 900 system; 15'' flat panel monitor; Customized CNC software with 5-axis machining capability; wireless or cable pendant.
Space Requirement	1.1 m wide x 0.8 m deep x 2.1 m high

Machining Spindle	Performance
Type	Water cooled aerostatic bearing
Stiffness	Radial: 4N/μm; Axial: 3N/μm
Maximum Speed	200,000 rpm
Load Capacity	Radial: 55N at spindle nose; Axial: 45N
Drive System	DC brushless motor
Power	400 Watts at 200,000 rpm
Motion Accuracy	<1.0 μm axial TIR and <2.0 μm radial TIR
Tool Clamping	3 mm collet, manual or automatic (optional)

Linear Axes	X	Y	Z
Type	Air bearing slides fitted with squeeze film dampers		
Stroke	230 mm	225 mm	160 mm
Feedrate	0-3000 mm/min	0-3000 mm/min	0-3000 mm/min
Drive System	DC brushless linear motor	DC brushless linear motor	DC brushless linear motor
Feedback	Optical linear encoder	Optical linear encoder	Optical linear encoder
Resolution	5 nm	5 nm	5 nm
Motion Accuracy	<1.0 μm over total travel	<1.0 μm over total travel	<1.0 μm over total travel

Rotational Axes	B (Spindle Swivelling)	C (Workpiece Rotary Table)
Type	Precision ball bearing	Air bearing fitted with squeeze film dampers
Stroke	± 90°	360°
Rotational Speed	0-30 rpm	0-100 rpm
Drive System	DC brushless torque motor	DC brushless torque motor
Feedback	Optical rotary encoder	Optical rotary encoder
Resolution	0.026 arcsec	0.02 arcsec

Appendix IV

- **Screenshots of HMI Programming**
- **Part of the HMI Programming Codes**
- **Part of the PLC Programming Codes**

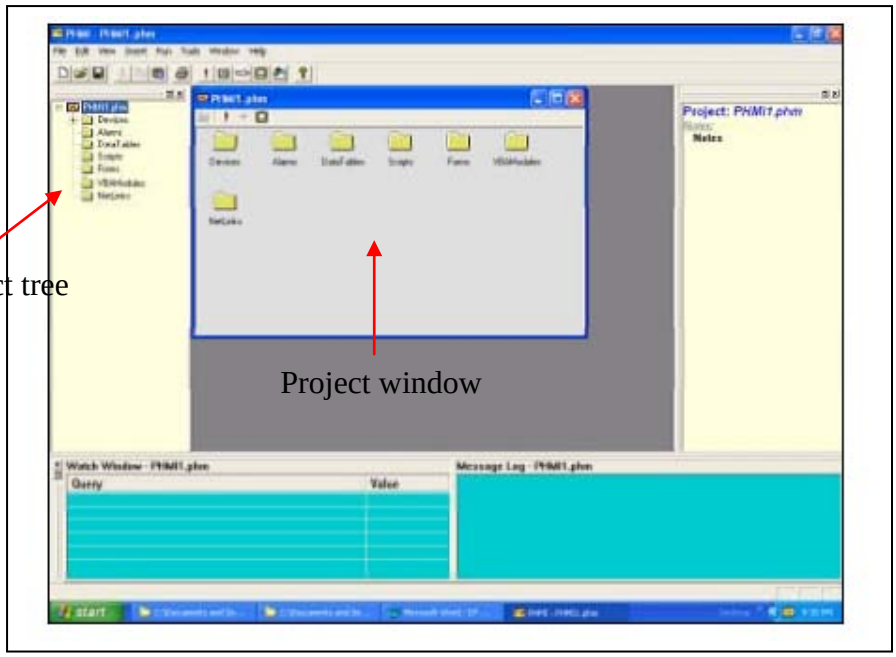

Fig. A-4.1 Screenshot of HMI customisation in VB

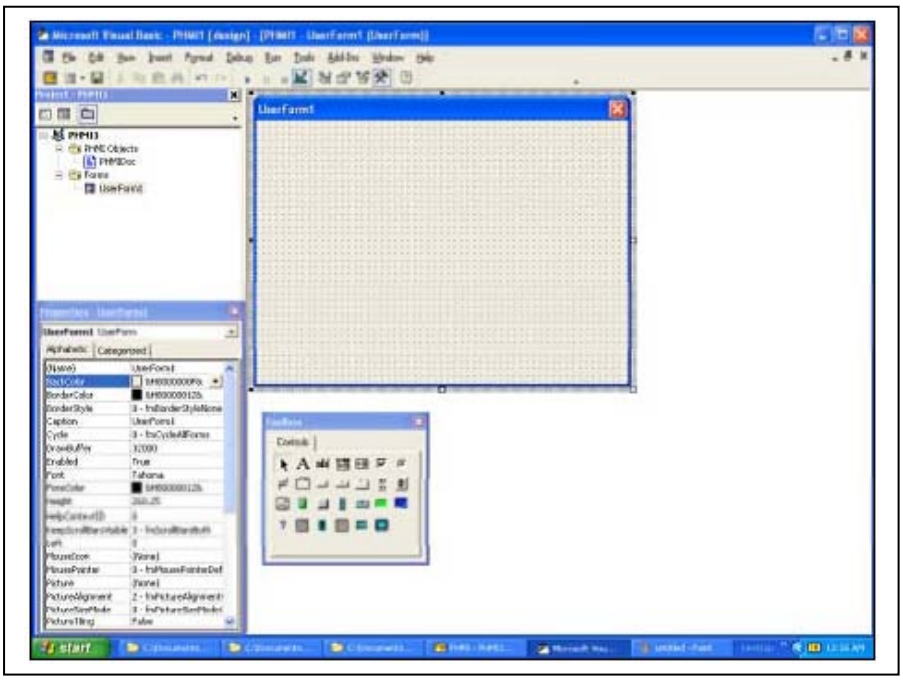

Fig. A-4.2 VB customisation window

\

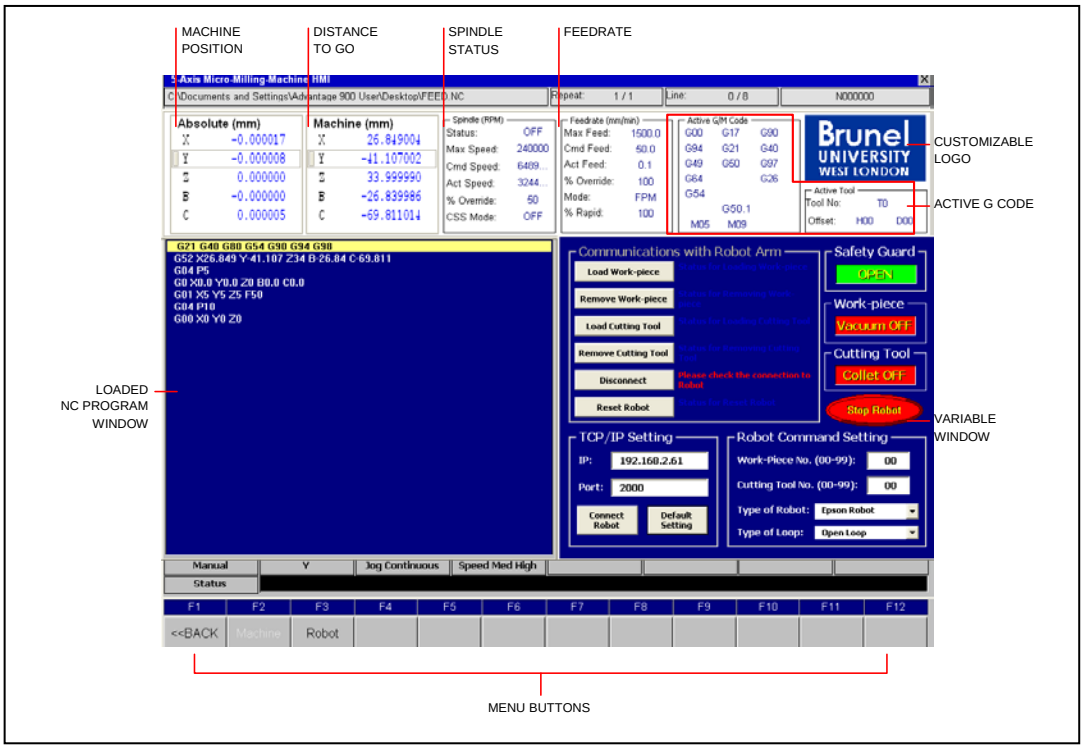

Fig. A-4.3 Designed HMI for Ultra-Mill

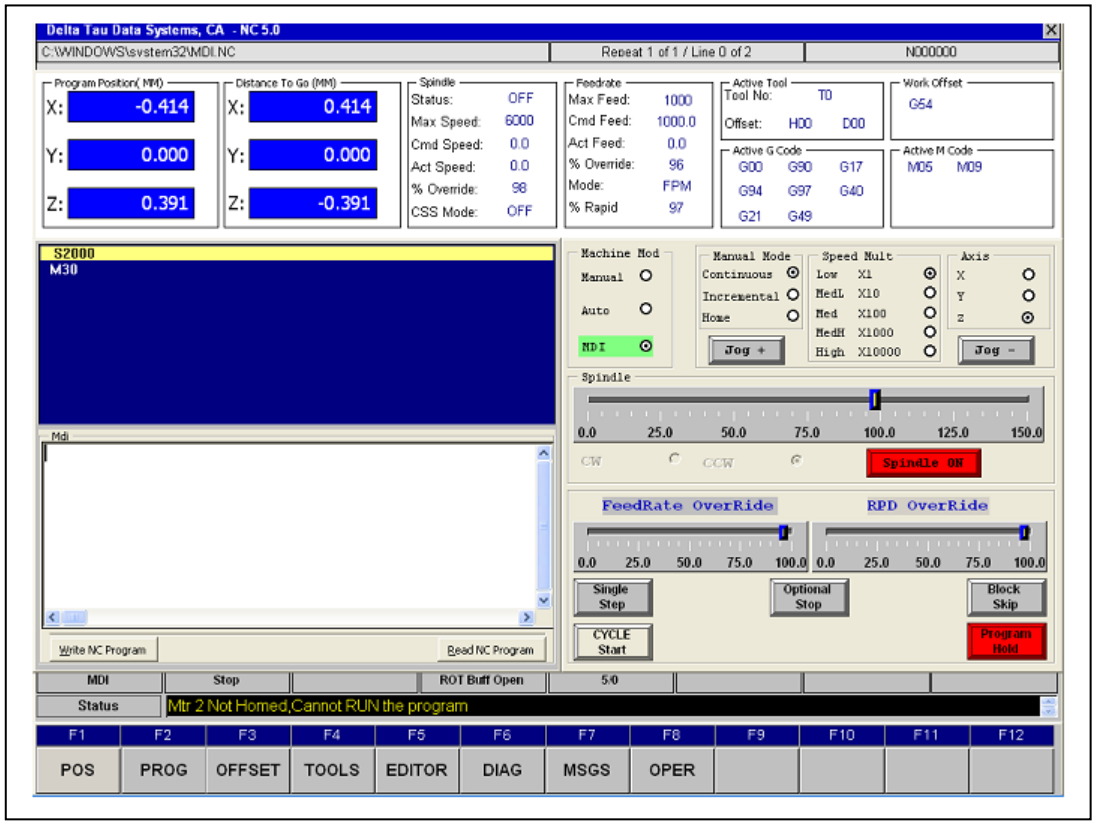

Fig. A-4.4 Initial HMI design

Part of the HMI Programming Codes:

```
' ---------------- Procedure DoFKey------------
' Handles F-Key functions for sub-menus
' ---------------------------------------------
Procedure DoFKey
	NUM nKey = GetArg(0)
	NUM CurrentMenu
	NUM UserPanelMode

	CurrentMenu = Query("DataTables.GlobalVars.CurrentMenu")

'	if (nKey = F12_KEY)
'		Dlg.MsgBox("Current Menu Error","F12 Pressed")
'	Endif
	if(CurrentMenu = 0)
		if (nKey = F1_KEY)
			Forms.SubMenuGroup.frmPositionMenu.Show
		elseif (nKey = F2_KEY)
			Forms.SubMenuGroup.frmProgramMenu.Show
		elseif (nKey = F3_KEY)
			Forms.SubMenuGroup.frmWorkOffsetMenu.Show
		elseif (nKey = F4_KEY)
			Forms.SubMenuGroup.frmToolMenu.Show
		elseif (nKey = F5_KEY)
			Forms.SubMenuGroup.frmEditorMenu.Show
		elseif (nKey = F6_KEY)
			Forms.SubMenuGroup.frmDiagnosticMenu.Show
		elseif (nKey = F7_KEY)
			Forms.SubMenuGroup.frmErrorsMenu.Show
		elseif (nKey = F8_KEY)
			UserPanelMode = Query("DataTables.GlobalVars.UserPanelMode")
			if(UserPanelMode = 1)
				Forms.SubMenuGroup.frmOperatorMenu.Show
			Endif
		endif
	elseif(CurrentMenu = 1)
		if (nKey = F1_KEY)
			Forms.SubMenuGroup.frmMainMenu.Show
		elseif (nKey = F2_KEY)
			Devices.PmacNC1.SetOrigin(1)
		elseif (nKey = F3_KEY)
			Devices.PmacNC1.SetOrigin(0)
		endif
	elseif(CurrentMenu = 2)
		if (nKey = F1_KEY)
			Forms.SubMenuGroup.frmMainMenu.Show
		elseif (nKey = F2_KEY)
			VBA.frmProgramMenu.Load
		elseif (nKey = F3_KEY)
			Devices.PmacNC1.ProgramRewind
		elseif (nKey = F4_KEY)
			VBA.frmProgramMenu.Search
		elseif (nKey = F5_KEY)
			VBA.frmProgramMenu.SearchLine
```

Part of the PLC Programming Codes:

```
OPEN PLC 8 CLEAR
IF(M800>0)
P806=M801
IF(P805=0)
IF(P806=0)
M479=1
M2000=1
M2001=0
M2006=0
M2007=0
M2008=0
ELSE
IF(P806=1)
M480=1
M2000=0
M2001=1
M2006=0
M2007=0
M2008=0
ELSE
IF(P806=6)
M549=1
M535=1
M480=0
M2000=0
M2001=0
M2006=1
M2007=0
M2008=0
ELSE
IF(P806=7)
M549=1
M536=1
```

Appendix V

- **Electrical Drawings**
- **EM Distribution Analysis**
- **CFD Thermal Analysis**

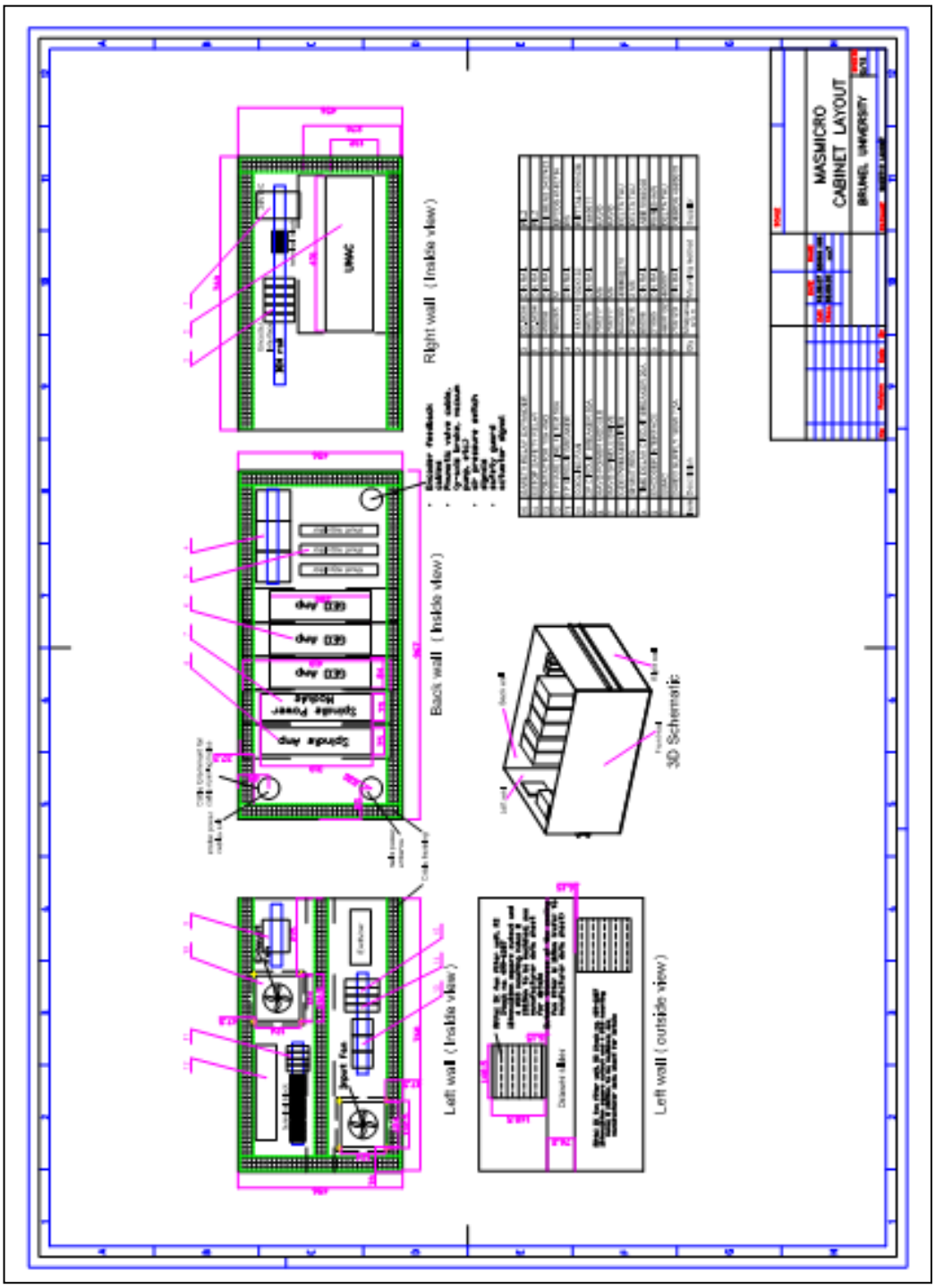

Fig. A-5.1 Electrical equipment layout

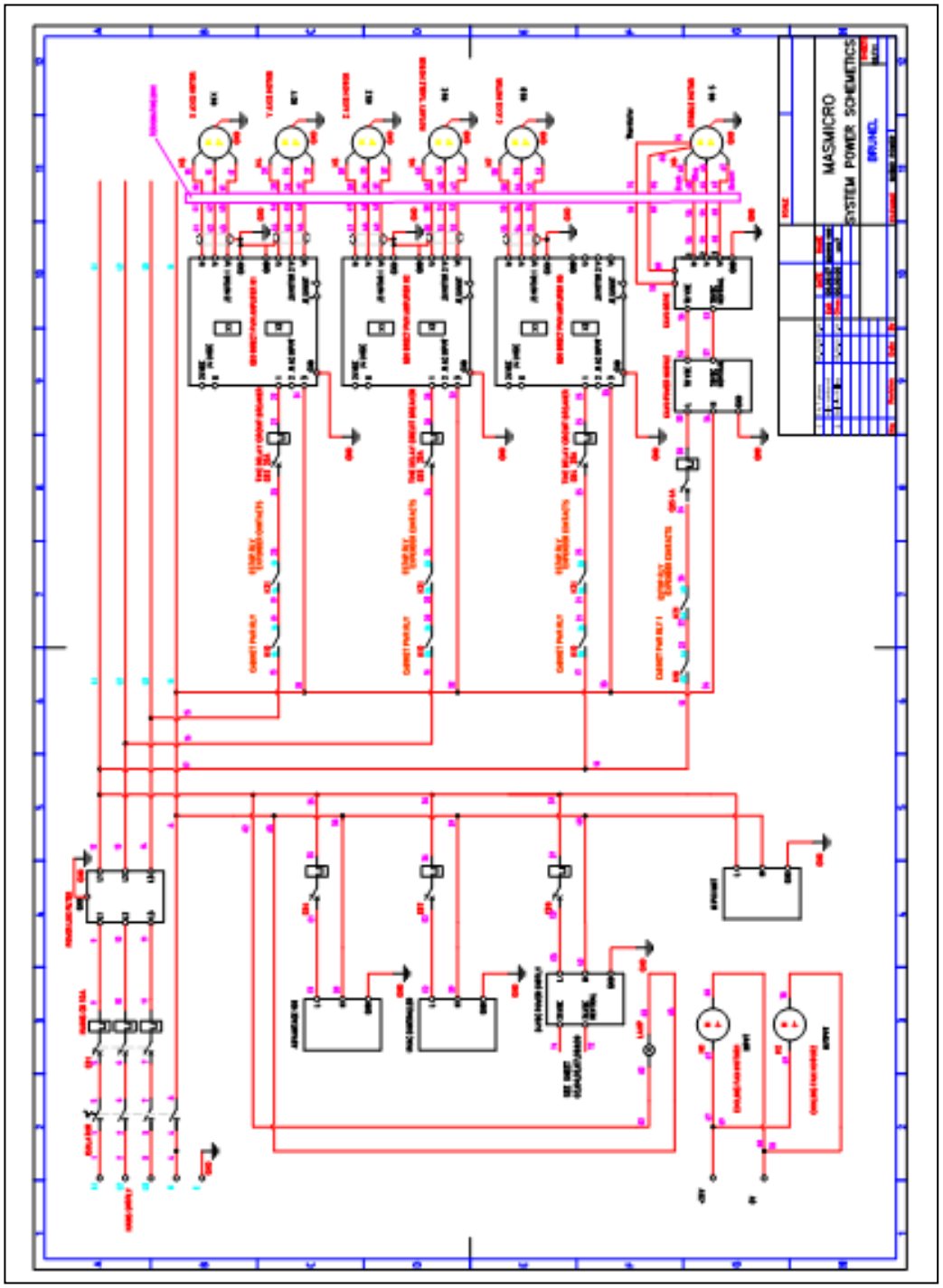

Fig. A-5.2 Electrical schematics

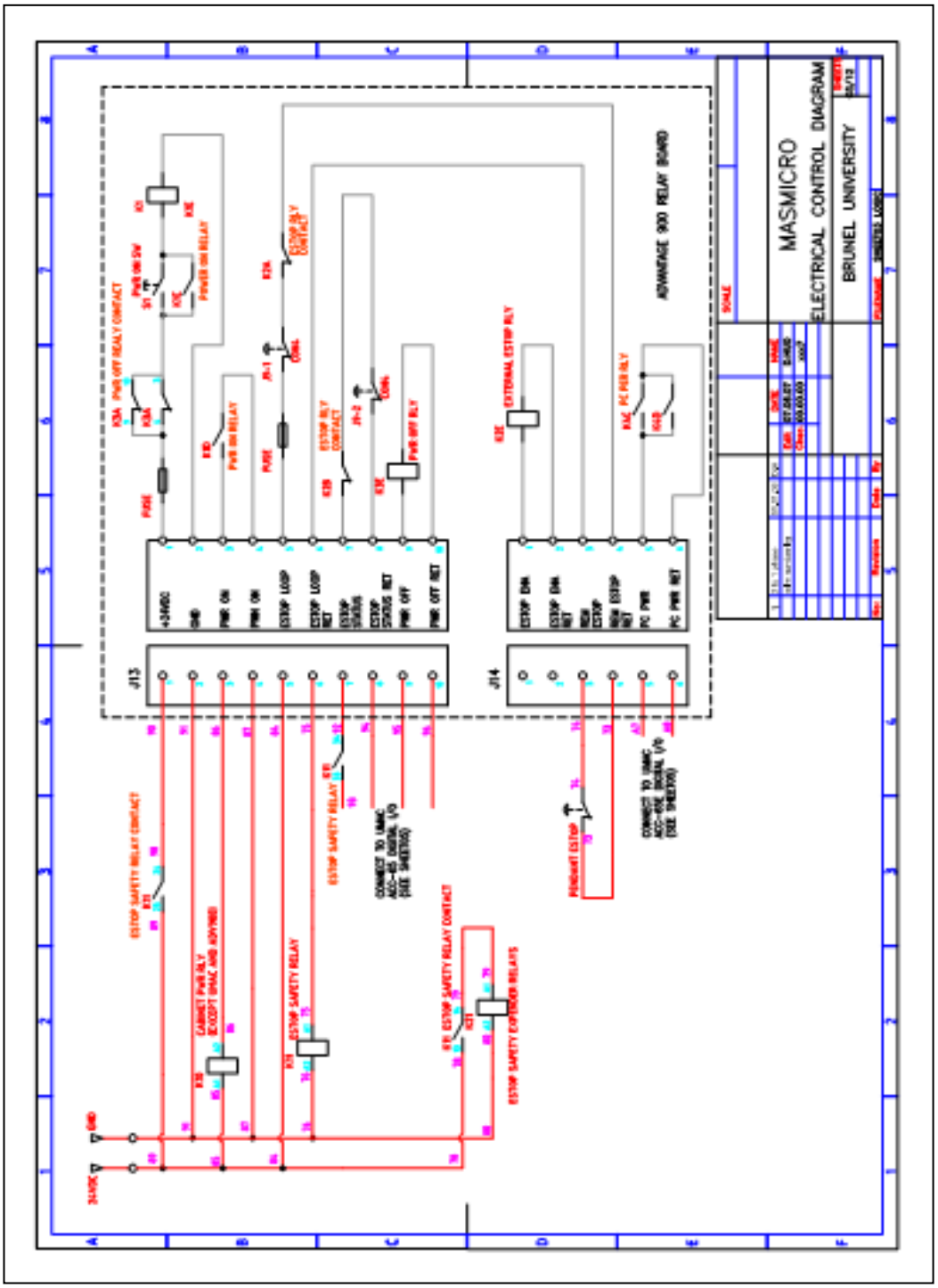

Fig. 5.3 A-Electrical control schematic

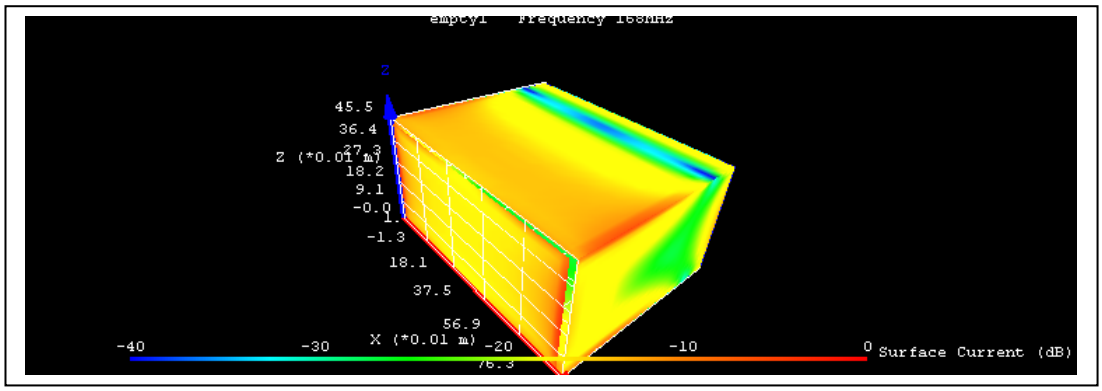

(a) 168 MHz

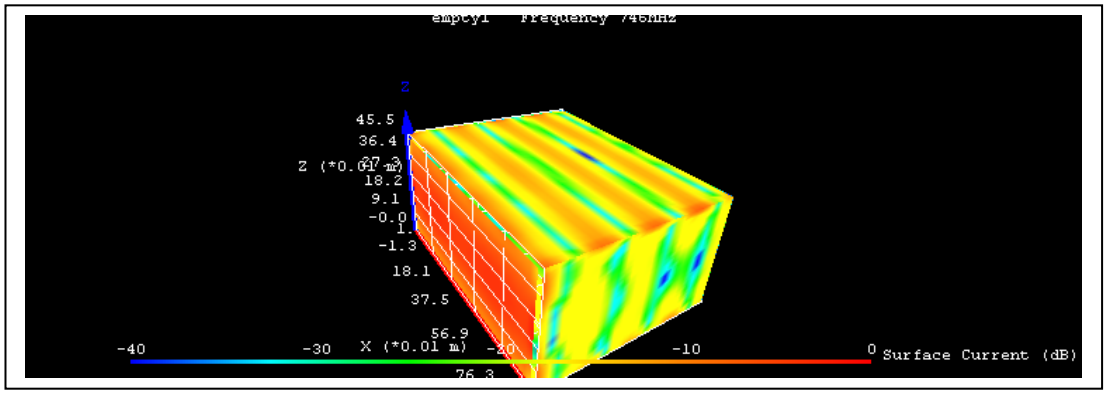

(b) 746 MHz

Fig. A-5.4 EM distribution of empty cabinet with lid

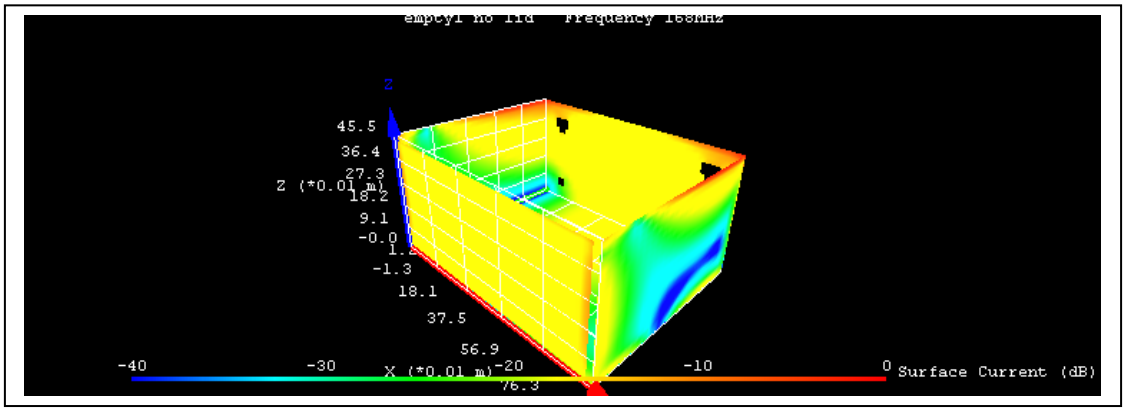

(a) 168 MHz

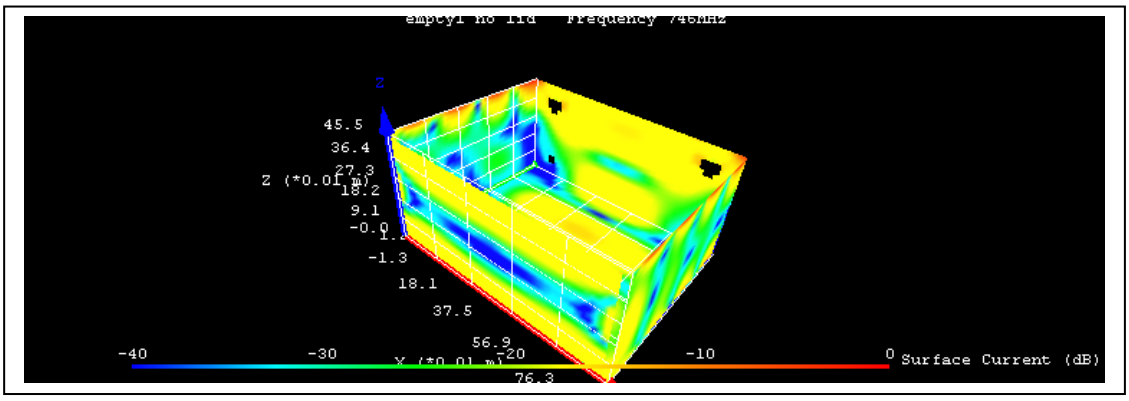

(b) 746 MHz

Fig. A-5.5 EM distribution of empty cabinet without lid

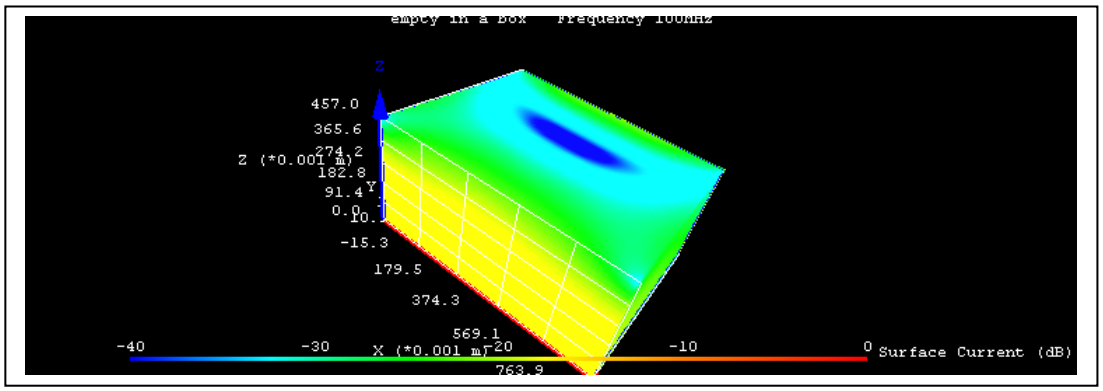

(a) 100 MHz

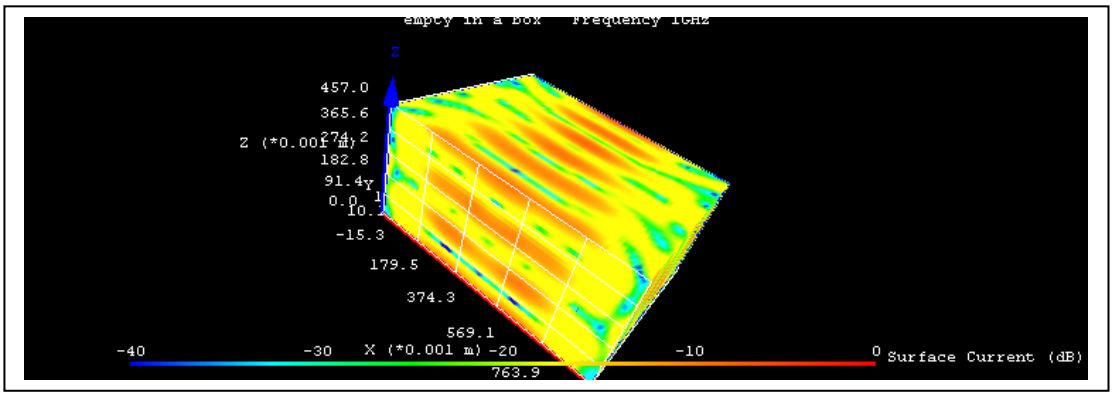

(c) 1 GHz

Fig. A-5.6 EM distribution of empty cabinet with lid within the machine frame

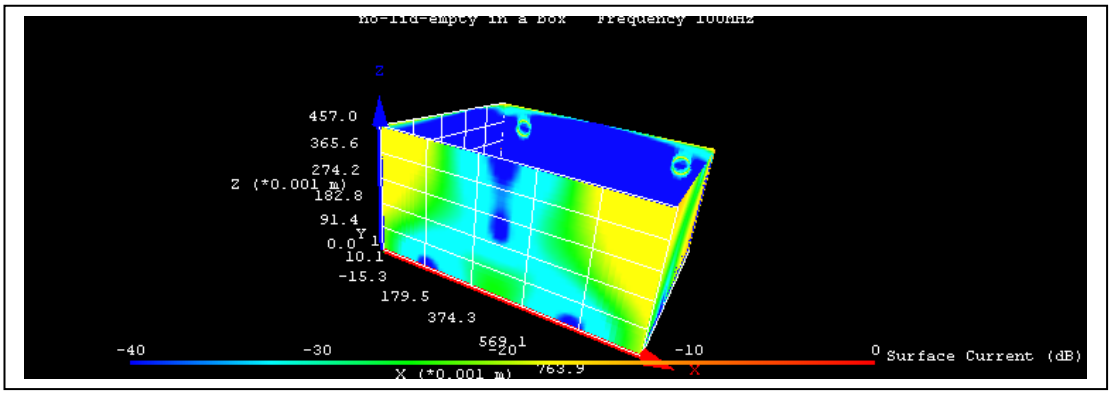

(a) 100 MHz

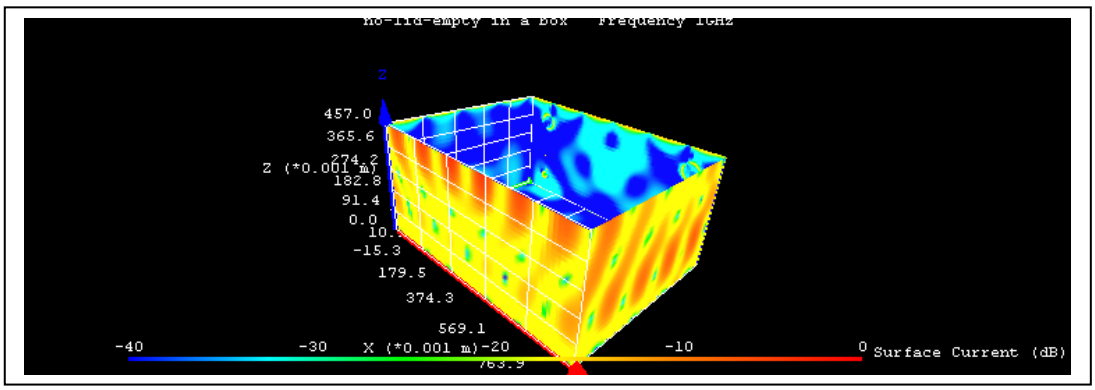

(b) 1GHz

Fig. A-5.7 EM distribution of empty cabinet without lid within the machine frame

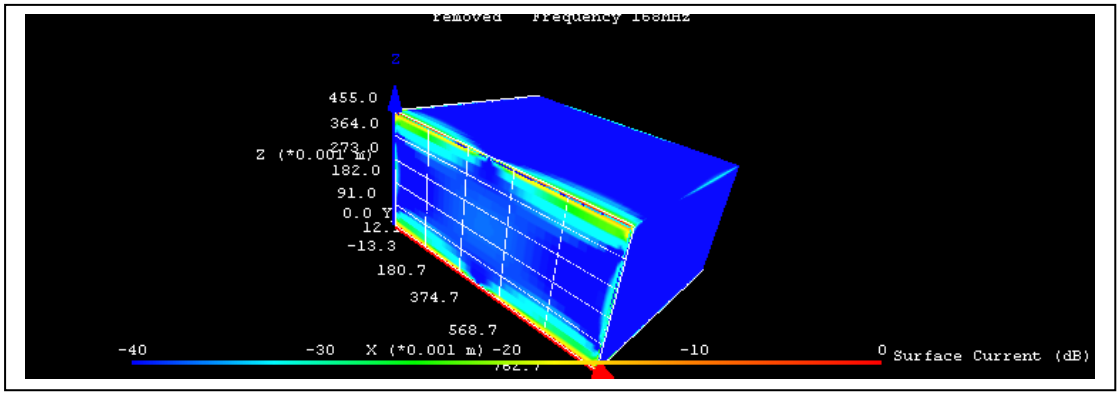

(a) 168 MHz

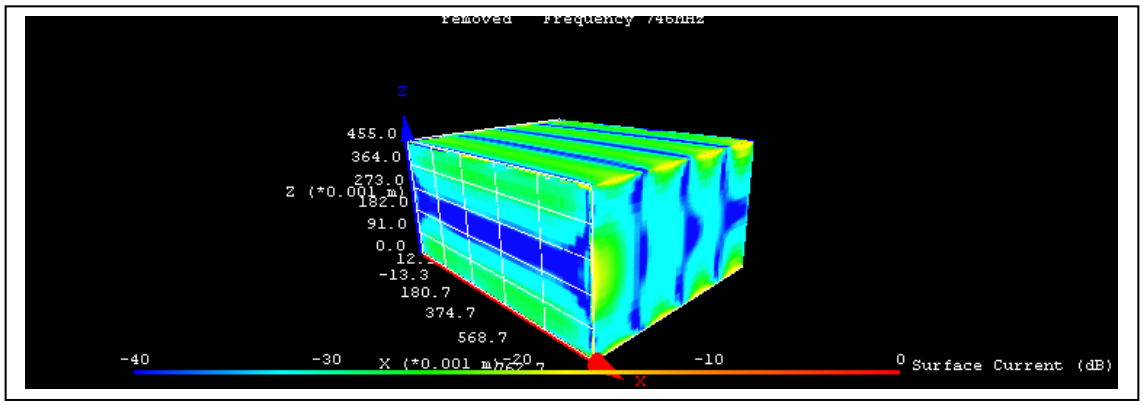

(b) 746 MHz

Fig. A-5.8 EM distribution of cabinet with trunking with lid in the machine frame

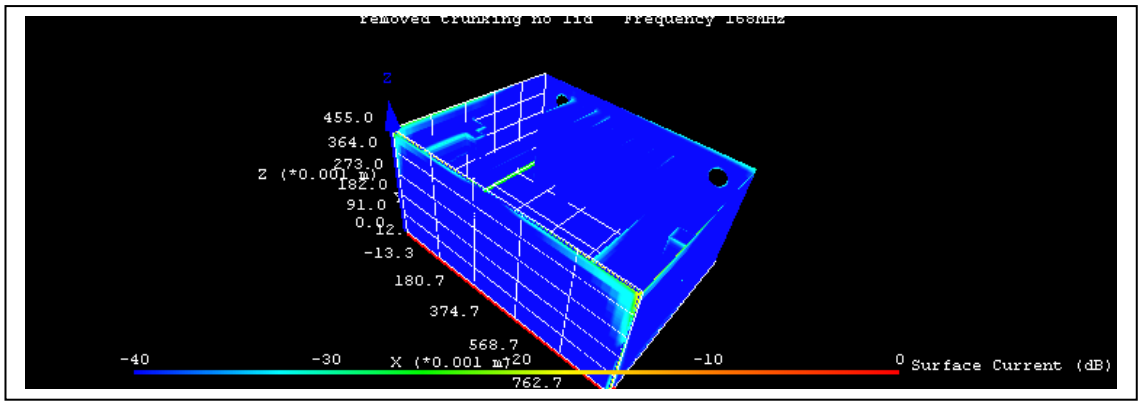

(a) 168 MHz

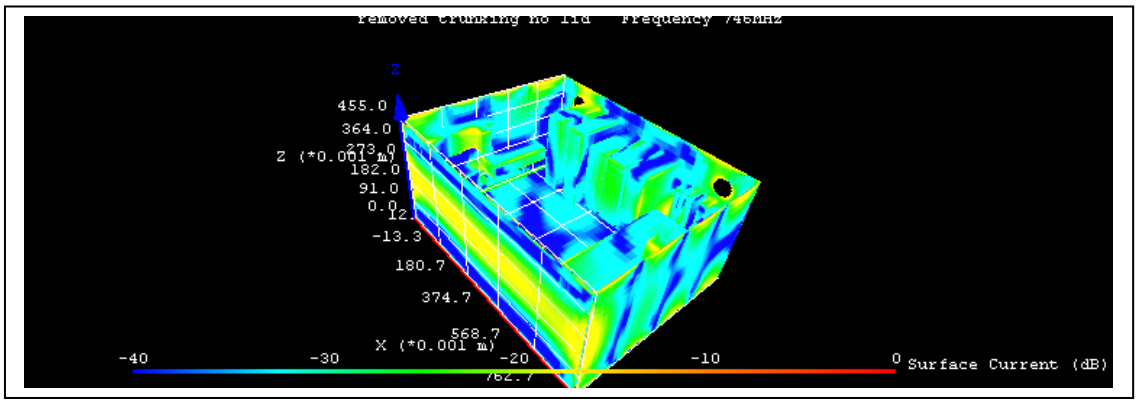

(b) 746 MHz

Fig. A-5.9 EM distribution of cabinet with trunking without lid in the machine frame

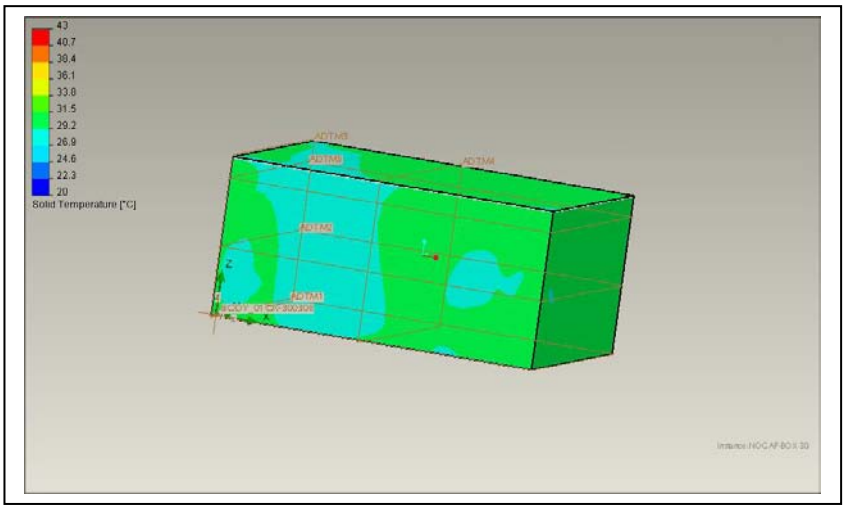

(a) Cabinet temperature

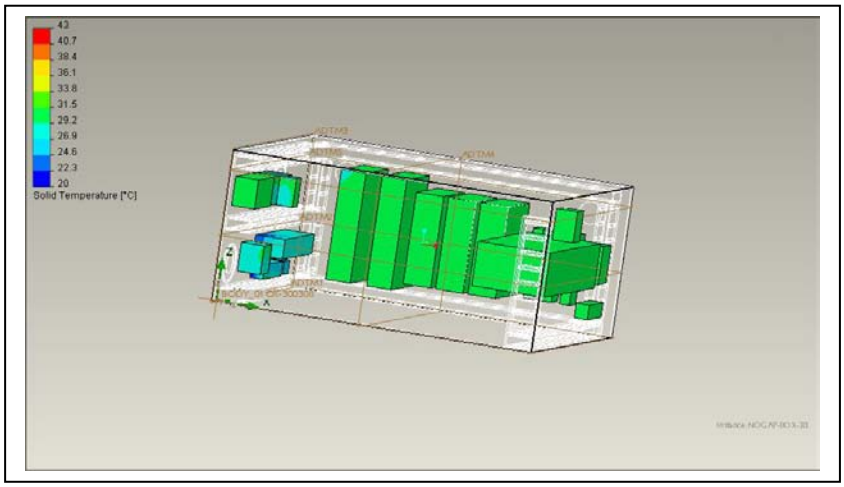

(b) Equipment temperature

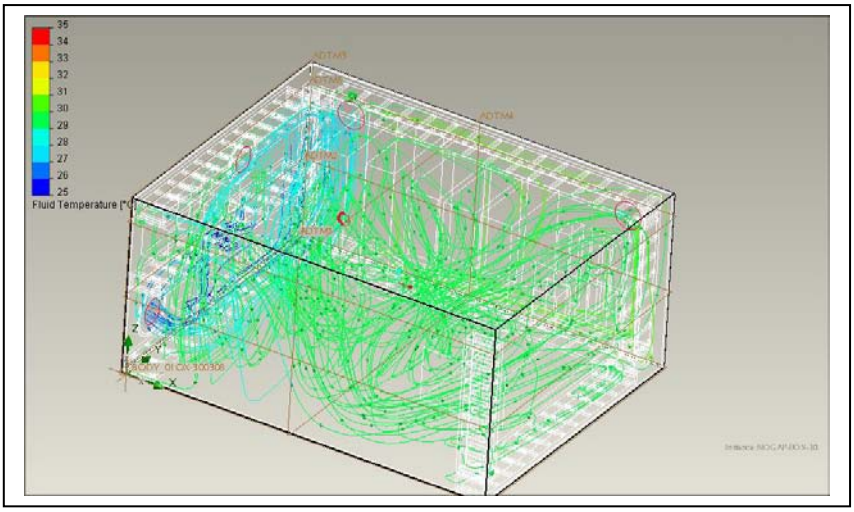

(c) Fluid temperature

Fig. A-5.10 CFD analysis of implemented design

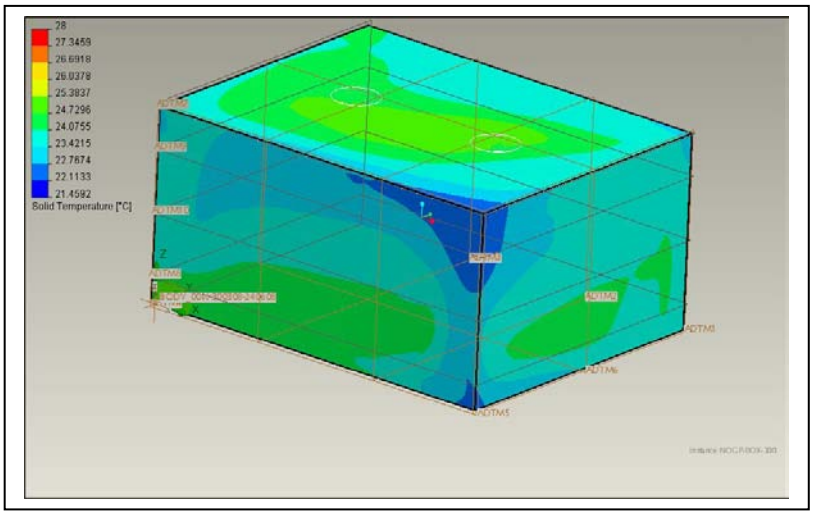

(a) Cabinet temperature

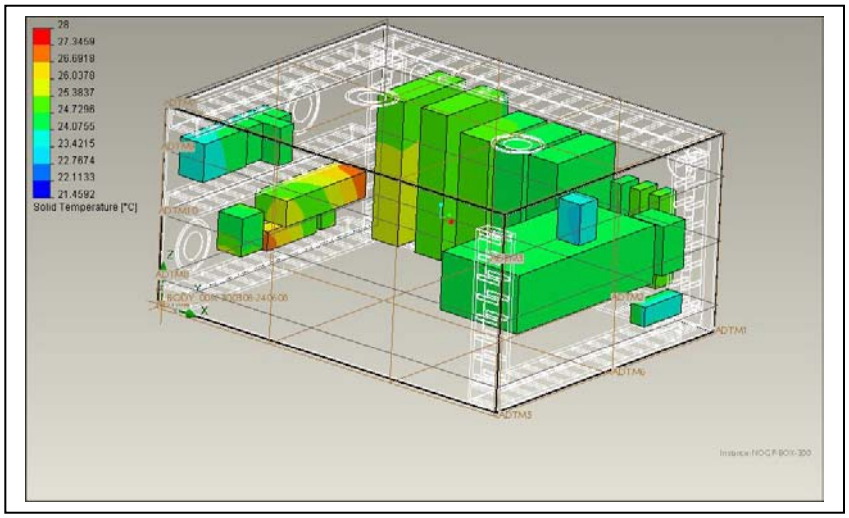

(b) Equipment temperature

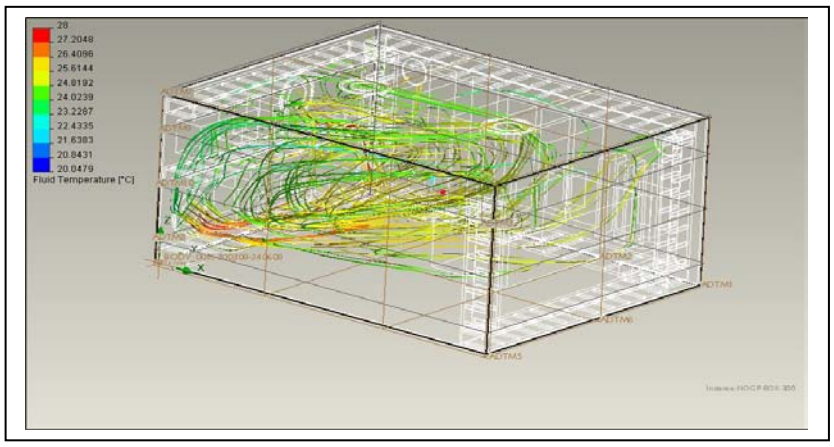

(c) Fluid temperature

Fig. A-5.11 CFD analysis with 2 input fans and 2 output fans

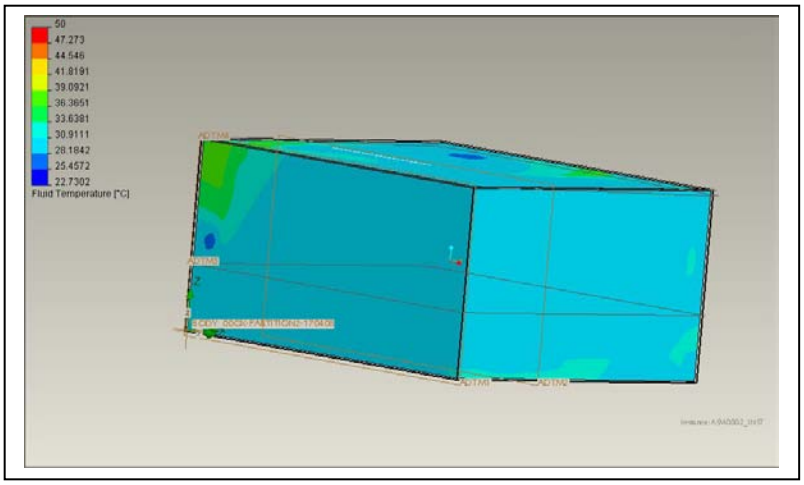

(a) Cabinet temperature

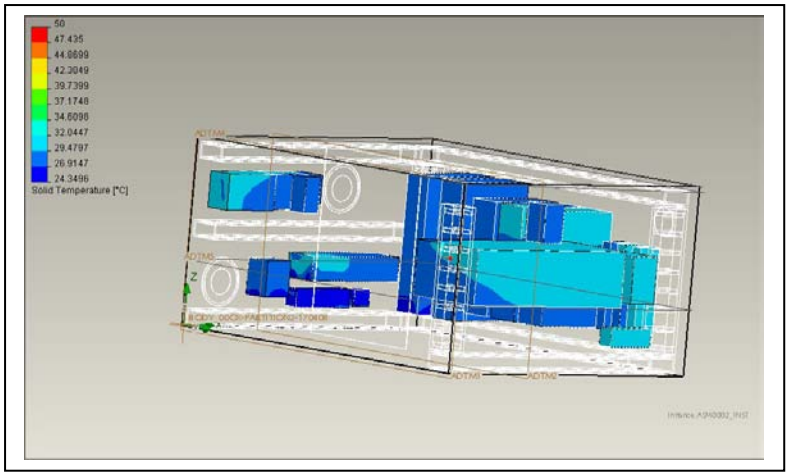

(b) Equipment temperature

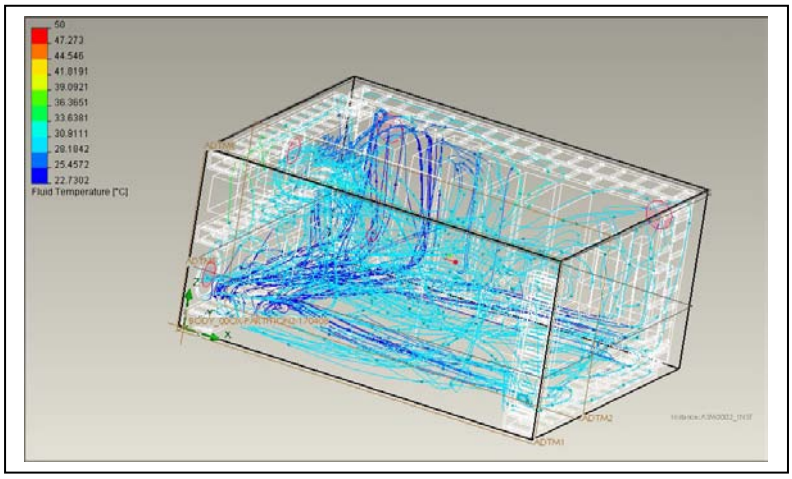

(c) Fluid temperature

Fig. A-5.12 CFD analysis with partitions (veins)

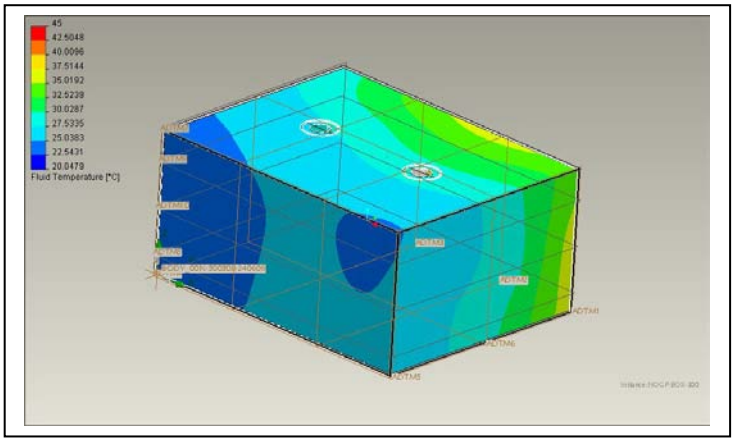

(a) Cabinet temperature

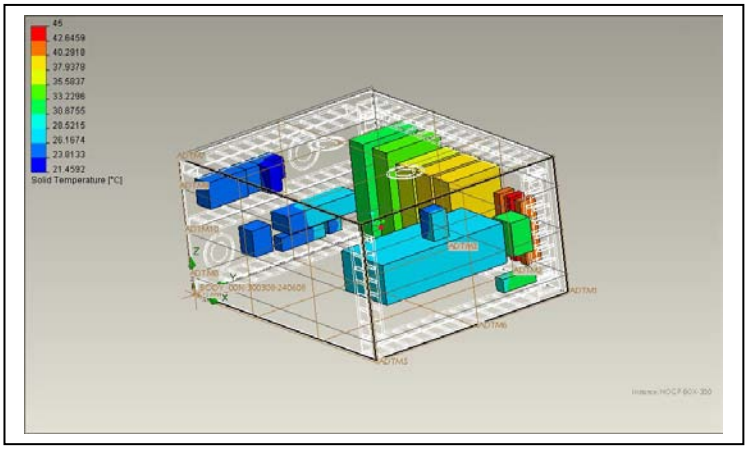

(b) Equipment temperature

Fig. A-5.13 CFD analysis with 2 output fans on the top

Appendix VI

- **Servo Tuning Analysis**

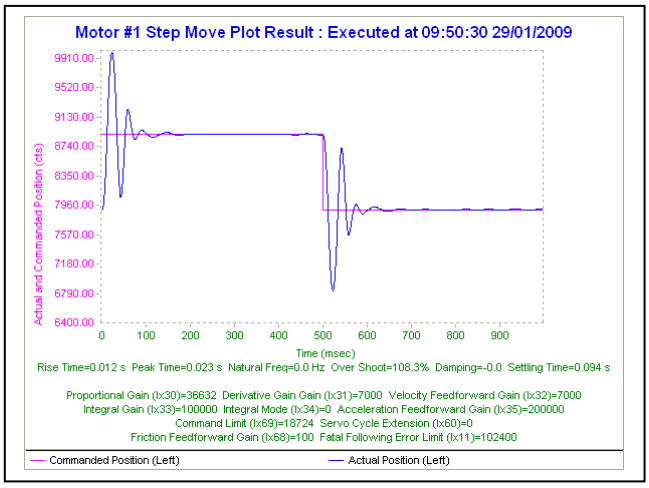

(a) Step move for X-axis (motor 1)

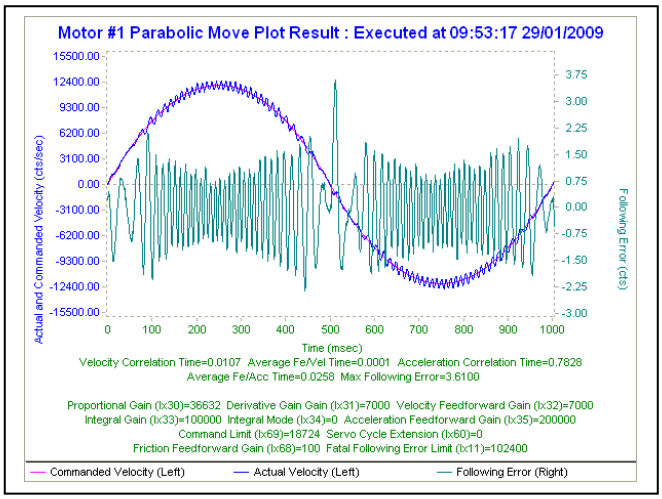

(b) Parabolic move for X-axis (motor 1)

Fig. A-6.1 Performance analysis of X-axis

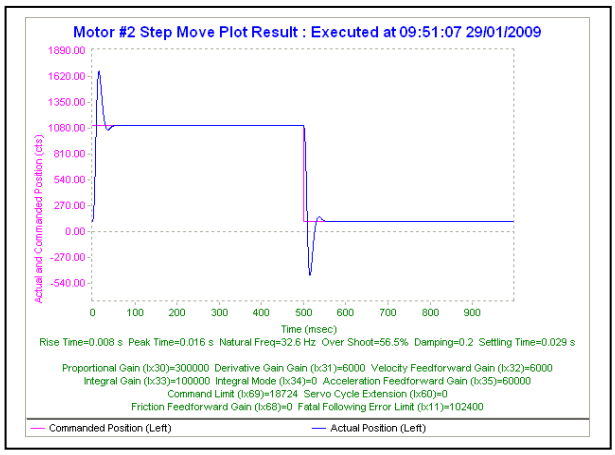

(a) Step move for Y-axis (motor 2)

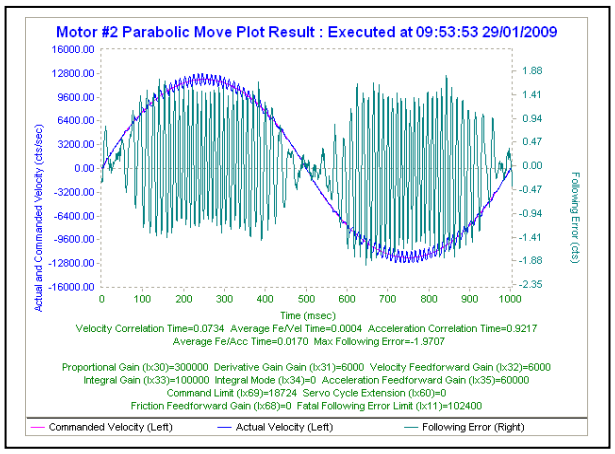

(b) Parabolic move for Y-axis (motor 2)

Fig. A-6.2 Performance analysis of Y-axis

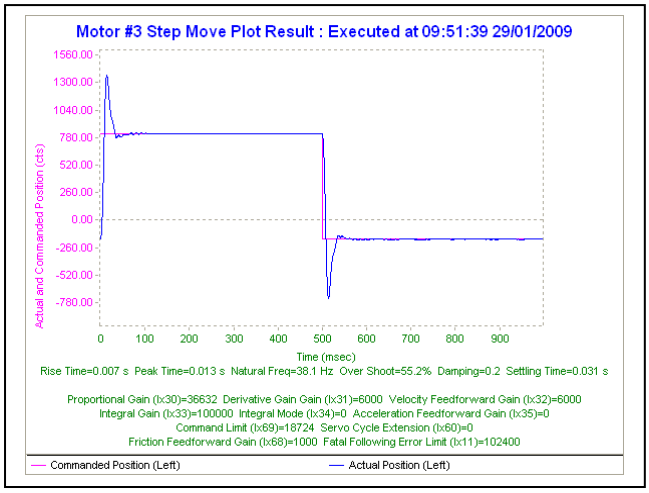

(a) Step move for Z-axis (motor 3)

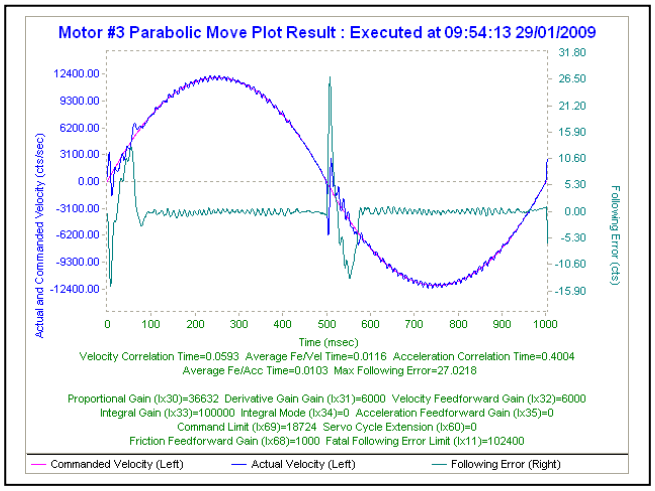

(b) Parabolic move for Z-axis (motor 3)

Fig. A-6.3 Performance analysis of Z-axis

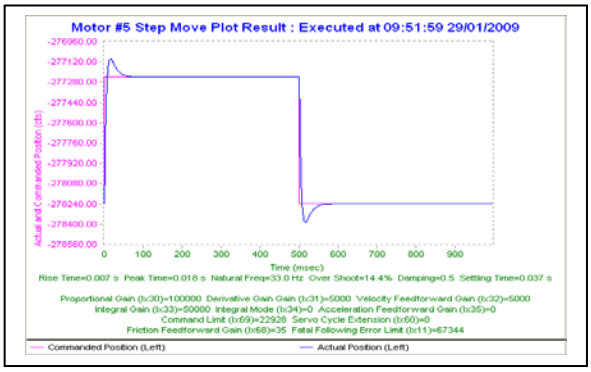

(a) Step move for B-axis (motor 5)

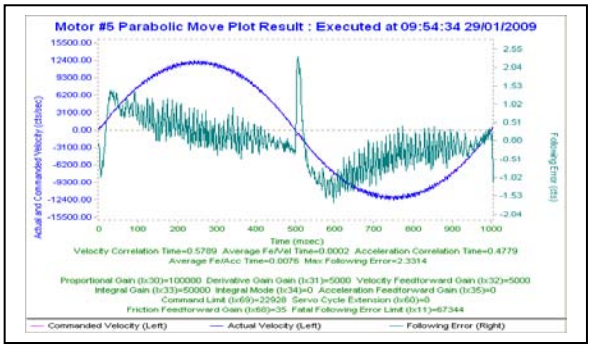

(b) Parabolic move for B-axis (motor 5)

Fig. A-6.4 Performance analysis of B-axis

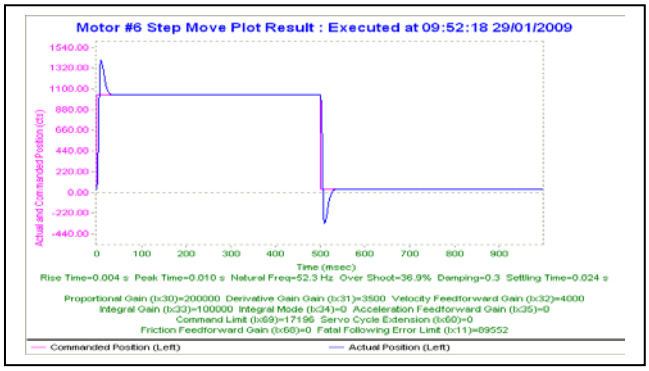

(a) Step move for C-axis (motor 6)

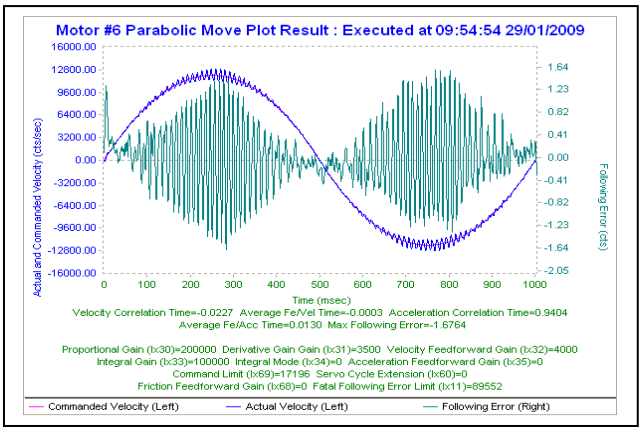

(b) Parabolic move for C-axis (motor 6)

Fig. A-6.5 Performance analysis of C-axis

Appendix VII

- **Part of the Program for Robot Communication**
  - **Cutting Forces Results**
- **Part of the Program for M-Code Macros**

A section of the robot communication with Ultra-Mill

```
Private SafetyGuardStatus As Integer
Private VacuumStatus As Integer
Private Sub Wsock_Disconnect()
   MsgBox "Please Check the Connection to the Robot!", vbOKOnly + vbCritical, "Communication Warning!"
   lblClosePort.ForeColor = vbYellow
   lblClosePort = "The Communication to Robot is not Established"
   lblLoadWorkpiece.ForeColor = vbBlue
   lblRemoveWorkpiece.ForeColor = vbBlue
   lblLoadCuttingTool.ForeColor = vbBlue
   lblRemoveCuttingTool.ForeColor = vbBlue
   Frame1.Enabled = False
   Frame2.Enabled = True
End Sub
Private Sub cmdClosePort_Click()
   Dim intReply As Integer
   If Wsock.State <> sckConnected Then Exit Sub
   intReply = MsgBox("Do you really want to close the connection to Robot?", vbYesNo + vbQuestion, "Close the Connection?")
   If intReply = vbYes Then
      Wsock.SendData "Close Port"
      Wsock.Close
      lblClosePort.ForeColor = vbYellow
      lblClosePort = "Port has been closed"
      lblLoadWorkpiece.ForeColor = vbBlue
      lblRemoveWorkpiece.ForeColor = vbBlue
      lblLoadCuttingTool.ForeColor = vbBlue
      lblRemoveCuttingTool.ForeColor = vbBlue
      Frame1.Enabled = False
      Frame2.Enabled = True
   End If
End Sub
Private Sub cmdConnection_Click()
   Wsock.Close
   Wsock.RemoteHost = txtIP.Text
   Wsock.RemotePort = txtPort.Text
   Wsock.Connect

   Timer1.Enabled = True
End Sub
```

Table A-7.1 Cutting forces in X, Y and Z on copper measured using a 3-axis Minidyn

Run	Factor 1	Factor 2	Factor 3			
	Spindle speed	Feedrate	DOC	Fx rms	Fy rms	Fz rms
	rpm	mm/min	µm	N	N	N
1	70,000	20	50	0.03	0.39	0.08
2	80,000	40	75	0.14	1.46	0.02
3	90,000	20	50	0.12	1.39	0.04
4	80,000	40	50	0.07	1.14	0.26
5	70,000	30	100	0.1	1.07	0.1
6	70,000	40	75	0.15	1.24	0.02
7	90,000	40	50	0	0.41	0.1
8	90,000	30	50	0.09	0.19	0.12
9	80,000	40	100	0.17	0.36	0.07
10	70,000	40	50	0.18	0.38	0.09
11	80,000	20	50	0.06	1.1	0.16
12	80,000	30	50	0.18	0.91	0
13	80,000	30	75	0.06	0.19	0.03
14	70,000	20	100	0.19	0.05	0.7
15	90,000	20	100	0.14	0.78	0.02
16	90,000	30	75	0.07	0.05	0.04
17	90,000	30	100	0.26	0.34	0.09
18	70,000	40	100	0.24	0.4	0.22
19	70,000	30	75	0.17	0.14	0.03
20	80,000	20	75	0.18	0.62	0.17
21	90,000	40	75	0.2	1.22	0.07
22	80,000	20	100	0.09	0.06	0.06
23	80,000	30	100	0.23	0.37	0.09
24	70,000	30	50	0.24	0.04	0.05
25	70,000	20	75	0.04	0.01	0.03
26	90,000	20	75	0.22	0.04	0.18
27	90,000	40	100	0.22	0.13	0.18

Table A-7.2 Cutting forces in X, Y and Z on aluminium measured using a 3-axis Minidyn

Run	Factor 1 Spindle speed rpm	Factor 2 Feedrate mm/min	Factor 3 DOC µm	Fx rms N	Fy rms N	Fz rms N
1	70,000	20	50	0.12	0.08	0.22
2	80,000	40	75	0.18	0.27	0.18
3	90,000	20	50	0.21	0.46	0.31
4	80,000	40	50	0.16	0.29	0.07
5	70,000	30	100	0.19	0.39	0
6	70,000	40	75	0.3	0.5	0.05
7	90,000	40	50	0.17	0.27	0.13
8	90,000	30	50	0.28	0.38	0.23
9	80,000	40	100	0.3	0.66	0.18
10	70,000	40	50	0.26	0.15	0.24
11	80,000	20	50	0.34	0.23	0.19
12	80,000	30	50	0.42	0.31	0.22
13	80,000	30	75	0	0	0
14	70,000	20	100	0	0	0
15	90,000	20	100	0	0	0
16	90,000	30	75	0	0	0
17	90,000	30	100	0	0	0
18	70,000	40	100	0	0	0
19	70,000	30	75	0	0	0
20	80,000	20	75	0	0	0
21	90,000	40	75	0	0	0
22	80,000	20	100	0	0	0
23	80,000	30	100	0	0	0
24	70,000	30	50	0	0	0
25	70,000	20	75	0	0	0
26	90,000	20	75	0	0	0
27	90,000	40	100	0	0	0

A section of the M-code macros

```
O9863
(REN BRKN TOOL PLUNGE)
IF[VRSTT NE 0]NRST
M130
PW=1(RPM CHK)
CALL O9760 PA=PA PC=PC PS=PS
PS=VC58
VNCOM[1]=VC38
IF[PH NE EMPTY]N1
PH=.5*VC79
N1 IF[PY NE EMPTY]N2
PY=0
N2 PT=VHCOD
PA=2(NO MOVES)
CALL O9761 PA=PA PT=PT
PV14=VC35
PV15=VC36
PV16=VC37
PV27=VC39
PV31=[VC[VC70]/VC57*VC79]-PV14
(MOVE TO XY CNTR)
CALL O9764 PX=[[VC[VC70+3]/VC57*VC79]-PV16]
(LASER OK CHK)
PV28=[VAPAZ-VMOFZ-VZOFZ[VACOD]]-VC66
PV29=PV28+[.1*VC50*VC79]
CALL O9763 PA=VC73 PT=PV29 PF=100 PW=2
IF[PH GE 0]N7
(LONG TL CHK)
PV27=0
PV28=PV31+[[ABS[PH]]*VC50]
(PV28=PV28+VTOFR[PT])
N6 CALL O9764 PZ=PV28
PV29=PV28-[.1*VC50*VC79]
CALL O9763 PA=VC73 PT=PV29 PF=100
G4F.1
VC98=0
IF[ABS[VC81-PV28] GT [VC95*10]]N7(OK TL)
VC98=2
PV27=PV27+1
IF[PV27 EQ 5]N9(BKN TL)
GOTO N6
N7 (SHORT TL CHK)
IF[VC[VC70+8] EQ 9]N15
IF[VC[VC70+8] NE EMPTY]N85
N15 (NON LATCH METHOD)
.....
.....
```

Appendix VIII

- **Cutting Trial Results**
- **Various Machined Test Parts**

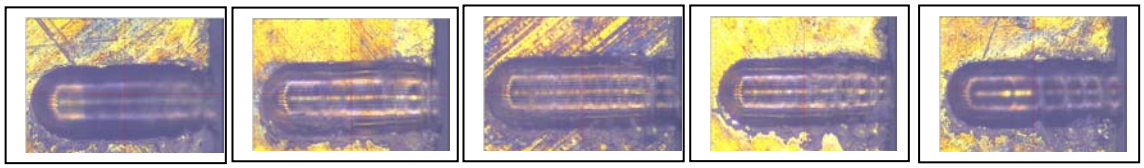

0º 90º 180º 270º 359.74º

(a) Cavities machined with standard tool.

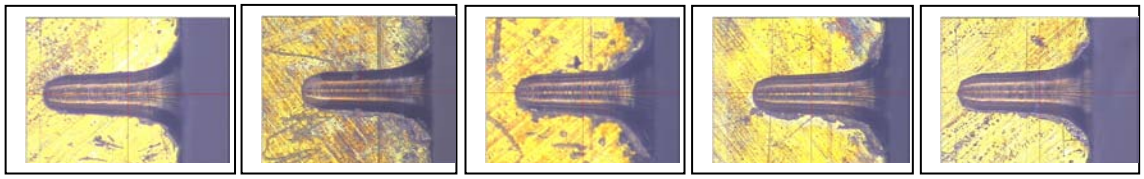

0º 90º 180º 270º 359.74º

(b) Cavities machined with bespoke tool.

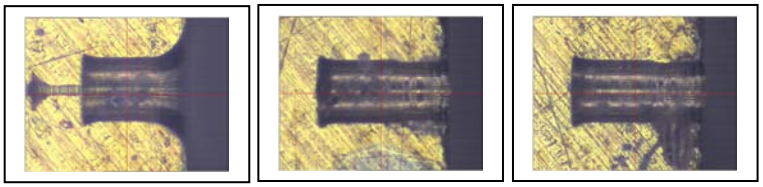

1st 3rd 5th

(c) Cavities machined with diamond tool.

Fig. A-8.1 Cavities machined with three different cutting tools

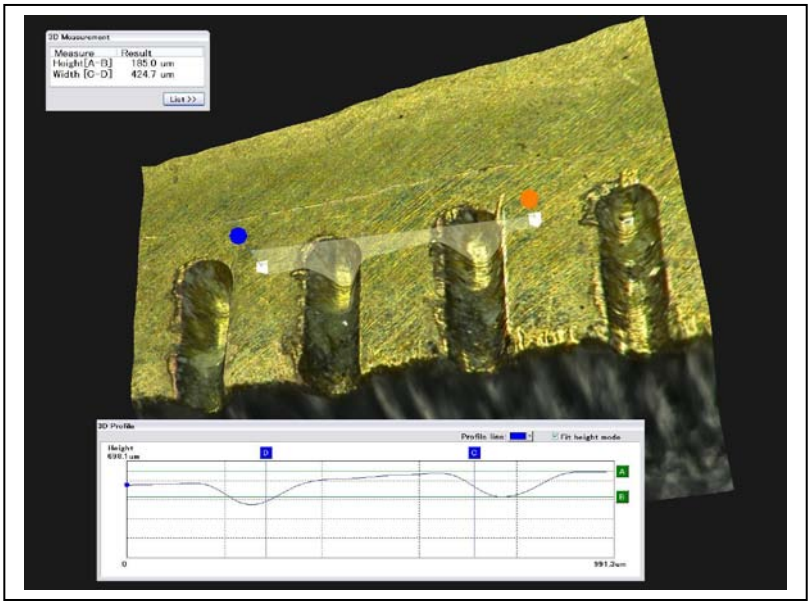

Fig. A-8.2 3D imaging of cavities

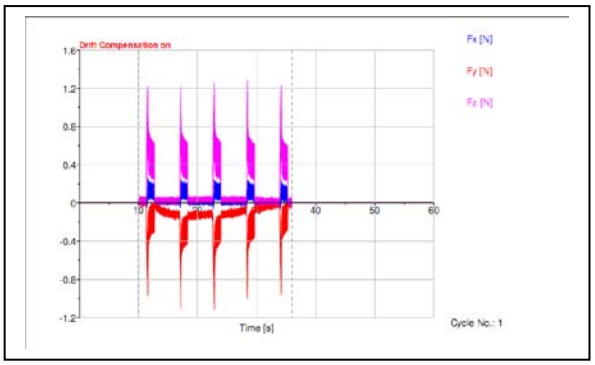

(a) 80,000 rpm and 20 mm/min

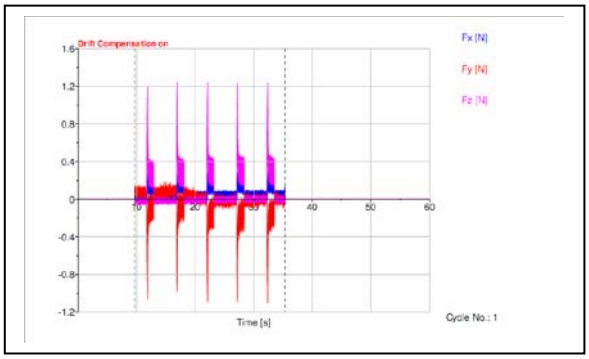

(b) 80,000 rpm and 30 mm/min

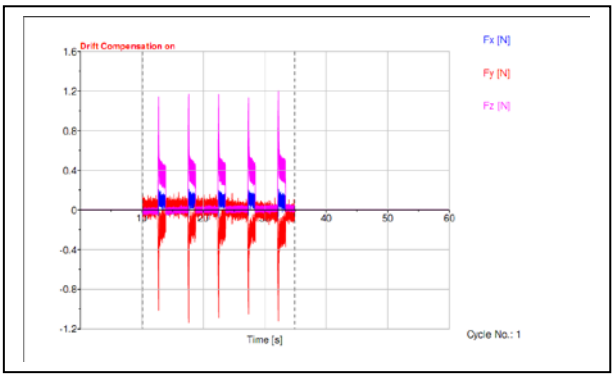

(c) 100,000 rpm and 40 mm/min

Fig. A-8.3 Cutting forces from the Aplix job

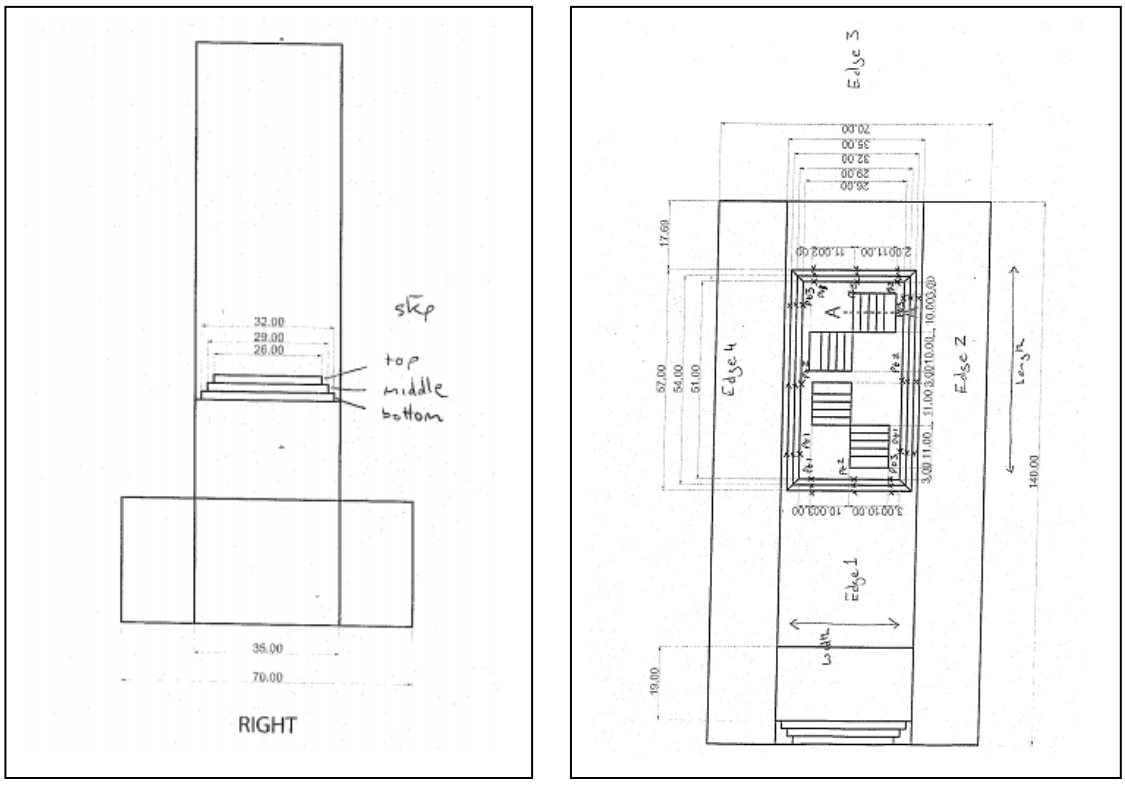

(a) (b)

Fig. A-8.4 Workpiece measurements identifier

Table A-8.1 Straightness measurements of the vertical pyramid

Straightness					
	Top z = -1.0		Middle z = -3.75		Bottom z = -5.75
Edge 1	0.000769	Edge 1	0.000709	Edge 1	0.001733
Edge 2	0.001590	Edge 2	0.001159	Edge 2	0.001289
Edge 3	0.002575	Edge 3	0.000050	Edge 3	0.000804
Edge 4	0.000369	Edge 4	0.001012	Edge 4	0.000955

Table A-8.2 Parallelism measurements of the vertical pyramid

Parallelism					
Top		Middle		Bottom	
Edge 1 & edge 3	0.001398	Edge 1 & edge 3	0.002215	Edge 1 & edge 3	0.001750
Edge 2 & edge 4	0.001688	Edge 2 & edge 4	0.001271	Edge 2 & edge 4	0.001455
	Top & middle		Top & bottom		
Edge 4	0.003815		0.003242		

Table A-8.3 Perpendicularity measurements of the vertical pyramid

Perpendicularity					
Top		Middle		Bottom	
Edge 1	0.001967	Edge 1	0.000847	Edge 1	0.002018
Edge 3	0.002602	Edge 3	0.002547	Edge 3	0.002707

Table A-8.4 Angles measurements of the vertical pyramid

Angles					
Top		Middle		Bottom	
Edge 1 to Edge 2	90.000941	Edge 1 to Edge 2	89.997359	Edge 1 to Edge 2	89.999147
Edge 2 to Edge 3	90.002157	Edge 2 to Edge 3	89.998797	Edge 2 to Edge 3	89.999761
Edge 3 to Edge 4	89.998056	Edge 3 to Edge 4	90.002937	Edge 3 to Edge 4	90.000713
Edge 4 to Edge 1	89.998846	Edge 4 to Edge 1	90.002937	Edge 4 to Edge 1	90.000379

Table A-8.5 Length measurements of the vertical pyramid

Length					
Top nominal = 51.00 mm		Middle nominal = 54.00 mm		Bottom nominal = 57.00 mm	
Pt 1	50.991875	Pt 1	53.984635	Pt 1	56.984762
Pt 2	50.990394	Pt 2	53.984571	Pt 2	56.983854
Pt 3	50.991835	Pt 3	53.984514	Pt 3	56.984028

Table A-8.6 Width measurements of the vertical pyramid

Width					
Top nominal = 26.00 mm		Middle nominal = 29.00 mm		Bottom nominal = 32.00 mm	
Pt 1	25.988736	Pt 1	28.989048	Pt 1	31.990154
Pt 2	25.989438	Pt 2	28.989740	Pt 2	31.990244
Pt 3	25.988297	Pt 3	28.993020	Pt 3	31.990687

Table A-8.7 Height measurements of the vertical pyramid

Height			
Top to step 1 nominal = 2.00 mm		Top to step 2 nominal = 2.00 mm	
Pt 1	2.755981	Pt 1	1.999584
Pt 2	2.749647	Pt 2	1.989631
Pt 3	2.757844	Pt 3	1.999602
Pt 4	2.760167	Pt 4	2.003377

Table A-8.8 Step width measurements of the vertical pyramid

Step width							
Top edge to step 1 edge nominal = 1.50 mm							
Edge 1		Edge 2		Edge 3		Edge 4	
Pt 1	1.496848	Pt 1	1.501276	Pt 1	1.498729	Pt 1	1.499036
Pt 2	1.498036	Pt 2	1.501163	Pt 2	1.498723	Pt 2	1.499139
Pt 3	1.497966	Pt 3	1.501584	Pt 3	1.497991	Pt 3	1.503139
Step 1 edge to step 2 edge nominal = 1.50 mm							
Edge 1		Edge 2		Edge 3		Edge 4	
Pt 1	1.504604	Pt 1	1.500833	Pt 1	1.498899	Pt 1	1.500274
Pt 2	1.504553	Pt 2	1.500625	Pt 2	1.499434	Pt 2	1.499879
Pt 3	1.503542	Pt 3	1.501322	Pt 3	1.499518	Pt 3	1.496344

Table A-8.9 Flatness measurements of the vertical pyramid

Flatness	
step 1	0.003575
step 2	0.003111

Table A-8.10 Planes parallelism measurements of the vertical pyramid

Parallelism (planes)	
Top to step 1	0.011833
Top to step 2	0.015465
step 1 to step 2	0.005404

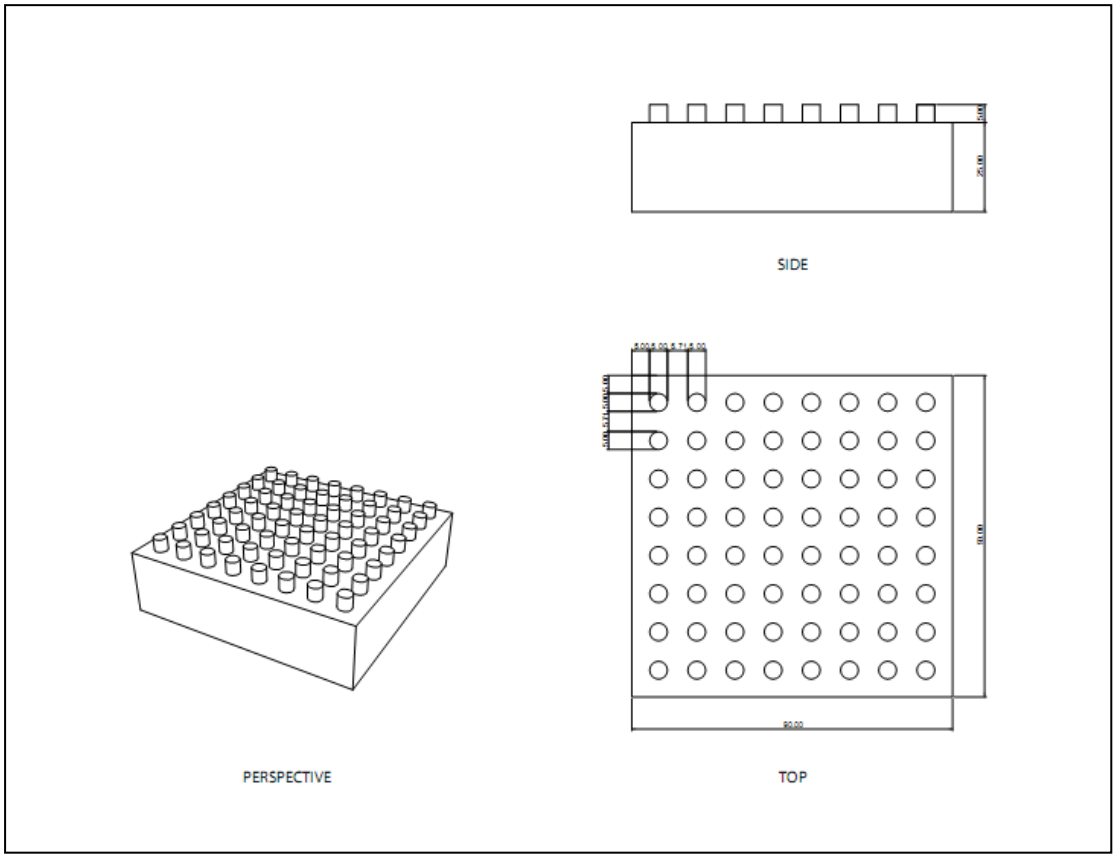

(a) 3D model

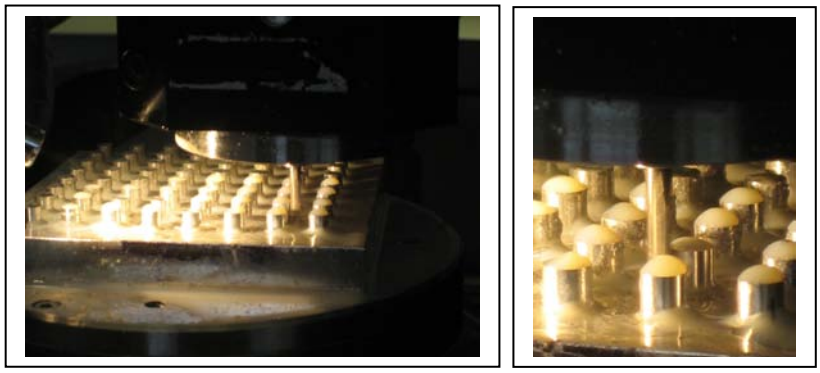

(b) Upstands machined

Fig. A-8.5 Machining of 64 circular upstands on aluminium (5 mm diameter, 5 mm height) using 3 mm tungsten carbide tool

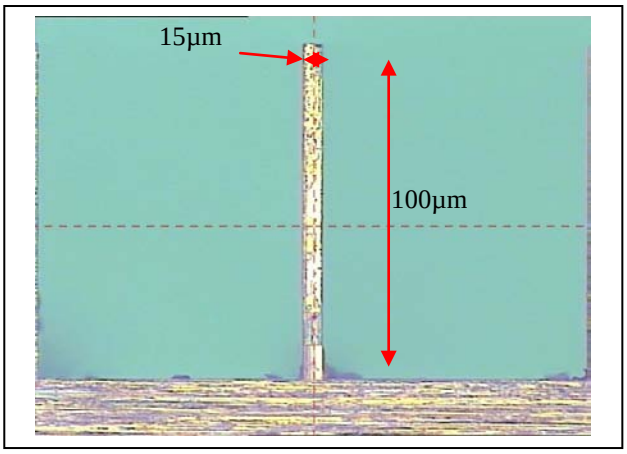

Fig. A-8.6 Micro channel on brass without burrs using 400 µm diamond milling tool

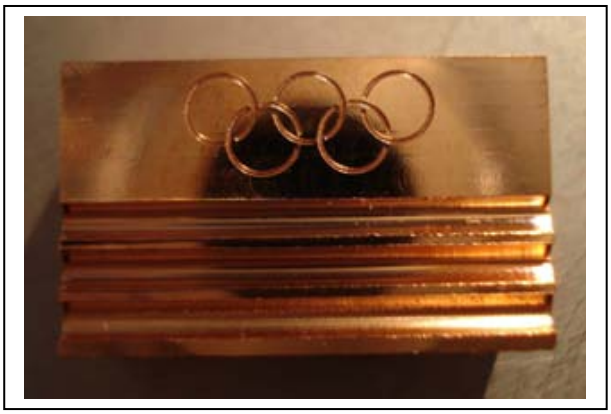

Fig. A-8.7 CVD milled grooves with optical surface finish

Fig. A-8.8 Micro drilling (200 µm carbide tools)

Fig. A-8.9 CVD milled trench with optical surface finish

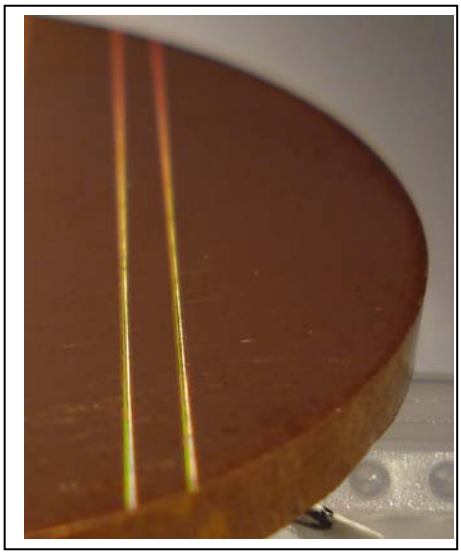

Fig. A-8.10 Diamond milled micro trenches
(400 µm wide, 15 nm Ra)